

Modulating Akt signalling to enhance CAR T-cell therapy

Vedika Mehra

University College London

PhD Supervisor: Dr Claire Roddie and Professor Karl Peggs

A thesis submitted for the degree of

Doctor of Philosophy

University College London

January 2023

Declaration

I, Vedika Mehra, confirm that the work presented in this thesis is my own. Where information has been derived from other sources, I confirm that this has been indicated in the thesis.

Abstract

CD19 targeting chimeric antigen receptor (CAR) T-cells deliver excellent clinical responses in relapsed/refractory acute lymphoblastic leukaemia (B-ALL) and high-grade B cell lymphoma. However, many patients do not respond or relapse post treatment because of poor CAR T-cell expansion and persistence. Adoptive cell transfer studies have shown that stem-cell memory/naïve/central memory (Tscm/Tn/Tcm) T-cell subsets compared to effector/terminal (Te/Tte) subsets, deliver superior T-cell expansion, persistence, and anti-tumour efficacy *in-vitro* and *in-vivo*. In patients, the proportion of Tn/Tcm subsets can vary considerably, and current manufacturing protocols prioritising mass cell expansion often give rise to Te/Tte skewed products. Studies have demonstrated that the *ex-vivo* inhibition of Akt signalling, an important mediator of T-cell activation and differentiation, can enrich such Tn/Tcm populations.

A novel CD19 targeting single chain fragment variable (scFv) was developed at UCL and named CAT. The CAT scFv was found to have lower affinity for the CD19 target over the FMC63 scFv, utilised in current FDA approved KymriahTM, YescartaTM and TecartusTM CAR therapies. This CAT CAR has demonstrated durable responses against paediatric/adult B-ALL and was used as a model to explore the effects of *ex-vivo* Akt inhibition. We describe a genetic engineering approach of Akt inhibition through the expression of a dominant negative Akt1 molecule and highlight the benefits of pharmacological Akt inhibition.

We assessed the incorporation of Akt inhibitor VIII (further referred to as VIII), originally developed by Merck Research Laboratories, Pennsylvania, USA (Compound 16g) into the CliniMACS Prodigy[®] manufacture process, utilised in current UCL based CAR T-cell trials, in both healthy/B-ALL patients at small/large scale. We show that *ex-vivo* Akt inhibition can promote enrichment of less differentiated Tscm/Tcm subsets with improved expansion and cytotoxicity against antigen expressing targets *in-vitro* and superior anti-tumour activity *in-vivo*. Inhibition using VIII supported enrichment of CD4 Th1 and Th17 subsets with no skew towards Th2 and Tregs, as previously reported resulting in increased T-cell polyfunctionality. Transcriptome and metabolic analysis

revealed a signature for autophagy in CAR CD8 T-cells validated by an increase in autophagic vesicles, not previously described in the context of *ex-vivo* Akt inhibition in CAR T-cells. VIII-treated CAR CD8 T-cells were found to have a unique metabolic profile with high mitochondrial membrane potential ($\Delta\Psi_m$) and increased fatty acid oxidation to support energy demands of enhanced expansion and cytotoxicity.

Lastly, we demonstrate that Akt inhibition can be incorporated into large scale automated manufacturing processes with the potential to generate functionally superior products compared to standard untreated products. This ultimately may help to improve clinical responses by rescuing patients/products at risk of CD19+ relapse.

Impact Statement

At UCL, a novel CD19 CAR called the CAT CAR with a fast off-rate CD19 binding domain, designed to reduce CAR T-cell immune toxicity, and improve engraftment, was developed and has shown promising clinical activity in both adult and paediatric acute lymphoblastic leukaemia (B-ALL). However, some patients do not respond or relapse post treatment because of poor CAR T-cell expansion and persistence. The incorporation of *ex-vivo* Akt inhibition with Akt inhibitor VIII (VIII) has shown promise in generating CAR T-cells with enhanced anti-tumour efficacy. However, this has only been tested at small-scale in CAR T-cells designed with a CD28 ζ endodomain. CD28 ζ CAR T-cells have been reported to suffer from exhaustion and diminished persistence over 41BB ζ CAR T-cells, attributed to basal signalling events in the absence of target. As vast majority of CAR T-cells therapies utilise a 41BB ζ endodomain, assessing the effects of *ex-vivo* Akt inhibition in a more clinically relevant model of 41BB ζ CAR T-cells is of significant impact to the CAR T-cell field. In this study, we show for the first time that *ex-vivo* VIII inhibition can provide phenotypic and functional benefits in the CAT CAR designed with a 41BB ζ endodomain and implicate several biological pathways contributing to this.

By directly comparing CAR T-cell products manufactured from B-ALL patients using conventional methods in parallel with VIII treatment, we show that Akt inhibition can enhance product phenotype and functionality in a series of *in-vitro* and *in-vivo* assessments. On the basis of this, we hypothesised that this manufacturing intervention may be able to rescue patients at risk of relapse from CD19+ disease due to poor CAR T-cell function.

We show that this method can be successfully scaled to the closed semi-automated CliniMACS Prodigy[®] CAR T-cell manufacturing platform to permit clinical scale manufacture of enhanced CAR T-cells. Such an automated manufacturing approach can help support the increasing demand for CAR T-cell manufacturing, providing a more standardised approach. The CliniMACS Prodigy[®] provides additional benefits by eliminating the requirement for high-classification manufacturing clean rooms and their

associated costs, reducing staffing requirements, and lowering the risks of contaminations or other operator handling errors. Work on this study led to the incorporation of this manufacturing method in an upcoming UCL based CAR T-cell trial against multiple myeloma (NCT04795882) with a chance to improve patient outcomes positively.

Acknowledgements

Firstly, I would like to thank Dr Claire Roddie, Professor Karl Peggs and Dr Martin Pule for giving me the opportunity to work on this project. Particularly Claire, thank you for taking a chance on an MSc student and providing endless opportunities, support, and guidance to achieve my goals over the years.

Next, I would like to thank all Pule and Translation Team members, past and present, in particular Gordon Weng-Kit Cheung, Marina Mitsikakou, Manar Shafat, Harriet Roddy, Morgan Palton, and Alastair Hotblack, for never turning away from my many requests for assistance. I have been fortunate to work with some great colleagues over the years who have made this an enjoyable experience. Especially Marina and Manar, we have shared many laughs and frustrations, and I'll always be grateful for your advice, unwavering support, and belief in my abilities, even in the absence of mine.

I'd also like to thank all RFH Translation Team members, especially Juliana Dias Alves Pinto, for accommodating my numerous requests as well as organising and overseeing all scale-ups. I'm grateful to Mahnaz Abbasian, Amaia Cadinanos Garai, Louisa Green, Mhairi Vaughan, Vitoria Meyer Cantinho Pereira, Leticia Bosshard-Carter and Ketki Vispute for their help executing scale-ups. I would also like to thank Giulia Agliardi for all the scientific guidance and immeasurable assistance with patient, *in-vivo* assessments and our many adventures with the Isoplexis platform.

Additionally, I would like to thank collaborators Dr Harry Dolstra, and Dr Anniek van der Waart for providing the GMP grade VIII inhibitor and for their helpful discussions over the years. I thank Tony Brooks and Niola Paola from the ICH genomics facility for assistance with RNA sequencing and analysis. Most importantly, I thank the patient's part of the ALLCAR19 trial for their consent to use surplus cellular material.

Lastly, I would like to thank my family and particularly my parents, I owe every opportunity to your hard work and care. This PhD has spanned many up/downs over the years, and none of this would have been possible without your infinite support.

Table of Contents

Abstract	3
Impact Statement	5
Acknowledgements	7
Table of Contents	8
Table of figures	12
List of tables	14
Abbreviations	15
Chapter 1. Introduction	18
1.1. Introduction	18
1.1.1. Cancer and the immune system	18
1.1.2. Chimeric Antigen Receptors (CARs)	22
1.1.3. CD19 CARs	23
1.1.4. Failure of CD19 CAR T-cell therapy	24
1.1.5. Importance of Tcm/Tscm subsets in CAR T-cell therapy	32
1.1.6. Akt and its role in T-cell signalling	34
1.1.7. Effects of pharmacological Akt inhibition in T-cells	39
1.2. Study rationale and aims	41
Chapter 2. Materials & Methods	44
2.1. Molecular Cloning	44
2.1.1. Construction of retroviral plasmids co-expressing dnAkt with CAT CAR	44
2.1.2. Moving CAT scFv into SFGmR.RQR8 scaffold	44
2.1.3. Replacing RQR8 with dnAkt	45
2.1.4. Adding a FLAG tag to dnAkt	46
2.1.5. Summary of plasmid constructs	48
2.2 Cell culture	48
2.2.1. Cell lines	48
2.2.2. Cell culture and maintenance	49
2.3 Virus production	50
2.3.1. Retrovirus vector production	50
2.3.2. Third generation lentivirus vector production, concentration, and titration	50

2.4. PBMC/T-cell isolation, cryopreservation, and recovery	51
2.4.1. PBMC isolation from whole blood	51
2.4.2. T-cell isolation from leucocyte cones	52
2.4.3. PBMC isolation from cryopreserved leukapheresis bags	52
2.4.4. PBMC cryopreservation and recovery	52
2.5. PBMC/T-cell activation and transduction	53
2.5.1. PBMC activation and retrovirus transduction.....	53
2.5.2. T-cell activation and lentivirus transduction.....	53
2.5.2. Scale-ups on the CliniMACS Prodigy®	54
2.6. Cell based assays	55
2.6.1. Co-culture assay	55
2.5.2. Flow cytometry based killing assay (FBK).....	55
2.7. Cytokine analysis.....	56
2.7.1. Cytokine Bead Array (CBA).....	56
2.7.2. Isoplexis	56
2.8. Flow Cytometry	57
2.8.1. General staining and analysis.....	57
2.8.2. Intracellular cytokine and transcription factor staining	58
2.8.3. Phosphoflow and FLAG tag staining.....	58
2.8.4. CytoID Staining	59
2.9. Mitochondrial/Metabolic Assessments.....	59
2.9.1. Mitrotracker staining.....	59
2.9.2. Mitochondrial membrane potential	60
2.9.3. Seahorse	60
2.10. RNA extraction, sequencing, and analysis.....	61
2.11. <i>In-vivo</i> Procedures.....	62
2.11.1. Establishment of a systemic leukaemia model and <i>in-vivo</i> imaging	62
2.11.2. Spleen Harvest and Staining	62
2.11.3. Bone Marrow Harvest and Staining.....	62
2.12. Statistical analysis	63
Chapter 3. Effects of pharmacologic and dnAkt mediated Akt inhibition on CAR T-	
cells	64

3.1. Introduction	64
3.2. Phenotypic and functional assessment of dnAkt and pharmacological Akt inhibition	66
3.2.1. Phenotypic and functional assessment of dnAkt in CAR T-cells	66
3.2.2. Effects of pharmacologic versus dnAkt mediated Akt inhibition on CAR T-cells	69
3.3. Discussion.....	74
3.4. Effects of early pharmacologic Akt inhibition in both 41BBζ/CD28ζ CAR T-cells.....	75
3.5. Conclusion.....	78
Chapter 4. Effects of pharmacological VIII inhibition in CAT CAR 41BBζ CAR T-cells, using the CliniMACS Prodigy[®] manufacturing protocol	81
4.1. Introduction	81
4.2. GMP Akt inhibitor VIII drug comparability and titration	86
4.2.1. Phenotype of CAR T-cells treated with Merck VIII vs GMP VIII Akt inhibitors	87
4.2.2. Function of CAR T-cells treated with Merck VIII vs GMP VIII Akt inhibitors	89
4.3. Assessing GMP inhibitor VIII in healthy donor T-cells	91
4.3.1. Effects of GMP Akt inhibitor VIII treatment on expansion and phenotype .	92
4.3.2. Effects of GMP Akt inhibitor VIII treatment on CAR T-cell function and cytokine secretion	96
4.3.3. Effects of GMP Akt inhibitor VIII treatment on CD4 T-helper (Th) cells and polyfunctionality.....	98
4.3.4. Effects of GMP Akt inhibitor VIII treatment on CAR T-cell transcriptome	104
4.3.5. Effects of GMP Akt inhibitor VIII treatment on CD8 CAR T-cell Autophagy, Mitochondria and Metabolism.....	109
4.3.6. Effects of GMP Akt inhibitor VIII treated CAR T-cells <i>in-vivo</i>	115
4.4. Discussion.....	118
Chapter 5. Effects of pharmacological VIII inhibition in patient derived CAT CAR T-cells, using the CliniMACS Prodigy[®] manufacturing protocol ..	123

5.1. Introduction	123
5.2. Assessing GMP Akt inhibitor VIII inhibitor in B-ALL patient derived T-cells	126
5.2.1. Effects of GMP Akt inhibitor VIII treatment on B-ALL patient phenotype	126
5.2.2. Effects of GMP Akt inhibitor VIII treatment on B-ALL patient derived CAR T-cell function and cytokines	129
5.2.3. Effects of GMP Akt inhibitor VIII treatment on B-ALL patient derived CD4 T-helper (Th) cells and polyfunctionality	132
5.2.4. Effects of GMP Akt inhibitor VIII treatment on B-ALL patient derived CAR T-cell autophagy and mitochondria	134
5.3. Discussion.....	136
Chapter 6. Large-scale manufacture of B-ALL patient CAR T-cells on the CliniMACS Prodigy® with VIII treatment	138
6.1. Introduction	138
6.2. Characteristics of clinically scaled CAR T-cells.....	139
6.3. <i>In-vivo</i> functionality of B-ALL patient CAR T-cells.....	141
6.4. Discussion.....	143
Chapter 7. General Discussion and Future Work	145
Reference List	152

Table of figures

Figure 1. Summary of CD4 T-helper subsets.....	19
Figure 2. CAR Structure	22
Figure 3. T-cell differentiation and associated markers.....	33
Figure 4. Akt structure and pathway	36
Figure 5. Role of Akt signalling in CD8 T-cell differentiation.....	38
Figure 6. Molecular cloning design of dnAkt CAT CAR construct	44
Figure 7. FLAG tag overlap PCR	47
Figure 8. CD19 and eGFP expression on target cell lines	49
Figure 9. Chemical Structure of Akt Inhibitor VIII	64
Figure 10. Illustration of dnAkt design	66
Figure 11. Method of CAR T-cell generation to evaluate the CAT CAR co-expressing the dnAkt. Schematic representation of the method used to generate CAT CAR T-cells co-expressing the dnAkt.....	67
Figure 12. Phenotypic and functional assessment of dnAkt in CAR T-cells.....	69
Figure 13. Method of CAR T-cell generation to evaluate the CAT CAR co-expressing the dnAkt with late pharmacological inhibition.....	70
Figure 14. Effects of pharmacologic versus dnAkt mediated inhibition of Akt on CAR T-cells	73
Figure 15. Method of 41BB ζ and CD28 ζ CAT CAR T-cell generation following early Akt inhibition	75
Figure 16. Effects of early pharmacologic Akt inhibition in both 41BB ζ /CD28 ζ CAR T-cells	77
Figure 17. Illustration of CAR T-cell manufacturing processes	81
Figure 18. Schema of manufacturing processes used in ALLCAR19 trial.....	84
Figure 19. Expansion, transduction, and phenotype of CAR T-cells manufactured in the ALLCAR19 trial	85
Figure 20. Phenotype of CAR T-cells treated with Merck VIII vs GMP VIII Akt inhibitors	88
Figure 21. Function of CAR T-cells treated with Merck VIII vs GMP VIII Akt inhibitors	90

Figure 22. Schema of CAR T-cell manufacturing process	92
Figure 23. Effects of GMP Akt inhibitor VIII treatment on expansion and phenotype .	95
Figure 24. Effects of GMP Akt inhibitor VIII treatment on CAR T-cell function and cytokine secretion.....	98
Figure 25. Effects of GMP Akt inhibitor VIII treatment on CD4 T-helper (Th) cells and polyfunctionality	104
Figure 26. Effects of GMP Akt inhibitor VIII treatment on CAR T-cell transcriptome	108
Figure 27. Autophagy signature in CD8 CAR T-cells and simplified autophagy pathway	110
Figure 28. Effects of GMP Akt inhibitor VIII treatment on CD8 CAR T-cell Autophagy, Mitochondria and Metabolism	115
Figure 29. Effects of GMP Akt inhibitor VIII treated CAR T-cells <i>in-vivo</i>	118
Figure 30. Phenotype comparison of T-cells from adult B-ALL patients with healthy donor and paediatric patients	125
Figure 31. Effects of GMP Akt inhibitor VIII treatment on B-ALL patient phenotype	129
Figure 32. Effects of GMP Akt inhibitor VIII treatment on B-ALL patient derived CAR T-cell function and cytokines.....	131
Figure 33. Effects of GMP Akt inhibitor VIII treatment on B-ALL patient derived CD4 T-helper (Th) cells and polyfunctionality	133
Figure 34. Effects of GMP Akt inhibitor VIII treatment on B-ALL patient derived CAR T-cell autophagy and mitochondria	135
Figure 35. The CliniMACS Prodigy®	138
Figure 36. Characteristics of clinically scaled CAR T-cells	140
Figure 37. <i>In-vivo</i> functionality of B-ALL patient CAR T-cells	142

List of tables

Table 1. Summary of factors contributing to the failure of CAR T-cell therapy	27
Table 2. Summary of clinical outcomes in B-ALL patients targeting CD19 antigen using CARs designed with a 41BB co-stimulatory domain	31

Abbreviations

AAV	Adeno Associated Virus
ACT	Adoptive Cell Therapy
ADCC	Antibody Dependent Cellular Cytotoxicity
AICD	Activation Induced Cell Death
ALC	Absolute lymphocyte counts
B-ALL	B cell Acute Lymphoblastic Leukaemia
B-cell	B lymphocyte
BLI	Bioluminescence Imaging
BMT	Bone Marrow Transplant
B-NHL	B cell Non-Hodgkin's lymphoma
CAR	Chimeric Antigen Receptor
CDC	Complement Dependent Cytotoxicity
CFE	Counter Flow Elutriation
CLL	Chronic Lymphocytic Leukaemia
CML	Chronic Myelogenous Leukaemia
CR	Complete Response
CTLA-4	Cytotoxic T lymphocyte Associated Protein 4
DC	Dendritic Cells
DLBCL	Diffuse Large B cell Lymphoma
dnAKT	Dominant Negative Akt
E:T	Effector to Target Ratio
eGFP	Enhanced Green Fluorescent Protein
EGFR	Epidermal Growth Factor Receptor
EMA	European Medicines Agency
FAO	Fatty Acid Oxidation
FASL	FAS Ligand
FDA	Food and Drug Agency
FDR	False Discovery Rate
FOXO	Forkhead Box Protein O
GM-CSF	Granulocyte Macrophage Colony Stimulating Factor
GMP	Good Manufacturing Practice
GSK3β	Glycogen Synthase Kinase 3 β
GVHD	Graft versus Host Disease
GVL	Graft versus Leukaemia
GZM	Granzyme
HER2	Upregulated Human Epidermal Growth Factor Receptor 2
ICOS	Inducible T-cell Co-stimulator
IDO	Indole 2,3-Dioxygenase
IL	Interleukin
IFN-γ	Interferon Gamma
IVC	Individually Ventilated Cages

Lck	Lymphocyte Specific Protein Tyrosine Kinase
LCMV	Lymphocytic Choriomeningitis Virus
mAb	Monoclonal Antibody
MAPK	Mitogen Activated Protein Kinase
MDSC	Myeloid Derived Suppressor Cells
MFI	Mean Fluorescence Intensity
MHC	Major Histocompatibility Complex
MiHA	Minor Histocompatibility
MM	Multiple Myeloma
MPEC	Memory Precursor Cells
MRD	Minimal Residual Disease
mTORC	Mammalian Target of Rapamycin Complex
NCI	National Cancer Institute
NK	Natural Killer Cells
NR	Non-Responders
NT	Non Transduced
PARP	Proliferator Activated Receptor
PBMC	Peripheral Blood Mononuclear Cell
PD	Progressive Disease
PD-1	Programmed Cell Death Protein 1
PDK1	3 Phosphoinositide Dependent Protein Kinase 1
PD-L1	Programmed Cell Death Ligand 1
PFS	Progression Free Survival
PH	Pleckstrin Homology Domain
PI3K	Pharmacological Phosphoinositide 3 kinase
PKB (Akt)	Protein Kinase B
PR	Partial Response
PSI	Polyfunctionality Strength Index
PTEN	Phosphatase and Tensin Homolog
r/r	Relapsed/Refractory
RAG	Recombinase Activating Gene
RBC	Red Blood Cell
RT	Room Temperature
RTK	Receptor Tyrosine Kinase
scFv	Single Chain Fragment Variable
SD	Stable Disease
Ser	Serine
SLEC	Short Lived Effector cells
T-cell	T lymphocyte
Tcm	Central Memory T-cell
TCR	T-cell Receptor
Te	Effector T-cell
Tfh	Follicular Helper T-cell

TGF	Transforming Growth Factor
Th	Helper T-cell
Thr	Threonine
TIL	Tumour Infiltrating Lymphocyte
Tn	Naïve T-cell
TNF	Tumour Necrosis Factor
TREG	Regulatory Tcell
TRUCK	T-cells Redirected for Universal Cytokine Mediated Killing
Tscm	Stem-cell Memory T-cell
Tte	Terminal T-cell
UT	Untreated
VEGF	Vascular Endothelial Growth Factor
VIII	Akt Inhibitor VIII
$\Delta\Psi_m$	Mitochondrial Membrane Potential

Chapter 1. Introduction

1.1. Introduction

1.1.1. Cancer and the immune system

Today, cancer is considered a genetic disease and remains a leading cause of mortality. Acquired gene abnormalities can contribute to several cancer hallmarks influencing uninhibited cancer cell expansion, invasion, and metastasis. Cancer dependent primary treatment consists of surgical resection, chemotherapy, and radiotherapy. Identification of genetic mutations and aberrant proteins has led to the development of many targeted therapies. Some include protein kinase inhibitors against upregulated/mutated epidermal growth factor receptor (EGFR) (Erlotinib/Osimertinib) (Leighl et al., 2020) or chromosomal fusion Bcr-Abl (Imatinib) (Iqbal and Iqbal, 2014). Other therapies utilise monoclonal antibodies to limit vascular endothelial growth factor (VEGF) regulated angiogenesis (Bevacizumab) (Braghiroli et al., 2012) or cell proliferation from upregulated human epidermal growth factor receptor 2 (HER2) (Trastuzumab) (Maximiano et al., 2016). Despite the development of many targeted therapies, cancers often develop resistance to such drugs (Hanahan and Weinberg, 2011).

More recently, growing evidence implicates the importance of the immune system in both driving and controlling cancer. The immune system consists of two parts, innate and adaptive immunity. Natural killer cells (NK), basophils, eosinophils, neutrophils, mast cells, dendritic cells (DCs) and macrophages contribute to innate immunity as a rapid first line defence against invading bacterial, viral, and parasitic pathogens. Adaptive immunity can take several days to develop but can generate long-term immunological memory. It involves B lymphocytes (B-cells) and T lymphocytes (T-cells) which confers antigen dependent responses to pathogens (Murphy and Weaver, 2016).

T-cells are further classified as CD8 cytotoxic T-cells, which recognise major histocompatibility complex (MHC) class I (MHC-I) molecules or CD4 T-helper T-cells, which recognise MHC class II (MHC-II). CD8 T-cells can directly kill infected cells presenting foreign antigens on MHC-I however, CD4 T-cells recognise MHC-II

predominately expressed by antigen expressing cells, including DCs, macrophages and B-cells (Murphy and Weaver, 2016). CD4 T-cells can develop into a variety of effector T-helper (Th) subsets such as Th1, Th2, Th9, Th17, Th22, Tfh (follicular helper T-cell) and TREG. These subsets can be identified by specific extracellular markers, transcription factors and cytokine profiles, as illustrated in Figure 1. Naturally, subsets can be evoked by different classes of pathogens. Based on their cytokine profiles, subsets can recruit a range of innate immune cells such as macrophages (Th1), eosinophils/basophils/mast cells (Th2) and neutrophils (Th17). Tfh and TREGs have more unique roles; B-cells can bind and process soluble molecules through the B-cell receptor (BCR). Protein components are internalised and processed into peptide fragments which can be displayed on the surface by MHC-II. Tfh can activate B-cells by recognising peptide/MHC-II presented to give rise to plasma cells which can produce neutralising, opsonising, NK/mast cell sensitising and complement activating antibodies. TREGs however have a regulatory function and can suppress T-cell and innate immune cell activity. Overall providing a regulated defence against pathogens (Murphy et al., 2017).



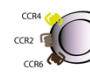
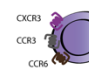



	Th1	Th2	Th17	Th9	Th22	iTreg	Tfh
							
Major cytokines driving differentiation	IL-12	IL-4	TGF β IL-6	TGF β IL-4	IL-6 TNF α	TGF β IL-2	IL-21
Master transcriptional regulator	T-Bet	GATA-3	ROR γ t	PU.1	AhR	FoxP3	Bcl-6
Major cytokines produced	IFN γ	IL-4	IL-17	IL-9	IL-22	IL-10 TGF β	IL-21
Chemokine receptors	CXCR3	CCR3, CCR4 CCR8	CCR2, CCR6, CCR4	CCR3, CCR6, CXCR3	CCR4, CCR10	CCR6	CXCR5

Figure 1. Summary of CD4 T-helper subsets

Summary of the different T-helper (Th) subsets naïve (Tn) CD4 T-cells can differentiate into. The figure highlights the polarising cytokines, transcriptional regulators, main cytokines produced and expression of surface chemokine receptors specific to each subset, adapted from (Kara et al., 2014).

Tumours can consist of a range of aberrant or mutated proteins that can elicit an immune response, a process termed as immunosurveillance. Studies in mice lacking the recombinase activating gene (RAG)-2 who fail to rearrange antigen receptors to produce T-cells and B-cells, mice depleted for NK cells and IFN- γ , a cytokine critical to support NK/T-cell cytotoxicity were more susceptible to chemically induced tumours (Dunn et al., 2004, Shankaran et al., 2001, Smyth et al., 2001). Clinical evidence supports that breast, lung, prostate, and colon cancers with tumour infiltrating lymphocytes (TILs), NK cells and macrophages positively correlated with survival (Corthay, 2014, Galon et al., 2006, Kawai et al., 2008, Mahmoud et al., 2011).

However, cancers can develop several mechanisms to evade immune attack registering evading immune destruction, an emerging hallmark of cancer (Hanahan and Weinberg, 2011). Some evasion mechanisms include the downregulation of MHC-1 to evade T-cell recognition (Anderson et al., 2021, Dhatchinamoorthy et al., 2021, Garrido et al., 1997). Infiltration of suppressive TREGs, M2 macrophages, myeloid derived suppressor cells (MDSCs) and increased production of immunosuppressive IL-10 and TGF- β cytokines (Vinay et al., 2015). TREG infiltration (Curiel et al., 2004, Stenström et al., 2021) and elevated serum TGF- β and IL-10 (Lippitz, 2013) have been associated with poor prognosis. Production of immunosuppressive enzyme indole 2,3-dioxygenase (IDO) produced by myeloid cells induces kynurenine, a metabolite of tryptophan that can suppress effector T-cell function and promote the generation of TREGs and MDSCs (Kim and Cho, 2022). T lymphocyte associated protein-4 (CTLA-4) expression by infiltrating TREGs can further influence tumour suppression. CTLA-4 can competitively bind CD80/CD86 ligands of co-stimulatory CD28 to limit T-cell activation (Sansom, 2000). Additionally, tumours can express programmed death-ligand 1 (PD-L1), which can dampen the activation of T-cells expressing programmed cell death protein-1 (PD-1) (He et al., 2015, Spranger et al., 2013).

Given the key role of the immune system in cancer, harnessing components of the immune response has led to the development of several therapies. One such approach is the production of therapeutic antibodies which can block tumour associated signalling pathways such as EGFR and VEGF, as discussed above. Antibodies can mediate

complement dependent cytotoxicity (CDC) and antibody dependent cellular cytotoxicity (ADCC), such as, CD20 targeting (Rituximab) against Non-Hodgkin lymphoma (NHL) (Weiner, 2010). Others include antibody and cytotoxic drug conjugates targeting human epidermal growth factor receptor-2 (HER2) such as (Trastuzumab-Emtansine) for breast cancer (Dhillon, 2014). Antibodies have further been developed to block negative immune regulators such as, (Ipilimumab (CTLA-4) and Nivolumab (PD-1) (Kooshkaki et al., 2020).

This ability of T-cells to recognise target antigens in a highly specific way has also been exploited by cancer researchers who have long investigated the utility of T-cells as adoptive cell therapies (ACT) for cancer. Pioneered in the early 1970s, bone marrow transplantation (BMT) for blood cancers demonstrated that allogeneic (donor) T-cells could recognise (patient) leukaemia cells as ‘foreign’ and deliver a graft versus leukaemia (GVL) effect. The major risk to these patients is graft versus host disease (GVHD), where the same allogeneic T-cells recognise and attack the patient’s normal tissues, often leading to fatal outcomes (Weiden et al., 1979, Sadelain et al., 2017).

BMT research paved the way for more sophisticated approaches to ACT without the attendant risks of GVHD. Autologous T-cells harvested directly from patient tumours (TILs), enriched for tumour-reactive clones, were first explored in clinical studies in the 1990s. TILs isolated from resected melanomas have been convincingly shown to mediate autologous tumour lysis (Rosenberg et al., 1994). However, TIL therapy is limited by the immune tolerance mechanisms, as discussed above, and T-cells can fail to initiate responses against tumour, as associated antigens are ‘self’ and not ‘foreign’. To overcome this, engineering approaches to introduce cancer antigen specific transgenic TCRs or chimeric antigen receptors (CARs) for specificity to tumour antigens have been extensively investigated (June and Sadelain, 2018).

1.1.2. Chimeric Antigen Receptors (CARs)

CARs are synthetic receptors designed to redirect T-cell effector functions by targeting cancer cell surface antigens in an MHC independent manner. CAR structure is illustrated in Figure 2 and comprises (Ghorashian et al., 2015):

- (1) An extracellular single chain variable fragment (scFv) antigen-binding domain consisting of heavy and light chains derived from a monoclonal antibody (mAb).
- (2) An extracellular spacer region, often derived from IgG, CD8 α or CD28, to project the binding domain off the cell membrane for optimal scFv orientation flexibility.
- (3) A transmembrane domain that anchors the CAR to the cell membrane, derived from CD8 α or CD28.
- (4) An intracellular signalling domain derived from the TCR ζ chain (CD3 ζ), 'first generation CARs'. More commonly, CD3 ζ is fused to T-cell co-stimulatory domains including, 4-1BB, CD28, OX40 and inducible T-cell co-stimulator (ICOS) to create 'second generation CARs'. Such second-generation CARs emulate endogenous primary T-cell receptor (TCR) stimulation and secondary co-stimulation required for complete T-cell activation.

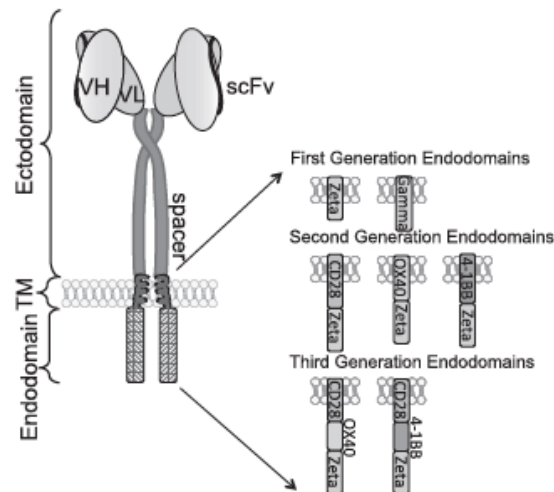


Figure 2. CAR Structure

The ectodomain is comprised of the antigen targeting scFv and spacer region. The spacer region links the transmembrane domain (TM) to the endodomain. The endodomain contains TCR derived CD3 ζ , where more efficacious second and third generation endodomains include one or

more T-cell derived co-stimulatory domains such as 4-1BB, CD28, OX40 and ICOS (Ghorashian et al., 2015).

The manufacture of CAR T-cells is a multi-step process. Peripheral blood mononuclear cells (PBMCs) are harvested from patients (autologous) or donors (matched or third party/universal) by leukapheresis, and the CAR transgene is most commonly introduced into T-cells via retroviral or lentiviral vectors (Ghorashian et al., 2015). Other platforms such as adeno-associated virus (AAV), CRISPR gene editing (Eyquem et al., 2017) and transposon-based non-viral integration methods have shown feasibility (Manuri et al., 2010). Following manufacture, the CAR product is then infused into the patient, and clinical studies have shown that these cells can engraft, traffic to and eradicate the tumour in an antigen-dependent manner (Schuster et al., 2017, Neelapu et al., 2017, Maude et al., 2018).

1.1.3. CD19 CARs

Numerous clinical studies have evaluated CAR therapy against a range of cancers, each varying in details of CAR design and T-cell integration methods used. To date, the greatest success described with CAR therapy is against CD19, an antigen with confined expression to cells of B-cell lineage, which is highly expressed in B-cell derived leukaemia and lymphomas. Off-tumour effects of CD19 targeting CAR T-cell therapy include complete B-cell aplasia and the attendant risks of infection, which can be readily managed with immunoglobulin replacement therapy (June and Sadelain, 2018).

Clinical studies of CD19 CARs have shown unprecedented responses in paediatric and adult patients with relapsed/refractory (r/r) B-cell acute lymphoblastic leukaemia (B-ALL) and Non-Hodgkin's lymphoma (B-NHL). These results have led to the release of three food and drug agency (FDA) approved therapies targeting CD19, Kymriah™ (tisagenlecleucel) for young adults r/r B-ALL and adult B-NHL (Hcp.novartis.com, 2019), Yescarta™ (axicabtagene ciloleucel) for adult r/r B-NHL (Yescarta.com, 2019) and Tecartus™ (brexucabtagene autoleucel) (TECARTUS®, 2022) for adult r/r mantle cell lymphoma and r/r B-ALL. While all therapies use second generation CAR structures with

the same CD19 binding scFv (FMC63) and CD3 ζ signalling domain, their transmembrane and co-stimulatory domains differ. With KymriahTM, gene transfer is mediated by lentiviral vector and the transgene codes for a CD8 transmembrane and 4-1BB co-stimulatory endodomain. In contrast, YescartaTM and TecartusTM gene transfer is mediated via retroviral vector, and the transgene encodes a CD28 transmembrane and co-stimulatory endodomain (Guedan et al., 2019, TECARTUS®, 2022).

Early results in the phase II ELIANA (KymriahTM) against r/r paediatric/young adult and ZUMA-3 (TecartusTM) r/r adult B-ALL trials demonstrated high complete responses (CRs), where 98%/97% responders were minimal residual disease negative (MRD-). Although promising, only 50% (Maude et al., 2018) and 52% (Shah et al., 2021) of responders remained relapse free at 12 months. Furthermore, clinical studies have shown that the likelihood of durable remission from CD19 CAR therapy for, B-NHL and other blood cancers, including chronic lymphocytic leukaemia (CLL) is lower still. The phase 2 trials JULIET (KymriahTM) and ZUMA-1 (YescartaTM) demonstrated ongoing complete responses (CR) in 40% of patients at 15.4 and 14 months, respectively (Neelapu et al., 2017, Schuster et al., 2019). There is more limited clinical data on CLL using CAR therapy. Of 134 reported cases, only a minority of patients (20-30%) achieved CR, with progression free survival (PFS) limited to 25% at 18 months (Lemal and Tournilhac, 2019). To date, KymriahTM and YescartaTM remain the only products approved by the European Medicines Agency (EMA).

1.1.4. Failure of CD19 CAR T-cell therapy

CD19 CAR T-cell therapy provides renewed hope for a previously untreatable subset of patients, yet it is not a cure for all. With 30-60% relapse rates, clinical studies have exposed several factors that can account for the failure of CAR T-cell therapy (Xu et al., 2019) as summarised, Table 1. The potential impact of CAR design, leukapheresis quality, intrinsic patient T-cell fitness and manufacturing challenges contributing to the failure of CAR T-cell therapy is discussed in more detail below.

Factors	Causes	Potential Solutions	References
Poor quality T-cells from patients	<ul style="list-style-type: none"> - Extensive chemotherapy - Age - Cancer mediated immunosubversion 	<ul style="list-style-type: none"> - Harvest T-cells at earlier disease time point - Allogeneic manufactures - Tscm/Tcm enrichment pre-manufacture - Use of cell signalling regulators <i>in-vivo</i> or <i>ex-vivo</i> to enhance Tscm/Tcm subsets and T-cell quality 	<p>(Singh et al., 2016) (Rajat K. Das, 2018) (Tu and Rao, 2016) (Riches et al., 2013) (Gattinoni et al., 2005) (Sommermeyer et al., 2016)</p>
Manufacturing Failures	<ul style="list-style-type: none"> - Poor quality patient manufacturing materials - Manufacturing variations/non-optimised manufacturing protocols - Length of manufacture 	<ul style="list-style-type: none"> - Allogeneic manufactures (Universal CAR T-cells) - Use of standardised, automated manufactures - Optimised manufactures to support the production of less differentiated cells via shorter manufactures, cytokine cocktails and <i>ex-vivo</i> use of cell signalling regulators 	<p>(Grupp SA, 2018) (Shah and Fry, 2019) (Schuster et al., 2017) (Roddie et al., 2019) (Vormittag et al., 2018) (Markley and Sadelain, 2010) (Mock et al., 2016) (Qasim, 2019)</p>

Tumour Microenvironment	<ul style="list-style-type: none"> - Complex network of tumour associated fibroblasts and blood vessels within the extracellular matrix (ECM) - Presence of immunosuppressive cells such as regulatory T-cells (Tregs), macrophages, myeloid-derived suppressor cells (MDSCs) - Immunosuppressive cytokines (TGFβ) - Immune checkpoint (PD1, PD-L1, CTLA-4) 	<ul style="list-style-type: none"> - Use of ‘Armoured’ CAR T-cells with chemokine receptors and ability to secrete pro T-cell cytokines in the microenvironment - Optimise CAR design with dominant negative TGFβ - Use of gene-editing for the knockdown of negative T-cell regulators such as PD1 - Combinatory CAR T-cell treatment with checkpoint blockade 	<p>(Ma et al., 2019) (Kershaw et al., 2002) (Cheng et al., 2019) (Xia et al., 2017) (Chen et al., 2018) (Anderson et al., 2017) (Burga et al., 2015) (Kloss et al., 2018) (Kueberuwa et al., 2018a) (Buchbinder and Desai, 2016) (Rupp et al., 2017)</p>
Antigen Loss	<ul style="list-style-type: none"> - Diminished or loss of expression through CD19 gene mutations - Alternative splicing variations - Presence of antigen negative clones before therapy - Prior therapy with CD19 targeting agents - Lineage switches - Enhanced CAR T-cell persistence 	<ul style="list-style-type: none"> - Simultaneous or successive treatments targeting multiple antigens. CD20, CD22 and CD123 are additional targets in B-cell malignancies 	<p>(Neelapu, 2018) (Rosenthal et al., 2018) (Sotillo et al., 2015) (Gardner et al., 2016) (Zoghbi et al., 2017) (Dorantes-Acosta and Pelayo, 2012) (Mejstrikova et al., 2017) (Bhojwani et al., 2019) (Maude et al., 2018) (Ghorashian et al., 2019) (Fry, 2015) (Ruella and Maus, 2016) (Amrolia, 2019) (Yates, 2018)</p>

CAR Design	<ul style="list-style-type: none"> - Variations in scFv, spacer and signalling domains can each alter signalling events - CD28 endodomains linked with tonic signalling and basal T-cell activation leading to early exhaustion 	<ul style="list-style-type: none"> - Retrospective analysis to determine optimal CAR design - 41BB CARs demonstrate greater long-term persistence and memory formation 	<p>(Kochenderfer et al., 2015) (Maude et al., 2018) (Kawalekar et al., 2016) (Salter et al., 2018)</p>
Murine source scFv's	<ul style="list-style-type: none"> - FDA approved FMC63 is murine derived and increases the risk of eliciting an immune response against CAR T-cells, leading to toxicity and limited persistence. 	<ul style="list-style-type: none"> - Use of fully humanised CAR T-cells 	<p>(Cheng et al., 2019) (Turtle et al., 2016) (Maus et al., 2013) (Maude, 2016)</p>
Tumour Burden vs CAR T-cell dose	<ul style="list-style-type: none"> - High tumour burden negatively impacts CAR T-cell expansion and persistence. 	<ul style="list-style-type: none"> - Bridging therapies during CAR T-cell manufacture and lymphodepletion chemotherapy pre-CAR T-cell infusion can reduce tumour burden and enhance CAR T-cell efficacy 	<p>(Hay and Turtle, 2017) (Hucks and Rheingold, 2019) (Cheng et al., 2019)</p>

Table 1. Summary of factors contributing to the failure of CAR T-cell therapy

The common factors that can lead to the failure of CAR T-cell therapy. Key: Tscm= stem-cell memory T-cell, Tcm= central memory T-cell, PD-1= programmed cell death protein 1, PD-L1= programmed death ligand 1 and CTLA4= cytotoxic T-lymphocyte associated protein 4.

The majority of studies use CARs designed with either a 41BB ζ /CD28 ζ endodomain which can influence persistence and clinical outcomes. Pre-clinical and clinical studies have shown that both 41BB ζ /CD28 ζ second generation CARs can mount effective cytotoxic responses against CD19 malignancies but have different characteristics. CD28 ζ CARs have shown rapid CAR expansion on antigen stimulation but suffer from early exhaustion and gain a more differentiated effector transcription profile (Kochenderfer et al., 2015). 41BB ζ CARs have instead shown more gradual CAR expansion, greater long-term persistence, efficacy upon chronic antigen stimulation and a less differentiated memory phenotype (Maude et al., 2018) (Kawalekar et al., 2016). A study attributed these differences to the presence of basal lymphocyte specific protein tyrosine kinase (Lck) association with the CD28 ζ endodomain and other phosphorylation events at resting state. This tonic signalling was accompanied by more rapid and intense protein phosphorylation events post-CAR activation in CD28 ζ versus 41BB ζ CARs and provides a mechanistic explanation (Salter et al., 2018). However, the direct comparison of CAR design is challenging. Trials can vary considerably in study design, patient populations and manufacturing methods. CARs design can possess variable scFv, spacer, transmembrane and signalling domains, each with their capacity to alter signalling events. Yet, we must consider that despite evidence suggesting that 41BB ζ CARs may be superior to CD28 ζ CARs, both have demonstrated broadly comparable outcomes in trials against CD19 (Schuster et al., 2019, Locke et al., 2019). As such, determining the ideal CAR design is challenging and whether tumours can benefit from both strong early efficacy and long-term persistence in a mixed CD28 ζ and 41BB ζ CAR therapy remains to be determined.

Another important consideration is optimal and timely CAR T-cell manufacturing and factors contributing to manufacturing failures. FDA approved CAR T-cell therapies utilise autologous T-cells for product generation, and from patients enrolled have described manufacturing failure rates of 7.6 and 7.3% in the ELIANA and JULIET trials, respectively (Maude et al., 2018, Schuster et al., 2019). More so, the median time taken from enrolment to product infusion was 45/54 days, respectively. Long periods to infusion can leave patients vulnerable to disease progression and other complications of active malignancy. This was highlighted in the ELIANA trial, where a further 7.6% of patients enrolled died before receiving the CAR product (Maude et al., 2018).

Several factors can attribute to manufacturing failures, with variations in the quality of apheresis among patients being the most prominent. Absolute lymphocyte counts (ALCs) can vary significantly between patients, with the National Cancer Institute suggesting that CAR T-cell manufacturing is feasible with lymphocyte counts of ≥ 150 cells/ μl identified in a 56 patient population with a range of (145-2144) cells/ μl (Shah and Fry, 2019). However, a trial using tisagenlecleucel against diffuse large B cell lymphoma (DLBCL) reported five manufacturing failures out of 38 enrolled patients, all of whom had ALCs ≤ 300 cells/ μl (Schuster et al., 2017). Further characteristics beyond cell quantity can also affect the success of manufacture. High contamination of apheresis with platelets, plasma and residual anticoagulant can alter T-cell responses to activation agents. Additional contamination with granulocytes and monocytes can inhibit T-cell expansion and transduction during the manufacturing process (Roddie et al., 2019, Stroncek et al., 2016).

T-cell subset composition can vary significantly between patients, impacted by factors such as age, chemotherapy exposure and underlying cancer diagnosis. Immunosenescence is a well characterised phenomenon describing the impairment of immune responses associated with ageing. Memory T-cells begin to show signs of senescence at approximately 65 years, and objective phenotypic changes include, loss of CD28 and progressive accumulation of highly differentiated Tte cells (CD45RA+CD28-CCR7-CD62L-) (Tu and Rao, 2016).

It is thought that intensive chemotherapy regimens can negatively impact CAR T-cell manufacture. Regimens containing cyclophosphamide and cytarabine can adversely impact early lineage T-cell populations (Singh et al., 2016) and both clofarabine and doxorubicin can lead to poor quality CAR products and even failed manufacture (Rajat K. Das, 2018).

Underlying disease can impact T-cell fitness, and nowhere is this better described than in CLL, where impaired T-cell phenotype/function is often present at diagnosis (Lemal and Tournilhac, 2019). CD4+ T-cells in CLL patients have been found to have an exhausted phenotype with high expression of programmed death-1 (PD-1), a negative regulator of

immune function. CD8⁺ T-cells in CLL are characterised by low proliferative and cytotoxic functionality (Riches et al., 2013).

Repeated T-cell stimulation can also adversely impact function, leading to activation induced cell death (AICD), functional exhaustion and replicative senescence (Akbar and Henson, 2011). An unfortunate quandary of CAR T-cell manufacturing is the fact that physiologically, processes of T-cell expansion and differentiation are coupled. With greater expansion, larger number of cells enter terminal differentiation, and where CAR manufacturing methods prioritise expansion to meet the target doses (often over 7-22 days) (Vormittag et al., 2018), the resulting products are often relatively differentiated.

To address this issue, researchers in Seattle altered their manufacturing protocol to enrich the leukapheresis for early lineage CD62L⁺ T-cells using immunomagnetic bead separation prior to CAR T-cell manufacturing. Using this method they reported improved short-term CAR T-cell expansion in patients but comparable persistence of ≤ 28 days when compared to CARs manufactured by standard methods (Wang et al., 2016). A deeper analysis of this study highlights that a median of 24 days of expansion was required to achieve the proposed trial dose using this method. Given the paradox between expansion and differentiation, it is likely that the initially selected early lineage populations were driven through differentiation during manufacture, which could further explain the lack of persistence observed in this study.

An overview of CD19 targeting CAR T-cell studies with a 41BB ζ design reveals comparable relapse rates but highlights variability in CD19^{+/-} relapses, Table 2. This could be attributed to limited follow ups and lack of uniform reporting but could also be representative of product variability. Overall, the data highlights that CD19⁺ relapses can account for up to 77.8% of total relapse, suggesting the loss of CAR T-cells or impaired activity could also be influenced by leukapheresis characteristics or manufactures.

Publication	Target Antigen	Co-stimulatory Domain	Number of Patients Treated	Patients with Early CR (%)	Patients with Relapse (%)	CD19+ Relapse	CD19- Relapse	Treatment Group
(Maude et al., 2014)	CD19	4-1BB	30	27(90%)	7(26%)	Unknown	4(57.1%)	Paediatric/Adult
(Turtle et al., 2016)	CD19	4-1BB	30	27(93%)	9(33%)	7(77.8%)	2(22.2%)	Adult
(Gardner et al., 2017)	CD19	4-1BB	43	40(93%)	18(45%)	11(61.1%)	7(38.9%)	Paediatric/Young Adult
(Maude et al., 2018)	CD19	4-1BB	75	61(81%)	22(36%)	1(4.5%)	15(68.2%)	Paediatric/Young Adult
(Frey et al., 2020)	CD19	4-1BB	35	24(69%)	9(38%)	Unknown	Unknown	Adult
(Ghorashian et al., 2019)	CD19	4-1BB	14	12(86%)	6(50%)	1(16.7%)	5(83.3%)	Paediatric/Young Adult
(Roddie et al., 2021)	CD19	4-1BB	20	17(85%)	8(40%)	4(50%)	4(50%)	Adult

Table 2. Summary of clinical outcomes in B-ALL patients targeting CD19 antigen using CARs designed with a 41BB co-stimulatory domain

% Early CR is calculated against total number of patients treated. % Relapse is calculated against number of patients with early CR. % CD19+/- relapse is calculated against number of relapse patients.

There are many advances in CAR T-cell manufacture to enhance products such as additional washes, ficoll and counter flow elutriation (CFE) and direct enrichment of lymphocytes using immunomagnetic bead separation to remove contaminating platelets, plasma, residual anticoagulant, and monocytes (Roddie et al., 2019). However, emerging data further highlights that less differentiated stem-cell memory/central memory T-cell subsets (Tscm/Tcm) outperform more differentiated effector/terminal T-cell subsets (Te/Tte). Patients with a greater number of Tscm/Tcm subsets before manufacturing or enrichment of such subsets through manufacturing manipulations are likely to improve the chances of generating a successful product (Sommermeyer et al., 2016, Singh et al., 2016) As such, manufacturing methods have moved towards protocols to enrich Tscm/Tcm subsets.

1.1.5. Importance of Tcm/Tscm subsets in CAR T-cell therapy

Clinical data highlights the importance of CAR T-cell persistence for ongoing responses, particularly in the context of B-ALL. The ELIANA trial identified that patients achieving CR had detectable CAR at a median of 5.5 months, whereas in non-responders (NR) this was limited to 1.6 months (Maude et al., 2018). Furthermore, the average time to reach peak CAR concentration was two times longer in cohorts of NR (20 days) versus CR (10 days). A similar trend was demonstrated in the JULIET trial where CR/partial responders (PR) had detectable CAR for an average of 9.5 months compared with 1.9 months in patients with stable (SD), progressive (PD) or unknown disease status (Schuster et al., 2019).

CAR T-cell function can be significantly impacted by T-cell subset composition. CD4/8 T-cells naturally undergo progressive differentiation through naïve (Tn), stem-cell memory (Tscm), central memory (Tcm), effector (Te) states until they reach terminal differentiation (Tte), Figure 3. While Tem can rapidly give rise to effector T-cells that can mount cytotoxic responses against a target antigen, they fail to persist long term. On the other hand, Tscm and Tcm can provide both long term persistence and rapid proliferation in response to antigen, generating both Tem and Tcm subsets. Tscm/Tcm populations are closely characterised by their expression of C-C chemokine receptor 7 (CCR7), L-selectin (CD62L) and co-stimulatory molecules CD27 and CD28, but differ in their expression of CD45RA. Tscm subsets express CD45RA; however, Tcm subsets lose this expression and gain CD45RO (Golubovskaya and Wu, 2016).

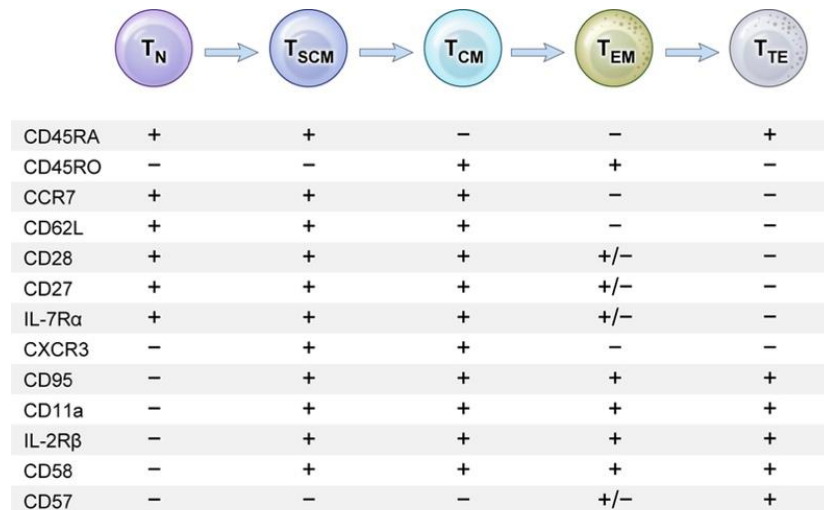


Figure 3. T-cell differentiation and associated markers

Progressive differentiation of T-cells from naïve (T_N), stem cell-like (T_{SCM}), central memory (T_{CM}), effector memory (T_{EM}) T-cells, to terminally differentiated effector T-cells (T_{TE}) and the common cell surface markers used to differentiate between subsets. As T-cells progress from T_N to T_{TE} , they lose stemness, proliferative potential, become increasingly antigen dependent, senescent and undergo a metabolic switch from lipid to glycolytic metabolism (Gattinoni et al., 2017).

Unsurprisingly, many pre-clinical and clinical studies of adoptive T-cell immunotherapy have demonstrated that CD8⁺ naïve Tscm/Tcm subsets outperform Tem/Tte subsets by providing greater proliferative capacity, enhanced metabolic T-cell fitness and longer-lasting/superior anti-tumour responses (Gattinoni et al., 2005, Graef et al., 2014, Hinrichs et al., 2011). Transcriptional profiling in a CD19 CAR T-cell study for CLL showed that patients who achieved CR had products enriched for memory related genes, whereas NR had an upregulation in genes involved in effector differentiation, exhaustion, apoptosis, and glycolysis. In this study, the presence of CD8⁺ CAR T-cells with a CD27⁺PD-1⁻ phenotype and expressing high levels of IL-6 positively predicted therapeutic response and tumour control (Fraiotta et al., 2018). A further clinical trial using a second generation CD19 CAR with a CD28 endodomain demonstrated that enrichment for CD62L⁺ Tcm in the CAR product positively correlated with engraftment and expansion of CAR T-cells in the peripheral blood (Xu et al., 2014b).

There is a substantial body of evidence that the transfer of Tscm/Tcm subsets for ACT correlates with improved tumour responses. As such, a range of small molecule compounds have been tested in cell manufacturing protocols for their ability to enrich such subsets. One example is the peroxisome proliferator-activated receptor (PPAR) agonist GW501516, an agent known to boost fatty acid oxidation (FAO). Tcm survival has been linked to a shift in metabolism from glycolysis (essential for Te function) to FAO. GW501516 increased FAO in CD8 T-cells, despite the high expression of the transcription factor T-bet, which is associated with Th1 fate decisions and is used by some as a marker of CD8 T-cell exhaustion, treated cells showed enhanced persistence and efficacy in an *in-vivo* adoptive cell therapy model (Saibil et al., 2019).

Another approach demonstrated by Luca Gattinoni and colleagues is the enhancement of Wnt signalling. The use of a glycogen-synthase-kinase-3 β (GSK3 β) inhibitor induced Wnt/ β -catenin signalling and arrested CD8 T-cell differentiation at the Tscm stage. Wnt signalling enabled the generation of Tscm subsets (CD44 low and CD62L high) with proliferative and anti-tumour capacities that exceeded responses seen from Tcm and Te/Tem subsets (Gattinoni et al., 2009). More recently, the use of pharmacological phosphoinositide-3-kinase (PI3K) and Akt inhibitors in CAR T-cell manufacture to promote the generation of Tcm subsets is gaining traction.

1.1.6. Akt and its role in T-cell signalling

Pharmacologic inhibition of the serine/threonine kinase Akt is a compelling prospect in the CAR manufacturing field. Akt (also known as protein kinase B (PKB)) has three known isoforms, Akt1, Akt2 and Akt3 (or PKB $\alpha/\beta/\gamma$). Each has a highly conserved structure comprising an N-terminal pleckstrin homology (PH) domain, a kinase domain, and a C-terminal regulatory tail, Figure 4A. Akt 1 is expressed in a wide range of tissues and has a role in cell growth and survival. Akt 2 expression is restricted to insulin dependent tissues such as muscle and adipocytes where it is involved in insulin mediated glucose homeostasis, whereas Akt3 expression is mostly confined to the brain and testes and plays a role in cell growth and survival (Hers et al., 2011).

Akt plays a primary role in the PI3K signalling pathway and can regulate many pathways related to metabolism, angiogenesis, proliferation, and survival. The PI3K family includes three classes, class I/II and III. Class I PI3Ks are further divided into class IA and IB heterodimeric enzymes with both regulatory and catalytic subunits. Class IA PI3Ks are activated by receptor tyrosine kinase (RTK), cytokine, co-stimulatory or antigen specific receptors, consisting of p85 α , p85 β , p55 γ regulatory and p110 α , p110 β and p110 δ catalytic subunits. Class IB PI3K are activated by G-protein-coupled receptors (GPCR) and have only one regulatory p101 and catalytic p110 γ subunit. Whilst less is known about the roles of Class II/III PI3Ks in lymphocytes, expression of the catalytic p110 δ and γ are restricted to leukocytes however, p110 α and β are expressed in all cell types (Vanhaesebroeck et al., 2012).

On activation, PI3K generates secondary lipid messengers to propagate signal. At the plasma membrane, class I PI3K convert phosphatidylinositol (4,5) bisphosphate PI(4,5)P₂ to phosphatidylinositol (3,4,5) trisphosphate (PI(3,4,5)P₃). Enzymes containing a PH domain can bind the lipid PI(3,4,5)P₃, including 3-phosphoinositide-dependent protein kinase 1 (PDK1) and Akt to propagate downstream signalling. Akt is usually held in an inactive state through phosphorylation at the T450 site on the C-terminus tail docking the PH domain to the kinase domain. The generation of PI(3,4,5)P₃ initiates recruitment of Akt and PDK1 to the cell membrane where they associate with the PI(3,4,5)P₃ lipid via their PH domains. Interaction with PI(3,4,5)P₃ induces a conformational change in Akt and permits PDK1 mediated phosphorylation of the threonine 308 (Thr308) site within the Akt kinase domain (Siess and Leonard, 2019). Phosphorylation at this site increases Akt activity by a 100-fold, but for maximum activity, concurrent phosphorylation at the serine 473 (Ser473) site located on the regulatory tail by mammalian target of rapamycin complex 2 (mTORC2) is required, Figure 4B/C (Hers et al., 2011). Akt can remain active as long as it is associated with PI(3,4,5)P₃. Conversion of PI(3,4,5)P₃ to PI(4,5)P₂ mediated by phosphate and tensin homolog (PTEN) leads to Akt dissociation and pathway downregulation (Siess and Leonard, 2019, Vanhaesebroeck et al., 2012).

Akt activation can modulate numerous downstream effectors to regulate cell proliferation, survival, and metabolism, as illustrated in Figure 4. Notable effects include activation of

mTORC1, the cytoplasmic sequestration of forkhead box protein O1 (FOXO1), a negative regulator of the PI3K/Akt pathway and the inhibitory phosphorylation of GSK3, all with the ability to mediate several pathways involved in cell proliferation, survival and metabolism (Hers et al., 2011), as illustrated in Figure 4C.

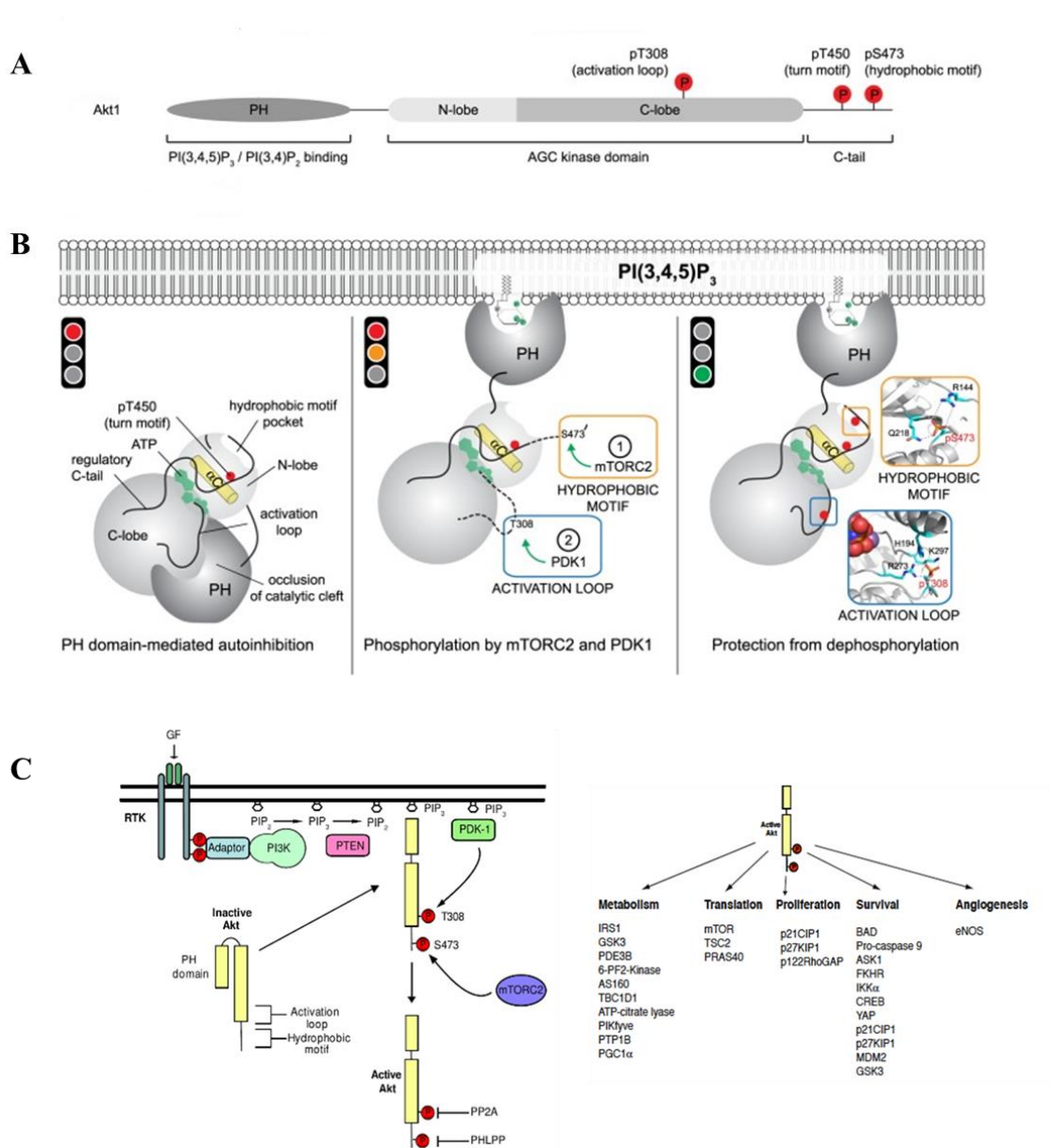


Figure 4. Akt structure and pathway

(A) Akt structure depicting the N-terminal pleckstrin homology (PH) domain, kinase domain, C-terminal regulatory tail, and associated phosphorylation sites. (B/C) Depict the activation of the PI3K pathway through RTK signalling, Akt recruitment and activation. Akt is held in an inactive state and activation of through RTK activates PI3K leads to the conversion of PI(4,5)P₂ to

PI(3,4,5)P₃. This reaction can be reversed by the PTEN lipid phosphatase. Association of Akt PH domain with the PI(3,4,5)P₃ lipid induces a conformational change in Akt, allowing membrane-associated PDK-1 to access and phosphorylate the Thr308 site in Akt. mTORC2 further phosphorylates the Ser473 site to fully activate Akt to regulate numerous downstream substrates. Regulation of such substrates can influence various cellular processes as depicted (Hers et al., 2011, Siess and Leonard, 2019).

Naïve CD4 T-cells (T_n) differentiate into T_{scm}, T_{cm}, T_e and T_{te} subsets. However, CD4 T-cells can acquire additional functional traits and are classified as Th1, Th2, T-helper Th17 and TREGs. The PI3K pathway has a critical function in T-cells where the p110 δ isoform of the PI3K catalytic subunit appears to be highly expressed in leukocytes. Studies have shown that maintaining a correct threshold of PI3K activity is critical to CD4 T-cell development. Mice with genetically silenced p110 δ (germline insertion of a kinase-dead p110 δ ^{D910A} allele) (Okkenhaug et al., 2002) have diminished Akt activity with an attendant reduction in CD4 effector and suppressive functionality, a reduction in Th1/2 cytokine secretion and the emergence of dysfunctional TREGs (Liu and Uzonna, 2010, Patton et al., 2006, Ali et al., 2014). Evidence suggests increased PI3K signalling skews CD4 T_n cells towards Th1/2/17 effector profiles and can negatively affect Tregs (Haxhinasto et al., 2008). This data suggests that PI3K signalling (and consequently Akt activation) must be tightly regulated to preserve normal CD4 T-cell differentiation and TREG function (Han et al., 2012).

Much like CD4 T-cells, PI3K/Akt signalling plays a crucial role in CD8 T-cell development and can drive several cellular processes to influence T-cell fate. In CD8 T-cells, Akt signalling is stimulated via the T-cell receptor (TCR), co-stimulatory receptors or via cytokines such as IL-2/7/15/21/12. Many studies have examined the impact of the strength and duration of Akt activation in CD8 T-cell differentiation and metabolism. The data indicates that while the absence of Akt signalling was not essential for CD8 proliferation, it was vital for the development of effector functions in activated CD8 T-cells (Kim and Suresh, 2013, Macintyre et al., 2011).

Strong Akt signalling can down-regulate the expression of CD62L and CCR7, indicating T-cell differentiation towards effector phenotype. Furthermore, terminal differentiation of CD8 T-cells caused by sustained IL-2 exposure is associated with increased Akt activation *in-vivo* (Kim et al., 2012). Additionally, constitutive mTORC1 activation, loss of FOXO and downregulation of the Wnt/ β -catenin pathway result in the terminal differentiation of CD8 T-cells (Kim and Suresh, 2013), Figure 5.

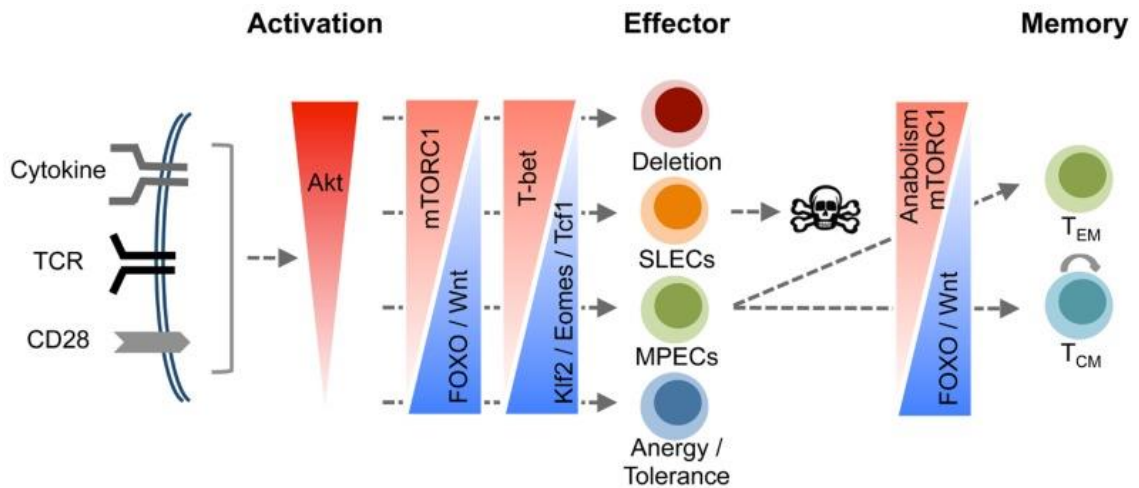


Figure 5. Role of Akt signalling in CD8 T-cell differentiation

This figure highlights the role of the Akt in CD8 T-cell differentiation. Akt signalling can be induced via cytokine, TCR and co-stimulatory molecules. Greater Akt activation and subsequent mTORC1 mediated signalling leads to T-cell deletion or the generation of short-lived effector cells (SLECs). However, lower Akt activation and increased Wnt/FOXO activation can give rise to memory precursor effector cells (MPECs). Here, if influenced by Akt activation can drive MPECs towards Tem cells and sustained low Akt activation form long-lived Tcm CD8 T-cells (Kim and Suresh, 2013).

Where Akt signalling is inhibited, CD62L and CCR7 expression is preserved and the CD8 transcriptome signature resembles that of a Tcm CD8 population (Macintyre et al., 2011). Akt signalling can also impact upon T-cell metabolism. Quiescent CD8 T-cells undergo FAO for cell maintenance. To allow for the rapid clonal expansion of Te CD8 T-cells in an antigen driven manner, metabolism must switch from FAO to glycolysis. This mechanism has been found to be driven by the transcription factor c-myc, regulated by Akt activation (Wang et al., 2011). CD8 T-cells with defective FAO induced by a

TRAF6 deficiency demonstrate Akt signalling hyperactivation and decreased CD8 memory formation. This defect in TRAF6 deficient CD8 T-cells can be countered by mTOR suppression via rapamycin, leading to improved memory formation (Pearce et al., 2009). Clearly, manipulation of Akt and its downstream targets appears to influence T-cell memory formation and its potential value to manufacture CAR T-cells for clinical application is of significant interest.

1.1.7. Effects of pharmacological Akt inhibition in T-cells

Several studies have evaluated the use of small-molecule drugs during the *ex-vivo* manufacture to enhance the function of adoptive cell therapies. These include, protein tyrosine kinase inhibitors, epigenetic/immuno and peptide-based modulators with an overlapping ability to limit T-cell differentiation. PI3K inhibitors, such as LY294002 (PI3K $\alpha/\beta/\delta$) (Zheng et al., 2018), Idelalisib (CAL-101) (PI3K δ) (Stock et al., 2019), Duvelisib (IPI-145) (PI3K δ/γ) (Funk et al., 2022) and Akt inhibitors, including MK2206 (Zhang et al., 2019), Ipatasertib (GDC-0088) (Mousset et al., 2018), Sirolimus (Rapamycin) (Nian et al., 2021) and VIII (Klebanoff et al., 2017, Urak et al., 2017, Van der Waart et al., 2014) remain popular for use in *ex-vivo* T-cell manufacture. Such protein tyrosine kinase inhibitors each in their own capacity have demonstrated preservation of less differentiated T-cell subsets and enhanced anti-tumour activity (Zhang et al., 2023).

Ex-vivo use of PI3K inhibitors such as Idelalisib (Petersen et al., 2018, Bowers et al., 2017), LY294002 (Zheng et al., 2018) and Duvelisib (Funk et al., 2022) have demonstrated reduced terminal differentiation and improved *in-vivo* efficacy using an anti-CD5 CAR with a CD28 ζ endodomain, an anti-CD33 CAR with a 41BB ζ endodomain and an anti-CD19 CAR with a CD28 ζ endodomain, respectively. The incorporation of PI3K inhibition in a clinical study of CAR T-cells is underway for multiple myeloma, CRB-402 (NTC03274219). CAR T-cells are manufactured in the presence of PI3K inhibitor BB007 to enrich for Tcm subsets. Early results are promising with 83% clinical responses, long term persistence and manageable cytokine related toxicities consistent to those seen with conventional CAR therapy (Berdeja et al., 2019).

The use of pharmacological Akt inhibitors have been tested both *in-vivo* and *in-vitro*. Early studies in mice of rapamycin to target mTOR (a downstream regulator of Akt) during both T-cell expansion and contraction greatly enhanced CD8 Tcm formation (Araki et al., 2009). Furthermore, sustained use of a pan Akt inhibitor (A-443654) following lymphocytic choriomeningitis virus (LCMV) infection in mice led to a significant increase in CD8 Tem populations suggesting that this population was rescued from terminal differentiation and apoptosis (Kim et al., 2012). This data prompted researchers to explore Akt inhibition in the T-cell manufacturing setting to enrich Tscm/Tcm subsets for adoptive T-cell therapy.

One such Akt inhibitor termed Akt inhibitor VIII (VIII) has been investigated for these properties. VIII was developed by researchers at Merck, and is compound 16g in their papers (Zhao et al., 2005, Lindsley et al., 2005). The compound is now off-patent offering flexibility for research use. Dr Harry Dolstra's group were the first to describe the advantages of *ex-vivo* T-cell culture in the presence of Akt inhibitor VIII (Van der Waart et al., 2014). In a minor histocompatibility (MiHA) assay of antigen-specific CD8 T-cells, the CD8 T-cells were stimulated with peptide-loaded dendritic cells (DCs) with or without VIII. There was an observed phenotypic shift towards early Tcm phenotypes (high CCR7, CD62L, CD27, CD28, CD45RO and CD95) in VIII-treated CD8 T-cells. VIII-treated cells additionally demonstrated superior expansion *in-vitro* and improved anti-tumour function in a multiple myeloma (MM) mouse model (Van der Waart et al., 2014). A similar study showed that *ex-vivo* propagation of TILs for 30 days with VIII promoted the expansion of TILs with a Tcm transcriptional, metabolic, and functional profile, that demonstrated enhanced anti-tumour functionality in a murine model of melanoma (Crompton et al., 2015).

In the CAR T-cell space, 2 groups have begun to evaluate the impact of VIII at a 1 μ M concentration during the *ex-vivo* transduction process of second generation (CD28 ζ) CD19 CARs. Both groups used different CD19 binding scFvs, different transduction/activation methods and different timelines. Klebanoff et al., used retroviral integration, soluble CD3 antibody activation and a 10 day *in-vitro* expansion (Klebanoff

et al., 2017) whereas, Urak et al. tested lentiviral integration and CD3/CD28 bead activation over a 17-21 day *ex-vivo* expansion (Urak et al., 2017).

Both studies conclude that VIII inhibition did not compromise CAR T-cell expansion, but increased Tcm phenotypes and improved anti-tumour activity in CD19+ tumour bearing mice. Furthermore, Klebanoff et al., mechanistically showed that Akt inhibition preserved mitogen-activated protein kinase (MAPK) activation and nuclear localisation of FOXO1, a transcriptional regulator of T-cell memory. Expression of an Akt resistant FOXO1 mutant mirrored the phenotypic T-cell changes observed with pharmacological suppression (Klebanoff et al., 2017). Interestingly, a study assessing a variety of pharmacological Akt inhibitors demonstrated that each had a variable impact on the ability to generate Tscm/Tcm subsets with VIII and GDC-0068 outperforming the other agents (Mousset et al., 2018).

1.2. Study rationale and aims

As a part of the UCL CAR T-cell programme, a novel CD19 targeting scFv referred to as ‘CAT’ was developed. The CD19 antigen-binding domain is derived from the murine CAT13.1E10 hybridoma, formatted as an scFv by linking the VH to the VL via a serine-glycine linker. The scFv was codon-optimised for transcript stability, fused to the stalk and transmembrane domains of human CD8 and to a human 41BB ζ endodomain to create a second generation CAR. This was subsequently cloned into a pCCL.PGK lentiviral transfer vector.

What distinguishes this CAR from other CD19 CARs in clinical trials or that have been FDA approved (all of which are based upon the FMC63 CD19-binding scFv), is the binding kinetic. CAT showed faster dissociation at $3.1 \times 10^{-3} \text{ s}^{-1}$ (9.8 seconds) vs $6.8 \times 10^{-5} \text{ s}^{-1}$ (21 minutes) for FMC63 despite binding the same or overlapping epitopes on CD19. Benefits of such a lower affinity CAR was seen through enhanced proliferation and anti-tumour activity in pre-clinical assessments against FMC63. The CAT scFv is the subject of two UCL based clinical trials for paediatric and adult B-ALL: CARPALL (NCT02443831) and ALLCAR19 (NCT02935257). The completed phase I CARPALL

study validated pre-clinical assessments with increased CAR T-cell expansion and persistence in comparison to published studies of KymriahTM/ FMC63 in a similar patient group (Ghorashian et al., 2019) and durable responses in adults patients from the phase I ALLCAR19 trial (Roddie et al., 2021). Cytokine release syndrome (CRS) and neurotoxicity are severe and detrimental side effects of CAR T-cell therapy. The most notable benefit of the low affinity CAT CAR in both paediatric and adult trials was its favourable safety profile with no severe incidences of CRS (Ghorashian et al., 2019, Roddie et al., 2021).

Given the clear benefit of Akt inhibition on the preservation of T-cell memory phenotypes and potentially on functionality, we initially planned to evaluate a gene-engineered, dominant-negative Akt1 molecule (dnAkt). The dnAkt is a non-functional counterpart of endogenous Akt to be expressed in tandem with the CAT CAR to overcome the requirement of *ex-vivo* pharmacological inhibition and to assess the impact of sustained Akt inhibition.

Early assessments highlighted the limitation of a gene engineered approach, discussed in chapter 3. Comparative evaluations against *ex-vivo* treatment using pharmacological Akt inhibitor VIII (VIII) showed promise, and the study was revised to assess its impact on the CAT CAR with a 41BB ζ endodomain, not previously assessed. The aims of the project include:

- To characterise the phenotypic, transcriptomic, and metabolic effects of *ex-vivo* VIII inhibition in healthy and B-ALL patient derived CD4/CD8 CAR T-cells, manufactured as per the UCL trial defined Miltenyi CliniMACS Prodigy[®] protocol.
- Assess how VIII treatment affects product polyfunctionality and test the impact on CAR T-cell function *in-vitro* using a CAR T-cell ‘stress’ model designed to replicate chronic antigen and subsequently *in-vivo*.

- Compare trial products delivered to patients on the ALLCAR19 trial with and without durable response and evaluate whether VIII treatment can rescue patients/products at risk of CD19+ relapse.
- Finally, we aim to review the integration of VIII treatment into the clinical scale Miltenyi CliniMACS Prodigy® process, comparing trial products with matched scale-ups incorporating VIII inhibition.

Chapter 2. Materials & Methods

2.1. Molecular Cloning

2.1.1. Construction of retroviral plasmids co-expressing dnAkt with CAT CAR

Existing CAR constructs were provided by Martin Pule's laboratory. The CAT CAR scFv was available in a pCCL lentiviral construct however, to allow for higher titres and improved native expression of the dnAkt, the CAT scFv was moved into a SFG retroviral construct with RQR8, a CD8a stalk and a 41BB/CD3 ζ endodomain. RQR8 is a marker/suicide gene separated by a 2A peptide to permit 1:1 suicide gene to CAR expression (Philip et al., 2014). This design allowed for a simplified downstream construction process by enabling the replacement of RQR8 with the dnAkt through simple cloning, Figure 6.

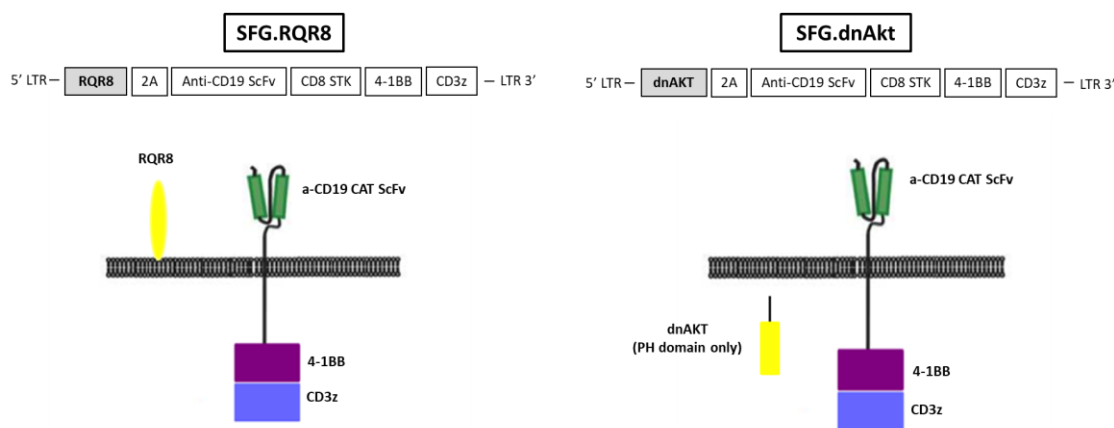


Figure 6. Molecular cloning design of dnAkt CAT CAR construct

This figure depicts the design of the dnAkt CAT CAR construct, where the RQR8 is replaced with the dnAkt expressing only the PH domain to ensure no kinase activity.

2.1.2. Moving CAT scFv into SFGmR.RQR8 scaffold

5 μ g of plasmids containing the CAT scFV and SFGmR.RQR8 scaffolds were digested using NcoI/BamHI (NEB) restriction enzymes. Digests were incubated in a thermocycler (DNA Engine Dyad[®]) at 37°C for 1 hour and run on 1.2% agarose gel (Biolone)

supplemented with SYBR[®] safe dye (ThermoFisher Scientific). Desired bands were cut out and DNA was extracted using the QIAquick[®] PCR & Gel Cleanup Kit (Qiagen). The SFG.RQR8 scaffold and CAT scFV were ligated at a 1:3 ratio using the Quick Ligase Kit (NEB) in a 20µl reaction. The ligation was subsequently transformed in NEB5α high-efficiency C2987H Escherichia Coli (E.coli) cells. Briefly, 2µl of ligation mix was added to 25µl of bacterial cells. The mixture was incubated for 30 minutes on ice, heat shocked at 42°C for 35 seconds and transferred into 250µl of SOC media. The mixture was incubated in a bacterial shaker at 200 RPM at 37°C for 40 mins prior to spreading onto LB agar plates supplemented with 100µg/ml Carbenicillin, plates were incubated at 37°C for 16 hours. Resulting colonies were grown in 3ml LB miniprep cultures supplemented with 100µg/ml Carbenicillin. DNA was extracted using the QIAprep[®] Spin Miniprep Kit (Qiagen) and screened using restriction enzymes to confirm ligation. Correct colonies were further validated by sanger sequencing. One correct colony was grown up to midipreps in 100mls TB supplemented with 100µg/ml Carbenicillin. Cultures were incubated in the shaker for 16 hours and plasmid DNA was extracted using the Macherey-Nagel Nucleobond[®] Xtra Midi kit. Eluted DNA was reconstituted in nuclease free water and quantified using the NanoDrop[™] spectrophotometer.

2.1.3. Replacing RQR8 with dnAkt

The dnAkt was constructed from the amino-terminal fragment of Akt1, a chain break before the kinase domain permits construction for the sole expression of the PH domain.

The amino-terminal amino acid sequence used for dnAkt construction from uniport P31749:

MSDVAIVKEGWLHKRGEYIKTWRPRYFLLKNDGTFIGYKERPQDVDQREAPLN
NFSVAQCQLMKTERPRPNTFIIRCLQWTTVIERTFHVETPEEREEWTTAIQTVAD
GLKKQEEEEEMDFRSGSP

The reverse translated dnAkt1 sequence:

ATGGGATCAGATGTCGCTATTGTTAAAGAGGGCTGGCTGCACAAAAGGGGG
GAGTATATAAAGACTTGGAGACCACGATATTTCTGCTCAAGAACGACGGA

ACGTTTATTGGATACAAGGAACGCCACAGGATGTCGATCAGCGCGAAGCA
 CCTCTCAATAACTTCTCCGTTGCCCAATGCCAGTTGATGAAGACCGAGCGCC
 CTCGACCAAACACCTTCATAATTCGATGCCTCCAGTGGACTACTGTGATTGA
 ACGCACGTTCCATGTCGAAACACCTGAGGAAAGAGAGGAATGGACCACTGC
 GATACAGACTGTGGCCGATGGGCTCAAGAAGCAAGAGGAAGAAGAGATGG
 ATTCAGGTCTGGGTCTCCA

An amino-terminal G was added after the initiating methionine to improve the kozak sequence.

To aid construction, DNA fragments spanning part of the SFG and 2A peptide regions were added to dnAkt design sequence upstream and downstream, respectively. The complete DNA fragment was synthesised as a double stranded DNA fragment (g-block) by integrated DNA technologies (IDT).

Primers were designed to allow for the amplification of the dnAkt g-block fragment. A 50µl PCR reaction was set up by mixing the DNA fragment with Phusion® High-Fidelity DNA Polymerase Buffer (NEB), Phusion® High-Fidelity DNA Polymerase (NEB), dNTPs and both forward and reverse primers. The mixture was placed in a thermocycler at 98°C for 2mins, 98°C for 40 seconds, 65°C for 40 seconds, 72°C for 1 minute. This programme was looped from 98°C for 40 seconds 35 times with a final step at 72°C for 10 minutes. The PCR product was run and extracted from a 1.2% agarose gel. DNA was extracted using the QIAquick® PCR & Gel Cleanup Kit (Qiagen). The design allowed both the amplified dnAkt g-block fragment and the SFG.RQR8.CATCAR plasmid constructed earlier to be digested using AgeI/NcoI (NEB) restriction enzymes, as described above. This allowed for the replacement of RQR8 with the dnAkt via ligation. The ligation mixture was similarly transformed in bacterial cells and screened. Correct colonies were further validated by sanger sequencing and grown up to midpreps for adequate DNA amounts for downstream applications.

2.1.4. Adding a FLAG tag to dnAkt

To permit the intracellular visualisation of dnAkt by flow cytometry the SFG.dnAkt.CAT plasmid was further modified to include a FLAG tag (DYKDDDDK) that could be

stained using an anti-FLAG tag antibody. The FLAG tag was designed to directly attach to the carboxyl terminal of dnAkt. To achieve this an overlap extension PCR was used using 4 specific primers. A primary PCR was set up using Phusion[®] High-Fidelity DNA Polymerase (NEB) to generate the two fragments. The first fragment was generated using forward primer 1 which included the upstream sequence to include the AgeI restriction site and reverse primer 2 which added the FLAG tag to the carboxyl terminal of the dnAkt. The second fragment was generated using forward primer 3 which also added the FLAG tag to the carboxyl terminal and reverse primer 4 which included the downstream sequence to include the NcoI restriction site. The overlap between primers 2 and 3 permits the fusion of the two fragments in a secondary PCR using primers 1 and 4. PCR settings were the same as stated above, except for the secondary PCR where the 72°C step was extended to 90 seconds to allow for adequate extension times. Figure 7 below illustrates the location of the primers used and the FLAG tagged construct generated via this method.

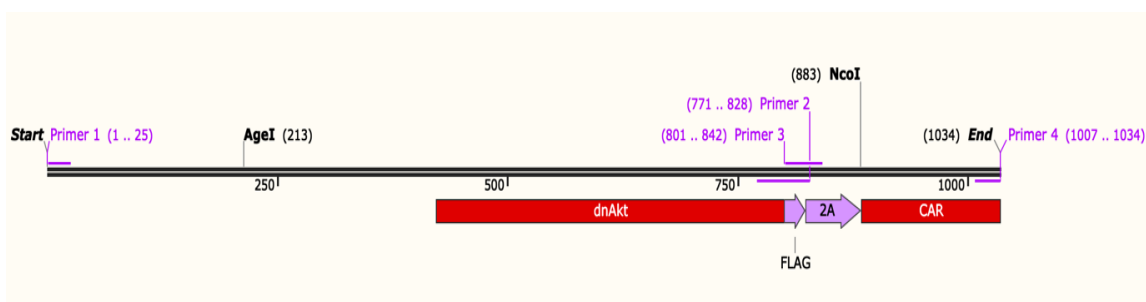


Figure 7. FLAG tag overlap PCR

This figure illustrates the locations of primers 1/4, upstream and downstream of AgeI/NcoI restriction sites, the location of primers 2/3, where they overlap and their role in the addition of a FLAG tag at the carboxyl terminal of the dnAkt.

DNA from the secondary PCR was run on a 1.2% agarose gel and the DNA was extracted. Both the FLAG tagged dnAkt DNA and original SFG.RQR8.CAT plasmid was digested using AgeI/NcoI (NEB) restriction enzymes. This allowed for the replacement of RQR8 with the FLAG tagged dnAkt via ligation. The ligation mix was subsequently transformed, screened, validated by sanger sequencing, and grown up to midpreps, as described above.

2.1.5. Summary of plasmid constructs

All other constructs used in this report were previously constructed in the laboratory. Below is a summary of all constructs used:

- SFG.RQR8.CATCAR.41BB-CD3 ζ
- SFG.dnAkt-FLAG.CATCAR.41BB-CD3 ζ
- SFG.RQR8.CATCAR.CD28-CD3 ζ
- pCCL.PGK.CATCAR.41BB-CD3 ζ

All plasmids were maintained at 1mg/ml in nuclease free water, stored at -20°C. Plasmids were regularly screened by restriction digests to ensure no plasmid degradation had occurred.

2.2 Cell culture

2.2.1. Cell lines

Martin Pule's laboratory provided all cell lines used in this report. Suspension cells used include SUPT1, a human T lymphoblastic lymphoma cell line, RAJI, B lymphocytes derived from a child with Burkitt's lymphoma (RAJI-WT) and RAJI CD19 knockout (KO) cells, where CRISPR CAS9 was used to knockdown CD19 surface expression (RAJI-KO). The RAJI-WT cell line previously transduced to express enhanced green fluorescent protein (eGFP) was also used (RAJI-GFP). CD19 and eGFP expression were confirmed by flow cytometry, as illustrated in Figure 8. NALM6, derived from an adult with acute lymphoblastic leukaemia (ALL) transduced to express the luciferase gene and K562s, derived from an adult with chronic myelogenous leukaemia (CML) were additional suspension cell lines used. K562s were transduced to secrete an anti-idiotypic antibody against the CAT CAR. The idiotype antibody was designed with a rabbit Fc, to permit secondary staining using a fluorochrome labelled anti-rabbit Fc antibody, allowing the visualisation of surface CAT CAR expression via flow cytometry. 293T human embryonic kidney cells were additional adherent cells used in this study.

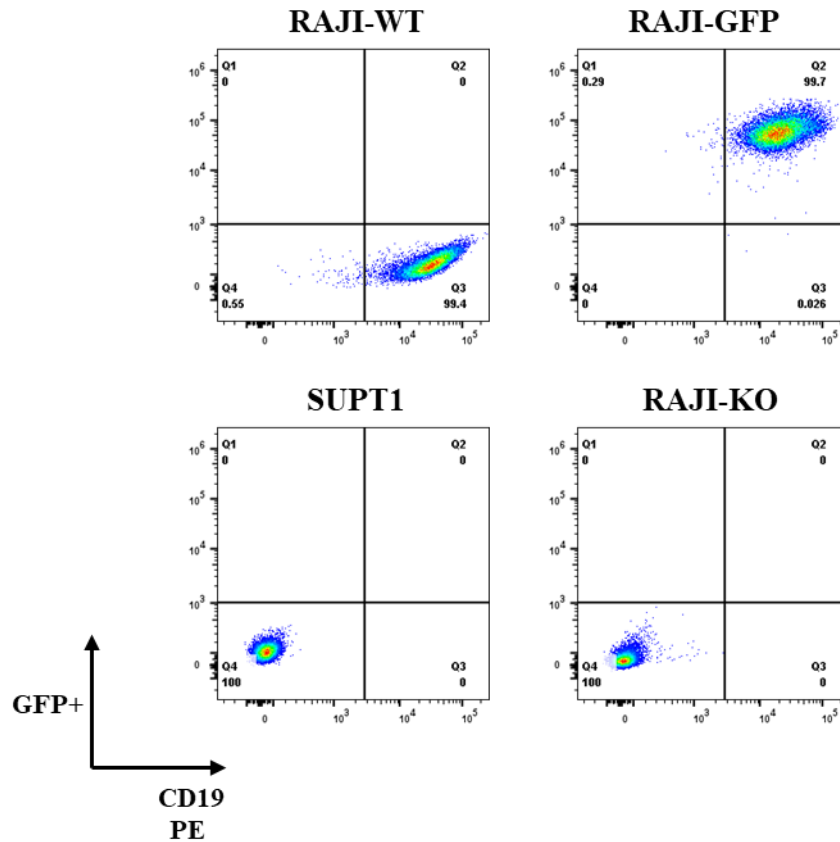


Figure 8. CD19 and eGFP expression on target cell lines

CD19 and eGFP expression on CD19+ (RAJI-WT), CD19+/GFP+ (RAJI-GFP), CD19-/GFP- (SUPT1 and RAJI-KO) cell lines determined by flow cytometry.

2.2.2. Cell culture and maintenance

All suspension cells except for the K562 cell line were cultured in T75cm² flasks containing 20mls RPMI medium (Lonza), supplemented with 10% fetal calf serum (FCS) and 1% glutamax (Gibco) (cRPMI). K562s were instead cultured in T75cm² flasks containing 20mls IMDM medium (Lonza) supplemented with 10% FCS and 1% glutamax (cIMDM). All cells were maintained with bi-weekly passages at a 1:10 ratio. Adherent 293T-cells were cultured in T175cm² flasks containing 20ml of cIMDM. The cells were also maintained with bi-weekly passages at a 1:10 ratio using trypsin EDTA (Sigma Aldrich). All cells were cultured in a humidified incubator at 37°C and 5%CO₂.

2.3 Virus production

2.3.1. Retrovirus vector production

293Ts were plated at a concentration of 2×10^6 cells in cIMDM per 10cm plate to ensure 50-60% confluency was reached post 24-hours. Plates were transfected by mixing 470ul plainIMDM (pIMDM) with 30ul genejuice (Merck Millipore) per plate. The mixture was incubated at room temperature (RT) for 5 minutes before the addition of 3.1 μ g of RDF (RD114) envelope, 4.7 μ g of PeqPam-env gagpol packaging plasmid and 4.7 μ g of the desired CAR plasmid per plate. The mixture was incubated for a further 15 minutes at room temperature and 500 μ l was added dropwise per plate. Plates were incubated till harvest at both 48 and 72-hours post transfection. Virus supernatants were pooled, filtered through a 0.45 μ m PES membrane, aliquoted and snap frozen in a dry ice and ethanol bath. Supernatants were stored at -80°C for downstream use.

2.3.2. Third generation lentivirus vector production, concentration, and titration

Third generation lentivirus was used to mimic the cGMP Prodigy CAR T-cell manufacturing process used in the UCL ALLCAR19 trial. Third generation lentiviruses have an improved safety profile over second generation where packaging plasmids are split into two, one containing Rev and the other Gag and Pol. This greatly eliminates the risk of recombination and the production of replication-competent viral particles. Whilst the risk of insertional mutagenesis and the potential activation of oncogenes with the use of integrating viruses cannot be completely eliminated, clinical studies utilising lentivirus for CAR delivery have a low risk profile (Milone and O'Doherty, 2018).

293Ts were plated at a concentration of 35×10^6 cells in cIMDM per Millicell HY-T1000 multilayer flask (Merck Millipore) to ensure 70-85% confluency was reached post 48-hours. Flasks were transfected by mixing 8550 μ l of pIMDM with 546 μ l genejuice per flask. The mixture was incubated for 5 minutes at RT before adding 73.8 μ g of pMDLg/RRE and 56.8 μ g RSV-rev packaging plasmids, 39.9 μ g of pMD.G2 envelope and 56.8 μ g of the desired CAR plasmid per flask. The mixture was incubated for a further 15

minutes at RT and added to the flask. Flasks were incubated for 48-hours before virus supernatant harvest. The supernatant was filtered through a 0.45µm PES membrane and immediately precipitated for concentration using the Lenti-X concentrator (Takara), following the manufacturer's instructions. The concentrated virus was aliquoted and frozen at -80°C for downstream use.

The titre of the concentrated virus was determined by flow cytometry by analysing CAR expression on 293Ts following transduction. 1×10^5 293T-cells were plated per well of a 12 well plate in 1ml cIMDM supplemented with 5µg/ml polybrene. Plated cells were incubated for 4 hours prior to the addition of viral vector. Various vector dilutions were added, starting from 2µl of the concentrated virus, and the vector was serially diluted at a 1:5 ratio. Plates were incubated for 72-hours and CAR expression was determined using flow cytometry. Only transduction efficiencies between 5-25% CAR+ cells were used to determine the titre using the formula below.

$$\text{Titre} \left(\frac{\text{IU}}{\text{ml}} \right) = \frac{\text{no. of cells at transduction} \times \frac{\% \text{ CAR positive cells}}{100}}{\text{End diluted vector volume (ml)}}$$

2.4. PBMC/T-cell isolation, cryopreservation, and recovery

2.4.1. PBMC isolation from whole blood

Whole blood PBMCs were isolated from healthy donors. Blood was collected into EDTA blood tubes, and PBMCs were isolated using density gradient centrifugation. Whole blood was diluted at a 1:1 ratio in plain RPMI (pRPMI) and layered on Ficoll® Paque (GE Healthcare). Tubes were spun at 750G for 40 minutes with no break and acceleration to generate plasma, PBMC, Ficoll and granulocyte/erythrocyte gradients. PBMCs were carefully collected and washed twice in pRPMI. Isolated PBMCs were either immediately depleted for natural killer (NK) cells using anti-human CD56 antibodies conjugated to a magnetic microbead (Miltenyi Biotec) or enriched for CD4/8 T-cells using a microbead based Pan T-cell isolation kit (Miltenyi Biotec), as per the manufacturer's instructions.

2.4.2. T-cell isolation from leucocyte cones

Leukocyte cones were processed using SepMate™ (Stemcell Technologies) tubes. These tubes utilise Ficoll® Paque density grade centrifugation and contain an insert to separate red blood cell (RBC) and PBMC layers. The tubes can be coupled with Stemcell Technologies RosetteSep™ reagent, which crosslinks unwanted cells to red blood cells (RBCs), permitting enrichment of desired cell subsets above the insert. 50ul of RosetteSep™ T-cell enrichment cocktail was added per ml of blood and incubated for 10 minutes at room temperature. Blood was diluted 1:1 in pRMPI and added above the Ficoll® Paque separating insert. Tubes were spun at 1200G for 10 minutes, and enriched CD4/8 T-cells were poured into a new tube. Cells were washed twice in pRPMI prior to use in downstream applications.

2.4.3. PBMC isolation from cryopreserved leukapheresis bags

Cryopreserved leukapheresis bags were thawed in a 37°C water bath. The contents were removed with a 50ml syringe and diluted at a 1:1 ratio with CliniMACS® buffer (Miltenyi Biotec). The buffer is a mix of PBS and EDTA to prevent leukapheresis coagulation. Cells were spun at a low speed at 120g for 15 minutes without break and acceleration. RBCs were immediately lysed by resuspending the resulting pellet in ACK Lysis Buffer (Thermofisher Scientific) for 10 minutes at room temperature. Cells were washed twice in CliniMACS® buffer and rested overnight in cRPMI, or TexMACS™ medium (Miltenyi Biotec) supplemented with 3% human serum (Sigma Aldrich, Life Science Production) at 37°C and 5%CO₂. Rested cells were enriched for CD4/8 T-cells using a microbead based Pan T-cell isolation kit (Miltenyi Biotec), as per the manufacturer's instructions.

2.4.4. PBMC cryopreservation and recovery

Excess PBMCs, enriched lymphocytes and end of process CAR transduced T-cells were cryopreserved in CS10 CryoStor® (Merck Millipore) at 10 to 50 million cells per ml. Vials were frozen at a controlled rate in Nalgene® Mr Frosty containers. Cryopreserved cell vials were placed in liquid nitrogen for long term storage. Cell vials were recovered

by rapidly thawing in a 37°C water bath. Cells were transferred dropwise into tubes containing 30mls of cRPMI or TexMACS™ medium supplemented with 3% human serum and spun at 300g for 10 minutes. Recovered PBMCs and enriched lymphocytes were rested overnight in serum supplemented media with no cytokines at 1×10^6 c/ml. All recovered CAR T-cells were instead rested overnight in TexMACS™ medium supplemented with 3% human serum (Sigma Aldrich, Life Science Production) and 10ng/ml IL-7/IL-15 (cTexMACS) at 1×10^6 c/ml. Recovery media for Akt inhibitor VIII (VIII) (Merck Millipore/Radboudumc) treated cells was supplemented with the inhibitor at working concentrations between 1-5µM.

2.5. PBMC/T-cell activation and transduction

2.5.1. PBMC activation and retrovirus transduction

PBMCs were resuspended at 2×10^6 c/ml in cRPMI and activated using 0.5mg/ml anti-CD3 (OKT3) and anti-CD28 (15E8) soluble antibodies (Miltenyi Biotec). PBMCs were activated for 48-hours prior to transduction. PBMCs were transduced on 24 well plates pre-coated with recombinant human fibronectin (Retronectin, Takara). 1.5mls of neat retrovirus supernatant was added per well to be transduced. Activated PBMCs were resuspended in cRPMI such that 3×10^5 cells were added to each transduction well in 500µl. IL-2 was added to the RPMI medium for a final concentration of 200IU/ml. Plates were spun at 1000G for 40 minutes before incubation for 72-hours. PBMCs were harvested and maintained at 1×10^6 c/ml in cRPMI supplemented with 200IU/ml IL-2 for 48-hours or further expanded for five days before use in downstream assays. Experiment dependent, in the treated arms, either 5µM or 1µM of VIII (Merck Millipore) was either added at transduction or activation. Once added, treated cells were maintained in media supplemented with the inhibitor until use in downstream assays. All cells were subjected to a media change every 48-hours.

2.5.2. T-cell activation and lentivirus transduction

This method was designed to mimic the cGMP Prodigy CAR T-cell manufacturing process used in the UCL ALLCAR19 trial. Selected T-cells were re-suspended at 1×10^6 c/ml in TexMACS™ medium (Miltenyi Biotec) supplemented with 3% human

serum and 10ng/ml IL-7/IL-15 (cTexMACS). Cells were activated for 24-hours by adding 10µl/ml of the TransAct™ (Miltenyi Biotec) reagent.

As above, T-cells were transduced on retronectin coated plates. The concentrated lentivirus was mixed with cTexMACS media to attain a multiplicity of infection (MOI) of 5 per well to be transduced. 500µl of this mix was added to the coated 24 well plates. Activated T-cells were resuspended in cTexMACS such that 3×10^5 cells were added to each transduction well in 500µl. Plates were spun at 1000G for 40 minutes before incubation for 72-hours. PBMCs were harvested and maintained at 1×10^6 c/ml in cTexMACS and expanded for four days prior to use in downstream assays. Experiment dependent, in the treated arm, 1 to 5µM of VIII (Merck Millipore/Radboudumc) was added at activation. Treated cells were continuously maintained in media supplemented with the inhibitor until use in downstream assays. All cells were subjected to a media change every 48-hours.

2.5.2. Scale-ups on the CliniMACS Prodigy®

The CAR T-cell products for patients on the ALLCAR19 trial are manufactured on semi-automated CliniMACS Prodigy® (Miltenyi Biotec) platform. To assess the feasibility of incorporating VIII onto this platform we carried out three manufacturing scale-ups. These were conducted at Royal Free Hospital by the ALLCAR19 trial manufacturing team. Excess frozen leukapheresis from patients recruited on ALLCAR19 trial was used for the scale-ups. This enabled downstream comparison of VIII scale-up CAR T-cells to trial products. The trial manufacturing protocol is as described in (Roddie et al., 2021). This scale-up method mimics this protocol where the only difference was the addition of VIII to the cTexMACS culture medium. A GMP grade version of the VIII AKT inhibitor was manufactured by ChemConnection BV and provided by Dr Harry Dolstra from Radboudumc.

Briefly, leukapheresis bags were thawed and loaded on the CliniMACS Prodigy®. In an automated cycle, the leukapheresis is first enriched for CD4/CD8 via microbeads (Miltenyi Biotec). 100-200 million enriched T-cells are transferred into a new bag to

proceed with automated activation and transduction steps. T-cells are transferred to the CentriCult unit for culture and maintained in TexMACS™ medium (Miltenyi Biotec) supplemented with 3% human serum (Life Science Production), 10ng/ml IL-7/IL-15 and 2.5µM of GMP grade VIII (Radboudumc) (cTexMACS VIII). Cells are activated with Miltenyi Biotec's TransAct™ reagent for 24-hours prior to the addition of lentivirus vector at an MOI of 5. Cells are cultured till Day 4, washed, and maintained in cTexMACS VIII till Day 8. Manufactured cells were harvested and frozen in a mixture of human serum albumin (Bio Products Laboratory) and 10% DMSO (Wak chemie medical GMBH) at a controlled rate in Nalgene® Mr Frosty containers and stored in liquid nitrogen.

2.6. Cell based assays

2.6.1. Co-culture assay

Before set-up, the transduction efficiency of all conditions was determined using flow cytometry. PBMCs/T-cell effectors were then re-suspended to 5×10^5 c/ml. RAJI-WT and RAJI-KO cell lines were irradiated at 60Gy. Targets were similarly resuspended to 5×10^5 c/ml. Cell number dependent, either 500µl or 1ml of effectors and targets were plated at a 1:1 in 48 or 24 well plates. Plates were incubated for 7 days prior to use in downstream assays. On day 3, 500µl of cell supernatant was harvested and frozen at -20°C for cytokine analysis. Subsequently, 500µl of cells were harvested on Day 6 for analysis by flow cytometry for viability, CD4, CD8, CAR, CD45RA, CD62L, CCR7, CD27, CD28 and CD95 expression. 10,000 CountBright™ counting beads (Thermofisher Scientific) were added to each sample during flow cytometry to determine absolute cell numbers. Co-cultures were either set up in serum supplemented RPMI or TexMACS media, with no additional cytokines. Where indicated, 1µM /5µM of VIII was added to the media throughout the co-culture.

2.5.2. Flow cytometry based killing assay (FBK)

FBK assays were either performed at the end of manufacture or at re-challenge where T-cells from the 7-day co-culture with RAJI-WT targets were restimulated in a killing assay.

Non-transduced PBMC/T-cell effectors were resuspended to 5×10^5 c/ml. Whereas, CAR transduced cells were resuspended to 5×10^5 c/ml CAR T-cells per ml. RAJI-GFP cells were resuspended to 5×10^5 c/ml. 5×10^4 effectors were serially diluted two fold in a 96 well U-bottom plate for a final volume of 100 μ l. 5×10^4 target cells in 100 μ l were mixed with the effectors for final effector to target ratios of 1:1, 1:2, 1:4 and 1:8. Cells were incubated for 72-hours and evaluated by flow cytometry to determine viability, CD3 and GFP expression. 10,000 counting beads were added to each sample during flow cytometry analysis to determine absolute cell numbers. Killing was assessed by determining the number of viable GFP+ target cells at the end of the assay. FBK assays were set up in serum supplemented RPMI or TexMACS medium with no additional cytokines or VIII.

2.7. Cytokine analysis

2.7.1. Cytokine Bead Array (CBA)

A CBA was performed on Day 3 cell culture supernatant obtained from the 7-day co-culture assay. The concentration of IL-2, IFN- γ , TNF- α , IL-4, IL-10, IL-6, IL-22, IL-17A and IL-17F cytokines was determined using the LEGENDplex™ Human Th Cytokine CBA kit (BioLegend), following the manufacturer's guidance. Fluorescence intensities were measured using the BD LSRFortessa™ flow cytometer, and concentrations were determined using the LEGENDplex™ software.

2.7.2. Isoplexis

Cryopreserved CAR T-cells were recovered and rested overnight in cTexMACS or cTexMACS VIII medium, as described above. Recovered cells were first stained with a violet membrane stain 405 provided with each kit. Labelled T-cells were then co-cultured with RAJI-WT targets at a 1:2 CAR:RAJI-WT ratio for 20 hours. Cells were harvested and split to individually select for CD4 and CD8 using magnetic microbeads on LS columns (Miltenyi Biotec), as per the manufacturer's instructions. Selected cells were then stained for CD4/8 using Alexa Fluor 647 conjugated antibodies provided in the kit. Cells were washed, counted, and resuspended to 1×10^6 c/ml in TexMACS medium

supplemented with 3% human serum. 30µl of 30,000 total cells were loaded onto each Isoplexis chip and loaded onto the machine.

Chips measure 31-plex cytokines grouped as, Effector (GranzymeB, IFN- γ , MIP-1 α , Perforin, TNF- α , TNF- β), Stimulatory (GM-CSF, IL-12, IL-15, IL-2, IL-5, IL-7, IL-8, IL-9), Chemoattractive (CCL-11, IP-10, MIP-1 β , RANTES), Regulatory (IL-10, IL-13, IL-22, IL-4, sCD137, sCD40L, TGF- β 1) and Inflammatory (IL-17A, IL-17F, IL-1 β , IL-6, MCP-1 and MCP-4). On the chip, single cells are loaded into lanes lined with antibodies against each cytokine. Chips are incubated in the machine at 37°C and 5%CO₂ to permit cytokine secretion from stimulated cells. Cytokine secretion is measured in an automated process using secondary antibodies and fluorescent microscopy. Lanes are barcoded to permit the identification of cytokines secreted from each cell.

Data from the chips were analysed using the company's proprietary image processing software Isospeak 2.9.0. The analysis provides data on the secretion frequency of each cytokine and permits the identification of the % of polyfunctional cells secreting 2 or more cytokines. The software further provides a polyfunctionality strength index (PSI) that is computed by identifying the % of polyfunctional cells and multiplying this by the mean fluorescence intensity (MFI) of each secreted cytokine.

2.8. Flow Cytometry

2.8.1. General staining and analysis

2.5×10^5 to 2×10^6 cells were used for flow cytometry staining. A primary stain using 250µl of cell supernatant obtained from K562 cells transduced to secrete an idiotype antibody against the CAT CAR scFv was performed to stain for CAT CAR expression. The idiotype antibody was designed to have a rabbit IgG, allowing the antibody to be visualised using a fluorochrome labelled anti-rabbit IgG antibody (Jackson ImmunoResearch) as a secondary stain. Fixable viability dyes, eFluor™ 780, eFluor™ 450 and eFluor™ 506 (Invitrogen™), were used to discriminate between live and dead cells. Antibodies used include, anti-human CD4 (RPA-T4), CD8 (RPA-T8), CD45RA

(HI100), CD62L (DREG-56), CCR7 (G025H7), CD27 (M-T271), CD28 (CD28.2), CD95 (DX2), CCR4 (L291H4), CCR6 (G034E3), CXCR3 (G025H7), CD127 (A019D5), CD25 (BC69), CD45 (HI30) and HA tag (16B12). All antibodies were purchased from BioLegend. Cells were primarily stained for CAR with anti-idiotypic supernatant for 30 minutes at 4°C, washed twice in PBS and stained for all other secondary antibodies, including viability dyes for an additional 30 minutes at 4°C. Cells were washed twice in PBS and analysed on BD LSRFortessa™, BD CytoFLEX, or Agilent Novocyte flow cytometers. All flow cytometry analysis was performed using FlowJo v10 software.

2.8.2. Intracellular cytokine and transcription factor staining

Prior to the detection of intracellular cytokines and transcription factors, 5×10^5 CAR T-cells were stimulated with RAJI-WT cells irradiated at 60Gy overnight in the presence of GolgiStop™ Protein Transport Inhibitor (BD Bioscience). Following primary CAR and subsequent secondary staining of cells, as described above, panel dependent, cells were either fixed and permeabilised using the BD Cytofix/Cytoperm™ solution or via the fixation buffer in the BD Pharmingen™ Transcription-Factor Buffer kit, as per the manufacturer's instructions. Following permeabilisation, cells were stained in respective permeabilisation/wash buffers containing intracellular antibodies for 30 minutes to 1 hour at RT. Cells were washed twice with the permeabilization/wash buffers and resuspended in PBS. Intracellular antibodies used include anti-human IL-2 (MQ1-17H12), IFN- γ (B27) (BD), TNF- α (Mab-11), GranzymeB (GB11) (BD), T-bet (4B10) (Invitrogen™), IFN- γ (B27) (BD), GATA3 (16E10A23), IL-4 (8D4-8) (BD), RORgt (AFKJS-9) (Invitrogen™), IL-17A (VL168), FoxP3 (PCH101) (Invitrogen™) and IL-10 (JES3-19F1) (BD), remaining antibodies were purchased from BioLegend.

2.8.3. Phosphoflow and FLAG tag staining

1×10^6 to 2×10^6 cells were first stained for CAR and subsequent secondary antibodies and viability dye, as described above. Cells were fixed with 4% formaldehyde (ThermoFisher Scientific) for 15 mins at RT. Cells were washed once in PBS supplemented with 0.5% Bovine Serum Albumin (BSA) (Sigma-Aldrich) and permeabilised with 250 μ l of 90%

methanol. Cells were incubated at 4°C for 30 minutes and washed twice with PBS/BSA before the addition of intracellular antibodies. Antibodies used included, fluorochrome conjugated Phospho-Akt Ser473 (D9E), Phospho-Akt Thr308 (D25E6) from Cell Signalling Technologies and Anti-DYKDDDDK (FLAG) (Miltenyi Biotech). Antibodies were stained in PBS/BSA for 1 hour at RT, washed twice and analysed.

2.8.4. CytoID Staining

Autophagy was measured using the CYTO-ID[®] Autophagy Detection Kit 2.0 (Enzo Life Sciences). This kit contains a 488nm excitable green fluorescent dye that can selectively label pre-autophagosomes, autophagosomes and autolysosomes in live cells. CYTO-ID[®] is a cationic amphiphilic tracer dye taken up by passive diffusion across the plasma membrane. Selection of titratable pH based functional moieties on the dye prevents the accumulation of the dye in lysosomes. Whilst potential background staining of lysosomes cannot be completely eliminated, CYTO-ID[®] has demonstrated proven specificity for autophagic vesicles (Chan et al., 2012, Oeste et al., 2013). 2.5×10^5 to 5×10^5 cells were primarily stained for viability, CD4, CD8 and CAR, as described above. The CYTO-ID[®] stain was diluted 1:1000 in assay buffer and 250µl was added to the cells. Cells were incubated in the dark at 37°C, 5%CO₂ for 30 minutes, washed in PBS and analysed by flow cytometry.

2.9. Mitochondrial/Metabolic Assessments

2.9.1. Mitrotracker staining

Total mitochondria were measured using the MitoTracker[™] Green FM (Invitrogen[™]), a 490/514nm excitable green, fluorescent stain. 2.5×10^5 to 5×10^5 cells were primarily stained for viability, CD4, CD8 and CAR, as described above. A 1mM stock solution of MitoTracker[™] was prepared in DMSO. The stock was diluted to 100nM in PBS and cells were stained at 37°C, 5%CO₂ for 30 minutes, washed in PBS and analysed by flow cytometry.

2.9.2. Mitochondrial membrane potential

Mitochondrial membrane potential was measured using the MitoProbe™ JC-1 Assay Kit. JC-1 is a membrane permeable dye that can accumulate in mitochondria in a potential dependent manner measured by a fluorescence emission shift from green (monomer) (514/528nm) to red (aggregate) (590nm). Membrane depolarisation can be measured by a decrease in red to green fluorescence ratios. A 200nM stock of JC-1 was prepared in DMSO. 2.5×10^5 to 5×10^5 cells were stained in 1ml cTexMACS or cTexMACS VIII media with a final JC-1 concentration of 2 μ M. Cells were incubated at 37°C, 5%CO₂ for 30 minutes washed twice with PBS and subsequently stained for viability, CD4, CD8 and CAR as described above. Cells were washed twice with PBS and analysed by flow cytometry.

2.9.3. Seahorse

Cryopreserved CAR T-cells were recovered overnight in cTexMACS or cTexMACS VIII as described above. Samples were enriched for CD8 T-cells using CD8 microbeads (Miltenyi Biotec), as per the manufacturer's instructions. Selected cells were further cultured overnight in cTexMACS or cTexMACS VIII medium at 1×10^6 c/ml. 2×10^5 cells were loaded per well of Seahorse XFe96 cell culture microplates coated with 0.1 mg/ml Poly-D-Lysine. Microplates were spun at 400G for 5 minutes to create cell monolayers. Seahorse XFe96 sensor cartridges were hydrated overnight in sterile water and incubated in XF Calibrant Solution for 1 hour in a 37°C, non CO₂ incubator prior to the addition of assay drugs as stated below. Microplates and sensor cartridges were loaded on the Seahorse XFe96 Analyzer where the oxygen consumption (OCR) and extracellular acidification (ECAR) rates were measured. Results were analysed using Agilent Seahorse Analytics and GraphPad Prism 9.3.1 Software.

Mitochondrial Stress and Long Chain Fatty Acid Oxidation Stress were measured using the Seahorse XF Long Chain Fatty Acid Oxidation Test Kit (Agilent). Cells were plated in Seahorse XF RPMI medium, pH 7.4 supplemented with 1mM pyruvate, 2mM glutamine and 10mM glucose. Long Chain Fatty Acid Assay drugs used include 4 μ M

Etomoxir, 2 μ M Oligomycin, 0.5 μ M FCCP and 0.5 μ M Rotenone/Antimycin A. As a control, cells were run in parallel without the addition of Etomoxir which was further used to inform Mitochondrial Stress.

Glycolysis was measured using the XF Glycolysis Stress Kit (Agilent). Cells were plated in Seahorse XF RPMI medium, pH 7.4 supplemented with only 2mM glutamine. Glycolysis Stress drugs used include, 10mM Glucose, 2 μ M Oligomycin and 50mM 2-DG.

2.10. RNA extraction, sequencing, and analysis

Cryopreserved CAR T-cells were recovered overnight in cTexMACS or cTexMACS VIII as described above. Cells were immediately stained for viability, CD4, CD8 and CAR. CAR expressing CD4 and CD8 T-cells were simultaneously sorted using the BD FACSAria™ III cell sorter into cTexMACS or cTexMACS VIII media and stored on ice. RNA was directly extracted from the sorted cells using the RNeasy Plus (Qiagen) kit, as per the manufacturer's instructions. RNA was eluted in nuclease free water and stored at -80°C.

Library preparation and sequencing were carried out by the UCL Great Ormond Street Institute of Child Health Genomics Facility. RNA was quality checked on the Agilent TapeStation. cDNA synthesis and library preparation were subsequently done using the KAPA mRNA HyperPrep Kit (Roche). Single end sequencing was performed on the Illumina NextSeq 500 using the high output 75 Cycle Kit. Approximately 33 million reads were generated per sample.

Output FASTQ files were mapped to the target genome and differential gene analysis was carried out by the genomics facility using the DESeq2 and EdgeR based R pipeline, SARTools (Varet et al., 2016). To identify enriched pathways, count-based gene enrichment tests were performed on differential gene data using the topGO package mapped against Gene Ontology Pathway Database.

2.11. *In-vivo* Procedures

2.11.1. Establishment of a systemic leukaemia model and *in-vivo* imaging

All protocols were performed in accordance to a UK Home Office approved project licence. 8-12 week old NOD scid gamma (NSG) mice housed in individually ventilated cages (IVCs) were used. Systemic leukaemia was established in mice via intravenous injection of 5×10^5 NALM6 luciferase transduced ALL tumour cell line in 200 μ l PBS via the tail vein followed by either 1×10^6 or 5×10^5 non-transduced or CAR T-cells 4 days later. Tumour burden was measured bi-weekly via bioluminescent imaging (BLI) using the IVIS spectrum *in-vivo* imaging system (PerkinElmer) following the intraperitoneal injection of 2mg D-luciferin in 200 μ l PBS. Photon emission from NALM6 cells was measured as photons/sec/cm²/steradian. Experiment dependent, mice were monitored for signs of sickness to evaluate survival or humanely euthanised at Day 21 where spleen and bone marrow samples were taken for downstream analysis.

2.11.2. Spleen Harvest and Staining

Spleens were excised and stored in cold Hanks Balanced Salt Solution (HBSS) (Sigma Aldrich). The spleens were gently pressed over a 70 μ m and subsequently a 30 μ m cell strainer to dissociate. Strainers were washed with PBS and cell suspensions were spun at 400G for 5 minutes to collect the cells. Cells were lysed with 2mls ACK lysis buffer for 10 minutes at RT to remove contaminating RBCs. Suspensions were washed again in PBS and immediately stained for flow cytometry analysis of viability, CD45, CAR, CD4, CD8 and HA tag (NALM6 tumour cells).

2.11.3. Bone Marrow Harvest and Staining

Mouse femurs were excised and stored in cold HBSS. Both ends of the bone were cut and the bone marrow was flushed out with PBS using a 25 gauge needle and syringe over a 70 μ m and subsequent 30 μ m cell strainer. The marrow was further pressed through the strainer and washed with PBS to maximise cell collection. Cell suspensions were spun at

400G for 5 minutes to collect the cells and pellets were lysed with 2mls ACK lysis buffer for 10 minutes at RT to remove RBCs. Suspensions were washed again in PBS and immediately stained for flow cytometry analysis of viability, CD45, CAR, CD4, CD8 and HA tag (NALM6 tumour cells).

2.12. Statistical analysis

Statistical tests were performed on data sets $n \geq 3$, the tests used are described in the figure legends. Statistical analysis was performed on GraphPad Prism 9.3.1. Statistical analysis for transcriptome data was carried out on R. Transcripts were filtered, where those with a mean count below 5 were removed. The remaining genes were fit in a negative binomial model for differential expression. A Wald test was used to identify significantly differentially expressed genes subsequently corrected for multiple testing using the Benjamin-Hochberg false discovery rate (FDR) method. The FDR rate was set to 5%. A Fisher test was used to identify significantly overrepresented gene fractions in each pathway at a $P < 0.05$ cut off.

Chapter 3. Effects of pharmacologic and dnAkt mediated Akt inhibition on CAR T-cells

3.1. Introduction

PI3K and Akt signalling pathway inhibitors have been widely investigated for use during the manufacture of T-cell therapies. Products manufactured in the presence of such pharmacological inhibitors were enriched in Tscm/Tcm subsets expressing CD62L and CCR7 T-cell homing markers and exhibited superior anti-tumour activity (Urak et al., 2017, Van der Waart et al., 2014, Crompton et al., 2015, Klebanoff et al., 2017, Bowers et al., 2017, Kim et al., 2012, Araki et al., 2009, Petersen et al., 2018, Zheng et al., 2018, Mousset et al., 2018, Funk et al., 2022). One such inhibitor, Akt inhibitor VIII (VIII), a PH domain dependent, cell permeable, and reversible allosteric inhibitor that inhibits Akt 1,2 and 3 activity at $IC_{50} = 58$ nM, 210 nM, and 2.12 μ M, respectively has been particularly investigated for these properties, Figure 9. In the CAR T-cell space, two groups have evaluated the impact of VIII during the *ex-vivo* manufacturing process of second generation CD19 targeting CAR T-cells with a CD28 ζ endodomain. Both groups used different CD19 scFvs, with variable manufacturing processes however, both studies conclude that VIII did not compromise CAR T-cell expansion, increased Tcm phenotypes and improved anti-tumour activity in CD19+ tumour bearing mice (Urak et al., 2017, Klebanoff et al., 2017).

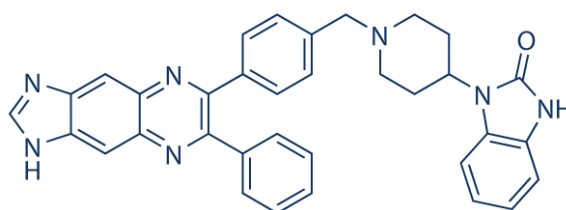


Figure 9. Chemical Structure of Akt Inhibitor VIII

This figure illustrates the chemical structure of Akt Inhibitor VIII, which is Compound 16g, originally developed by Merck Laboratories, Pennsylvania, USA (Lindsley et al., 2005). A cell permeable and reversible drug that can potently inhibit Akt1/2 in a PH domain dependent manner.

Given the benefit of VIII mediated Akt inhibition, we evaluated a gene engineered dominant negative Akt1 molecule (dnAkt) expressed in tandem with a novel CD19 targeting scFv referred to as the 'CAT CAR'. The dominant negative Akt is a non-functional counterpart of endogenous Akt. Transient expression of dnAkt constructs using adenovirus have shown successful Akt inhibition in other studies. A double mutant Akt with alanine substitutions at the Ser-473 and Thr-308 sites successfully inhibited insulin-induced endogenous Akt activity in hepatoma cells (Kotani et al., 1999). A further triple mutant kinase dead Akt created with alanine substitutions within Lys-179 (involved in ATP binding) and in Ser473/Thr-308 phosphorylation sites, enabled apoptosis and growth arrest in pancreatic cancer cell lines (Stoll et al., 2005).

Here, we propose the use of a novel dnAkt design of Akt1 with sole expression of the PH domain. We predict this will permit competitive lipid membrane binding with endogenous Akt without subsequent kinase activity and Akt activation. Whilst transient Akt downregulation can be achieved through the expression of the dnAkt using non-integrating viruses such as adenovirus and the use of short hairpin RNAs (shRNAs)/short interfering RNAs (siRNAs), we hypothesise that this strategy of dnAkt co-expression with the CAT CAR, as illustrated in Figure 10 will result in down regulated Akt signalling exclusively in CAR transduced cells sparing effects on total T-cell populations. As prior data with transient dnAkt expression led to growth arrest and apoptosis (Stoll et al., 2005), it is possible that this strategy of permanently expressing a dnAkt in CAR T-cells could significantly impact survival however, does provide us with a model to determine the long term effects of Akt downregulation on CAR T-cell phenotype and function.

We primarily set out to evaluate the impact of the dnAkt transgene via T-cell phenotyping and through functional assessments of proliferation and cytotoxicity compared to CAR alone. As an additional control, we tested this along the pharmacological Akt inhibitor VIII guided by its demonstrated effects on CAR T-cells and comparable activity on the Akt PH domain.

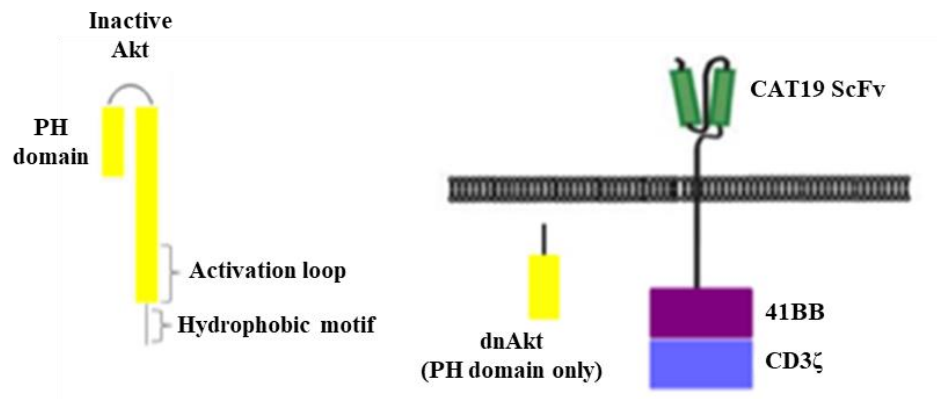


Figure 10. Illustration of dnAkt design

(A) Depicted here is the normal structure of inactivated Akt. (B) Illustration of novel dnAkt design expressing the PH domain only in combination with a second-generation CAT CAR with a 41BB and CD3 ζ endodomain.

3.2. Phenotypic and functional assessment of dnAkt and pharmacological Akt inhibition

3.2.1. Phenotypic and functional assessment of dnAkt in CAR T-cells

As per previous studies, we set out to determine whether expression of the dnAkt could enrich for Tcm subsets and provide any functional benefits. We began by retrovirally transducing PBMCs with the CAT CAR or CAT CAR dnAkt constructs. 2 days post transduction, CAR T-cells were assessed for T-cell phenotype by flow cytometry, as summarised in Figure 11. Transduced T-cells were further assessed for their killing and proliferative abilities. Killing assays were performed by co-culturing either non-transduced (NT) PBMCs or CAR transduced PBMCs with CD19 expressing RAJI-GFP cells at 1:1, 1:2 and 1:4 effector to target ratios (E:T) for 72-hours. Killing was determined by assessing the reduction in GFP target cells by flow cytometry. Proliferation was assessed by co-culturing CAR transduced PBMCs with either CD19 negative SUPT1s or CD19 expressing RAJI-WT targets. Proliferation was measured after 7-days by determining absolute cell counts for each subset using flow cytometry.

CAR T-cell Tn, Tcm, Te and Tte phenotype subsets were characterised via flow cytometry using CD62L and CD45RA markers. dnAkt expressing CD4/CD8 CAR T-cells failed to show any enrichment in Tcm subsets. Both conditions showed comparable phenotype with predominantly Te subsets, Figure 12A. Functionally, CD4/CD8 CAR T-cells expanded more against RAJI-WT over SUPT1 targets, as expected however both CAR T-cell groups were found to have the same proliferative and cytotoxic capabilities, Figure 12B and C.

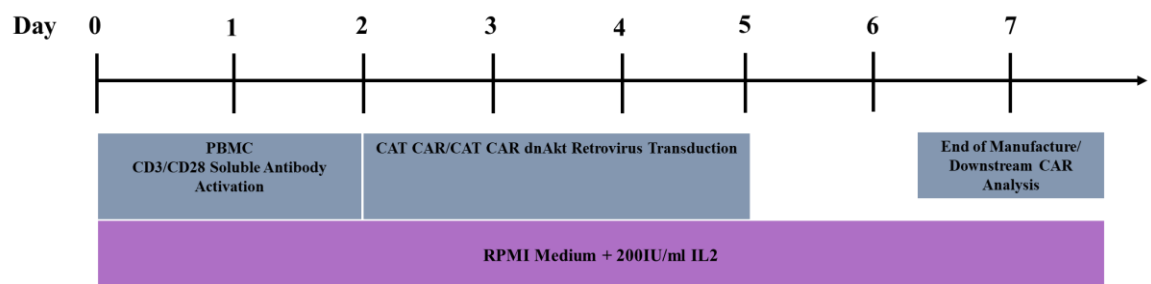


Figure 11. Method of CAR T-cell generation to evaluate the CAT CAR co-expressing the dnAkt. Schematic representation of the method used to generate CAT CAR T-cells co-expressing the dnAkt.

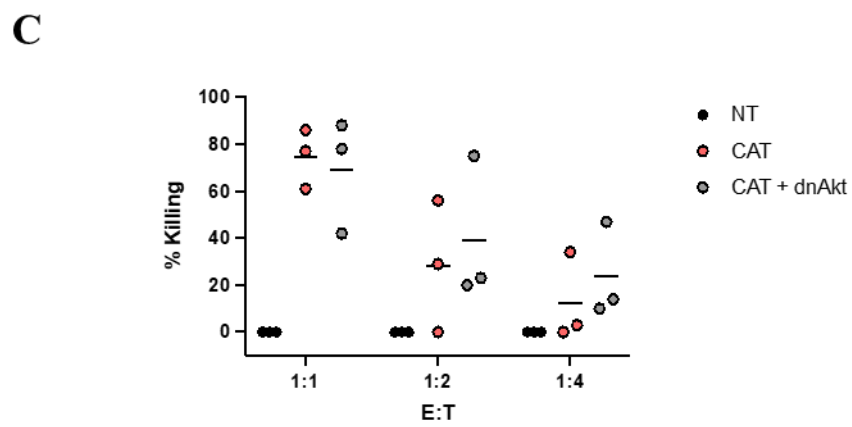
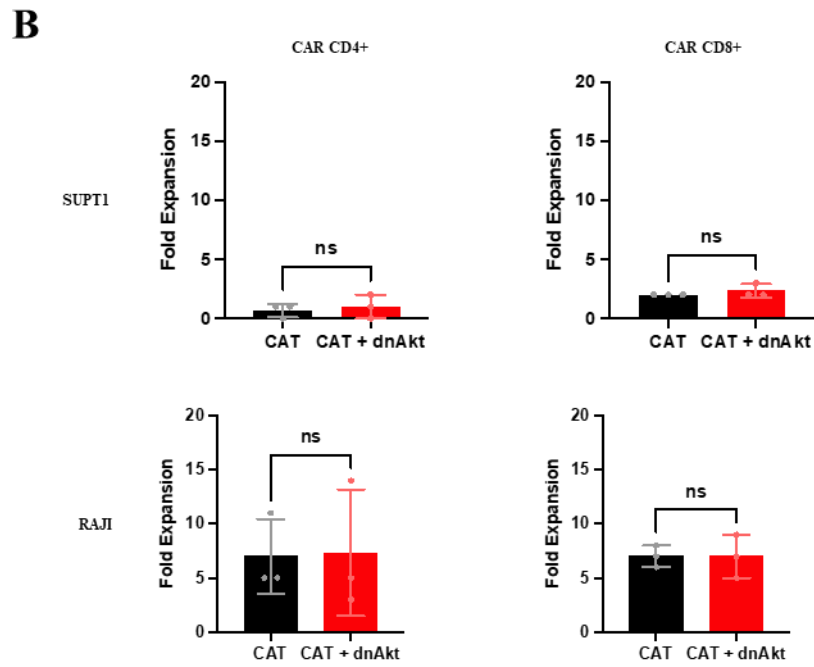
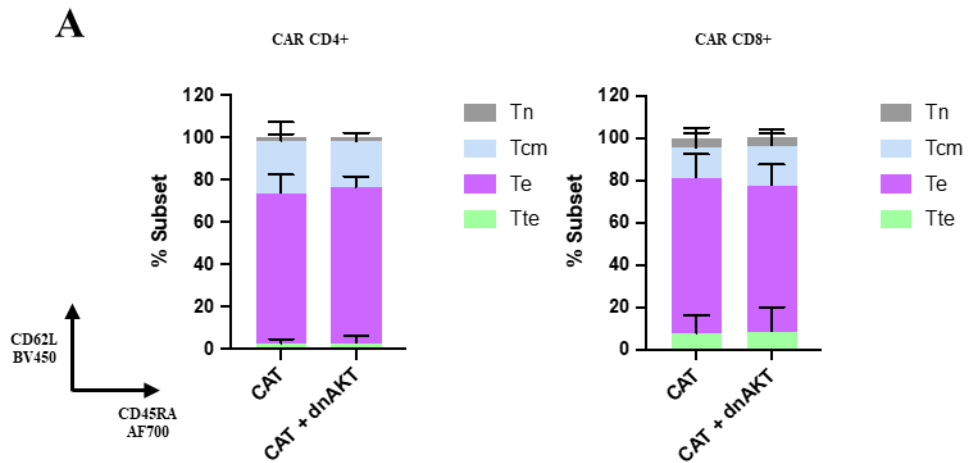


Figure 12. Phenotypic and functional assessment of dnAkt in CAR T-cells

(A) Phenotype characterised by CD62L and CD45RA expression. Subsets, Tn (CD62L+/CD45RA+), Tcm (CD62L+/CD45RA-), Te (CD62L-/CD45RA-), Tte (CD62L-/CD45RA+) in CAR CD4/CD8 T-cells. (B) Fold expansion of CD4/CD8 CAR T-cells following 7-day co-culture with SUPT1 and RAJI-WT cell lines. (C) Graph representing the percentage killing of targets post co-culture of transduced PBMCs in a 72-hour killing assay against RAJI-GFP target cells. Results depicted are normalised against NT PBMCs at each E:T ratio. All data sets are n=3 per condition \pm SD (A)/(B) or individual data points (C). No statistical significance was found via two-way ANNOVA corrected for multiple comparisons by Tukey's test (A)/(C) or two tailed Mann-Whitney U test (B).

3.2.2. Effects of pharmacologic versus dnAkt mediated Akt inhibition on CAR T-cells

As initial experiments showed no apparent phenotypic enrichment for Tcm subsets in the dnAkt or functional benefit in VIII conditions, we questioned the expression of the dnAkt and the feasibility of this strategy. We used a new dnAkt construct designed with a FLAG tag to enable intracellular visualisation of the dnAkt as a confirmation of protein expression. As a control for this strategy, we looked to compare dnAkt with pharmacological inhibition using Akt inhibitor VIII, as summarised in Figure 13. Studies have shown Tcm enrichment in T-cells using this inhibitor at concentrations between 1-18 μ M (Urak et al., 2017, Van der Waart et al., 2014, Klebanoff et al., 2017, Mousset et al., 2018).

As the dnAkt would only be expressed post transduction, to enable direct comparison, 5 μ M VIII was only added post transduction and maintained in culture throughout. CAR T-cell phenotype was assessed by flow cytometry, and proliferative capacity was assessed in a 7-day co-culture with CD19 negative SUPT1s or CD19 expressing RAJI-WT targets. To further assess if the dnAkt can reduce native Akt signalling compared to VIII, CAR T-cells were stained for Akt phosphorylation sites Thr308 and Ser473, indicative of moderate and strong signalling through Akt, respectively.

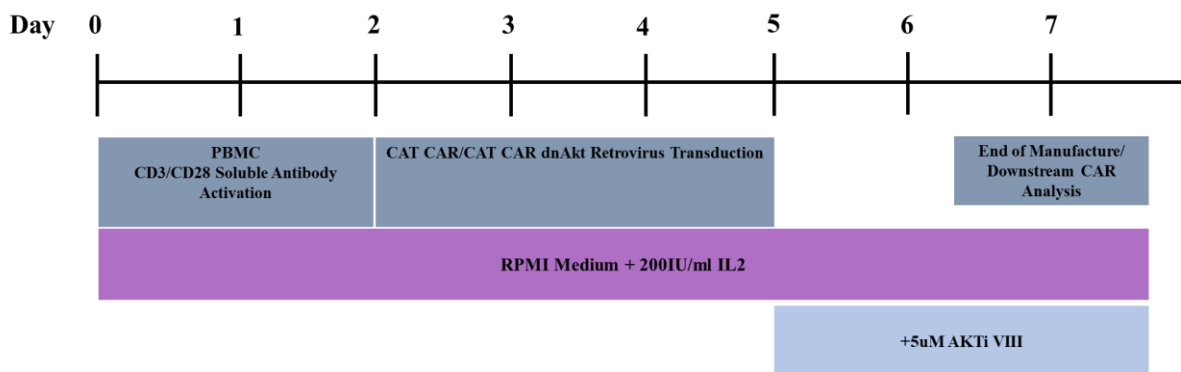


Figure 13. Method of CAR T-cell generation to evaluate the CAT CAR co-expressing the dnAkt with late pharmacological inhibition

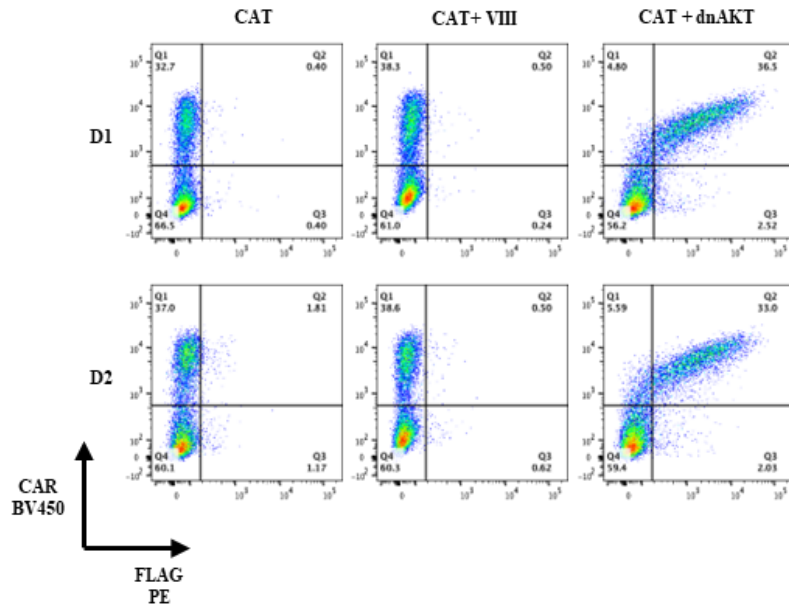
Schema of CAT CAR T-cell generation to evaluate the effects of the CAR CAR co-expressing the dnAkt with late pharmacological inhibition where Akt inhibitor VIII was added at Day 5 to mimic when the dnAkt expression would arise in transduced T-cells.

3 days post transduction, cells were stained to determine surface CAR and intercellular dnAkt expression, Figure 14A. This demonstrated successful and comparable transduction between CAT CAR alone, CAT + VIII and CAT + dnAkt conditions. dnAkt expression was confirmed by intracellular expression of the FLAG tag using an anti-FLAG antibody. Flow cytometry analysis showed a clear 1:1 expression of CAR to dnAkt. However, at this time point no difference in CAR T-cell phenotype was observed as characterised by both CD62L, CCR7 and CD45RA expression, Figure 14B. Subsets in all conditions were predominantly Te, as seen previously.

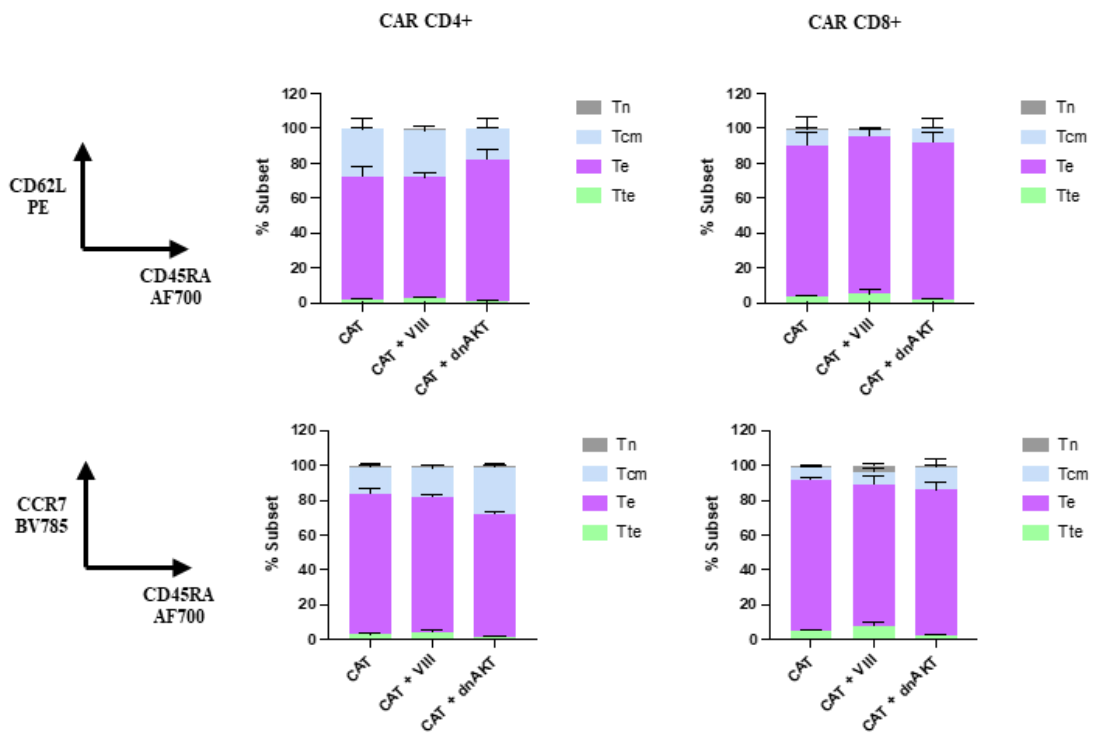
As expected, minimal CAR T-cell expansion was observed when cells were co-cultured with SUPT1s. Greater expansion was observed following co-culture with RAJI-WT cells. No differences in expansion were observed between CAT CAR alone and CAT + dnAkt conditions. To mimic dnAkt, VIII was continually added during the co-culture in VIII-treated cells at 5 μ M. CAR T-cells in this condition showed dramatically reduced CAR expansion in all conditions, Figure 14C. This may be attributed to sustained Akt inhibition causing T-cell toxicity. Akt inhibition during the co-culture may have further had cytotoxic effects on the SUPT1/RAJI target cells used, contributing to the lack of expansion.

To assess if the dnAkt could reduce native Akt signalling, CAR T-cells were stained for phosphorylation at Thr308 and Ser473, 2 days post transduction. The mean fluorescence intensity (MFI) of each antibody shows a reduced pThr308 and pSer473 staining in dnAkt expressing CAR T-cells. The same however was not seen in the VIII-treated arm. Here, pThr308 remained unchanged and a small variable donor dependent decrease in pSer473 MFI was seen, Figure 14D.

A



B



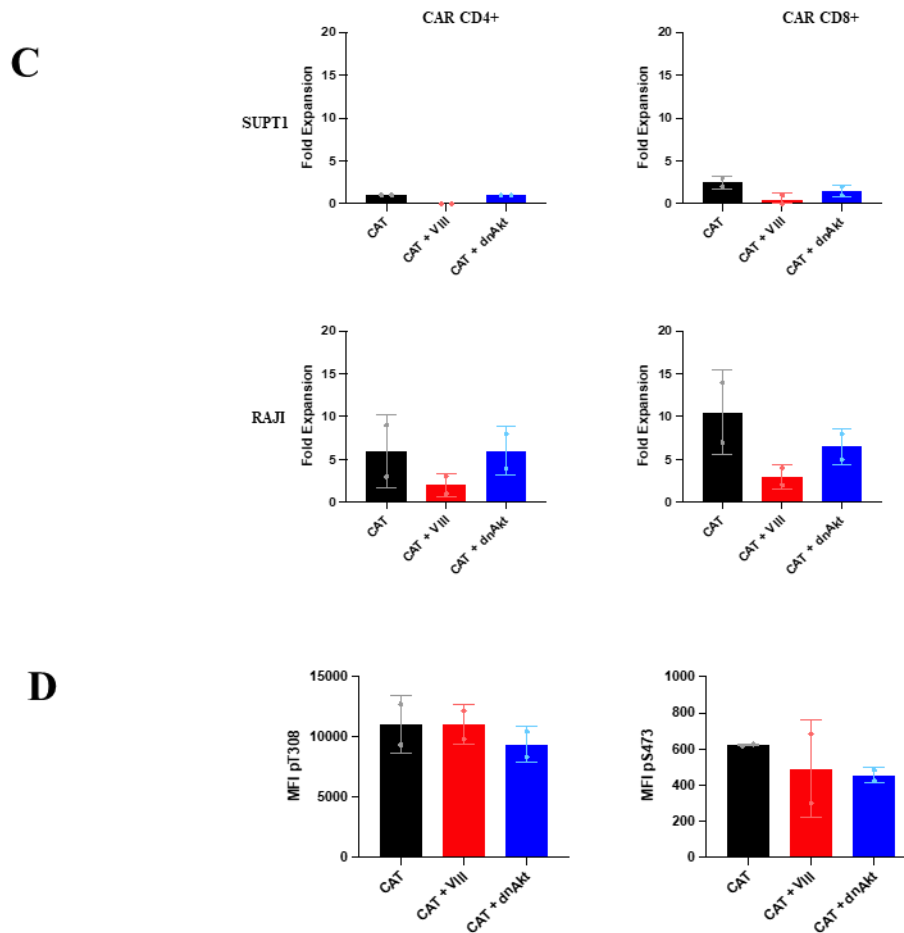


Figure 14. Effects of pharmacologic versus dnAkt mediated inhibition of Akt on CAR T-cells

(A) Flow cytometry plots depicting transduction efficiencies between CAR alone, CAR + VIII and CAR + dnAkt, 3 days post transduction. (B) Phenotype characterised by both CD62L, CCR7 and CD45RA expression. Subsets, Tn (CD62L+/CD45RA+)/(CCR7+/CD45RA+), Tcm (CD62L+/CD45RA-)/(CCR7+/CD45RA-), Te (CD62L-/CD45RA-)/(CCR7-/CD45RA-) and Tte (CD62L-/CD45RA+)/(CCR7-/CD45RA+) in CAR CD4/CD8 T-cells. (C) Fold expansion of CD4/CD8 CAR T-cells following 7-day co-culture with SUPT1 and RAJI-WT-cell lines. (D) Graph representing MFI of anti pThr308 and pSer473 antibodies in CAR T-cells 3 days post transduction. All data sets are n =2 per condition \pm SD (B) and/or individual data points (C)/(D).

3.3. Discussion

Whilst the data suggests dnAkt may be actively competing for binding sites with native Akt and reducing phosphorylation of pSer473 and pThr308, phenotypically no shift towards T_{cm} or functional benefit against CD19⁺ targets was observed. This naturally leads to question whether the dnAkt is truly functional and if the 1:1 expression of dnAkt:CAR is enough for substantial and sustained suppression of Akt signalling. However, no subset enrichment or functional benefits was seen in the CAR/VIII condition either. This raises an important consideration of when the Akt pathway is stimulated in T-cells and from which point Akt signalling should be inhibited to achieve phenotypic and functional gains.

Akt signalling can be initiated upon engagement of TCRs, cytokine receptors and costimulatory molecules (e.g. CD28) and we know that activated T-cells can lose expression of markers such as CD62L in an Akt1/2 dependent manner (Kim et al., 2012, Kim and Suresh, 2013, Macintyre et al., 2011). In preclinical studies of the pharmacological Akt inhibitor VIII where CD62L/CCR7 expression was preserved, VIII was added at the point of T-cell activation (Urak et al., 2017, Klebanoff et al., 2017), 48-hours earlier than our tested protocol. Therefore, one possible explanation for this data is that the potency of Akt signalling and the downstream effects initiated following T-cell activation, proceeding unhindered over 48-hours, outcompetes the ability of the CAR/dnAkt and even CAR/VIII to suppress this axis.

A further point of consideration is the potential for Akt inhibition to be variably impactful dependent upon the CAR endodomain used. The co-stimulatory receptor CD28 directly signals through the PI3K/Akt pathway and CD28 ζ endodomain CARs have been shown to have basal activation of Akt signalling, even in the absence of antigenic target (Salter et al., 2018). With this in mind, it may be that Akt inhibition strategies would be of maximal impact in CD28 CARs. In the experiments above we used a CAR incorporating a 41BB ζ endodomain. Native 41BB signals through a TRAF pathway and not directly through Akt. 41BB ζ endodomain CAR T-cells demonstrate greater long-term persistence and memory formation over CD28 ζ endodomain CAR T-cells (Milone et al., 2009, Dai

et al., 2020). Thus, in our next assessments, we wanted to investigate whether earlier Akt inhibition at activation is enough for Tcm enrichment and functional benefits in 41BB ζ endodomain CAR T-cells or if sustained Akt signalling through CD28 is required for optimal benefits.

3.4. Effects of early pharmacologic Akt inhibition in both 41BB ζ /CD28 ζ CAR T-cells

To evaluate if Akt inhibition at the point of T-cell activation is key to enriching for Tcm subsets with preserved CD62L/CCR7 expression, a protocol by (Klebanoff et al., 2017) was adopted for use in this experiment. PBMCs were either untreated (UT) or treated with 1 μ M of VIII at the point of T-cell activation with anti-CD3/CD28 soluble antibodies. The inhibitor was maintained in the culture of the treated arm throughout transduction until functional assessment as depicted in Figure 15. To assess if there is a differential effect of pharmacological Akt inhibition based on CAR endodomain, this method was evaluated in CAT CAR T-cells designed with both 41BB ζ and CD28 ζ endodomains. Phenotype was again assessed by flow cytometry, and proliferative capacity was assessed in a 7-day co-culture with CD19 expressing RAJI-WT targets.

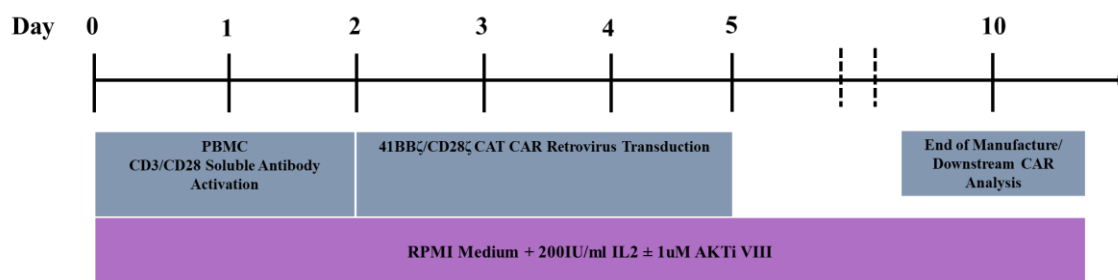


Figure 15. Method of 41BB ζ and CD28 ζ CAT CAR T-cell generation following early Akt inhibition

Schema of the generation of CAT CAR T-cells with either a 41BB ζ or CD28 ζ endodomain where pharmacologic Akt inhibitor VIII was added from the start of manufacture and maintained till the end of manufacture Day 10.

Phenotype subsets were identified using CD62L, CCR7 and CD45RA markers. At Day 9 of the CAR T-cell transduction/expansion process, enrichment of Tcm and decrease in Te was observed in both CD4/CD8 CD28 ζ endodomain CAR T-cells treated with VIII from activation using both CD62L/CCR7 markers. However, VIII-treated 41BB ζ CAR T-cells showed only a minimal increase in CD4/CD8 CAR Tcm characterised by CD62L staining. CCR7 staining failed to show an enrichment in 41BB ζ CAR CD4 T-cells but showed a marked increase in Tcm in CAR CD8 T-cells, Figure 16A. To assess functionality, CAR T-cell proliferation was tested in a 7-day co-culture with CD19 expressing RAJI-WT targets. Improved expansion of both CD4/CD8 CAR T-cells was seen in both 41BB and CD28 endodomain CARs. A modest 3.4/4.9-fold increase in VIII-treated 41BB ζ CD4/8 CAR T-cells was seen compared to a far greater 30/35.8 9-fold increase in VIII-treated CD28 ζ CD4/8 CAR T-cells post stimulation with CD19 target, Figure 16B.

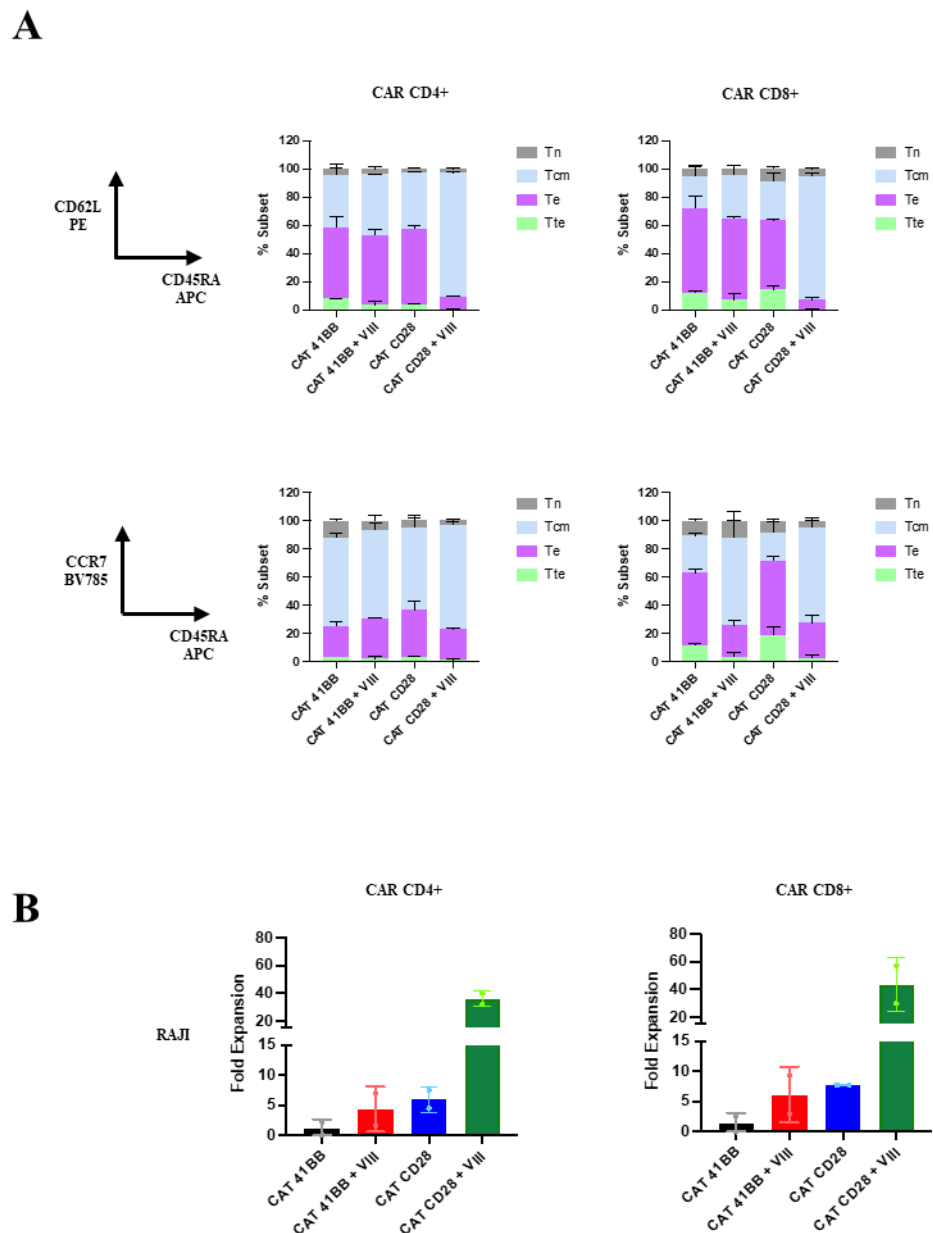


Figure 16. Effects of early pharmacologic Akt inhibition in both 41BB ζ /CD28 ζ CAR T-cells
(A) Phenotype characterised by both CD62L/CCR7 and CD45RA expression. Subsets, Tn (CD62L+/CD45RA+)/(CCR7+/CD45RA+), Tcm (CD62L+/CD45RA-)/(CCR7+/CD45RA-), Te (CD62L-/CD45RA-)/(CCR7-/CD45RA-) and Tte (CD62L-/CD45RA+)/(CCR7-/CD45RA+) in CAR CD4/CD8 T-cells. **(B)** Fold expansion of CD4/CD8 CAR T-cells following 7-day co-culture with RAJI-WT cell line. All data sets are n=2 per condition \pm SD **(A)** and/or individual data points **(B)**.

3.5. Conclusion

Taken together, this data suggests that early Akt inhibition prior to T-cell activation is key to preserving less differentiated T-cell phenotypes leading to improved CAR T-cell function.

The literature has established that CD28 ζ CAR T-cells demonstrate rapid CAR expansion and cytotoxicity upon antigen stimulation. A consequence of this however is maturation towards a more effector phenotype, a transcriptional profile of T-cell exhaustion and poor persistence *in-vivo*. This has been attributed to basal CD28 signalling activity at rest and post target mediated activation, which triggers signalling through the PI3K/Akt pathway, driving T-cell differentiation (Kawalekar et al., 2016, Salter et al., 2018). Thus, as predicted, it is unsurprising that early Akt inhibition provides a greater phenotypic and functional benefit in CAR T-cells with a CD28 ζ endodomain. *Ex-vivo* inhibition of Akt is likely protecting against basal/cell activation induced Akt activity, halting early T-cell differentiation during the CAR manufacturing process. Although the question remains whether this advantage gained *in-vitro* is lost early *in-vivo* when potent CD28 ζ CAR activation and downstream Akt signalling overwhelm the balance and drives these Tcm populations towards exhaustion.

Persistence following *ex-vivo* Akt inhibition in CD28 ζ CAR T-cells has not been demonstrated in previous studies. Despite early expansion, improved cytotoxicity and overall survival, studies observed no significant improvement in the persistence of CD28 ζ CD19 CAR T-cells in immunodeficient NOD scid γ (NSG) mouse models between VIII-treated and untreated arms (Urak et al., 2017, Klebanoff et al., 2017). This suggests a short-term gain in function but not one sustained long-term. Conversely, *ex-vivo* Akt inhibition studies in tumour reactive and tumour infiltrating T-cells generated interesting results. Under physiological TCR signalling, *ex-vivo* T-cell expansion in the presence of an Akt inhibitor resulted in Tcm enriched cell populations which upon adoptive transfer into a murine model of melanoma, showed greater expansion and enhanced persistence compared with controls. Long-lived populations of memory T-cells could be detected in lymphoid and non-lymphoid organs up to 600 days post transfer (Crompton et al., 2015).

41BB ζ CAR T-cells activate PI3K/Akt signalling to a lesser degree than CD28 ζ CAR T-cells. The biology of 41BB ζ CARs compared to CD28 ζ is of more gradual expansion, a Tcm skew, greater long-term persistence, and ongoing efficacy despite chronic antigen stimulation (Jang et al., 1998, Lee et al., 2003, van der Stegen et al., 2015). It is therefore understandable that *ex-vivo* Akt inhibition provides a lesser benefit in 41BB ζ CAR T-cells.

Both endodomains provide distinct functional properties and different malignancies may benefit from each. Third generation CAR T-cells incorporating two co-stimulatory domains in succession with a CD3 ζ endodomain have been evaluated in both pre-clinical and clinical assessments. Third generation CAR T-cells incorporating both 41BB ζ and CD28 ζ endodomains have shown variable results. Whilst some studies demonstrated improved persistence and anti-tumour responses from third generation CAR T-cells compared to second generation (Zhao et al., 2015, Zhong et al., 2010), other studies failed to show a benefit (Abate-Daga et al., 2014, Milone et al., 2009). Although clinical data remains promising where a study co-administered second generation CAR T-cells with a CD28 ζ endodomain and third generation CAR T-cells with both 41BB ζ and CD28 ζ endodomains demonstrated improved expansion and longer persistence of third generation CAR T-cells over second generation (Ramos et al., 2018). Despite this, conclusive evidence of the clinical benefit of third generation CAR T-cells is yet to be determined. A key limitation with the combination of multiple co-stimulatory domains is the potential of increased tonic signalling and CAR T-cell exhaustion, where the ideal CAR T-cell design remains to be determined.

Clinical response to CAR T-cell therapy has been linked to enhanced *in-vivo* expansion and long-term persistence, further correlated with less differentiated T-cell phenotypes. Given the characteristics of the 41BB ζ endodomain, and as our early experiments suggests that early Akt inhibition can limit activation induced differentiation in 41BB ζ CAR T-cells, enrich Tcm subsets, and provide a functional benefit, we wanted to explore this further in the context of the CAT CAR.

At UCL, the current paediatric and adult ALL clinical trial protocols utilise the CAT CAR with a 41BB ζ endodomain, delivered by a lentivirus vector and manufactured under Tcm supporting cytokines IL-7 and IL-15. Trial manufactures for the adult ALL study is performed using the semi-automated CliniMACS Prodigy[®] platform (Miltenyi Biotec). We next set out to determine if the inclusion of the Akt inhibitor VIII in the current trial manufacturing process can deliver functionally superior 41BB ζ CAR T-cells.

Chapter 4. Effects of pharmacological VIII inhibition in CAT CAR 41BB ζ CAR T-cells, using the CliniMACS Prodigy[®] manufacturing protocol

4.1. Introduction

Methods of CAR T-cell production vary considerably between studies, as summarised in Figure 17. The majority of manufacturing processes utilise anti-CD3/CD28 paramagnetic beads, with lentivirus CAR delivery and expansion in a rocking bioreactor such as WAVE[™]/ Biostat[®] RM/Xuri[™] systems, a process used as a part of trials evaluating Kymriah[™] (CTL019) (Schuster et al., 2019, Maude et al., 2018). Manufacture times further vary from less than 10 to greater than 30 days, majority of which are manufactured under 20 days (Roddie et al., 2021, Vormittag et al., 2018, Kalos et al., 2011, Tumaini et al., 2013, Lu et al., 2016).

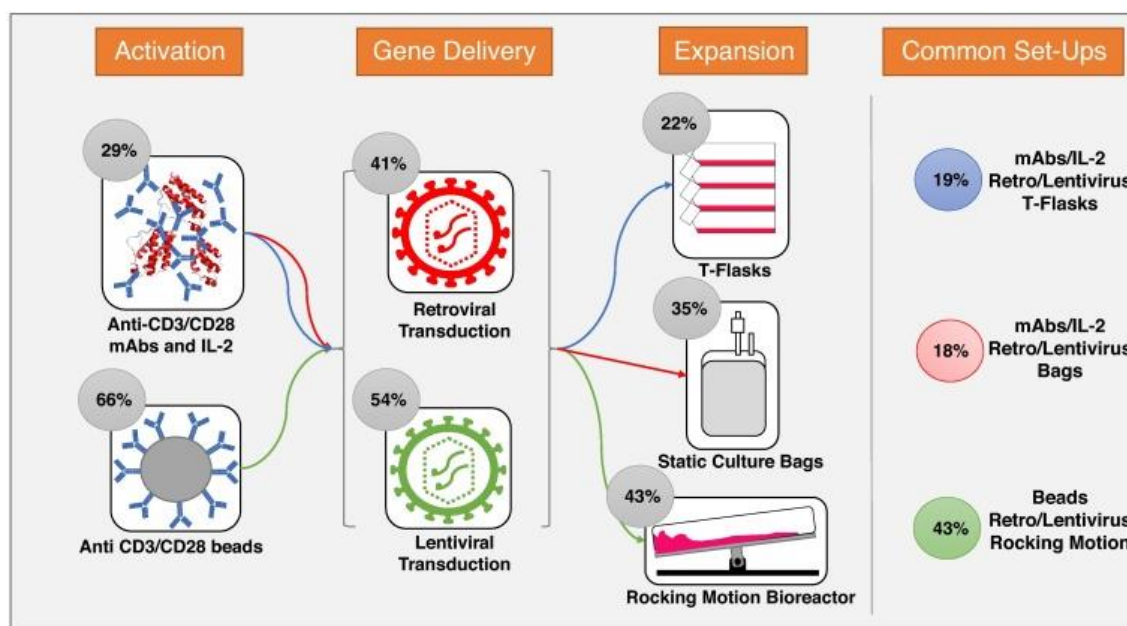


Figure 17. Illustration of CAR T-cell manufacturing processes

Commonly used clinical CAR T-cell manufacturing methods. Frequency of each method used is shown as percentages over each illustration as summarised from published studies, (Vormittag et al., 2018).

Additional variability in manufacturing comes from the use of enrichment/depletion steps commonly utilising the CliniMACS[®] system. Whilst some studies assessed the impact of directly selecting CD4/CD8 T-cell subsets to infuse defined ratios (Turtle et al., 2016), others enriched for Tcm (CD62L⁺) subsets (Wang et al., 2016), whole CD3⁺ T-cells (Roddie et al., 2021) or depleted NK cells (CD56⁺) (Singh et al., 2013). The use of cytokines can further impact products. Expansion is commonly achieved using interleukin-2 (IL-2) at highly variable concentrations. The use of IL-2 has been associated with driving T-cells toward a more exhausted Te phenotype with increasing evidence supporting a shift towards the use of interleukin-7/15/21 (IL-7/IL-15/IL-21), shown to enrich for less differentiated T-cell phenotypes (Ghassemi et al., 2016, Kaneko et al., 2009).

Current manufacturing methods generate products with highly variable transduction efficiencies, phenotype, and expansion, all of which can have consequences on patient outcomes. This is further exacerbated by unavoidable variability in patient apheresis used in autologous manufacture, often impacted by age, disease, and prior therapy. A study showed between 23.6 to 385-fold variability in the expansion of clinical products and retroviral transduction efficiencies ranging from 4%-70% (Brentjens et al., 2011). A study utilising lentiviral vector demonstrated similar variability from 5.5%-45.3% (Guo et al., 2016). However, despite such variability, a study forced to infuse 0.03-0.48x10⁶ CAR T-cells/kg, lower than the planned 1-3x10⁶ CAR T-cells/kg dose demonstrated that patients achieved stable disease, complete minimal residual (MRD) negative disease and had similar numbers of circulating CAR T-cells in the blood as those treated with the planned dose (Lee et al., 2015). The lack of standardised manufacturing methods and no uniformity in testing/reporting product characteristics make it difficult to determine the impact of manufacturing on CAR T-cell therapy outcomes.

As CAR T-cell therapy expands, the need for scalable, standardised, good manufacturing practice (GMP) compliant automated production process is high. With the emergence of new automated platforms such as the Cocoon[®] by Lonza, the most popular platform has been the use of the CliniMACS Prodigy[®] by Miltenyi Biotech. The Prodigy[®] allows for automated T-cell selection, activation, and expansion steps. Additional benefits of an

automated platform are the reduced requirements for high-classification manufacturing clean rooms and their associated costs. More so, such platforms require reduced staff interaction, further lowering costs and risks of contaminations or other operator handling errors (Roddie et al., 2019).

At UCL, a direct comparison of manual versus automated manufacturing was made as a part of the phase I ALLCAR19 (NCT02935257) trial (Roddie et al., 2021). Here, 6 patient products were manufactured using manual process A, where fresh apheresis was activated with human CD3/CD28 Dynabeads™ (CTS™, Gibco) in X-Vivo™ 15 (Lonza) medium supplemented with 5% human AB serum (Life Science Production). 500x10⁶ CD45+ haematopoietic cells were transduced with lentiviral vector encoding the CAT CAR at an MOI of 2.5-5. Cells were expanded on the Xuri™ Wave Bioreactor (GE Healthcare). Post expansion, Dynabeads™ were removed with the CTS™ DynaMag™ magnet and cells were incubated for an additional 2 hours prior to dose cryopreservation after a total of 9 days of culture. Manufacture was designed for the use of no exogenous cytokines however if expansion was impaired, cultures were supplemented with IL-2, as summarised in Figure 18.

An additional 18 products were manufactured in an automated process B, using the CliniMACS Prodigy®. CD4/CD8 T-cells were first selected in an automated process. 100-125x10⁶ selected T-cells were reloaded for automated activation using TransAct®, (a polymeric nanomatrix conjugated to human CD3/CD28, Miltenyi Biotech), lentiviral transduction with the CAT CAR at an MOI of 2.5-5 and expansion steps. Cultures were maintained in TexMACs™ (Miltenyi Biotech) supplemented with 3% human AB serum (Life Science Production). Cultures were further supported with IL-7 and IL-15 cytokines and cryopreserved after a total of 8 days of culture, as summarised in Figure 18.

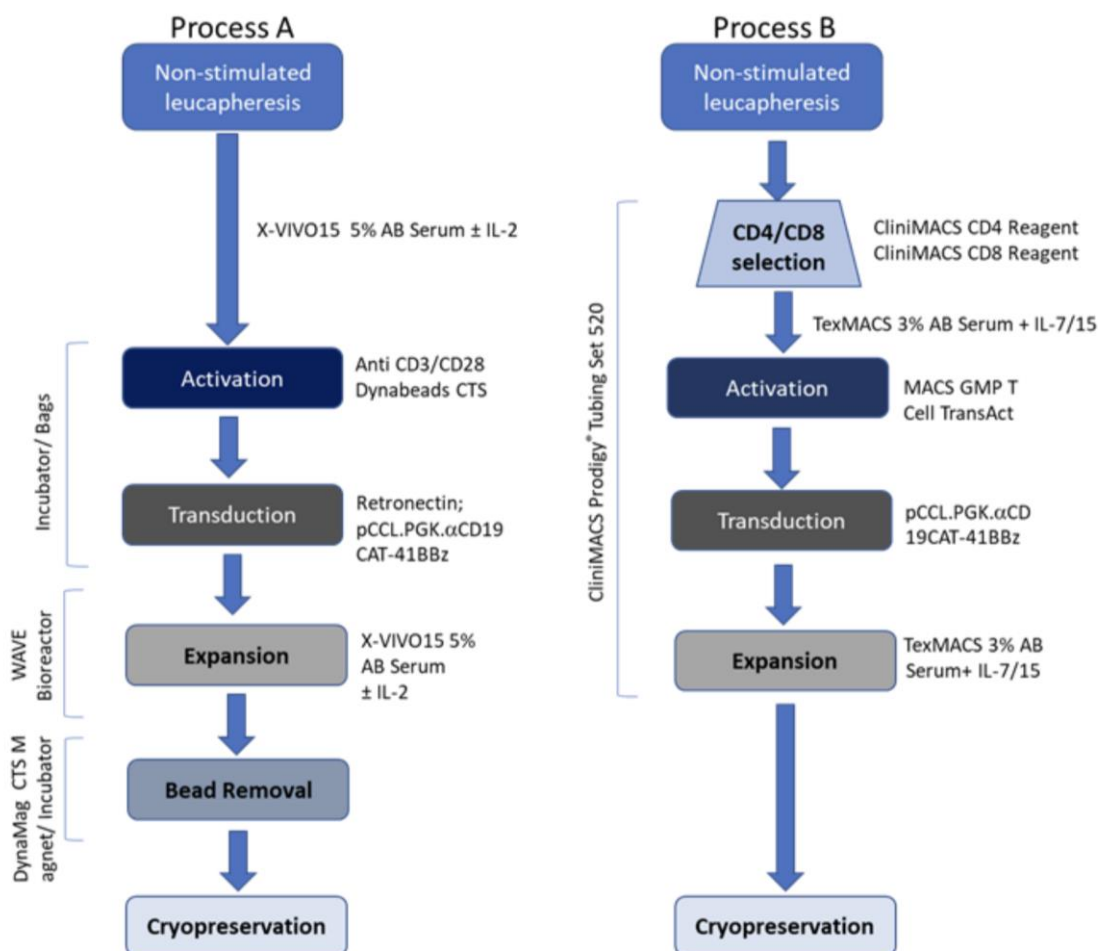


Figure 18. Schema of manufacturing processes used in ALLCAR19 trial

CAR T-cell products were generated from autologous PBMCs using either manual (Process A), n=6 or automated (Process B), n=18 (Roddie et al., 2021).

The goal of each manufacture was to successfully generate a total dose of 410×10^6 CAR T-cells. The dose was successfully reached for all but one patient manufactured by each process. Unpublished data provided by Dr Claire Roddie showed no significant differences between the total number of CAR T-cells generated from both manufactures, Figure 19A. Supplementary findings plotted from (Roddie et al., 2021) further showed no significant differences in transduction or phenotype by CCR7/CD45RA staining, Figure 19B/C. However, a significant reduction in PD-1 expression, a negative regulator of immune function was seen in products manufactured via the automated Prodigy®

platform, Figure 19D. Despite lack of significance, the distribution of data points demonstrates more consistent end of manufacture CAR T-cell doses and transduction in automated process B manufactures. More so, a trend towards enrichment in Tn (mean (A) 9.8% vs (B) 14.5%) and Tcm (mean (A) 23.3% vs (B) 30.5%) subsets can be seen in automated manufactures versus manual, Figure 19A/B/C.

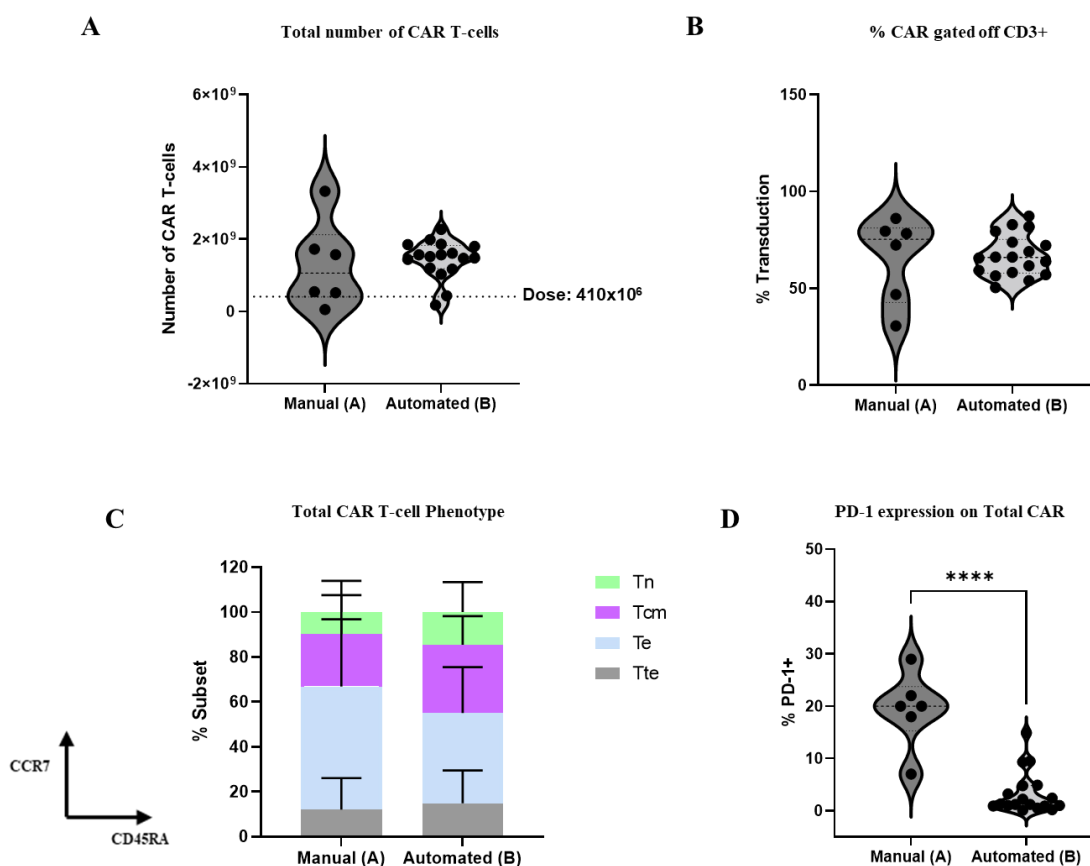


Figure 19. Expansion, transduction, and phenotype of CAR T-cells manufactured in the ALLCAR19 trial

(A) Volcano plot of total number of CAR T-cells generated at the end of manual or automated manufactures, dose required was 410×10^6 CAR T-cells, Process A, $n=6$ and Process B, $n=17$. Two tailed Mann-Whitney U test, ns $P>0.05$. (B) Volcano plot of percentage transduction of CD3+ cells. Two tailed Mann-Whitney U test, ns $P>0.05$. (C) Phenotype characterised by CCR7 and CD45RA expression. Subsets, Tn (CCR7+/CD45RA+), Tcm (CCR7+/CD45RA-), Te (CCR7-/CD45RA-) and Tte (CCR7-/CD45RA+). Two tailed Mann-Whitney U test, ns $P>0.05$

(D) Volcano plot depicting PD-1 expression on CAR T-cells. Two tailed Mann-Whitney U test, **** P<0.0001. (A-D) Process A, n=6 and Process B, n=18.

Given the scalability and consistency of automated manufactures on the CliniMACS Prodigy[®] platform, this manufacturing method is set to be used in a larger Phase II trial NCT04404660I. As our early assessments showed improved phenotype and function in CAT CAR T-cells manufactured in the presence of the VIII inhibitor. Our next aim was to assess if the use of the Akt VIII could be incorporated into the Prodigy[®] manufacturing protocol and evaluate subsequent effects on CAR T-cell phenotype and function.

4.2. GMP Akt inhibitor VIII drug comparability and titration

We established a collaboration with Dr Harry Dolstra's group, who were the first to describe the advantages of *ex-vivo* T-cell culture in the presence of Akt inhibitor VIII, Merck Millipore in 2014. CD8 tumour reactive T-cells were stimulated *ex-vivo* with dendritic cells (DC's) ±VIII for 14 days. VIII-treated T-cells had an enriched early memory phenotype and demonstrated superior expansion and antitumor activity in an *in-vivo* myeloma model (Van der Waart et al., 2014). Following this, other studies have described similar benefits in CAR T-cells, as described earlier (Klebanoff et al., 2017, Urak et al., 2017).

In a move towards the use of this Akt VIII inhibitor for clinical manufacturing, Dr Dolstra led the production of the VIII drug to GMP specifications with ChemConnection BV, following a 2 step synthesis and purification steps, as described in literature (Craig W. Lindsley, 2003, Lindsley et al., 2005). In collaboration with Dr Dolstra's group, we were provided with the GMP grade inhibitor to perform subsequent testing. As the literature standard was the VIII drug from Merck Millipore, we first set out to test the comparability of both drugs and titrate the GMP drug to identify the optimal concentration.

4.2.1. Phenotype of CAR T-cells treated with Merck VIII vs GMP VIII Akt inhibitors

Both drugs were tested by mimicking the Prodigy[®] manufacture at small-scale. Briefly, CD4/CD8 T-cells were enriched and activated overnight using TransAct[®] (Miltenyi Biotech) reagent. Activated T-cells were transduced the next day with lentivirus encoding the CAT CAR at an MOI of 5. Virus was removed and cells were washed 72-hours post transduction. Cells were expanded for an additional four days prior to downstream experiments. Cultures were maintained in TexMACs[™] (Miltenyi Biotech) supplemented with 3% human AB serum (Life Science Production) and 10ng/ml IL-7/IL-15 (Miltenyi Biotech) cytokines. In VIII conditions, the drug was added at testing concentrations from activation and maintained throughout the culture, as outlined in Figure 22. A direct comparison of 1 μ M Merck vs 1 μ M GMP VIII was made. The GMP VIII drug was further tested at 2.5 μ M and 5 μ M to identify the optimal concentration.

Total T-cell expansion remained unchanged between untreated (UT) and treatment with 1 μ M of Merck VIII Akt inhibitor. Expansion with 1 μ M of the GMP VIII inhibitor was comparable to the Merck drug however, higher concentrations of the GMP drug at 2.5 μ M and 5 μ M limited T-cell expansion by 45.3% and 52.4%, respectively, Figure 20A.

A greater effect on CAR T-cell phenotype was seen in CAR CD8 T-cells. Thus, the CD8 T-cells were used to compare the effect of each drug and concentration on phenotype. Here, all Merck and GMP VIII-treated T-cells demonstrated a comparable increase in Tcm subsets characterised by both CD62L and CCR7. Subsets CD62L⁺/CD45RA⁻ and CCR7⁺/CD45RA⁻ were designated as Tcm, Figure 20B. Further extended phenotyping demonstrated that all VIII-treated T-cells had comparably higher proportions of CD27⁺/CD28⁺ double positive cells, Figure 20C. CD27 and CD28 are T-cell surface co-stimulation proteins and are lost as T-cells differentiate towards Te/Tte. Loss of these markers in T-cells has also been linked to senescence (Gattinoni et al., 2017, Tu and Rao, 2016).

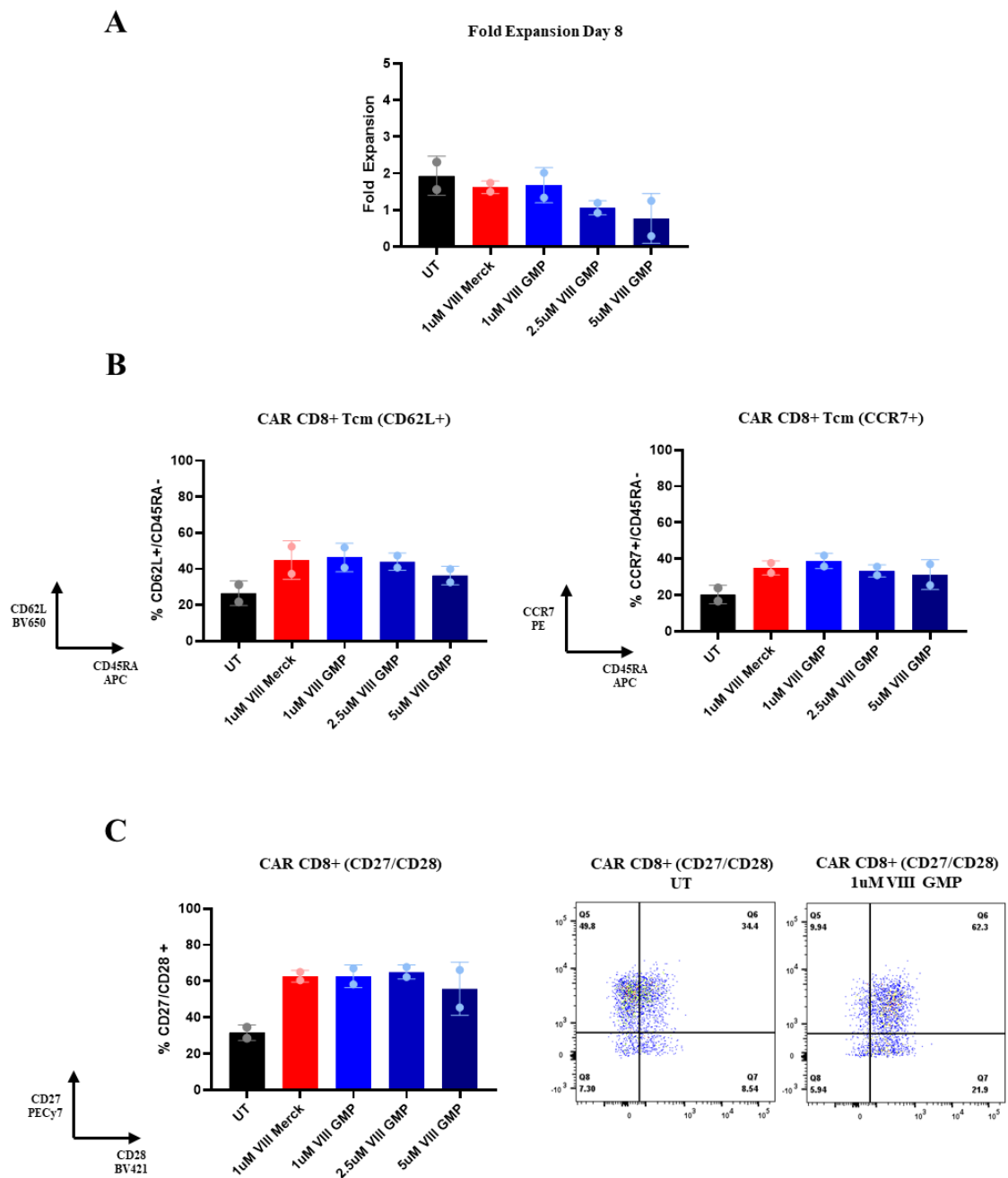


Figure 20. Phenotype of CAR T-cells treated with Merck VIII vs GMP VIII Akt inhibitors
(A) Total T-cell fold expansion by the end of manufacture at Day 8. **(B)** % Tcm subset in CAR CD8s at Day 8, determined by flow cytometry as (CD62L+/CD45RA-) and (CCR7+/CD45RA-). **(C)** Extended phenotyping depicting % CD27/CD28 double positive cells characterised by flow cytometry. Representation flow cytometry plots from one donor in the UT and 1µM VIII GMP are depicted to the right. All data sets are n=2 per condition ± SD and individual data points.

4.2.2. Function of CAR T-cells treated with Merck VIII vs GMP VIII Akt inhibitors

Following the 8 day manufacture of the CAR T-cells, cells were tested for functionality. CAR T-cell proliferation was tested in a 7-day co-culture with irradiated CD19 expressing RAJI-WT targets. Expansion of the CAR CD4 T-cells remained unchanged regardless of treatment however, a marked increase in expansion was seen in all VIII-treated CAR CD8 T-cells. A 7.7, 12.6, 14.2 and 11.2 average fold increase was seen in all 1 μ M Merck, 1 μ M GMP, 2.5 μ M GMP and 5 μ M GMP VIII conditions, respectively, Figure 21A.

Killing abilities were tested on re-challenge. Non-transduced (NT) or CAR T-cells were harvested from the 7-day co-culture used to assess proliferation and re-challenged in a killing assay against CD19 expressing RAJI-GFP targets. CAR T-cells and targets were co-cultured at 1:1, 1:2, 1:4 and 1:8 Effector:Target (E:T) for 72-hours. No killing of RAJI targets was observed by NT T-cells. All VIII-treated CAR T-cells showed improved killing at all E:T ratios. Killing between 1 μ M treated Merck and GMP VIII Akt inhibitors were comparable. However, greater killing was observed in CAR T-cells treated with the higher 2.5 μ M and 5 μ M of the GMP VIII drug, with 2.5 μ M providing the greatest killing capabilities at all E:Ts, Figure 21B.

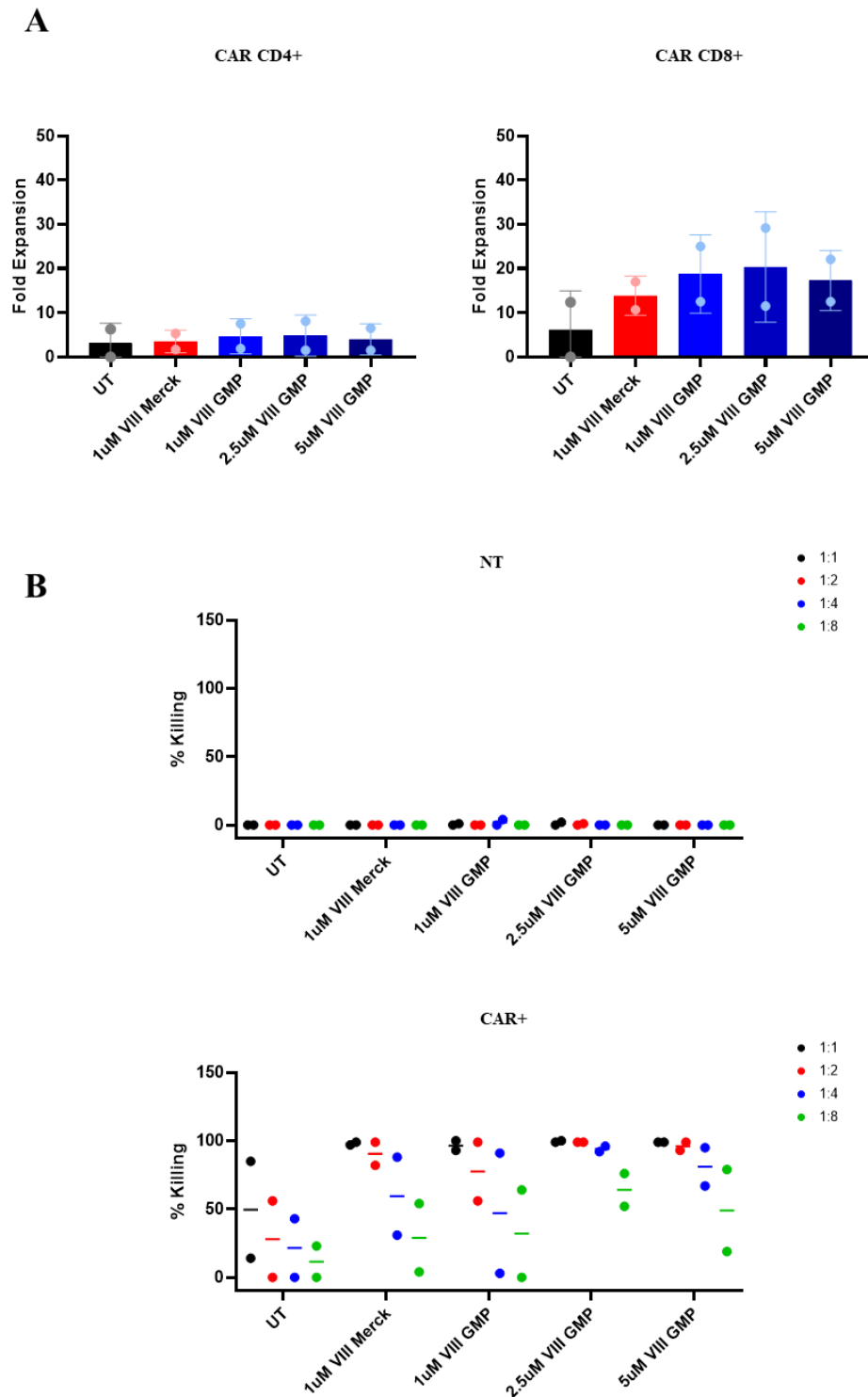


Figure 21. Function of CAR T-cells treated with Merck VIII vs GMP VIII Akt inhibitors
(A) CD4/CD8 CAR fold expansion following a 7-day co-culture with irradiated RAJI-WT target cell lines. **(B)** Graphs depicting % killing of RAJI-GFP target cells post re-challenge of NT or CAR T-cells in a 72-hour killing assay. Results from all conditions were normalised to the

untreated NT condition at each E:T ratio. All data sets are n=2 per condition \pm SD and individual data points (A) or only individual data points (B).

Ex-vivo manufacture of CAR T-cells in the presence of the new GMP VIII inhibitor showed comparable enhancement of phenotype, CAR CD8 expansion and killing against RAJI targets to the Merck Millipore VIII inhibitor at the 1 μ M concentration. Further titration of the GMP VIII inhibitor demonstrated improved killing of RAJI target cells at rechallenge, particularly at lower E:T ratios at a higher concentration of 2.5 μ M however, at a cost of reduced overall T-cell expansion.

Comparability of the GMP VIII inhibitor to Merck Millipore VIII was encouraging. Following these findings, we next set out to explore the effects of *ex-vivo* AKT inhibition across multiple donors. Evaluating in depth effects on phenotype, function, cytokine release and metabolism. The GMP VIII inhibitor at a concentration of 2.5 μ M was used for all future experiments.

4.3. Assessing GMP inhibitor VIII in healthy donor T-cells

All assessments were carried out as before by manufacturing CAR T-cells at a small-scale following the CliniMACS Prodigy[®] protocol. CD4/CD8 T-cells were enriched from healthy donor PBMCs and activated with TransAct[®] (Miltenyi Biotech) and transduced the next day with lentivirus encoding the CAT CAR at an MOI of 5. Virus was removed and cells were washed 72-hours post transduction. Cells were expanded for four days prior to downstream experiments. Cultures were maintained in TexMACs[™] (Miltenyi Biotech) supplemented with 3% human AB serum (Life Science Production) and 10ng/ml IL-7/IL-15 (Miltenyi Biotech) cytokines. Cells were either maintained as UT or VIII-treated, where 2.5 μ M GMP VIII was added from the start till the end of manufacture, as summarised in Figure 22.

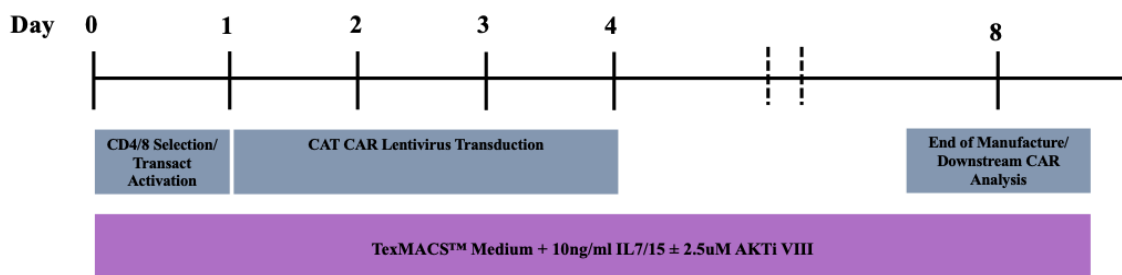


Figure 22. Schema of CAR T-cell manufacturing process

Process of CAR T-cell manufacturing at small-scale following the CliniMACS Prodigy® protocol.

CAR T-cells were assessed at Day 8 post manufacture. Cells underwent in-dept analysis for the effects of VIII inhibitor treatment on CAR T-cell phenotype, transduction, function, cytokine secretion, CD4 T-helper subsets, transcriptome analysis for gene enrichment signatures and metabolism.

4.3.1. Effects of GMP Akt inhibitor VIII treatment on expansion and phenotype

Total T-cell expansion was determined throughout the CAR T-cell manufacturing process from Day 0 – Day 8. Like previous experiments, manufacture in the presence of the GMP VIII inhibitor at the higher 2.5 μ M significantly impacted expansion. Despite initiating manufactures with the same number of selected T-cells, VIII-treated cells had reduced expansion by 52.5%, 52.5% and 60.4% at Day 4, 6 and 8, respectively, Figure 23A. A small significant increase was found in overall CAR T-cell transduction in VIII-treated cells however, average transduction was generally comparable at 61.2% (UT) and 67.7% (VIII), Figure 23B.

Like previous experiments, an improved phenotype was also observed at the end of manufacture in VIII-treated CAR CD4/CD8 T-cells. CCR7/CD45RA staining showed significant enrichment of less differentiated T_{cm} subsets and a significant reduction in more differentiated T_e and T_{te} subsets in both CD4/CD8 CAR T-cells. A more marked

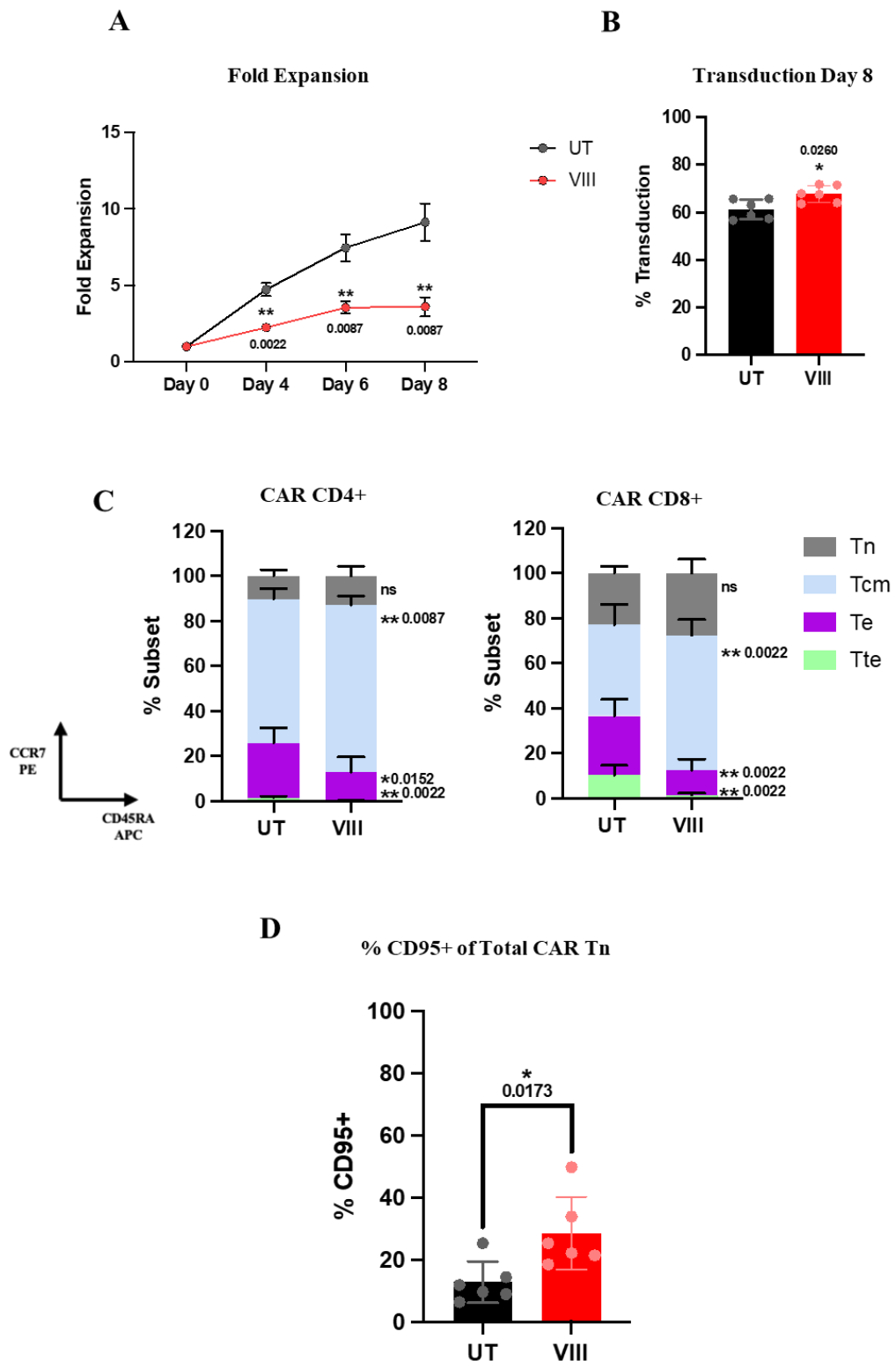
Tcm enrichment was seen in VIII-treated CAR CD8s where, CAR CD4s only demonstrated a 10.2% average increase but CAR CD8s increased by 19.2%, Figure 23C.

Although no marked changes were seen in Tn subsets, we performed extended phenotyping to identify stem cell like memory subsets (Tscm). Tscm subsets can be identified in Tn (CCR7+/CD45RA+) pools by sub gating for FAS receptor CD95. Tscm subsets are known to have a robust proliferative capacity and possess the ability to rapidly acquire effector functions following stimulation, much like memory T-cells. Transcriptional analysis shows Tscm subsets to have a unique gene profile with some features closely related to Tcm subsets (Gattinoni et al., 2011). In this experiment, flow cytometry analysis of Tn subsets sub gated to identify CD95 expression showed a significant increase in Tscm subsets in VIII-treated total CAR T-cells from mean 12.8% (UT) to 28.5% (VIII), Figure 23D.

Flow cytometry plots demonstrating representative CCR7/CD45RA staining in pre-manufactured CD8 T-cells and CAR CD8 T-cells throughout the manufacture are depicted in Figure 23E. The phenotype of starting CD8 T-cells comprises of mostly Tn subsets. This subset was found to expand post T-cell activation and differentiate towards Tcm, as the manufacture progresses. UT CAR T-cells eventually differentiate towards, Te/Tte subsets. However, VIII-treated cells retain greater CCR7 expression and have greater proportions of Tcm subsets at the end of manufacture.

For further extended phenotyping, like previous experiments we looked at the expression of CD27 and CD28, markers associated with less differentiated T-cell subsets (Gattinoni et al., 2017, Tu and Rao, 2016). A small non-significant increase in the percentage of CD27/28 double positive CAR CD4s was seen in VIII-treated cells. However, a marked average increase of 55.4% double positive cells was seen in VIII-treated CAR CD8s, Figure 23F. Additionally, we investigated IL-2 and Granzyme B secretion by CAR T-cells following stimulation. The literature shows that Tcm memory subsets can produce high levels of IL-2 but not cytotoxic molecules including Perforin and Granzymes (Mahnke et al., 2013, Sallusto et al., 1999, Xu and Larbi, 2017). We similarly saw a significantly greater proportion of both CAR CD4/CD8 T-cells producing IL-2 but not

Granzyme B following manufacture in the presence of the VIII inhibitor. CD4 CAR T-cells have greater proportions of IL-2+/Granzyme B- cells at 10.2% (UT) vs 29.8% (VIII) whereas CD8 CAR T-cells were lower 0.3% (UT) vs 4.8% (VIII), Figure 23F.



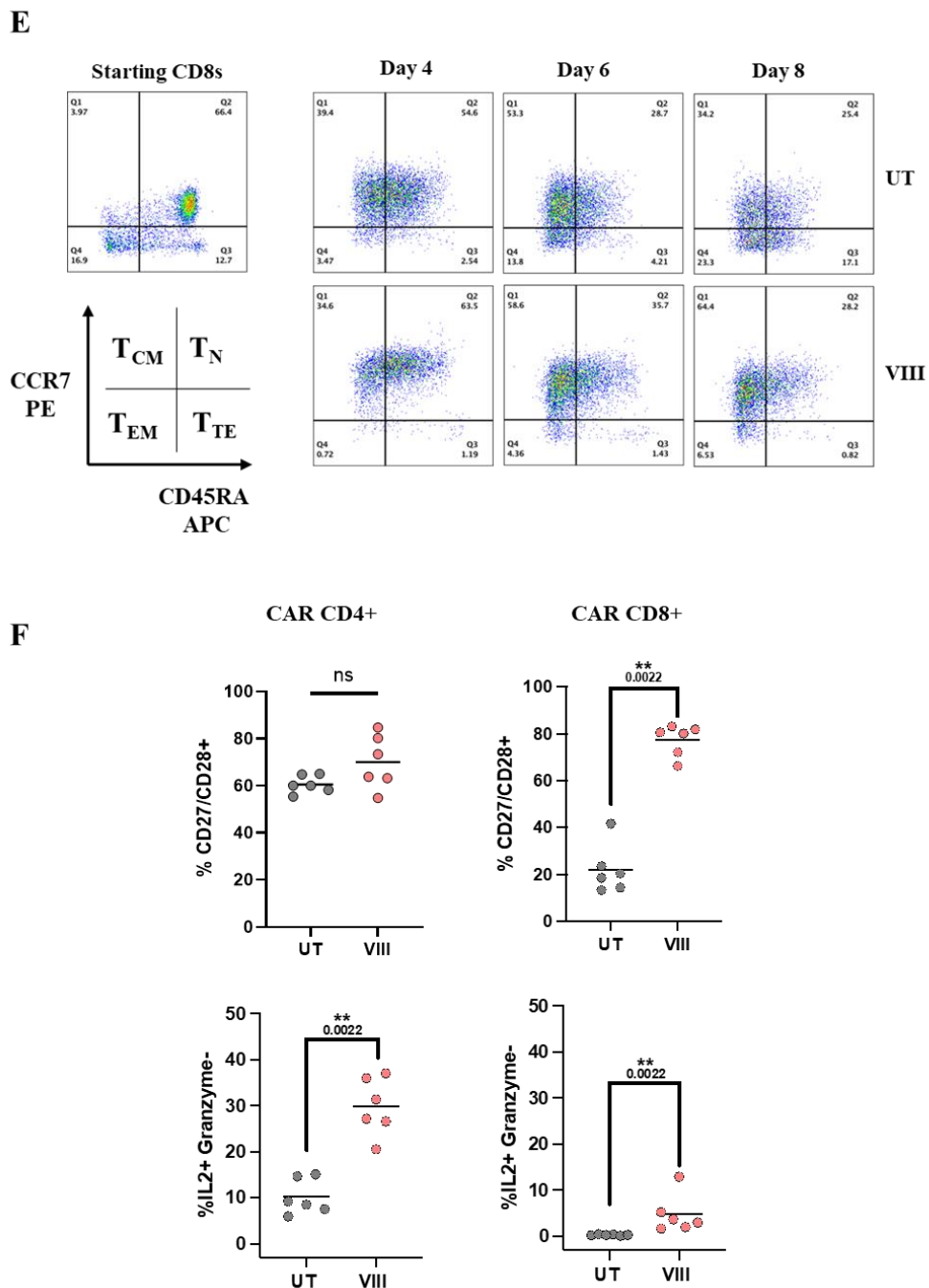


Figure 23. Effects of GMP Akt inhibitor VIII treatment on expansion and phenotype

(A) Total T-cell fold expansion throughout manufacture, \pm SEM. (B) CAT CAR T-cell transduction at end of manufacture Day 8, \pm SD/individual data points. (C) Graphical representation of T_n (CCR7⁺/CD45RA⁺), T_{cm} (CCR7⁺/CD45RA⁻), T_e (CCR7⁻/CD45RA⁻) and T_{te} (CCR7⁻/CD45RA⁺) subsets in CD4/CD8 CAR T-cells determined by flow cytometry, \pm SD. (D) Percentage CD95⁺ positive, sub gated from T_n population, \pm SD/individual data points. (E) Representative flow cytometry plot from one donor demonstrating CCR7/CD45RA staining in T-cell starting material and subsequently in CAR CD8s throughout manufacture. (F) Percentage

CD27⁺/CD28⁺ and IL-2⁺/Granzyme⁻ in CD4/8 CAR T-cells at end of manufacture, determined by flow cytometry, graphs depicting individual data points. (A-D/F) n=6, Two tailed Mann-Whitney U test, ns P>0.05. *P<0.05 and ** P<0.01.

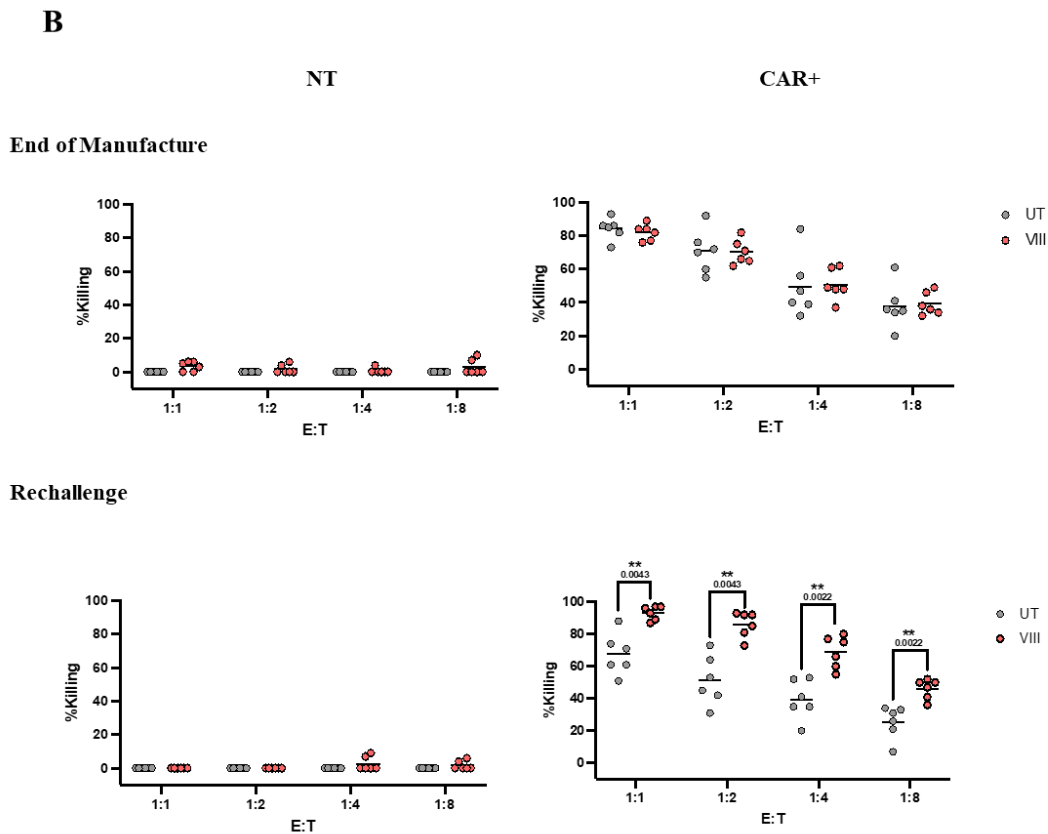
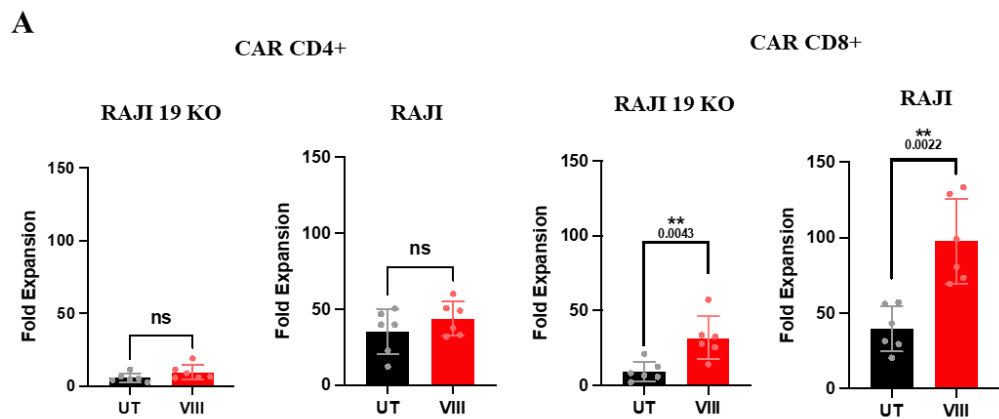
4.3.2. Effects of GMP Akt inhibitor VIII treatment on CAR T-cell function and cytokine secretion

Similar to previous experiments, T-cell proliferation was first assessed in a 7-day co-culture with RAJI-WT targets. As an improved control, proliferation was compared against RAJI-KO cells, where CD19 expression was knocked out using CRISPR. Killing was assessed at two time points, the first directly at end of manufacture, Day 8 and subsequently at rechallenge. Here, NT and CAR T-cells cultured with RAJI-WT targets in the 7-day co-culture were harvested and rechallenged in a killing assay against RAJI-GFP targets at 1:1, 1:2, 1:4 and 1:8 E:T for 72-hours. Killing was determined by measuring the reduction in GFP by flow cytometry. Cytokine secretion was measured from media supernatant collected at Day 3 of the 7-day co-culture using the LEGENDplex™ Human Th Cytokine Bead Array (CBA) kit (BioLegend), against IL-2, IFN- γ , TNF- α , IL-4, IL-10, IL-6, IL-22, IL-17A and IL-17F cytokines.

No significant change in expansion was seen in CAR CD4 T-cells following VIII treatment against both RAJI-KO and RAJI-WT cell lines. However, a marked benefit was seen in CAR CD8 T-cells where improved survival and a 22.4-fold increase in expansion was observed in the absence of target against RAJI-KO targets. A far more significant 57.9-fold increase in expansion was seen against CD19 expressing RAJI targets, Figure 24A.

Assessment of killing abilities at the end of manufacture showed no killing by NTs and comparable killing between both UT and VIII-treated CAR T-cells. A greater difference in killing was seen at rechallenge where, VIII-treated CAR T-cells exhibited a 26%, 35%, 30% and 21% increase at 1:1, 1:2, 1:4 and 1:8 E:T, respectively, Figure 24B.

Cytokine analysis by CBA showed VIII-treated cells were able to produce significantly more cytokines associated with effector functions. A 2.9, 4.6 and 2.7-fold increase in IL-2, IFN- γ and TNF- α secretion, respectively was observed. Assessment of other regulatory and inflammatory cytokines showed a significant increase in IL-4 following VIII treatment, although present at low concentrations at an average of 49.3 and 121.3 pg/ml. Significant increases in IL-6, IL-22 and IL-17A were also seen following VIII treatment however, no differences were seen in IL-10 and IL-17F, Figure 24C.



C

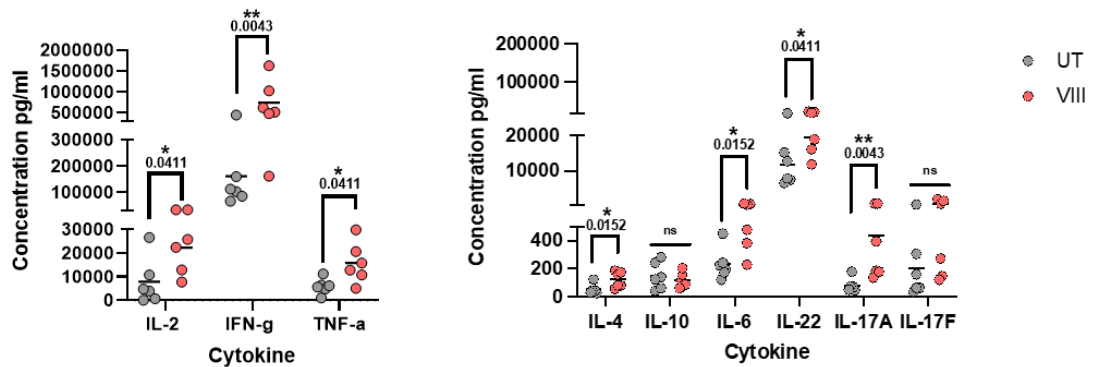


Figure 24. Effects of GMP Akt inhibitor VIII treatment on CAR T-cell function and cytokine secretion

(A) CD4/CD8 CAR fold expansion following a 7-day co-culture with irradiated RAJI-KO or RAJI-WT target cell lines, \pm SD/individual data points. (B) Graphs depicting % killing of RAJI-GFP target cells at the end of manufacture or post re-challenge by NT or CAR T-cells in a 72-hour killing assay. Results from all conditions were normalised to the untreated NT condition at each E:T ratio, graphs show individual data points. (C) Cytokine concentrations measured by CBA from Day 3 of the 7-day co-culture with RAJI-WT targets, graphs show individual data points. (A-C) $n=6$, Two tailed Mann-Whitney U test, ns $P>0.05$. * $P<0.05$ and ** $P<0.01$.

4.3.3. Effects of GMP Akt inhibitor VIII treatment on CD4 T-helper (Th) cells and polyfunctionality

In the context of tumour immunity, Th1, Th2, Th17 and TREG subsets have been evaluated. Th1 demonstrates superior anti-tumour activity due to their ability to secrete IFN- γ which can enhance the expansion of CD8 T-cells (Nishimura et al., 1999, Nishimura et al., 2000). Th1 can further help recruit components of the innate immune system such as endogenous macrophages to aid tumour elimination (Corthay et al., 2005).

The contribution of Th2 and Th17 to tumour immunity is more controversial. Whilst some studies suggest Th2 can offer anti-tumour effects by recruiting endogenous macrophages and eosinophils (Tepper et al., 1992) others show that tumour antigen specific Th2 cells can promote tumour growth. IL-5 produced by Th2 cells has been correlated with

progressive disease in follicular lymphoma (Rawal et al., 2011), melanoma (Tatsumi et al., 2002), pancreatic (Ochi et al., 2012) and prostate (Nappo et al., 2017) cancer patients. Intratumor IL-17 from Th17 cells has been shown to promote angiogenesis (Numasaki et al., 2005) and can induce inflammatory processes (Langrish et al., 2005) promoting a pro-tumour environment. Other studies show that the transfer of polarised Th17 cells had greater anti-tumour activity than Th1 polarised cells. This correlated with the recruitment of leukocytes and CD8 T-cell priming (Martin-Orozco et al., 2009, Muranski et al., 2008). Spontaneous antigen specific Th17 cells from lung cancer patients have also demonstrated the ability to produce IFN- γ (Hamaï et al., 2012).

TREG cells conversely have an entirely pro-tumour association. Their ability to produce cytokines such as IL-10, IL-35 and transforming growth factor- β (TGF- β) can down regulate the activity of effector T-cells and antigen presenting cells (APCs). TREGs further have a high dependency on IL-2, depleting it from the surroundings and constitutively express cytotoxic T lymphocyte antigen 4 (CTLA4) that can bind CD80/86 on APCs reducing their ability to activate effector T-cells (Togashi et al., 2019). Tumours enriched with TREGs, strongly correlate with poor prognosis in multiple cancer types (Curiel et al., 2004, Stenström et al., 2021).

The composition of CD4 T-helper subsets in CAR T-cell products is rarely characterised. Whilst CD4 T-cells can enhance CD8 T-cell activity through cytokine production, studies have shown CD4 CAR T-cells play an important role with comparable cytotoxic capabilities to CD8 CAR T-cells (Wang et al., 2018, Csaplár et al., 2021). Moreso, CD4 CAR T-cells demonstrate better persistence and less exhaustion following repeated antigen exposure than CD8 counterparts (Agarwal et al., 2020, Melenhorst et al., 2022).

(Mousset et al., 2020) reported concerns that the inclusion of CD4 T-cells in mixed cultures could reduce the beneficial effects of VIII inhibition on CD8 T-cells. Polyfunctionality is the ability of T-cells to secrete two or more cytokines and in the setting of mixed CD4/CD8 T-cell cultures, *ex-vivo* VIII inhibition of T-cells stimulated with dendritic cells (DCs) skewed CD4 Th differentiation towards Th2. This resulted in diminished favourable effects on CD8 T-cells, particularly reducing CD8 T-cell

polyfunctionality. (Mousset et al., 2020) suggest a split culture process where CD4 T-cells are manufactured independently without VIII treatment and CD8 T-cells with. Whilst they clearly outline the rationale for this, practically this is a more complicated, labour-intensive, and costly approach of limited feasibility where broad delivery of CAR T-cells for multiple patients is the desired goal and bulk cell culture is the current gold standard.

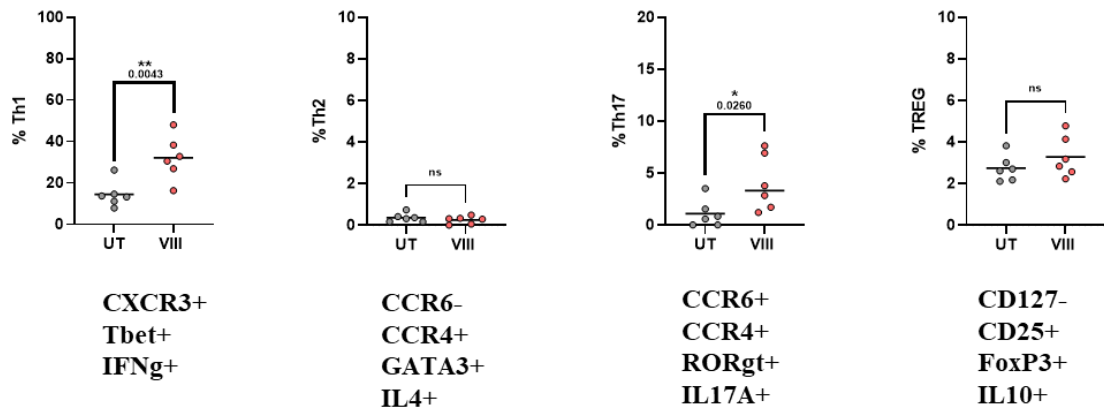
To identify functional CAR CD4 subsets at the end of CAR T-cell manufacture, T-cells were stained for Th1, Th2, Th17 and TREG specific surface markers and transcription factors. Expression of such surface markers and transcription factors can be associated with many functions particularly influenced by T-cell activation. To overcome this and generate an accurate representation of CD4 subsets, intracellular cytokines specific to each subset were also assessed. End manufacture CAR T-cells were stimulated overnight 1:1 with CD19 expressing RAJI-WT targets, stained for all markers, and evaluated by flow cytometry. Markers, transcription factors and cytokines used to characterise each subset were Th1 (CXCR3, T-bet, IFN- γ), Th2 (CCR4, CCR6, GATA3, IL-4), Th17 (CCR4, CCR6, ROR γ t, IL-17A) and TREG (CD127, CD25, FOXP3, IL-10).

Results demonstrated a significant 2.2 and 3.7-fold enrichment of Th1 and Th17 subsets in CD4 CAR T-cells manufactured in the presence of VIII inhibitor. No significant differences were seen Th2 or TREG subsets following VIII treatment, Figure 25A.

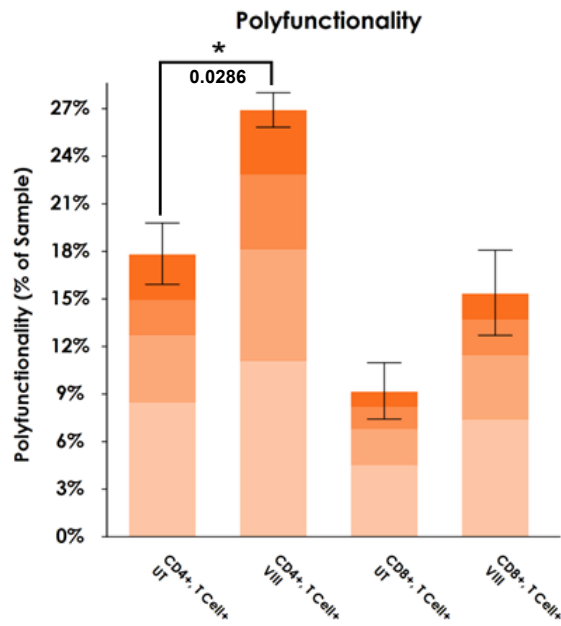
To further evaluate changes in polyfunctionality, end manufacture CAR T-cells were assessed on the Isoplexis platform. This platform can uniquely identify cytokine secretion from single cells, identifying overall percentages of polyfunctional T-cells and the polyfunctionality strength index (PSI). VIII-treated T-cells showed an increase in the proportion of both CD4/CD8 polyfunctional cells however, more significantly in CD4 T-cells, Figure 25B. Calculated PSI further showed a 1.6-fold overall increase in VIII-treated CD4/CD8 T-cells. Particularly, a marked increase in cytokines represented by effector and stimulatory subsets in CD4/CD8 T-cells. Results were significant in CD4s with CD8 T-cells demonstrating the same trend. Additionally, no significant increase in the regulatory cytokine subsets was seen in VIII-treated cells, Figure 25C. Principal

component analysis computed by the Isospeak software further illustrates far more robust CD4/CD8 polyfunctional populations in VIII-treated cells with a skew towards effector and stimulatory GM-CSF, IL-2, TNF- α and TNF- β cytokines, Figure 25D.

A



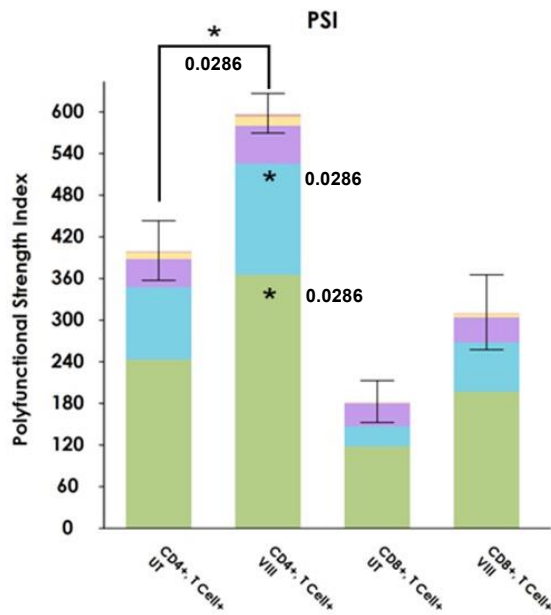
B



Key



C

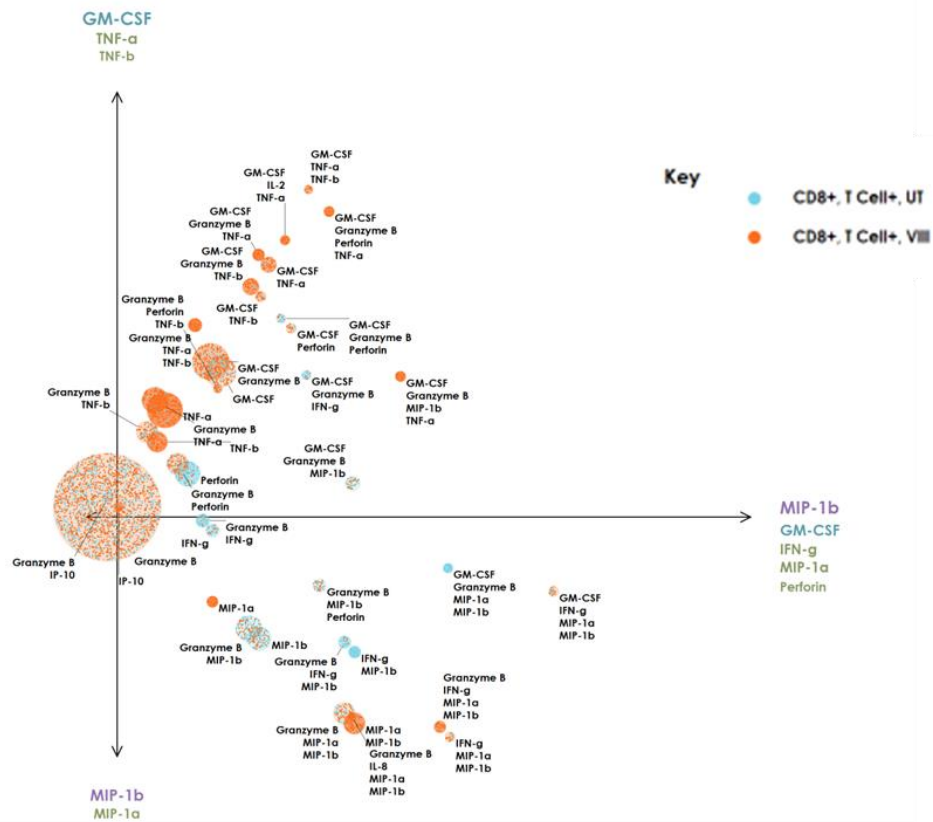


Key



D

CAR CD8+ PAT PCA



CAR CD4+ PAT PCA

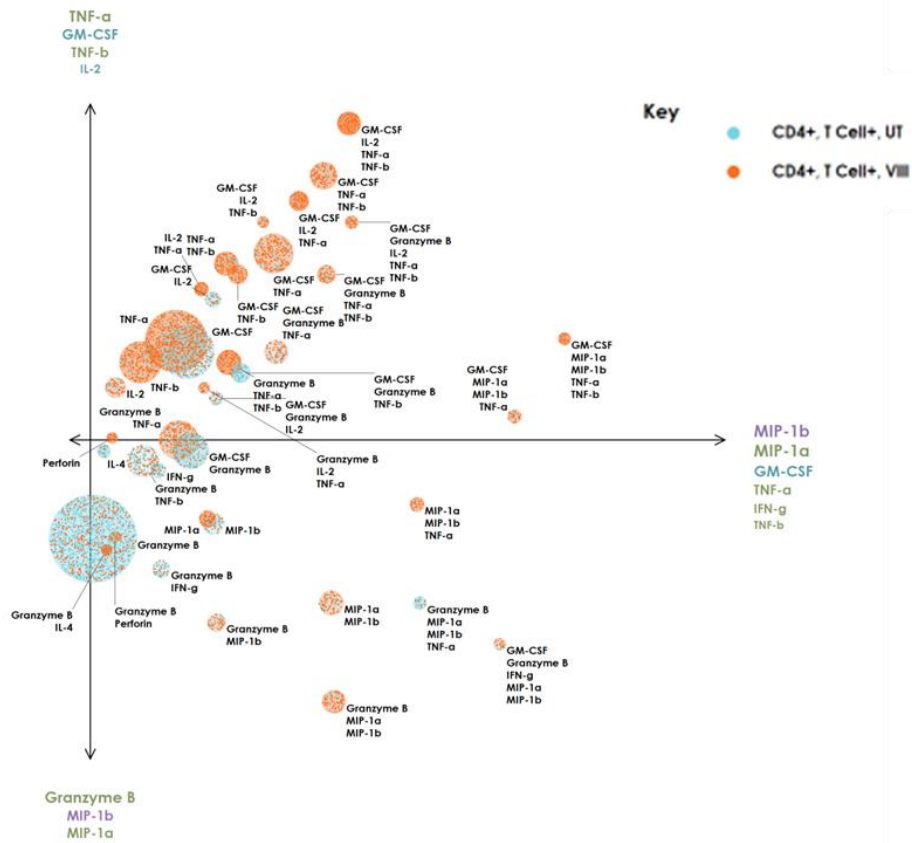


Figure 25. Effects of GMP Akt inhibitor VIII treatment on CD4 T-helper (Th) cells and polyfunctionality

(A) Graphs representing percentage of CAR CD4 Th1, Th2, Th17 and TREG subsets determined by flow cytometry post overnight stimulation at 1:1 with RAJI-WT targets, graphs show individual data points. (B) Total percentage of polyfunctional cells per sample \pm SD. Statistical comparisons were made against paired UT samples (C) Polyfunctionality Strength Index (PSI) calculated by multiplying the total percentage of polyfunctional cells with the secretion intensity of each cytokine grouped into effector, stimulatory, chemoattractive, regulatory and inflammatory subsets \pm SD. All statistical comparisons were made against paired UT sample in each subset. (D) Polyfunctionality Activity Topography (PAT), Principal Component Analysis (PCA) of CD4/CD8 subsets demonstrating primary polyfunctional profiles of CD4/CD8 T-cells where radius is proportional to secretion frequency. (A) n=6, (B-D) Determined using Isoplexis™ platform, following 20 hour 2:1 RAJI-WT:CAR stimulation, n=4. (A-C) Two tailed Mann-Whitney U test, ns P>0.05. *P<0.05 and ** P<0.01.

4.3.4. Effects of GMP Akt inhibitor VIII treatment on CAR T-cell transcriptome

To attain a global assessment of the effects of VIII treatment we next performed transcriptome analysis of CAR CD4/CD8 subsets from three independent donors. UT or VIII-treated CAR T-cells cryopreserved at end of manufacture were thawed and immediately sorted for CAR+ populations by flow cytometry. RNA was extracted and sequenced. Analysis revealed 417 and 609 significantly differentially expressed transcripts in CAR CD4s and CD8s, respectively. Principal Component Analysis (PCA) revealed some variability between donors analysed however, showed general clustering based on treatment, Figure 26A.

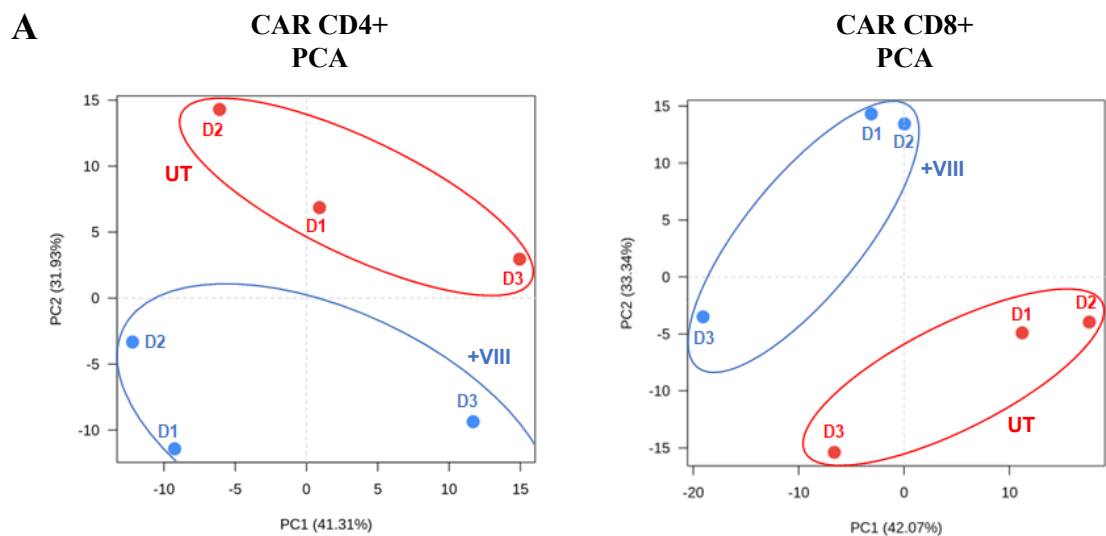
Count based enrichment tests on differential genes mapped to the Gene Ontology Pathway Database demonstrated downregulation of transcripts specific to leukocyte migration, activation, lymphocyte differentiation and proliferation pathways in CAR CD4 T-cells treated with VIII, Figure 26B. Conversely, CAR CD8 T-cells treated with VIII instead revealed upregulation of transcripts specific to leukocyte migration, T-cell activation, and autophagy, Figure 26C.

Further analysis of individual genes represented in CAR CD8 pathways showed a large, significantly upregulated signature for T-cell activation following VIII treatment, including co-stimulatory CD28 and ICOS transcripts, consistent with increased CD28 expression seen by flow cytometry. We additionally saw significantly downregulated Granzyme A (GZMA), Granzyme M (GZMM) and FASLG transcripts specific to effector function. Consistent with the decreased Granzyme B (GZMB) expression seen by flow cytometry, Figure 26C.

These findings were comparable with previous transcriptome analysis of CD19 targeting CAR T-cells with a CD28 ζ endodomain following *ex-vivo* manufacture with or without VIII. This study found VIII to act in a manner dependent on the FOXO1 transcription factor (Klebanoff et al., 2017). FOXO1 has been described as essential for the maintenance and longevity of Tn cells (Kerdiles et al., 2009), it is sequestered in the cytoplasm under active Akt signalling conditions and shows nuclear accumulation following Akt inhibition (Greer and Brunet, 2005). The study showed upregulated transcripts for SELL, IL7R, KLF2, S1PR1 and S1PR2 (Klebanoff et al., 2017), which are directly regulated by FOXO1 (Kerdiles et al., 2009) following VIII treatment. Additionally, overexpression of a mutant phosphorylation resistant FOXO1, permitted nuclear accumulation and generation of CAR T-cells with a memory profile like those treated with VIII (Klebanoff et al., 2017). On the assessment of our transcripts, VIII-treated CD8 CAR T-cells showed a similar dependency on FOXO1 with significantly upregulated transcripts of SELL, IL7R, KLF2 and S1PR1, Figure 26C. Despite seemingly differential pathway effects between CD4/8 CAR T-cells, CD4 CAR T-cells also showed upregulated FOXO1 dependent, SELL and IL7R transcripts and upregulated co-stimulatory CD28 and ICOS transcripts like CD8 CAR T-cells following VIII treatment, Figure 26D. Suggesting that inhibition of Akt signalling has some comparable effects on both CD4/8 CAR T-cells. Almost identical transcriptional profiles were also seen in an independent study of spleen and lymph node derived CD8 T-cells activated and cultured in the presence of VIII (Macintyre et al., 2011).

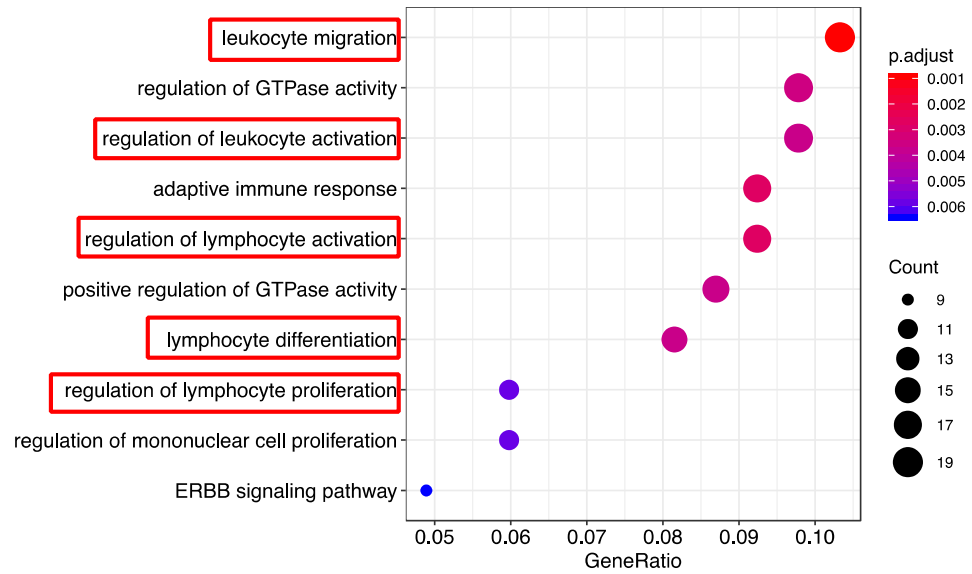
Overall, transcript profiles following VIII treatment correlate with less differentiated Tn and Tcm subset profiles. SELL, the gene encoding CD62L was significantly upregulated

in both CAR CD4/CD8 T-cells. CD62L expression is associated with Tn/Tcm subsets where expression correlates with effective adoptive therapies (Klebanoff et al., 2012). CD62L expression is often lost following T-cell activation in a Akt dependent manner (Abu Eid et al., 2015) but shows preservation here following VIII inhibition. Other transcripts including IL7R, KLF2 have further been associated with Tcm and T-cell persistence (Kerdiles et al., 2009, Macintyre et al., 2011). Upregulation of costimulatory CD28 and ICOS transcripts may further enhance CAR T-cell function by enhancing activation signals where CAR T-cells designed with both CD28 and ICOS endodomains show potent anti-tumour activity (Frigault et al., 2015). CD28 expression and downregulation of granzymes are also associated with less differentiated non effector Tn/Tcm subsets (de Koning et al., 2010, Gattinoni et al., 2017, Takata and Takiguchi, 2006), supported here with upregulated CD28 and reduced GZMA and GZMM transcripts.

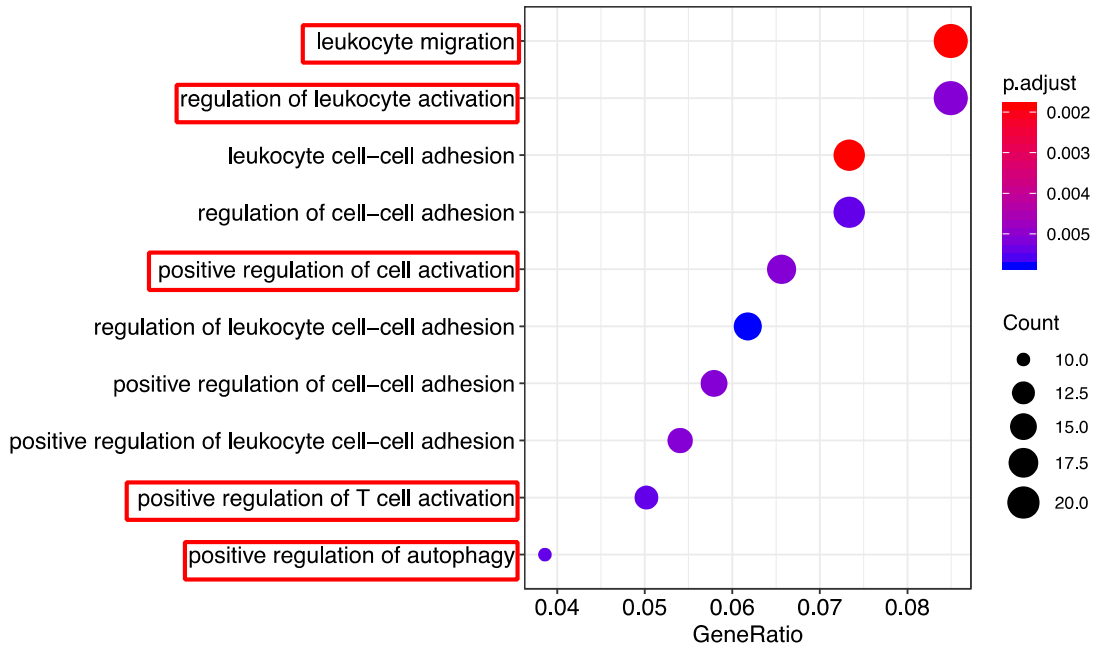


B

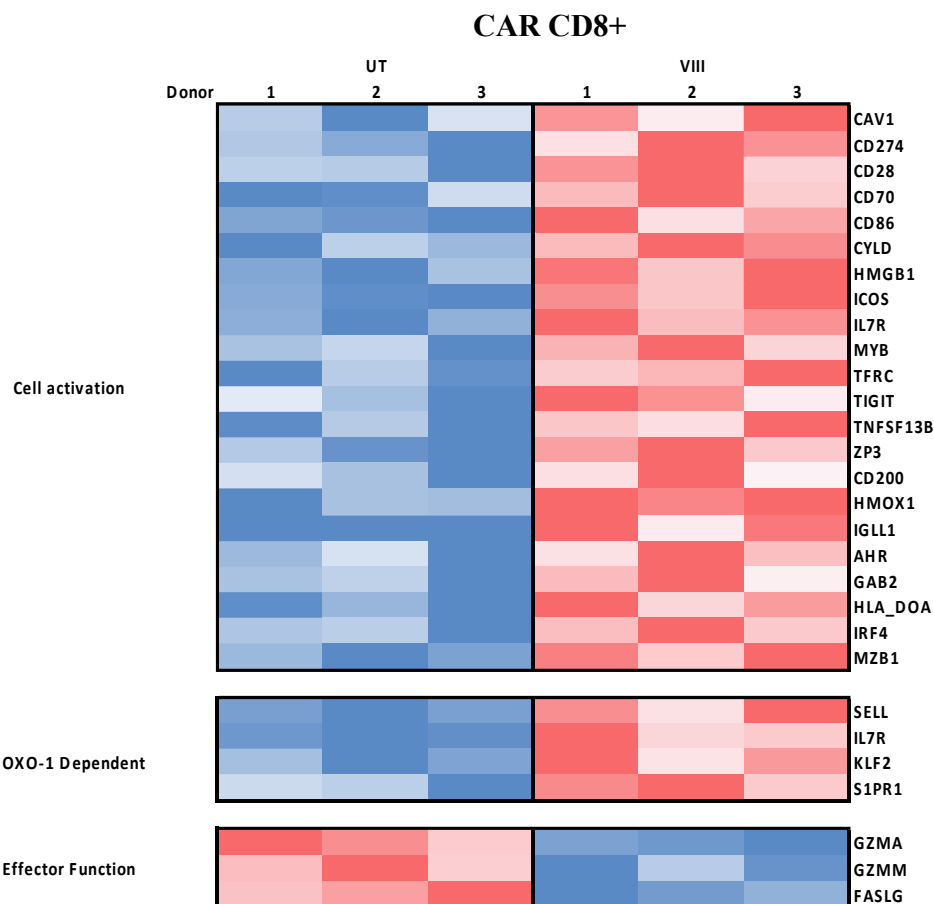
**CAR CD4+
Downregulated Pathways**



**CAR CD8+
Upregulated Pathways**



C



D

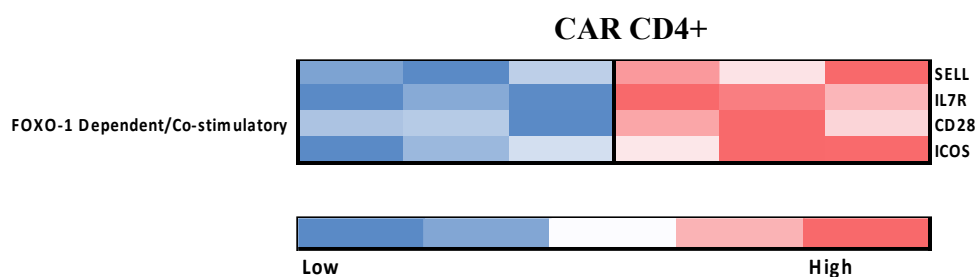


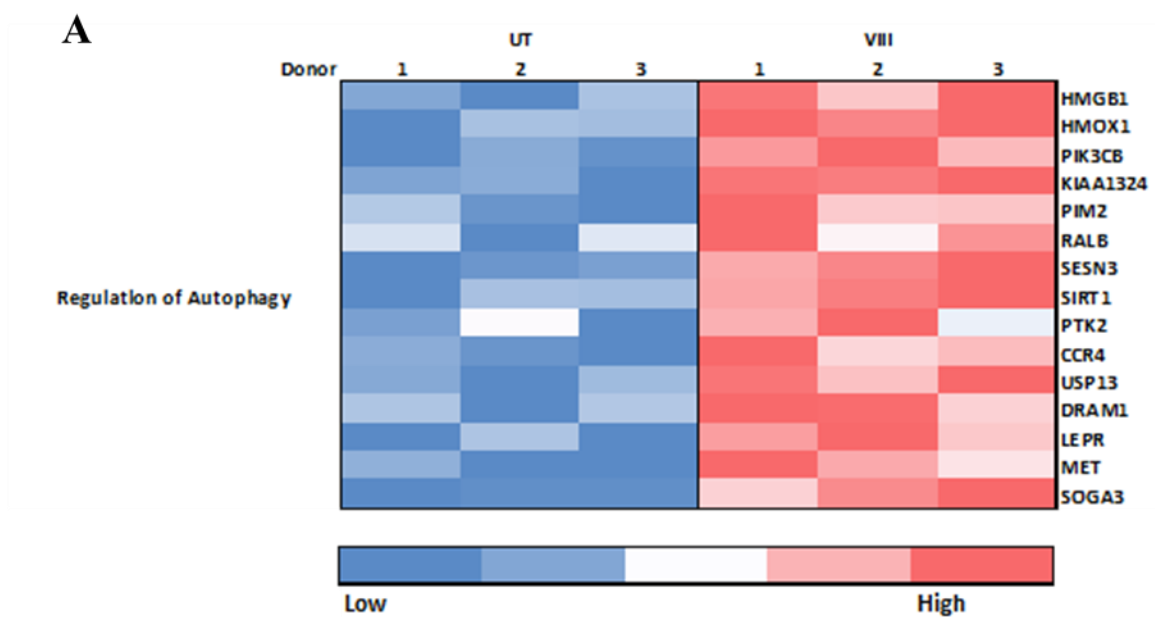
Figure 26. Effects of GMP Akt inhibitor VIII treatment on CAR T-cell transcriptome

(A) Principal component analysis (PCA) depicting transcript variation in CD4/CD8 CAR T-cells manufactured with (VIII) or without (UT) VIII treatment. Percentages represent variance in each component. (B) Dot plots of cellular pathways mapped to Gene Ontology database. Size of dots represents the number of genes contributing to a pathway, dot colour represents adjusted p-values and x-axis shows the fraction of mapped genes in each pathway. (C) Heat map representation of transcripts specific to cell activation, FOXO1 and effector function in CD8 CAR T-cells. (D) Heat

map representation of transcripts specific to FOXO1 and co-stimulatory transcripts in CD4 CAR T-cells. (C) and (D) Colour represents low to high transcript expression. Rows are specific to each gene and columns highlights expression in each donor following manufactured with (VIII) or without (UT) VIII treatment. Only significantly differentially expressed pathways and genes are included in figures at a $p < 0.05$ cut off. All data sets represent $n=3$.

4.3.5. Effects of GMP Akt inhibitor VIII treatment on CD8 CAR T-cell Autophagy, Mitochondria and Metabolism

Transcriptome analysis of CAR CD8 T-cells additionally revealed an upregulation in transcripts specific for autophagy following VIII inhibition, Figure 26B and Figure 27. Autophagy encompasses lysosome mediated degradation of cellular material to maintain cell homeostasis or for the removal of damaged organelles, misfolded proteins, or intracellular pathogens. Autophagy is orchestrated through a complex process and is inhibited during active PI3K/Akt signalling through mTOR (Glick et al., 2010), as summarised in Figure 27B. Inhibition has been shown to be reversible using rapamycin, an mTOR inhibitor. As Akt is a positive regulator of mTOR, it is unsurprising that VIII inhibition of Akt1/2 resulted in increased autophagy transcripts.



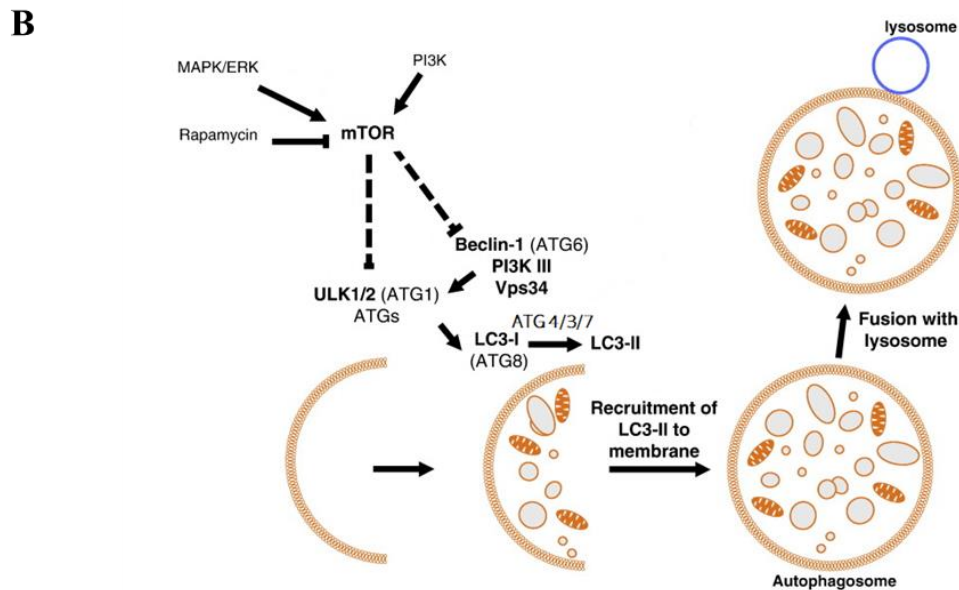


Figure 27. Autophagy signature in CD8 CAR T-cells and simplified autophagy pathway

(A) Heat map representation of autophagy signature in CAR CD8 T-cells. Colour represents low to high transcript expression. Rows are specific to each gene and columns highlights expression in each donor following UT/VIII manufacture. (B) Autophagy is initiated through phagophore formation via ULK1/2-ATG and Beclin-1/Vps34 complexes which can be directly inhibited by the mTOR pathway. LC3-I is converted to LC3-II via ATG4/7/3 to permit elongation and circularisation of autophagosomes. Fusion with lysosomes completes the degradation of cellular content, Adapted from (Deas et al., 2011).

The CYTO-ID[®] stain permits the detection of pre-autophagosomes, autophagosomes, and autolysosomal vesicles as a phenotypic measure of autophagy. Here, CYTO-ID[®] mean fluorescence intensity (MFI) assessment of VIII-treated total CAR and CD8⁺ CAR T-cell subsets showed increased autophagy by 61% and 46%, respectively, Figure 28A.

What role autophagy may play in CAR T-cells is unclear. Autophagy has been shown to aid T-cell survival by the removal of dysfunctional mitochondria (mitophagy) (Gupta et al., 2019, Glick et al., 2010) and has been implicated in fatty acid oxidation (FAO) (O'Sullivan et al., 2014). To investigate these, we used MitoTracker[™] Green to quantify the mitochondrial mass in live cells at end of manufacture which demonstrated a small

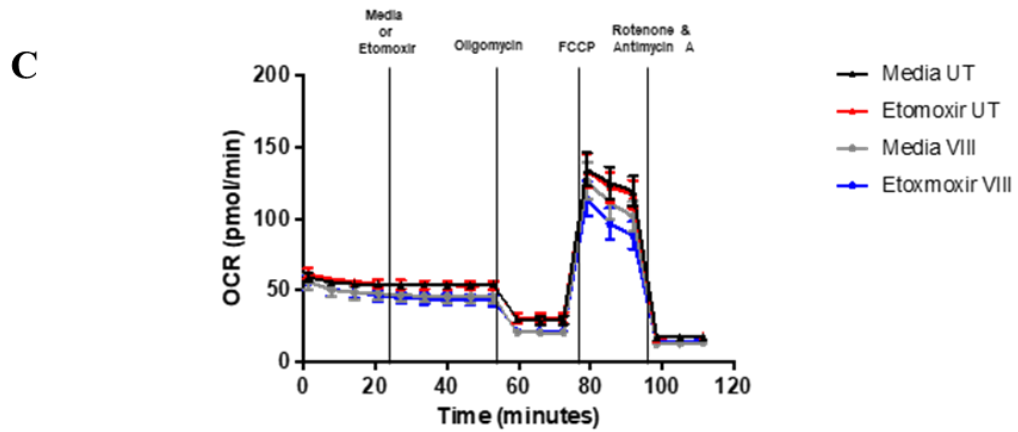
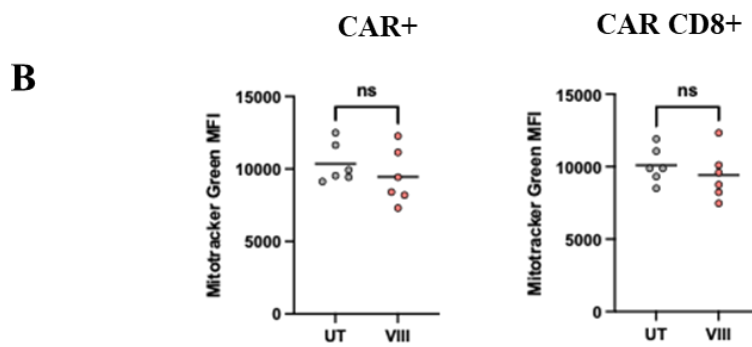
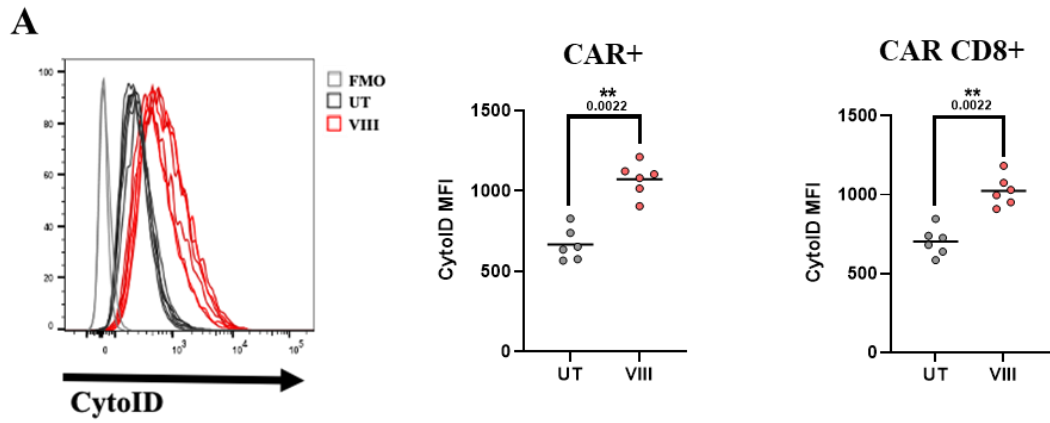
reduction in VIII-treated total CAR (-9%) and CD8⁺ CAR T-cell subsets (-7%), Figure 28B. To characterise FAO by oxygen consumption rate (OCR), CD8 T-cells were treated with etomoxir, a long chain fatty acid oxidation inhibitor of carnitine palmitoyltransferase-1 (CPT-1). FAO-dependent cultures show inhibition of maximal respiration following etomoxir treatment. The effect on maximal respiration can be assessed against a media only control. We showed a 2.8-fold reduction in maximal respiration following etomoxir treatment in VIII-treated CD8s, Figure 28C/D. Overall, this data suggests a trend towards increased mitophagy and FAO in VIII-treated CD8s, consistent with autophagy.

Tcm subsets have additionally been shown to have a greater capacity for mitochondrial respiration over Tn/Te/Tte as measured by OCR reading for spare respiratory capacity (SCR) (van der Windt et al., 2012). An increase in SCR has been reported in VIII-treated TILs (Crompton et al., 2015) however, the same was not replicated in another study of tumour reactive T-cells, which showed no change following VIII treatment. This may be attributed to variations in VIII concentrations used or stimulation methods. Here, despite phenotypic trends towards Tcm, OCR readings showed no change in SCR in VIII-treated CAT CAR CD8 T-cells, Figure 28C/D.

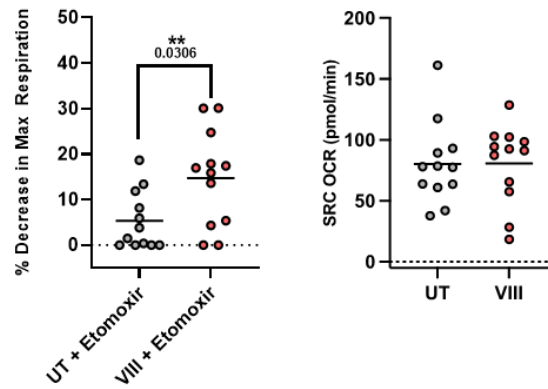
Metabolic CAR T-cell fitness correlates with anti-tumour efficacy (Kawalekar et al., 2016, Sabatino et al., 2016). Research has shown that PI3K inhibitors and the mTOR inhibitor rapamycin can increase mitochondrial membrane potential ($\Delta\Psi_m$) however, the effects of VIII treatment on CAR T-cell $\Delta\Psi_m$ have not been characterised. In T-cells, low- $\Delta\Psi_m$ has been associated with superior persistence (Sukumar et al., 2016) however, high- $\Delta\Psi_m$ represents energy stored that can ultimately be used to produce ATP and has been shown to enhance CD8 effector function (Amitrano et al., 2021). $\Delta\Psi_m$ measurements using the JC-1-dye revealed a 4/4.9-fold increase in $\Delta\Psi_m$ in VIII-treated total CAR and CAR CD8s, respectively, Figure 28E, representing an increased capacity to produce ATP.

Whilst AKT can regulate glycolysis (Frauwirth et al., 2002, Wieman et al., 2007), investigators report variable effects of VIII treatment on glycolysis (Klebanoff et al., 2017, Mousset et al., 2018). This may be attributed to experimental variations, with assessments

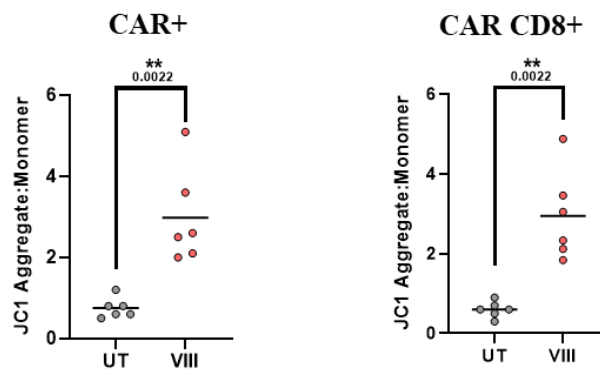
in bulk T-cells and failure to report whether assessments were carried out in the presence/absence of VIII. Time post stimulation and stimulation methods may have further impacts. Here, we focused our assessments on end of manufacture VIII-treated CD8s which showed no changes in basal or glycolytic capacity compared to UT CD8s following assessments in the absence of continual VIII treatment, Figure 28F/G. Together, the data demonstrates a metabolically charged phenotype in VIII-treated CD8s capable of supporting enhanced function.



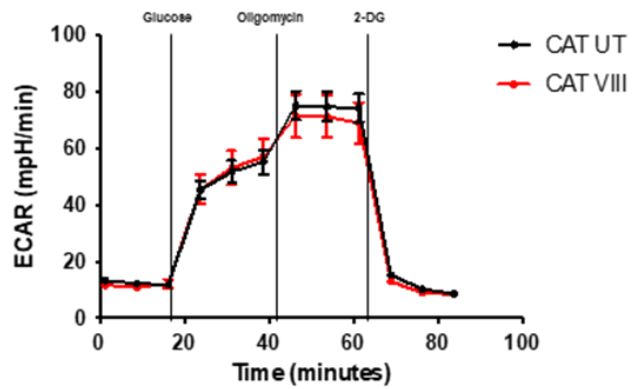
D



E



F



G

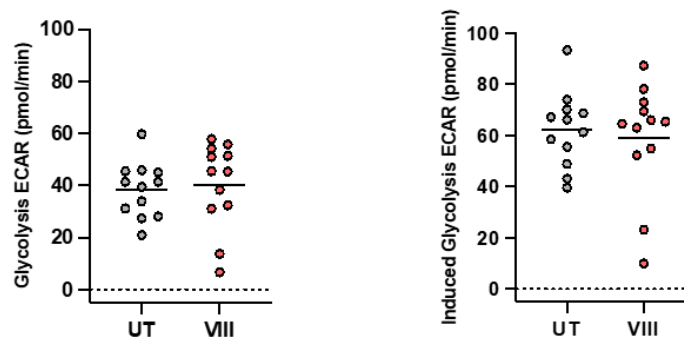


Figure 28. Effects of GMP Akt inhibitor VIII treatment on CD8 CAR T-cell Autophagy, Mitochondria and Metabolism

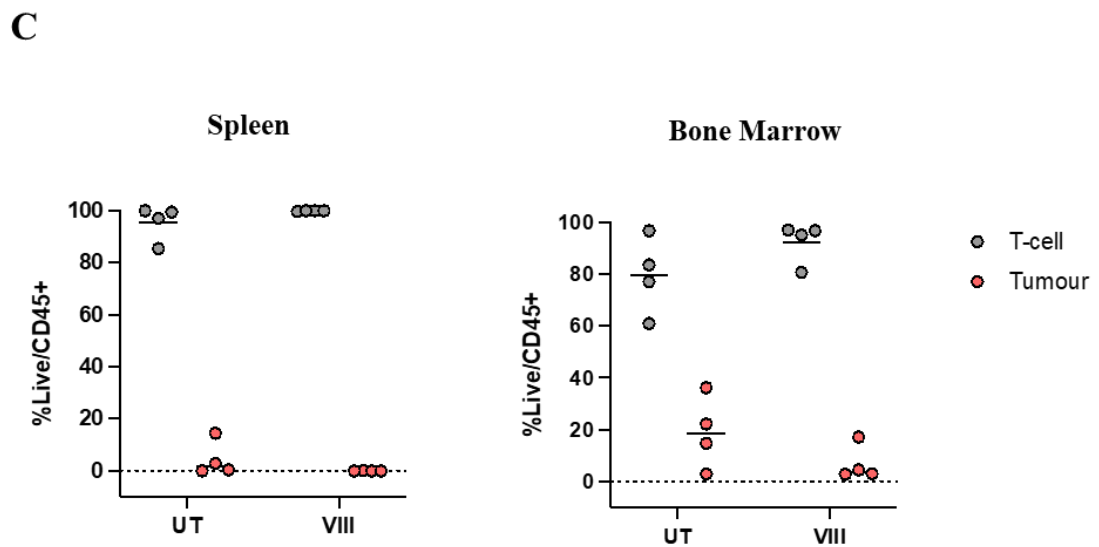
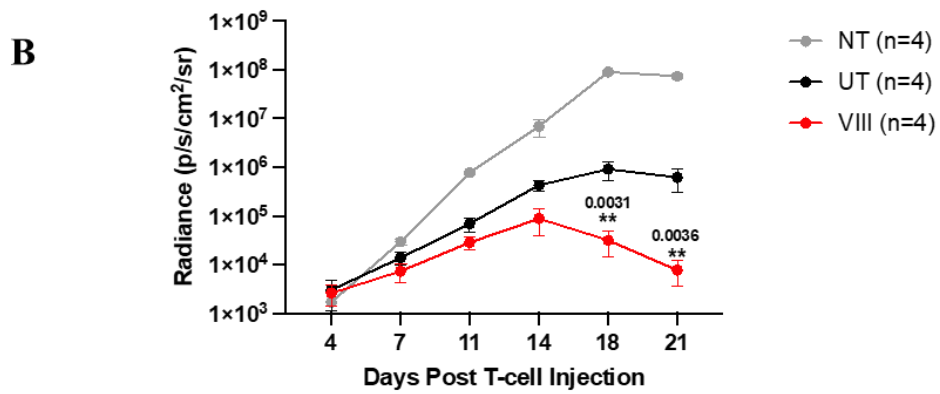
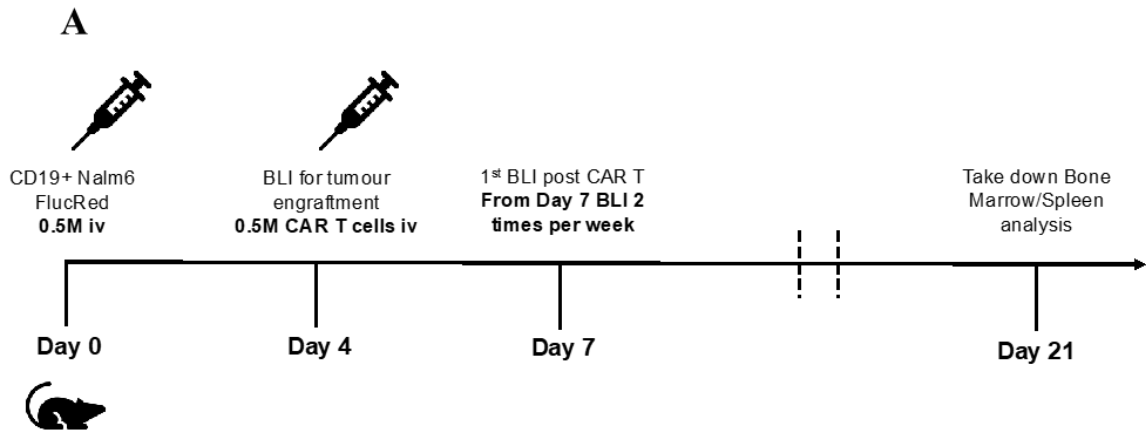
(A) Histogram and MFI representation of CytoID[®] staining for autophagic vesicles in total CAR and CD8 CAR T-cells. (B) Mitochondrial mass determined using MitroTracker Green[™] measured by MFI in total CAR and CAR CD8 T-cells. (C) Oxygen consumption rates (OCR) in CD8 T-cells treated with etomoxir or media control. (D) Graphs representing decrease in maximal respiration following etomoxir treatment compared to media alone and mitochondrial spare respiratory capacity (SCR). (E) $\Delta\Psi_m$ of total CAR and CAR CD8 T-cells using the JC-1[™] dye, ratio of aggregate (red) to monomer (green) fluorescence. (F) Extracellular acidification rates (ECAR) in CD8 T-cells. (G) Graph representing basal and maximal glycolysis. (A/B/E) n=6, depicting individual data points. (C/D/F/G) Seahorse experiments represent pooled data from two independent experiments, n=6 each \pm SEM. (A/B/D/E/G) Two tailed Mann-Whitney U test, ns $P>0.05$. * $P<0.05$ and ** $P<0.01$.

4.3.6. Effects of GMP Akt inhibitor VIII treated CAR T-cells *in-vivo*

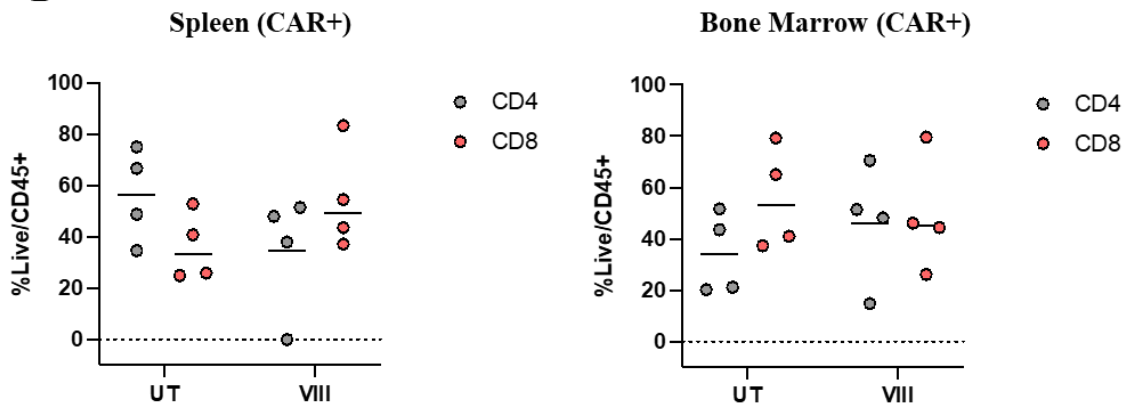
Following Tcm phenotypic traits, increased cytokine release, improved expansion, and increased cytotoxicity at rechallenge, we lastly determined whether VIII-treated CAR T-cells could improve anti-tumour activity *in-vivo*. Systemic ALL was established in NOD scid γ (NSG) mice using B-ALL cell line, NALM6. Mice were either treated with a low dose of 5×10^5 untreated (UT), VIII-treated (VIII) CAR T-cells or non-transduced (NT) T-cells as a control, from a single healthy donor Figure 29A. Bi-weekly bioluminescent imaging (BLI) revealed improved tumour control in all mice treated with CAR over NT T-cells. VIII-treated mice had significantly reduced tumour burden compared to the UT group Figure 29B. At Day 21, the VIII-treated group showed persisting T-cells and a virtual absence of tumour in the spleen and BM over the UT group, Figure 29C.

Isolated CAR T-cells revealed greater preservation of VIII-treated CD8s in the spleen and increased proportions of VIII-treated CD4s in the BM, revealing a more balanced CD4:CD8 ratio at the late D21 timepoint, Figure 29D. Phenotype analysis demonstrated a trend of preserved Tn/Tcm and reduced Te CAR subsets in the BM of VIII-treated mice, Figure 29E. Total VIII-treated CAR cells from the BM had greater proportions of CCR7⁺/CD27⁺ total CAR T-cells and CD27⁺/CD28⁺ VIII-treated CD8s at the D21

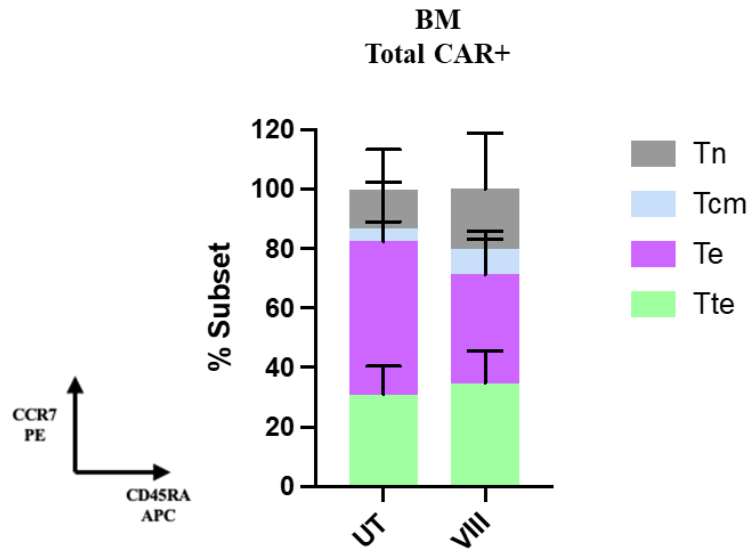
timepoint, Figure 29F , where such phenotypes have been found to positively correlate with response (Deng et al., 2020, Fraietta et al., 2018).



D



E



F

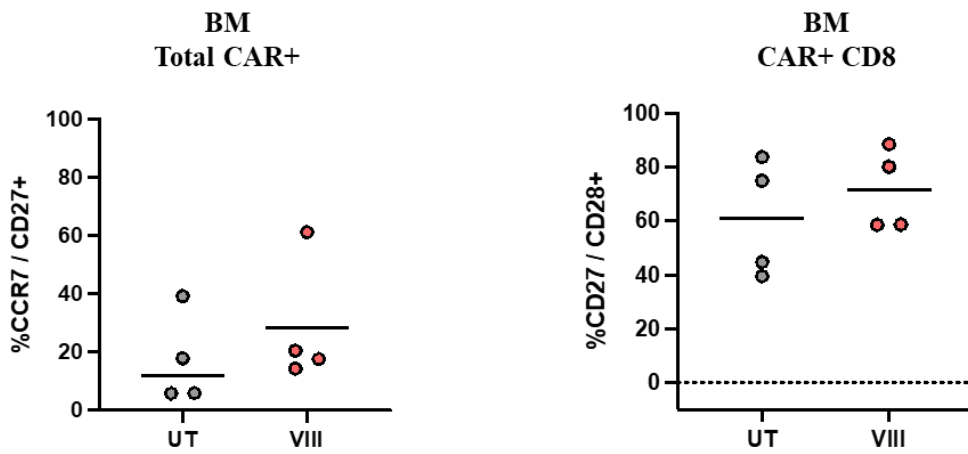


Figure 29. Effects of GMP Akt inhibitor VIII treated CAR T-cells *in-vivo*

(A) Schematic of tumour mouse model. (B) Tumour burden measured by BLI in NALM6 tumour established mice treated with NT T-cells or UT/VIII CAR T-cells, \pm SEM (C) Residual percentages of total T-cell and tumour cells in mouse spleen and BM at Day 21, individual data points (D) Percentage of CAR+ CD4/8s in spleen and BM at Day 21, individual data points. (E) Graphical representation of Tn (CCR7+/CD45RA+), Tcm (CCR7+/CD45RA-), Te (CCR7-/CD45RA-) and Tte (CCR7-/CD45RA+) subsets in total CAR T-cells at Day 21, \pm SD. (F) Frequencies of (CCR7+/CD27+) in total CAR T-cells and (CD27+/CD28+) in CD8 CAR T-cells from BM at Day 21, depicting individual data points. (B-F) Cells derived from one healthy donor, n=4 mice per group. (B) Two-way ANNOVA corrected for multiple comparisons by Tukey's test on log transformed data, ns P>0.05 and ** P<0.01. (C/D) Two-way ANNOVA corrected for multiple comparisons by Bonferroni's test, ns P>0.05. (E/F) Two tailed Mann-Whitney U test, ns P>0.05.

4.4. Discussion

Pre-clinical and clinical studies of adoptive T-cell immunotherapy demonstrate that Tscm/Tcm subsets outperform Tem/Tte subsets providing greater proliferative capacity, enhanced metabolic T-cell fitness and superior anti-tumour responses (Gattinoni et al., 2005, Graef et al., 2014, Hinrichs et al., 2011).

Prior studies manufacturing CD19-targeting CAR T-cells with VIII inhibition show Tcm subset enrichment and superior *in-vivo* anti-tumour responses (Klebanoff et al., 2017, Urak et al., 2017). The clinical use of VIII is confounded by its lack of availability in GMP grade. We overcame this by procuring the drug at GMP grade. Titration revealed a higher 2.5 μ M concentration over 1 μ M previously tested (Klebanoff et al., 2017, Urak et al., 2017) affected expansion throughout manufacture, but resulting CAR T-cells conferred superior expansion and cytotoxicity against tumour target. As expansion drives differentiation (Ghassemi et al., 2018, Akbar and Henson, 2011), this provided an additional advantage of limiting unnecessary expansion. Consistent with prior studies, manufacture of CAT CAR with VIII inhibition conferred Tscm/Tcm enrichment, superior *in-vitro* expansion and cytotoxicity against target (Klebanoff et al., 2017, Urak et al.,

2017) We found superior tumour control *in-vivo* with a trend towards a greater proportion of circulating Tn/Tcm and CCR7+/CD27+ CAR T-cells, previously found to positively correlate with response (Deng et al., 2020, Fraietta et al., 2018).

Transcriptional analysis primarily implicated an upregulation of transcripts regulated by transcription factor FOXO1 and autophagy. Transcriptional dependency on FOXO1 has been previously demonstrated by other studies following Akt inhibition (Macintyre et al., 2011, Klebanoff et al., 2017) and is increasingly implicated as a target to enhance CAR T-cell therapy. FOXO1 is required for the maintenance of Tscm properties in T-cells (Delpoux et al., 2021) and inducible expression of FOXO1-3A, resistant to Akt mediated phosphorylation with sustained nuclear retention in CAR T-cells led to a preserved less differentiated Tscm/Tcm phenotype and improved CAR T-cell expansion in an *in-vivo* ovarian tumour model (Smole et al., 2022). This data highlights that evaluating the role of FOXO1 beyond CAR T-cell manufacturing for maintained functional benefits *in-vivo* is worthy of further investigation.

Our investigations are the first to describe enhanced autophagy in CAR T-cells following *ex-vivo* Akt inhibition. Previous work in CD8 virus specific T-cells found autophagy was critical to the survival of effector T-cells that form memory during the T-cell contraction phase, by aiding the elimination of misfolded or protein aggregates, reactive oxygen species (ROS) and dysfunctional or damaged mitochondria (mitophagy) (Xu et al., 2014a). CD8 T-cells with increased autophagy have been shown to have improved proliferation, cytotoxicity, and cytokine production. Whereas blocking autophagy led to the accumulation of depolarised mitochondria associated with T-cell exhaustion (Swadling et al., 2020). Autophagy has further been shown to regulate fatty acid oxidation (FAO) via the breakdown of lipid stores (Singh et al., 2009), vital for the generation and maintenance of memory T-cells (Sabatino et al., 2016). Autophagy related Atg7 molecule deficient tumour cells have been shown to have reduced FAO and defective mitochondria (Guo et al., 2013). Mitophagy has additionally been shown to promote self-renewal and persistence (Vannini et al., 2016, Kishton et al., 2017). Consistent with prior studies, our assessments of mitochondrial mass and FAO shows increased mitophagy and FAO in

VIII-treated CD8s, supporting survival. The results implicate that modulating autophagy is an attractive target of further investigation to enhance CAR T-cell therapy.

A potential caveat of utilising VIII inhibition was reported where T-cells stimulated with dendritic cells (DCs), cultured with VIII skewed CD4 Th differentiation towards Th2, impairing CD8 T-cell polyfunctionality (Mousset et al., 2020). A similar effect was seen in CAR T-cells treated PI3K inhibitor duvelisib, with increased frequencies of proliferating Th2 cells although this was accompanied by Th1 polarisation (Funk et al., 2022). Here, single cell cytokine assessments on the IsoplexisTM platform and intracellular staining following CD19-target stimulation failed to show a skew towards Th2 or TREGs. This may be attributed to the testing of CAR T-cells versus endogenous T-cells, differential stimulation methods and the higher 18 μ M VIII concentrations previously tested (Mousset et al., 2020). Although CBA analysis from co-culture with targets revealed an increase in IL-4 and IL-10 cytokines following VIII treatment, these were detected at low concentrations of ≤ 121.3 pg/ml. Th1/Th2 responses demonstrate some cross-regulation where responses are often described as co-inhibitory, dominated by either Th1 or Th2 (Fishman and Perelson, 1994). Whilst we see a cytokine pattern dominated by Th1 we also saw an increase in Th2 cytokines, although without a skew towards Th2 subsets by Isoplexis and flow cytometry characterisation. This could partly be explained by cross-regulation where a study demonstrated that IL-2/IFN- γ significantly enhanced IL-4 production from Th2 in the presence of B-cells (Singh and Agrewala, 2006). Additionally, CBA measurements were carried out in supernatant from mixed CD4/8 co-cultures and evidence indicates that CD8 T-cells can also produce cytokines associated with Th2 (Lev Bar-Or, 2000, Nakamura et al., 2005).

Our results instead revealed a skew toward Th1 and Th17 profiles with the production of predominantly effector and stimulatory GM-CSF, IL-2, TNF- α and TNF- β cytokines. Th1 subsets are associated with superior anti-tumour activity for their ability to secrete IFN γ and support CD8 T-cells (Nishimura et al., 2000, Wilde et al., 2012). Other studies show that the transfer of polarised Th17 cells has greater anti-tumour activity than Th1 polarised cells with a less differentiated phenotype, akin to Tscm (Muranski et al., 2011, Martin-Orozco et al., 2009). This provides them with a capacity to self-renew and harbour

a degree of plasticity. Indeed, repetitive stimulation of Th17 cells *in-vitro* has been shown to result in progeny with Th1 features (Muranski et al., 2011, Hamaï et al., 2012). Th1/Th17 subset enrichment may be attributed to ICOS, which we observed to be enriched in VIII-treated CAR CD4 T-cells by transcriptome analysis. Previous studies implicate ICOS in the induction and regulation of Th1/Th2 and Th17 responses (Wilson et al., 2006, Wikenheiser and Stumhofer, 2016). This is further supported in CAR T-cells where CAR T-cells engineered with an ICOS endodomain conferred Th1/Th17 bipolarisation with improved persistence compared to CD28 ζ /4-1BB ζ endodomain CAR T-cells (Guedan et al., 2014). IL-6 was also found to be increased in VIII-treated CAR T-cells and has been shown to drive Th17 differentiation and maintenance (Korn and Hiltensperger, 2021), further supporting the Th17 skew observed in our VIII-treated CAR co-cultures. IL-6 additionally positively correlated with therapeutic response and tumour control in a study of CAR T-cell treated chronic lymphocytic leukaemia (CLL) patients (Fraietta et al., 2018).

The effects of VIII inhibition on oxidative phosphorylation (OXPHOS) and glycolysis have varied between studies. Studies have shown differential effects on non-engineered T-cells and CAR T-cells where the presence of the signalling endodomain in the latter can directly impact metabolism (Crompton et al., 2015, Klebanoff et al., 2017, Mousset et al., 2018). Tn/Tcm subsets are recognised to be dependent on oxidative phosphorylation (OXPHOS) and FAO whereas activated Te cells are associated with enhanced glycolysis (Zhang et al., 2021). Overall, our metabolic profiles demonstrate hybrid features of longevity (Tn/Tcm) and effector (Te) function.

The literature suggests that low- $\Delta\Psi_m$ is associated with superior T-cell persistence (Sukumar et al., 2016), and that high- $\Delta\Psi_m$ is associated with CD8 effector function (Amitrano et al., 2021), supporting a Te profile. Our data shows results consistent with a Te profile, in that we observe no overt change in glycolysis, no increase in SRC and high- $\Delta\Psi_m$ in VIII-treated CD8 T-cells. A small increase in FAO in our experiments supports the emergence of a Tcm profile following VIII treatment, but in the absence of a change in glycolysis or SRC, it is likely that this is mechanistically an autophagy driven process rather than a global metabolic shift. Together, these findings support the presence of

multiple active metabolic pathways to support the energy requirements of rapid activation, expansion, and longevity in VIII-treated CD8s, corroborated by functional tests.

Together, the data demonstrates several mechanisms to support enhanced functionality following VIII treatment. As all experiments were carried out on healthy donor material, we next wanted to assess if VIII treatment could provide the same benefits in T-cells derived from B-ALL patients. CAR T-cell manufacture in adult patients is challenging, due to several factors which contribute to poor quality T-cells. We used T-cells from 6 patients enrolled on the ALLCAR19 trial, and manufactured CAR T-cells with and without VIII using our small-scale version of the Prodigy[®] manufacturing protocol to evaluate the effects on CAR T-cell phenotype and function.

Chapter 5. Effects of pharmacological VIII inhibition in patient derived CAT CAR T-cells, using the CliniMACS Prodigy[®] manufacturing protocol

5.1. Introduction

As highlighted in chapter 1, T-cell subset composition can vary significantly between patients, impacted by factors such as age, chemotherapy exposure and underlying cancer diagnosis (Lemal and Tournilhac, 2019, Rajat K. Das, 2018, Riches et al., 2013, Singh et al., 2016, Tu and Rao, 2016). Consistent with these, a study in DLBCL showed that patient T-cells had significantly fewer CD27+/CD28+ cells following chemotherapy, and cells lacking CD27/CD28 expression failed to proliferate following stimulation (Petersen et al., 2018).

We addressed this in our samples by comparing the baseline phenotype of B-ALL patient total T-cells to healthy donors using CCR7/CD45RA and CD27/CD28 markers. This revealed lower proportions of Tn (mean, 54.2% vs 29.4%) and greater Te (mean, 22.4% vs 31.1%)/Tte (mean, 6.3% vs 10.5%) subsets in adult patient material over healthy donors Figure 30A, with significantly fewer CD27+/CD28+ T-cells at baseline (mean, 81.7% vs 51.6% Figure 30B).

We further assessed the phenotype of CAT CAR T-cells manufactured as part of ALLCAR19 and CARPALL trials for adult and paediatric B-ALL, respectively. A subset of patients on the CARPALL trial were manufactured on the automated CliniMACS Prodigy[®] process (B), as depicted in Figure 18. The data was provided by Dr Claire Roddie and allowed us to compare products from the automated process (B) cohort from the adult ALLCAR19 trial with paediatric patients. We found baseline paediatric products had phenotypic profiles that more closely matched that of healthy donors, Figure 30A. Resulting CAR T-cell products from paediatric patients were significantly enriched in Tcm phenotypes and the frequency of memory phenotypes in adults was impaired where products composed primarily of Te subsets, characterised by CCR7/CD45RA (Roddie et al., 2021, Ghorashian et al., 2019), Figure 30C.

These findings support an overall poorer quality of T-cells derived from adult B-ALL patients compared with healthy donor and paediatric B-ALL patients. It was important to address if VIII inhibition could positively impact patient T-cells as per healthy donors or if VIII treatment would exhibit limitations in this suboptimal starting material.

CAR T-cells were manufactured at small-scale following the CliniMACS Prodigy[®] protocol as illustrated in, Figure 22 using excess leukapheresis from six B-ALL patients on the ALLCAR19 trial. These specific patient samples were selected as they represent two distinct groups with respect to outcome on the study. Three patients achieved long-term remission, and three patients relapsed with CD19+ disease following a loss of CAR T-cell persistence. We wished to determine whether the CAR T-cell product profile/functionality between the groups differed and whether VIII treatment could impact/improve these products with respect to phenotype, function, cytokines, autophagy, and mitochondrial activity/mass.

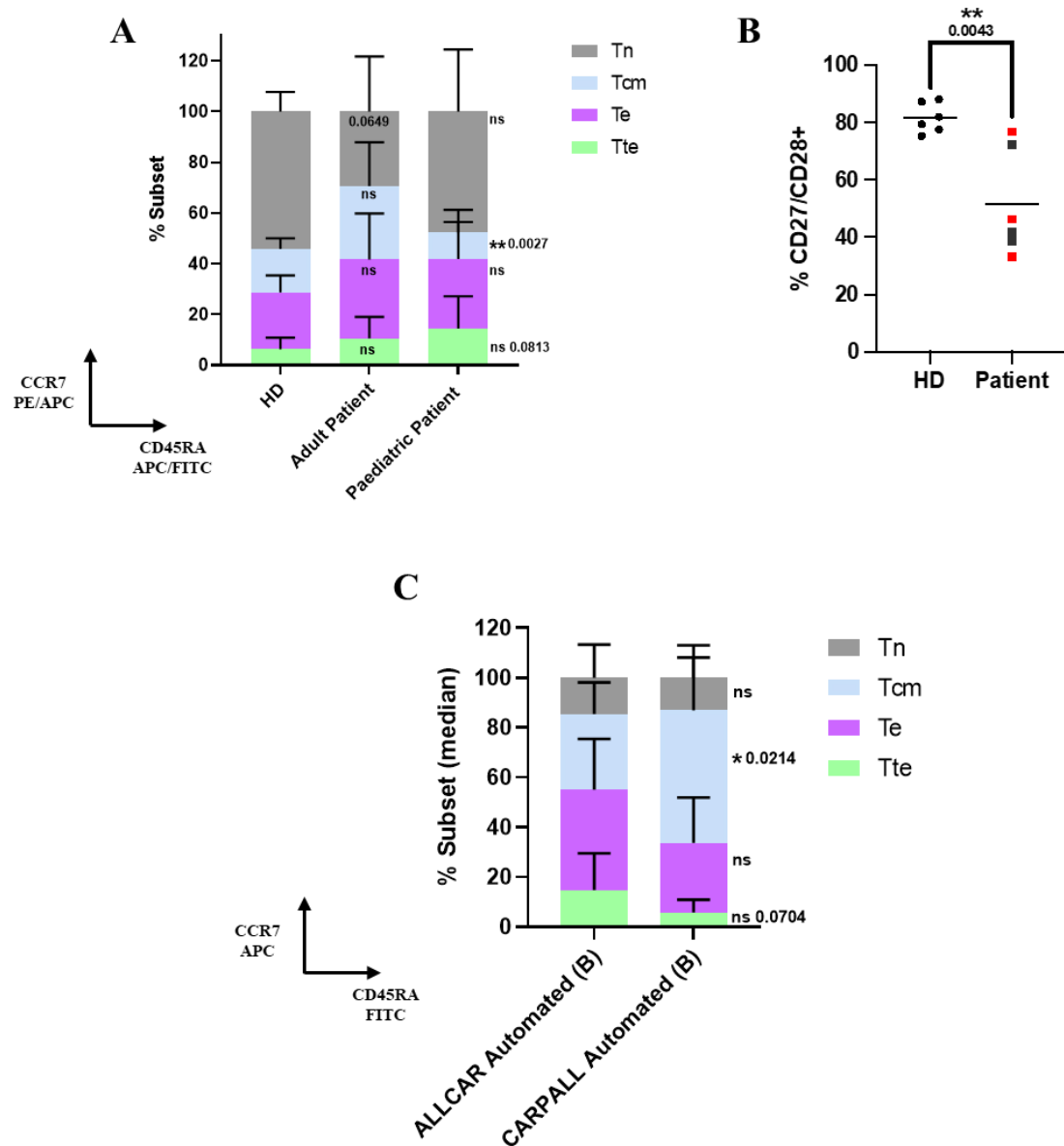


Figure 30. Phenotype comparison of T-cells from adult B-ALL patients with healthy donor and paediatric patients

(A) Graphical representation of Tn (CCR7+/CD45RA+), Tcm (CCR7+/CD45RA-), Te (CCR7-/CD45RA-) and Tte (CCR7-/CD45RA+) subsets in total T-cells from healthy donor (HD) (n=6), B-ALL adult (n=6) and B-ALL paediatric patients (n=8) at baseline determined by flow cytometry, \pm SD. (B) Percentage CD27+/CD28+ in total T-cells from HD and adult B-ALL patients at baseline, depicting individual data points. Black squares in patient group represent patients in remission and red squares represent patients with CD19+ relapse. (C) Mean CAR phenotype characterised as, Tn (CCR7+/CD45RA+), Tcm (CCR7+/CD45RA-), Te (CCR7-

/CD45RA-) and Tte (CCR7-/CD45RA+) subsets from adult and paediatric B-ALL patients manufactured as a part of ALLCAR19 (n=18) and CARPALL (n=8) trials, \pm SD. (A-C) Two tailed Mann-Whitney U test, ns $P > 0.05$, * $P < 0.05$ and ** $P < 0.01$. Statistical comparisons for (A) were made against HD for each patient group.

5.2. Assessing GMP Akt inhibitor VIII inhibitor in B-ALL patient derived T-cells

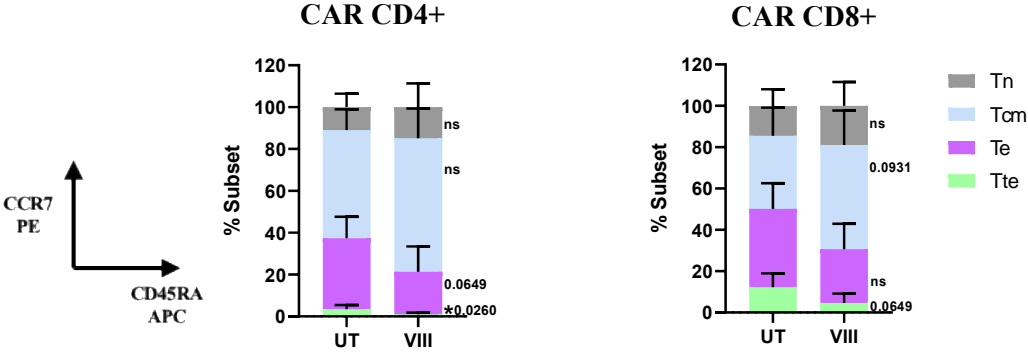
5.2.1. Effects of GMP Akt inhibitor VIII treatment on B-ALL patient phenotype

T-cells from six B-ALL patients were manufactured at small-scale, with/without GMP VIII inhibitor at 2.5 μ M. End of manufacture phenotype analysis by flow cytometry showed improved phenotype in VIII-treated CAR CD4/8 T-cells. Subsets were characterised using CCR7/CD45RA markers and showed general trends towards increased Tn/Tcm and decreased Te/Tte subsets following VIII treatment. Similar to healthy donors, a more marked Tcm enrichment was seen in VIII-treated CAR CD8s where, CAR CD4s demonstrated a 23.4% average increase but CAR CD8s increased by 42.6%, Figure 31A. The Tn subset was sub gated for FAS receptor CD95 expression to identify Tscm subsets known to confer superior persistence and proliferative capacity (Biasco et al., 2021, Gattinoni et al., 2011). VIII-treated total CAR T-cells showed a significant increase from mean 8.4% (UT) to 18.3% (VIII), Figure 31B.

Further extended phenotyping was carried out with CD27/CD28 markers. The absence of these markers is associated with T-cell senescence and differentiation (Gattinoni et al., 2017, Tu and Rao, 2016). A small non-significant increase in the percentage of CD27+/CD28+ CAR CD4s was seen in VIII-treated cells. However, a marked average increase by 3-fold of double positive cells was seen in VIII-treated CAR CD8s, Figure 31C. We also investigated IL-2 and Granzyme B secretion by CAR T-cells following stimulation where literature characterises Tcm subsets as IL-2 secreting but lacking cytotoxic molecules including Perforin and Granzymes (Mahnke et al., 2013, Sallusto et al., 1999, Xu and Larbi, 2017). Much like healthy donors, we similarly saw a significantly greater proportion of both CAR CD4 and CD8 T-cells producing IL-2 but not Granzyme B following manufacture in the presence of the VIII inhibitor. CD4 CAR T-cells had

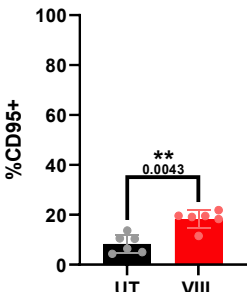
greater proportions of IL-2+/Granzyme B- cells at 2.5% (UT) vs 20.3% (VIII) whereas, CD8 CAR T-cells were lower 0.1% (UT) vs 4% (VIII), Figure 31D.

A

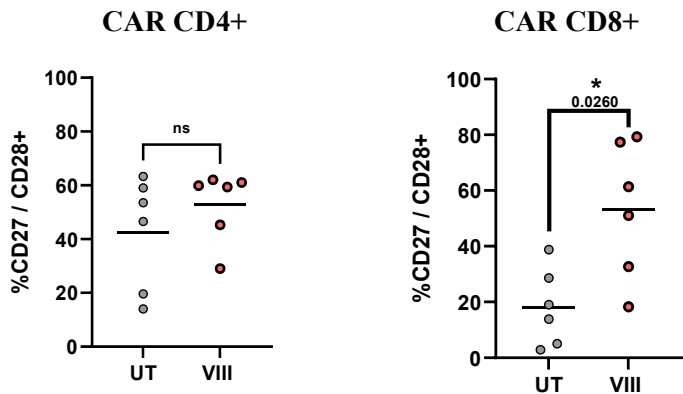


% CD95+ of Total CAR Tn

B



C



D

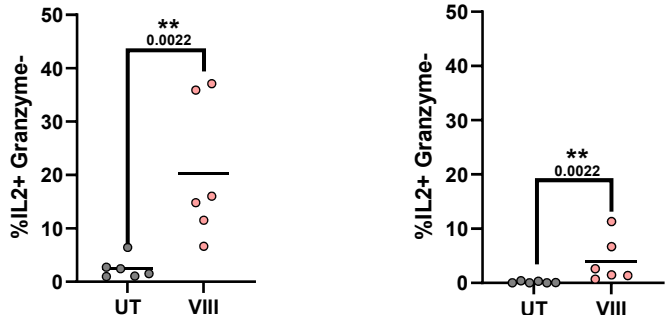


Figure 31. Effects of GMP Akt inhibitor VIII treatment on B-ALL patient phenotype

(A) Graphical representation of Tn (CCR7+/CD45RA+), Tcm (CCR7+/CD45RA-), Te (CCR7-/CD45RA-) and Tte (CCR7-/CD45RA+) subsets in CD4 and CD8 CAR T-cells determined by flow cytometry, \pm SD. (B) Percentage CD95+ positive, sub gated from Tn population, \pm SD/individual data points. (C) Percentage CD27+/CD28+ in CD4/8 CAR T-cells (D) Percentage of IL-2+/Granzyme- in CD4/8 CAR T-cells. (C-D) Markers at end of manufacture, determined by flow cytometry, graphs depicting individual data points. (A-D) n=6, Two tailed Mann-Whitney U test, ns P>0.05. *P<0.05 and ** P<0.01.

5.2.2. Effects of GMP Akt inhibitor VIII treatment on B-ALL patient derived CAR T-cell function and cytokines

Proliferative abilities of CAR T-cells were assessed in a 7-day co-culture against CD19+ RAJI-WT and CD19- RAJI-KO cell lines. Killing was assessed at both end of manufacture and at rechallenge where NT and CAR T-cells cultured with RAJI-WT targets in the 7-day co-culture were harvested and rechallenged in a killing assay against RAJI-GFP targets for 72-hours. Killing was determined by measuring the reduction in GFP by flow cytometry. Cytokine secretion was measured from media supernatant collected on Day 3 of the 7-day co-culture using the LEGENDplex™ Human Th Cytokine Bead Array (CBA) kit (BioLegend), against IL-2, IFN- γ , TNF- α , IL-4, IL-10, IL-6, IL-22, IL-17A and IL-17F cytokines.

In healthy donors, a marked increase in proliferation was seen in CD8 CAR T-cells but no change in expansion was seen in CAR CD4 T-cells following VIII treatment. Interestingly, in patient derived CAR T-cells VIII-treated CAR CD4 and CD8 T-cells both showed improved survival in absence of CD19 target against RAJI-KO and significant 5.7 and 5.3-fold expansion against RAJI-WT expressing CD19, Figure 32A.

Killing assessments in healthy donors revealed comparable killing against RAJI-GFP cells at the end of manufacture. Patient derived CAR T-cells however, retained high killing capabilities but showed a small reduction in cytotoxicity in VIII-treated conditions compared to UT at all E:T ratios. Yet, at rechallenge, VIII-treated CAR T-cells showed

improved cytotoxicity for all donors and by an average of 2.1, 3.1, 4.9 and 6.7-fold at 1:1, 1:2, 1:4 and 1:8 E:T, respectively, Figure 32B.

Cytokine analysis by CBA showed the same trend as healthy donors where VIII-treated cells were able to produce more cytokines associated with effector functions. A 403.4, 6.9 and 8.3-fold increase in IL-2, IFN- γ and TNF- α secretion, respectively was observed. Similarly, increases in IL-6, IL-22 and IL-17A were also seen following VIII treatment, and no differences were seen in IL-17F. Assessment of other regulatory cytokines showed a significant increase in IL-4 and IL-10 following VIII treatment, although present at low concentrations at an average of 21.4 (UT) vs 57 (VIII) pg/ml IL4 and 17 (UT) vs 63.6 (VIII) pg/ml, IL-10, Figure 32C.

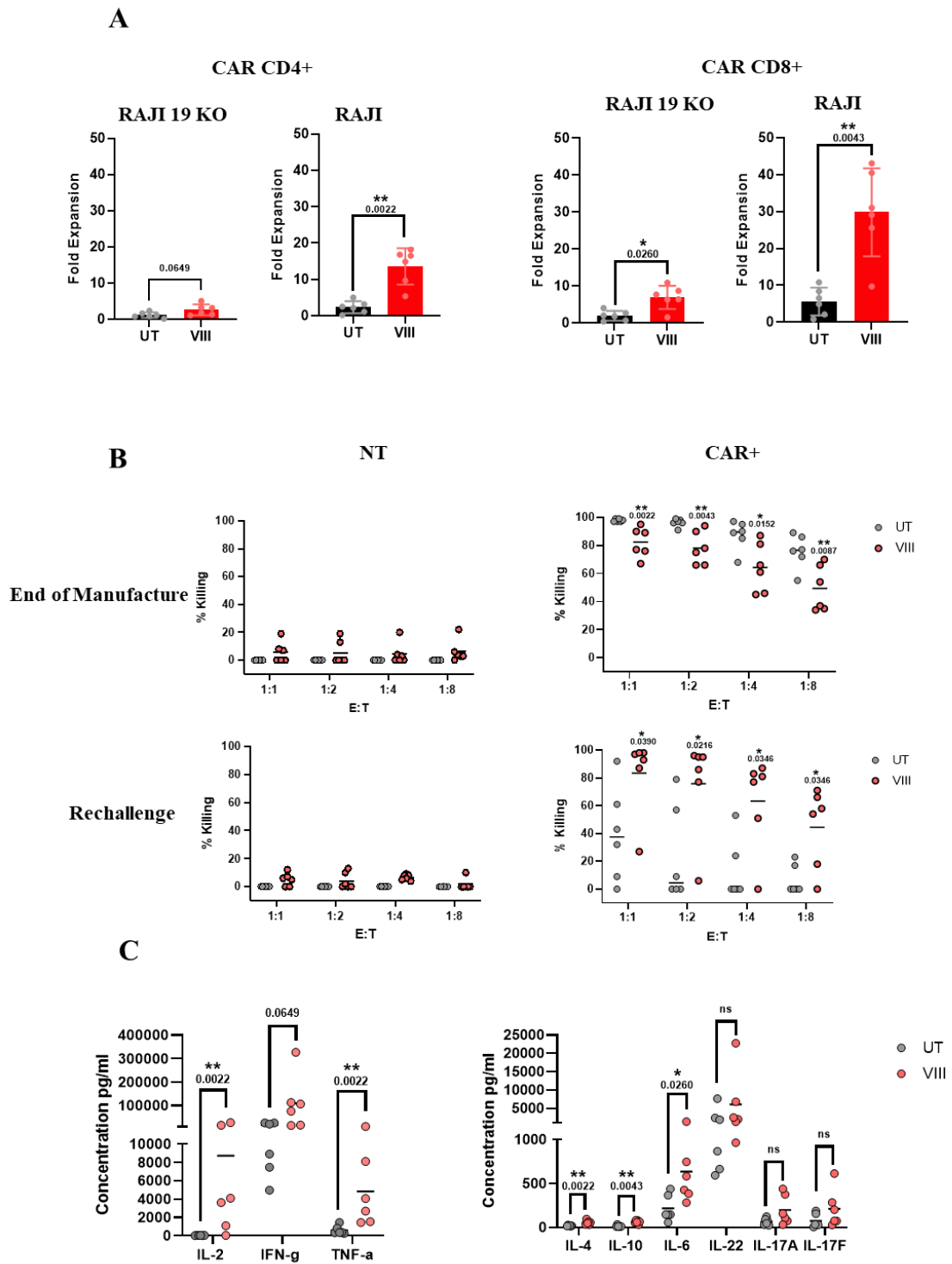


Figure 32. Effects of GMP Akt inhibitor VIII treatment on B-ALL patient derived CAR T-cell function and cytokines

(A) CD4/CD8 CAR fold expansion following a 7-day co-culture with irradiated RAJI-KO or RAJI-WT target cell lines. \pm SD/indivual data points. (B) Graphs depicting % killing of RAJI-

GFP target cells at the end of manufacture or post re-challenge by NT or CAR T-cells in a 72-hour killing assay. Results from all conditions were normalised to the untreated NT condition at each E:T ratio, graphs show individual data points. (C) Cytokine concentrations measured by CBA from Day 3 of the 7-day co-culture with RAJI-WT targets, graphs show individual data points. (A-C) n=6, Two tailed Mann-Whitney U test, ns P>0.05. *P<0.05 and ** P<0.01.

5.2.3. Effects of GMP Akt inhibitor VIII treatment on B-ALL patient derived CD4 T-helper (Th) cells and polyfunctionality

To identify functional CAR CD4 subsets at the end of CAR T-cell manufacture, T-cells were stained for Th1, Th2, Th17 and TREG specific surface markers and transcription factors. End manufacture CAR T-cells were stimulated overnight 1:1 with CD19 expressing RAJI-WT targets, stained for all markers, and evaluated by flow cytometry. Markers, transcription factors and cytokines used to characterise each subset were Th1 (CXCR3, T-bet, IFN- γ), Th2 (CCR4, CCR6, GATA3, IL-4), Th17 (CCR4, CCR6, ROR γ t, IL-17A) and TREG (CD127, CD25, FOXP3, IL-10). Overall, results in patients were more variable but demonstrated the same trend as healthy donors with 1.7 and 9-fold enrichment of Th1 and Th17 subsets in CD4 CAR T-cells manufactured in the presence of VIII inhibitor. No differences were seen Th2 or TREG subsets following VIII treatment, Figure 33A.

We have previously shown that VIII treatment predominantly impacts measures of polyfunctionality through the production of the effector cytokines IL-2, IFN- γ , TNF- α and GZMB. For this reason, we assessed polyfunctionality for B-ALL patient-derived products using intracellular flow cytometry for these cytokines/chemotoxins following stimulation with RAJI-WT targets. Consistent with results from the Isoplexis platform in healthy donor T-cells, patient VIII-treated CAR T-cells showed increased production and polyfunctionality in relation to effector cytokines and a reduction in GZMB, Figure 33B.

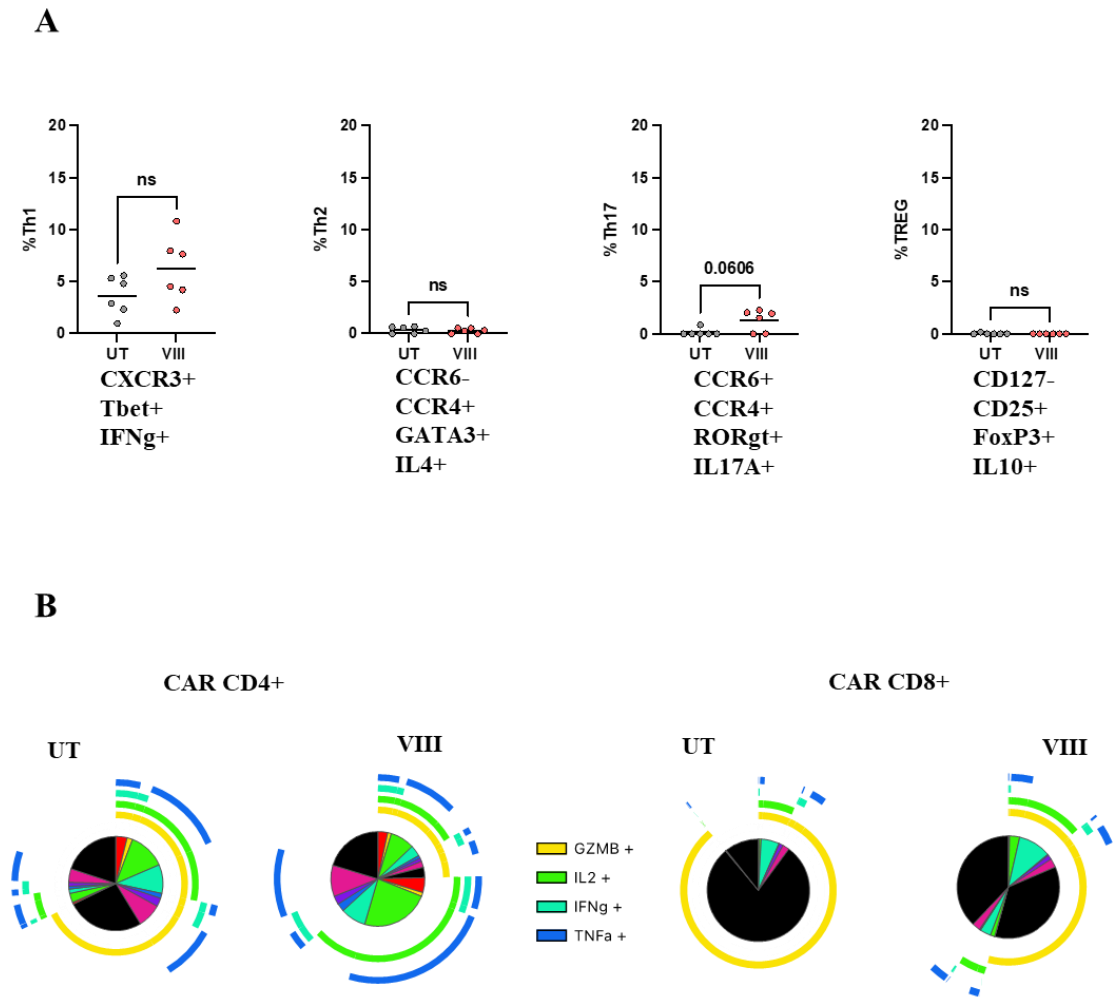


Figure 33. Effects of GMP Akt inhibitor VIII treatment on B-ALL patient derived CD4 T-helper (Th) cells and polyfunctionality

(A) Percentage of CAR CD4 Th1, Th2, Th17 and TREG subsets determined by flow cytometry post overnight stimulation at 1:1 with RAJI-WT targets, graphs show individual data points, n=6, Two tailed Mann-Whitney U test, ns P>0.05. (B) Pie chart of proportion of intracellular cytokines/chemotoxins measured following RAJI-WT stimulation. Arcs represent proportion of single or polyfunctional secretion, n=6.

5.2.4. Effects of GMP Akt inhibitor VIII treatment on B-ALL patient derived CAR T-cell autophagy and mitochondria

Healthy donor T-cells showed a marked autophagy gene signature in CAR CD8 T-cells. As a phenotypic measurement of autophagy, CYTO-ID® staining of total CAR T-cells confirmed the presence of increased pre-autophagosomes, autophagosomes, and autolysosomal vesicles following VIII-treatment. The same was seen in patient derived CAR T-cells. MFI assessment of VIII-treated total CAR and CD8+ CAR T-cell subsets showed increased autophagy by 107.3% and 69.5%, respectively, Figure 34A.

We additionally assessed mitophagy using the MitoTracker™ Green to quantify the mitochondrial mass in live cells at end of manufacture which demonstrated a significant reduction in VIII-treated total CAR (-20%) and CD8+ CAR T-cell subsets (-19.7%), Figure 34B. Further, $\Delta\Psi_m$ measurements using the JC-1-dye revealed a 2-fold increase in $\Delta\Psi_m$ in both VIII-treated total CAR and CAR CD8s, Figure 34C representing an increased capacity to produce ATP and comparable trends to healthy donors.

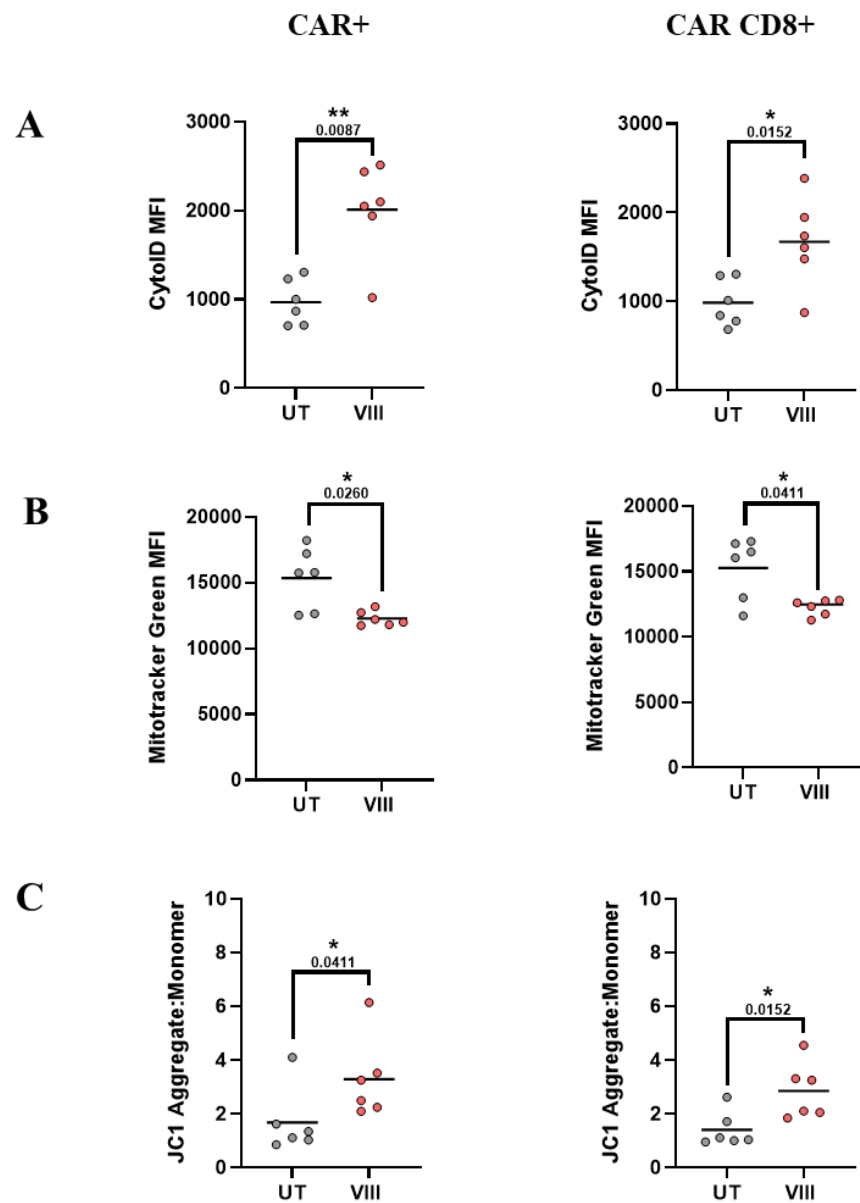


Figure 34. Effects of GMP Akt inhibitor VIII treatment on B-ALL patient derived CAR T-cell autophagy and mitochondria

(A) CytoID[®], (B) MitoTracker Green[™] and (C) JC-1[™] staining of CAR and CAR CD8 T-cells for autophagy, mitochondrial mass and $\Delta\Psi_m$, respectively. (A-C) All graphs depicting individual data points, n=6, Two tailed Mann-Whitney U test, ns P>0.05. *P<0.05 and ** P<0.01.

5.3. Discussion

CAR T-cells manufactured in the presence of VIII treatment from B-ALL patients showed increased Tscm/Tcm subsets and Tcm supporting CD27+/CD28+ and IL-2+/GZMB- profiles. Functionally, they exhibited improved total CAR T-cell expansion against target and enhanced cytotoxicity at rechallenge. Treated cells additionally demonstrated increased effector cytokine release and polyfunctionality with increased autophagy, $\Delta\Psi_m$, decreased mitochondrial mass and CD4 Th1/Th17 skew which no enrichment of Th2/TREG regulatory subsets.

Overall, B-ALL patient derived CARs had increased variability which impacted significance in some assessments but followed the same trends as healthy donor derived CAR T-cells. In general, fold expansion against targets and levels of cytokines produced were lower in patient CAR T-cells in comparison to healthy donor. Interestingly, VIII-treated CAR T-cells from patients showed an overall improvement in total CAR T-cells and not predominately in CAR CD8s as seen with healthy donors. There was improved expansion following VIII treatment of both CD4/8 CAR T-cells against target, and a significant increase in cytotoxicity at tumour rechallenge. VIII treatment further remarkably improved both IL-2 and TNF- α production.

Analysis of the metabolism data from healthy donors led us to speculate that the increased autophagy observed could be contributing to mitophagy to enhance T-cell survival. Mitophagy has been shown to promote self-renewal and persistence (Vannini et al., 2016, Kishton et al., 2017) where terminally exhausted TILs show decreased mitophagy with the accumulation of depolarised mitochondria (Denk et al., 2022). However, healthy donor T-cells only had small reductions of 9% and 7% in mitochondrial mass in total CAR and CD8+ CAR T-cells, respectively. This was further validated in patient CAR T-cells which showed a more significant reduction in mitochondrial mass by 20% and 19% in total CAR and CD8+ CAR T-cells, respectively. Chemotherapy has been shown to have a profound impact resulting in T-cells with small, depolarised, damaged mitochondria with disrupted energy reserves (Das et al., 2020). Thus, the presence of

increased damaged mitochondria in baseline B-ALL patient T-cells is not unlikely and could explain the greater impact of mitophagy in patient T-cells.

Taken together, this data demonstrates that a functional benefit could be achieved by all patient CAR T-cells manufactured with *ex-vivo* VIII inhibition and may be of particular value in patients where impaired ‘T-cell fitness’ is recognised to compromise *in-vivo* function, with the attendant risks of CD19+ disease relapse post CAR T-cell therapy. Our final step in the project was to assess if this manufacturing protocol could be adapted to large-scale manufacture on the CliniMACS Prodigy[®] platform.

Chapter 6. Large-scale manufacture of B-ALL patient CAR T-cells on the CliniMACS Prodigy[®] with VIII treatment

6.1. Introduction

The CliniMACS Prodigy[®] is a semi-automated platform for the manufacture of CAR T-cells, Figure 32. This platform can perform automated T-cell selection, activation, transduction, and expansion steps and was used for the manufacture of products for the UCL based ALLCAR19 trial for adult B-ALL and has shown greater product consistency, as discussed in Chapter 4.



Figure 35. The CliniMACS Prodigy[®]

Illustration of the CliniMACS Prodigy[®] platform for semi-automated CAR T-cell manufacturing.

All prior experiments were carried out at small-scale, designed to mimic the CliniMACS Prodigy[®] protocol and the next step was to assess if the protocol could be adapted in large-scale GMP to provide the same phenotypic and functional benefits. Here, CAR T-cells were manufactured using excess leukapheresis material from 3 patients on the ALLCAR19 trial. In an automated process, outlined in Figure 18, CD4/8 T-cells were enriched and manufactures were initiated with 100-200 million total T-cells. Cells were subsequently activated with Transact[™] and transduced the following day. Cells were

washed on Day 4 and expanded until Day 8, maintained throughout in TexMACS™ supplemented with 10ng/ml IL-7/15 and 2.5µM of GMP VIII. The resulting products were evaluated against non-VIII exposed CAR T-cell trial products, manufactured for the same 3 patients during the trial.

6.2. Characteristics of clinically scaled CAR T-cells

To test whether the desirable phenotypic and functional profiles of VIII treatment *in-vitro* and *in-vivo* can be reproduced at GMP clinical scale, we used surplus leukapheresis from three B-ALL patients on ALLCAR19 and manufactured with VIII treatment (VIII). The resulting products were compared with surplus products manufactured as a part of the trial (UT). As per small-scale findings, T-cell expansion was reduced following VIII-treatment by 73.6%, similar to the 60.4% reduction seen at small-scale. Despite this, scaled manufacture comfortably generated the 410×10^6 target dose as specified in the ALLCAR19 study. Mean transduction efficiency was broadly comparable between the two conditions 72.6 (UT) and 79% (VIII), Figure 36A.

End of manufacture phenotype was analysed by flow cytometry. Subsets were characterised using CCR7/CD45RA markers. Tcm subsets were increased by 2.2 and 3.6-fold in VIII-treated CAR CD4/8 T-cells, respectively, Figure 36B. The Tn subset was sub gated for FAS receptor CD95 expression to identify Tscm subsets. VIII-treated total CAR T-cells showed an increase from mean 17.8% (UT) to 41.5% (VIII), Figure 36B.

As prior results showed marked effects on the production of effector cytokines IL-2, IFN- γ , TNF- α and GZMB. We assessed polyfunctionality in products using intracellular flow cytometry for these cytokines/chemotoxins following stimulation with RAJI-WT targets. Consistent with previous results, VIII-treated CAR T-cells showed increased production and polyfunctionality in relation to IL-2 and TNF- α effector cytokines and a reduction in GZMB, Figure 36C.

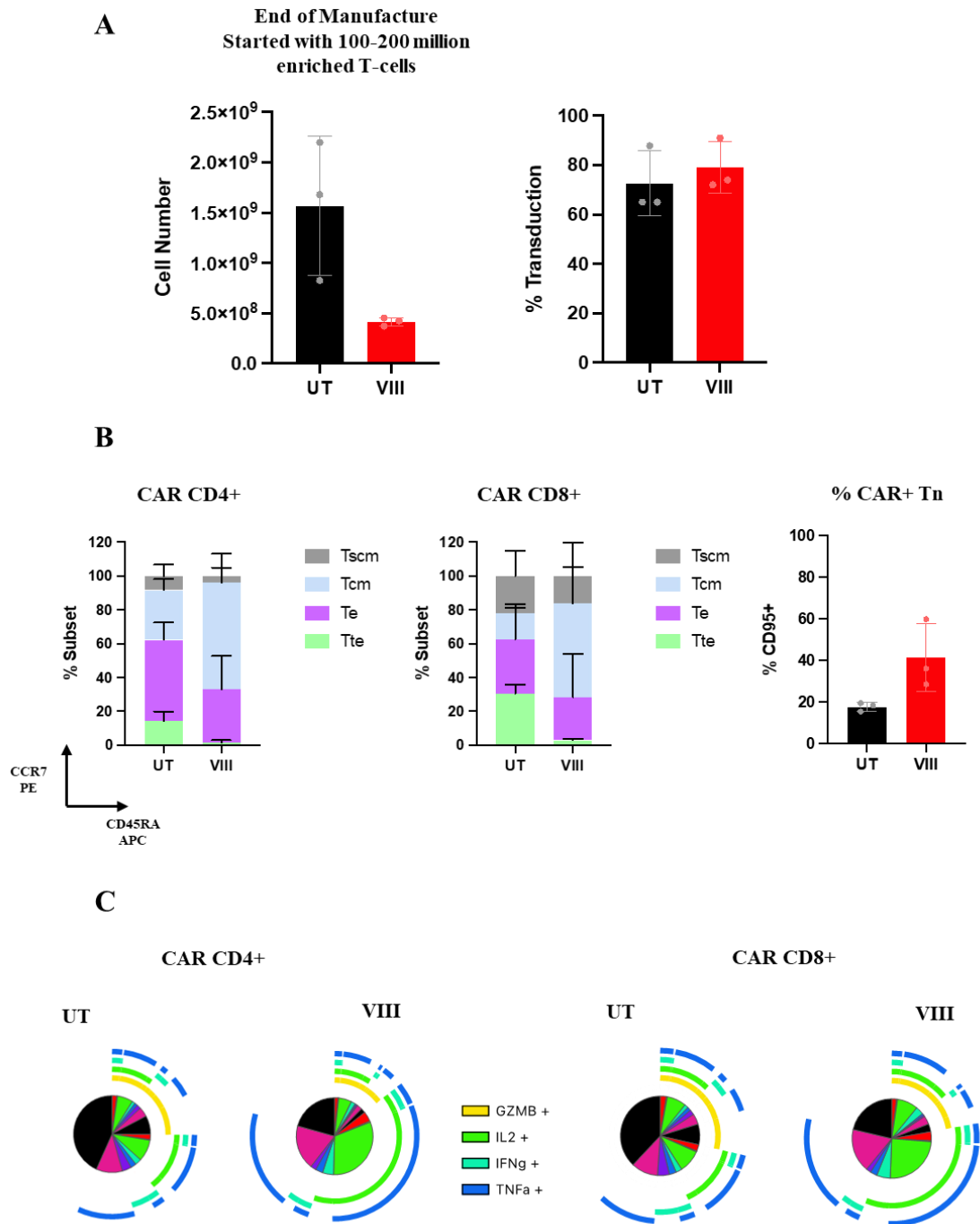


Figure 36. Characteristics of clinically scaled CAR T-cells

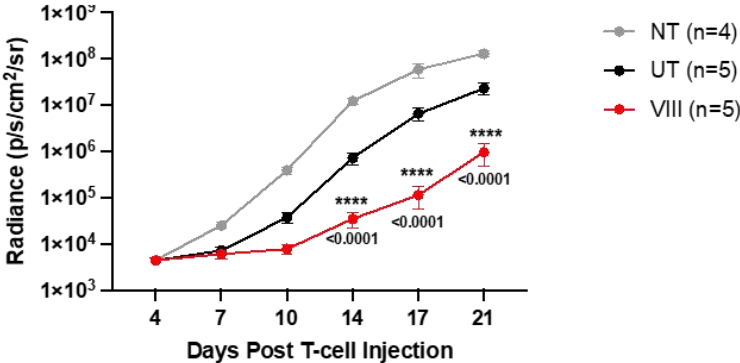
(A) Total number of T-cells and CAT CAR transduction percentage at the end of scaled manufactures with (VIII) or without (UT), individual data points \pm SD. (B) Graphical representation of Tn (CCR7+/CD45RA+), Tcm (CCR7+/CD45RA-), Te (CCR7-/CD45RA-) and Tte (CCR7-/CD45RA+) subsets in CD4 and CD8 CAR T-cells determined by flow cytometry, \pm SD and percentage CD95+ positive, sub gated from Tn population, \pm SD/indivial data points. (A-

B) n=3, Two tailed Mann-Whitney U test, ns $P > 0.05$. **(C)** Pie chart of proportion of intracellular cytokines measured following RAJI-WT stimulation. Arcs represent proportion of single or polyfunctional secretion, n=3.

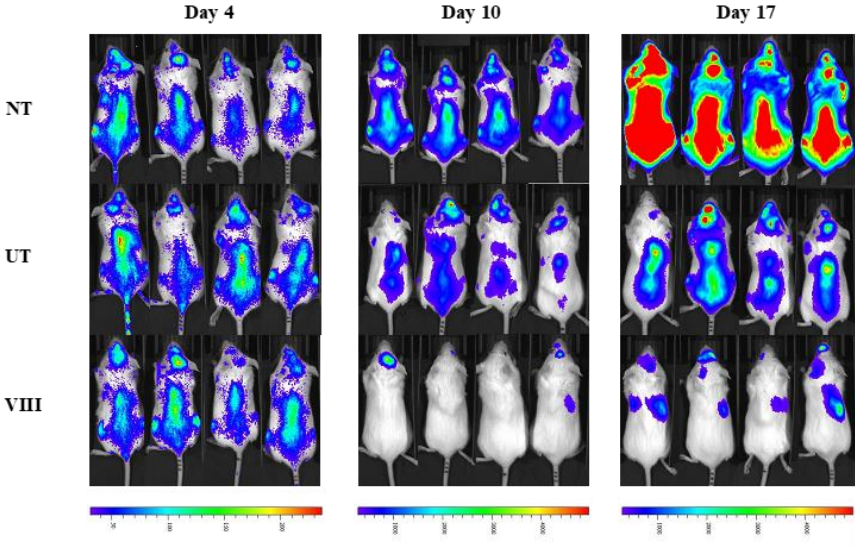
6.3. *In-vivo* functionality of B-ALL patient CAR T-cells

To assess functionality, CAR T-cells generated from a trial patient who developed CD19+ relapse with and without VIII treatment were tested *in-vivo* using the NSG NALM6 mouse model as defined in Figure 29A. As small-scale experiments showed that patient derived CAR T-cells had lower fold-expansion than healthy donor, mice were treated with a higher dose of 1×10^6 NT, UT, or VIII-treated T-cells. Bi-weekly BLI revealed significantly improved tumour control Figure 37A/B and survival Figure 37C in all VIII-treated CAR T-cell mice over NT and UT groups.

A



B



C

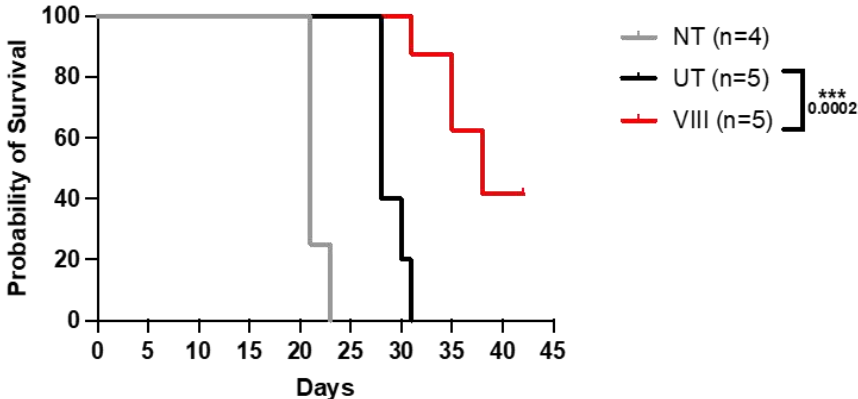


Figure 37. *In-vivo* functionality of B-ALL patient CAR T-cells

(A) Tumour burden measured by bioluminescent imaging (BLI) in NALM6 tumour established mice treated with NT T-cells or CAR T-cells manufactured with (VIII) or without (UT) VIII ±

SEM. (B) Representative BLI images of 4 mice per NT/CAR treatment group, pre CAR (Day 4) and post CAR (Day 10/17). (C) Overall survival of mice. (A-C) Cells derived from one ALL patient, n=5 mice per group. Two-way ANNOVA corrected for multiple comparisons by Tukey's test on log transformed data, ns P>0.05, *** P<0.001 and **** P<0.0001. Differences in survival were determined using Mantel Cox test.

6.4. Discussion

Results demonstrate the feasibility of large-scale clinical manufacture of CAR T-cells with *ex-vivo* VIII inhibition. Expansion of VIII-treated scaled products was similarly affected as per previous assessments however, the stipulated 410×10^6 target dose defined by ALLCAR19 trial was reached for all donors. This further aided in limiting expansion mediated differentiation resulting in Tscm/Tcm enrichment and increased effector cytokine production and polyfunctionality in VIII-treated CAR T-cells.

Cytokine assessments further validate a more effector cytokine profile and unaffected polyfunctionality of CD8 CAR T-cells following VIII inhibition in a mixed CD4/8 culture, unlike previously described by (Mousset et al., 2020). We acknowledge that findings failed to reach significance due to variability from B-ALL patient donors as seen in small-scale assessments and due to replication constraints associated with the costs of large-scale manufactures. Yet, VIII-treated products showed the same phenotypic and functional trends to small-scale assessments in healthy and B-ALL patient donors.

Most encouragingly, *in-vivo* assessments of mice with systemic leukaemia treated with CAR T-cells derived from a donor who previously relapsed with CD19+ disease on trial following conventional CAR T-cells treatment showed improved tumour control and significantly enhanced survival in the VIII-treated group. Mice were treated with a low dose of 1×10^6 CAR T-cells to provide a stress factor to identify differences between UT and VIII groups. Results highlight that complete tumour clearance and long-term survival could be achieved with a larger CAR T-cell dose.

We show that this method can be successfully incorporated into the CliniMACS Prodigy[®] manufacture to provide superior CAR T-cell products for patients. The success of large-scale GMP production has led to the approval of this manufacturing protocol for future UCL based CAR T-cell trials.

Chapter 7. General Discussion and Future Work

There are many factors that require consideration for optimal CAR T-cell therapy in adults. To date, TECARTUS™ (brexucabtagene autoleucel) based on the FMC63 scFv remains the only CAR T-cell therapy with FDA approval for adult B-ALL. Approval was based on findings of the phase II ZUMA-3 trial with 52% complete remissions (CR) at 12 months. However, there were high incidences of cytokine release syndrome (CRS) in ALL patients at 26% Grade ≥ 3 and 35% Grade ≥ 3 neurological events (TECARTUS®, 2022, Shah et al., 2021). At UCL, the phase I adult B-ALL ALLCAR19 trial with the CAT scFv revealed similar response rates at 50% CR at 12 months but holds promise for its superior safety profile of no Grade ≥ 3 CRS and lower Grade 3 neurotoxicity at 15%, attributed to fast off rate kinetics (Roddie et al., 2021).

The manufacture of CAR T-cell products in adults can be challenging. Previous studies report impaired phenotypes in patients treated with chemotherapy (Petersen et al., 2018), which our assessment corroborated in comparison to healthy donor T-cells, Figure 30A. Age related senescence also seemed to contribute where end CAT CAR products manufactured for paediatric B-ALL patients on the CARPALL trial had better enrichment of less differentiated Tcm subsets than adults, Figure 30C. Interestingly, as per Table 2, CD19+ relapses in paediatric patients only accounted for 16.7% whereas the remaining relapses were due to loss of CD19 antigen. Whereas in adults, CD19+ relapses on the ALLCAR19 trial were more frequent and may be addressed by optimised CAR T-cell products.

The ZUMA-3 trial used a non-automated protocol with T-cell enrichment prior to activation with subsequent retroviral CAR transduction and expansion in the presence of IL-2 for 6 to 10 days (Sabatino et al., 2016). The UCL ALLCAR19 trial validated the use of the automated CliniMACS Prodigy® platform with T-cell enrichment, activation, lentiviral CAR transduction and expansion in the presence of IL-7/IL-15 for 8 days (Roddie et al., 2021, Shah et al., 2021). Despite trial variations, both trials suffered from high 48-50% relapse rates (Roddie et al., 2021, Shah et al., 2021). This highlights the importance of addressing CAR T-cell manufacture to limit failure in patients with

impaired starting material. Prior studies have assessed shortened manufactures and the incorporation of small molecule compounds to target several pathways from Wnt/ β -catenin signalling, FAO to phosphoinositide-3-kinase (PI3K)/AKT pathways (Funk et al., 2022, Gattinoni et al., 2009, Klebanoff et al., 2017, Petersen et al., 2018, Urak et al., 2017), with a common aim to arrest T-cell differentiation during *ex-vivo* T-cell manufacture.

The only clinically tested compound in the manufacture of 41BB ζ CAR T-cells is PI3K inhibitor BB007, part of the CRB-402 (NTC03274219) trial targeting multiple myeloma. Results correlate the presence of memory markers in drug products with increased peak expansion and superior clinical outcomes (Raje et al., 2021). Remaining pre-clinical studies have predominantly assessed the use of PI3K and AKT inhibitors in CD28 ζ CAR T-cells, manufactured with CD3/CD28 dynabead or CD3 antibody stimulation coupled with IL-2 supplementation (Funk et al., 2022, Klebanoff et al., 2017, Petersen et al., 2018, Urak et al., 2017).

As functional characteristics of CD28 ζ /4-1BB ζ endodomains and their reliance on the AKT pathway differ (Salter et al., 2018, Kawalekar et al., 2016), it was important to explore the effects of VIII in 4-1BB ζ CAR T-cells. We were the first to investigate this in a manufacturing process using TransActTM stimulation and IL-7/IL-15 cytokine supplementation to further support the production of less differentiated T-cells. Our results showed that *ex-vivo* VIII inhibition was a successful method leading to Tscm/Tcm enrichment, superior expansion against target and sustained cytotoxicity at re-challenge. We additionally found dependency on the FOXO1 transcription factor as previously described with a novel signature for autophagy which we suspect may be contributing to mitophagy and FAO to aid survival. We found the presence of multiple active metabolic pathways to support energy demands of superior functionality and enhanced production and polyfunctionality of cells producing effector cytokines. Unlike prior studies (Funk et al., 2022, Mousset et al., 2020), we found no skew to regulatory Th2 CD4 subsets and instead a skew toward Th1/Th17 with no negative impacts on the polyfunctionality of CD8 CAR T-cells, Chapters 4/5. We were further successful in scaling this to clinical manufacture, validating that *ex-vivo* VIII inhibition is a valuable addition to our current

manufacturing process which can enhance functionality in adult patients vulnerable to relapse, Chapter 6.

Ex-vivo VIII treatment does have some limitations, a key feature of the CAT CAR is the low incidences of CRS (Ghorashian et al., 2019, Roddie et al., 2021). Our results show an increase in effector cytokines as well as the inflammatory cytokine, IL-6 following VIII treatment. IL-6 positively associates with superior clinical outcomes (Fraietta et al., 2018) but may enhance the risk of Grade ≥ 3 CRS events. Whether this exceeds incidences seen with the FMC63 CAR remains to be determined however, 41BB ζ CAR T-cells used in CRB-402 trial manufactured with *ex-vivo* PI3K inhibitor maintained tolerable toxicities (Raje et al., 2021) and the use of anti-IL-6 monoclonal antibody, tocilizumab to treat CRS is common clinical practice in CAR T-cell therapy, (Si and Teachey, 2020).

A previous report suggests that VIII treatment fails to provide phenotypic benefits in manufactures initiated with entirely differentiated Te/Tte T-cells (Klebanoff et al., 2017). This supports a VIII mechanism of limiting activation induced differentiation over reprogramming of differentiated T-cells and highlights that VIII may not be a solution in incidences where Tn/Tcm populations are entirely absent from patient baseline starting material.

More recent studies have assessed shortened 1-3 day manufacturing processes (Ghassemi et al., 2018) some without an T-cell activation step (Ghassemi et al., 2022). Biotech companies such as Novartis (TchargeTM) (Novartis), and Gracell Biotechnologies (F-CAR-T) (Yang et al., 2022) are in the race to shrink the manufacture process to 1-4 days *in-vitro* with the potential advantages of less time in cGMP with subsequent impacts on lowering costs of staff/room hire per product and a reduction in vein-to-vein time, which is particularly important for patients with rapidly progressive chemo-refractory disease. From a product perspective, shorter *ex-vivo* expansion is proposed to preserve T-cell stemness in the final product and provide a functional improvement by limiting activation/expansion related CAR T-cell differentiation during manufacture (Ghassemi et al., 2022, Yang et al., 2022).

As the technology stands currently, shorter manufacture protocols possess several challenges which may impede their broad deliverability into the clinic. First, whilst shortened manufacturing to 3 days with T-cell activation was able to increase CAR T-cell proliferation against target in healthy donors, it failed to provide a benefit in CAR products from B-ALL patients. Researchers further highlight that producing viable products within 3 days was more challenging in patient derived T-cells, attributed to significantly fewer Tn and increased Te subsets in baseline material (Ghassemi et al., 2018). Shortened manufacture without activation is yet to be tested on patient derived T-cells and we hypothesise that this method is likely to encounter similar difficulties in Te/Tte enriched patient leukapheresis, but this requires further research. Secondly, much higher T-cell numbers are required at baseline for a non-expansion protocol, and this may be difficult to obtain from lymphopenic patient leukapheresis. Third, high viral vector volumes are required to modify large cell numbers *ex-vivo*, thus negatively impacting the cost per patient product, as vector is the most expensive component of current CAR-T manufacture processes. Further, from a practical perspective, shortened manufacture must be accompanied by shortened duration release testing and quality sign-off to realise a truly shortened vein-vein time. Despite advances in technical know-how, the issue of expedited release remains a major bottleneck.

By contrast, VIII based manufacture does not require higher starting T-cell numbers, nor higher vector volumes, and consistently yields Tscm/Tcm enrichment, even in heavily pre-treated patient starting material, Chapter 5/6. Ultimately, whether VIII driven effects on phenotype, autophagy/metabolism, or whether the incorporation of VIII in a shortened process can provide additional functional benefits over current shortened manufacturing processes requires testing in comparison.

Other potential methods to improve CAR T-cell products beyond exogenous VIII treatment include transcriptional reprogramming of Te/Tte material, where overexpression of transcription factors such as FOXO1 and BACH2, may be able to induce and maintain less differentiated Tn populations (Lu et al., 2020, Yao et al., 2021). Another approach to overcome the problems associated with poor quality starting material is the use of healthy donor derived allogeneic CAR T-cells or universal CAR T-

cells where gene editing can be utilised to knock-down TCR/MHC expression in healthy donors to eliminate the risks of GvHD and CAR T-cell allojection observed with allogeneic CAR T-cell therapy (Lin et al., 2021).

Whilst studies support that increased frequencies of Tscm subsets support long term persistence (Biasco et al., 2021), even CAR T-cell products enriched for such subsets are likely to eventually reach exhaustion upon repetitive stimulation *in-vivo*. We acknowledge that our assessments are not designed to directly assess the impact of VIII treatment on long-term persistence. Although 41BB ζ endodomain CAR T-cells are known for superior persistence over CD28 ζ and our assessments show better long-term cytotoxicity, *in-vivo* assessments failed to show any definitive effects in persistence following spleen/BM analysis at the D21 timepoint, Figure 29. Whilst there was a degree of variability between mice which underpowered this study, xenogeneic B-ALL murine models are challenging to model persistence, due to the inevitability of xenogeneic GvHD. It is possible that a syngeneic fully murine model such as the A20 B-cell leukaemia model (Kueberuwa et al., 2018b) treated with murine CAR T-cells may begin to answer these questions. However, such an approach also poses challenges for its lack of comparability to a human therapeutic and difficulty modelling the specific characteristics of existing CAR T-cell therapies.

Taken together, we propose the following future assessments that would add value to this project.

1. An *in-vivo* rechallenge model, where mice are treated with a high dose of patient derived CAR T-cells and re-challenged with tumour cells following primary clearance would help inform persistence.
2. Additional functional assessments comparing shortened manufacturing methods with *ex-vivo* pharmacologic inhibition to delineate the pro's and con's of both approaches.
3. Lastly, to combat eventual *in-vivo* exhaustion a combinatorial approach of transient rest *in-vitro* with VIII treatment and subsequently *in-vivo* to prolong anti-

tumour efficacy as seen with the use of the tyrosine kinase inhibitor Dasatinib to reversibly dampen CAR signalling (Weber et al., 2021) can also be assessed.

Furthermore, CAR T-cells have shown reduced efficacy against solid tumours. Although CAR T-cells offer increased specificity to tumour they are likely to suffer similar inhibitory factors caused by the tumour environment affecting other cell therapies such as TILs as discussed in Chapter 1. With a move towards the treatment of solid tumours, *ex-vivo* VIII inhibition still provides an attractive universal approach to improve the functionality of CAR T-cells but will likely require other combinatory strategies to protect against or reshape the tumour microenvironment to favour CAR T-cells.

Some strategies include the blocking of growth factors such as granulocyte macrophage colony stimulating factor (GM-CSF) to inhibit immunosuppressive MDSCs (Burga et al., 2015). The expression of a dominant negative TGF β receptor in CAR T-cells has demonstrated superior anti-tumour activity, resistance to exhaustion and long-term *in-vivo* persistence in a prostate cancer model (Kloss et al., 2018). The increased presence of pro T-cell cytokines such as IL-2, IL-12 and IL-15 could aid in overcoming the immunosuppressive factors and improve CAR T-cell therapy. One approach includes the use of CAR T-cells that permits constitutive or inducible cytokine expression. These CAR T-cells are referred to as T-cells redirected for universal cytokine mediated killing (TRUCKs). With this approach, a murine lymphoma model demonstrated tumour clearance and the recruitment of host immune cells using CD19 targeting CAR T-cells secreting IL-12 (Kueberuwa et al., 2018a). A further glioblastoma model demonstrated improved anti-tumour activity *in-vivo* using IL-13R α 2 targeting CAR T-cells secreting IL-15 (Krenciute et al., 2017). Other strategies using checkpoint inhibitors against PD-1, CTLA-4 and PD-L1 have demonstrated improved T-cell response in patients (Buchbinder and Desai, 2016). Further novel strategies including designing CAR T-cells to secrete anti-PD-L1 antibodies (Suarez et al., 2016) have also demonstrated reduced tumour progression with increasing work to evaluate the potential use of CRISPR gene editing to allow for the complete knockout of negative T-cells regulators. A study demonstrated reduced tumour burden in PD-1 knockout CD19 targeting CAR T-cells when compared

to control CAR T-cells in a CD19 myelogenous leukaemia model engineered to overexpress PD-L1 (Rupp et al., 2017).

Nonetheless, in applicable patients, VIII treatment forms an attractive approach as we demonstrate its ability to improve tumour response and survival in patients who have failed CAR T-cell therapy. *Ex-vivo* VIII in culture can also be an additional advantage in other adoptive cell therapies that may require long term *ex-vivo* culture including, TIL and virus specific T-cell therapies. Work on this study had led to the incorporation of this manufacturing method in an upcoming UCL based CAR T-cell trial against multiple myeloma (NCT04795882).

Reference List

- ABATE-DAGA, D., LAGISETTY, K. H., TRAN, E., ZHENG, Z., GATTINONI, L., YU, Z., BURNS, W. R., MIERMONT, A. M., TEPER, Y., RUDLOFF, U., RESTIFO, N. P., FELDMAN, S. A., ROSENBERG, S. A. & MORGAN, R. A. 2014. A novel chimeric antigen receptor against prostate stem cell antigen mediates tumor destruction in a humanized mouse model of pancreatic cancer. *Hum Gene Ther*, 25, 1003-12.
- ABU EID, R., FRIEDMAN, K. M., MKRTICHYAN, M., WALENS, A., KING, W., JANIK, J. & KHLEIF, S. N. 2015. Akt1 and -2 inhibition diminishes terminal differentiation and enhances central memory CD8(+) T-cell proliferation and survival. *Oncoimmunology*, 4, e1005448.
- AGARWAL, S., HANAUER, J. D. S., FRANK, A. M., RIECHERT, V., THALHEIMER, F. B. & BUCHHOLZ, C. J. 2020. In Vivo Generation of CAR T Cells Selectively in Human CD4(+) Lymphocytes. *Mol Ther*, 28, 1783-1794.
- AKBAR, A. N. & HENSON, S. M. 2011. Are senescence and exhaustion intertwined or unrelated processes that compromise immunity? *Nat Rev Immunol*, 11, 289-95.
- ALI, K., SOOND, D. R., PINEIRO, R., HAGEMANN, T., PEARCE, W., LIM, E. L., BOUABE, H., SCUDAMORE, C. L., HANCOX, T., MAECKER, H., FRIEDMAN, L., TURNER, M., OKKENHAUG, K. & VANHAESEBROECK, B. 2014. Inactivation of PI(3)K p110 δ breaks regulatory T-cell-mediated immune tolerance to cancer. *Nature*, 510, 407-411.
- AMITRANO, A. M., BERRY, B. J., LIM, K., KIM, K.-D., WAUGH, R. E., WOJTOVICH, A. P. & KIM, M. 2021. Optical Control of CD8+ T Cell Metabolism and Effector Functions. *Frontiers in Immunology*, 12.
- AMROLIA, P., WYNN, R, HOUGH, R, VORA, A, BONNEY, D, VEYS, P, CHIESA, R, RAO, K, CLARK, L, AL-HAJJ, M, CORDOBA, S, ONUOHA, S, KOTSOPOULOU, E, KHOKHAR, N, PULE, M. AND PEDDAREDDIGARI, V 2019. Phase I Study of AUTO3, a Bicistronic Chimeric Antigen Receptor (CAR) T-Cell Therapy Targeting CD19 and CD22, in Pediatric Patients with Relapsed/Refractory B-Cell Acute Lymphoblastic Leukemia (r/r B-ALL): Amelia Study. . *Blood*, 134, 2620.
- ANDERSON, K. G., STROMNES, I. M. & GREENBERG, P. D. 2017. Obstacles Posed by the Tumor Microenvironment to T cell Activity: A Case for Synergistic Therapies. *Cancer Cell*, 31, 311-325.
- ANDERSON, P., APTSIAURI, N., RUIZ-CABELLO, F. & GARRIDO, F. 2021. HLA class I loss in colorectal cancer: implications for immune escape and immunotherapy. *Cell Mol Immunol*, 18, 556-565.

- ARAKI, K., TURNER, A. P., SHAFFER, V. O., GANGAPPA, S., KELLER, S. A., BACHMANN, M. F., LARSEN, C. P. & AHMED, R. 2009. mTOR regulates memory CD8 T-cell differentiation. *Nature*, 460, 108-12.
- BERDEJA, J. G., ALSINA, M., SHAH, N. D., SIEGEL, D. S., JAGANNATH, S., MADDURI, D., KAUFMAN, J. L., MUNSHI, N. C., ROSENBLATT, J. & JASIELEC, J. K. 2019. Updated Results from an Ongoing Phase 1 Clinical Study of bb21217 Anti-Bcma CAR T Cell Therapy. American Society of Hematology Washington, DC.
- BHOJWANI, D., SPOSTO, R., SHAH, N. N., RODRIGUEZ, V., YUAN, C., STETLER-STEVENSON, M., O'BRIEN, M. M., MCNEER, J. L., QUERESHI, A., CABANNES, A., SCHLEGEL, P., ROSSIG, C., DALLA-POZZA, L., AUGUST, K., ALEXANDER, S., BOURQUIN, J. P., ZWAAN, M., RAETZ, E. A., LOH, M. L. & RHEINGOLD, S. R. 2019. Inotuzumab ozogamicin in pediatric patients with relapsed/refractory acute lymphoblastic leukemia. *Leukemia*, 33, 884-892.
- BIASCO, L., IZOTOVA, N., RIVAT, C., GHORASHIAN, S., RICHARDSON, R., GUVENEL, A., HOUGH, R., WYNN, R., POPOVA, B., LOPES, A., PULE, M., THRASHER, A. J. & AMROLIA, P. J. 2021. Clonal expansion of T memory stem cells determines early anti-leukemic responses and long-term CAR T cell persistence in patients. *Nature Cancer*, 2, 629-642.
- BOWERS, J. S., MAJCHRZAK, K., NELSON, M. H., AKSOY, B. A., WYATT, M. M., SMITH, A. S., BAILEY, S. R., NEAL, L. R., HAMMERBACHER, J. E. & PAULOS, C. M. 2017. PI3Kdelta Inhibition Enhances the Antitumor Fitness of Adoptively Transferred CD8(+) T Cells. *Front Immunol*, 8, 1221.
- BRAGHIROLI, M. I., SABBAGA, J. & HOFF, P. M. 2012. Bevacizumab: overview of the literature. *Expert Rev Anticancer Ther*, 12, 567-80.
- BRENTJENS, R. J., RIVIERE, I., PARK, J. H., DAVILA, M. L., WANG, X., STEFANSKI, J., TAYLOR, C., YEY, R., BARTIDO, S., BORQUEZ-OJEDA, O., OLSZEWSKA, M., BERNAL, Y., PEGRAM, H., PRZYBYLOWSKI, M., HOLLYMAN, D., USACHENKO, Y., PIRRAGLIA, D., HOSEY, J., SANTOS, E., HALTON, E., MASLAK, P., SCHEINBERG, D., JURCIC, J., HEANEY, M., HELLER, G., FRATTINI, M. & SADELAIN, M. 2011. Safety and persistence of adoptively transferred autologous CD19-targeted T cells in patients with relapsed or chemotherapy refractory B-cell leukemias. *Blood*, 118, 4817-28.
- BUCHBINDER, E. I. & DESAI, A. 2016. CTLA-4 and PD-1 Pathways: Similarities, Differences, and Implications of Their Inhibition. *Am J Clin Oncol*, 39, 98-106.
- BURGA, R. A., THORN, M., POINT, G. R., GUHA, P., NGUYEN, C. T., LICATA, L. A., DEMATTEO, R. P., AYALA, A., JOSEPH ESPAT, N., JUNGHANS, R. P. & KATZ, S. C. 2015. Liver myeloid-derived suppressor cells expand in response to liver metastases in mice and inhibit the anti-tumor efficacy of anti-CEA CAR-T. *Cancer Immunol Immunother*, 64, 817-29.

- CHAN, L. L., SHEN, D., WILKINSON, A. R., PATTON, W., LAI, N., CHAN, E., KUKSIN, D., LIN, B. & QIU, J. 2012. A novel image-based cytometry method for autophagy detection in living cells. *Autophagy*, 8, 1371-82.
- CHEN, G., HUANG, A. C., ZHANG, W., ZHANG, G., WU, M., XU, W., YU, Z., YANG, J., WANG, B., SUN, H., XIA, H., MAN, Q., ZHONG, W., ANTELO, L. F., WU, B., XIONG, X., LIU, X., GUAN, L., LI, T., LIU, S., YANG, R., LU, Y., DONG, L., MCGETTIGAN, S., SOMASUNDARAM, R., RADHAKRISHNAN, R., MILLS, G., LU, Y., KIM, J., CHEN, Y. H., DONG, H., ZHAO, Y., KARAKOUSIS, G. C., MITCHELL, T. C., SCHUCHTER, L. M., HERLYN, M., WHERRY, E. J., XU, X. & GUO, W. 2018. Exosomal PD-L1 contributes to immunosuppression and is associated with anti-PD-1 response. *Nature*, 560, 382-386.
- CHENG, J., ZHAO, L., ZHANG, Y., QIN, Y., GUAN, Y., ZHANG, T., LIU, C. & ZHOU, J. 2019. Understanding the Mechanisms of Resistance to CAR T-Cell Therapy in Malignancies. *Front Oncol*, 9, 1237.
- CORTHAY, A. 2014. Does the immune system naturally protect against cancer? *Front Immunol*, 5, 197.
- CORTHAY, A., SKOVSETH, D. K., LUNDIN, K. U., RØSJØ, E., OMHOLT, H., HOFGAARD, P. O., HARALDSEN, G. & BOGEN, B. 2005. Primary Antitumor Immune Response Mediated by CD4+ T Cells. *Immunity*, 22, 371-383.
- CRAIG W. LINDSLEY, Z. Z. 2003. *Fused quinoxaline derivatives as inhibitors of akt activity*, WO2003086404A1.
- CROMPTON, J. G., SUKUMAR, M., ROYCHOUDHURI, R., CLEVER, D., GROS, A., EIL, R. L., TRAN, E., HANADA, K., YU, Z., PALMER, D. C., KERKAR, S. P., MICHALEK, R. D., UPHAM, T., LEONARDI, A., ACQUAVELLA, N., WANG, E., MARINCOLA, F. M., GATTINONI, L., MURANSKI, P., SUNDRUD, M. S., KLEBANOFF, C. A., ROSENBERG, S. A., FEARON, D. T. & RESTIFO, N. P. 2015. Akt inhibition enhances expansion of potent tumor-specific lymphocytes with memory cell characteristics. *Cancer Res*, 75, 296-305.
- CSAPLÁR, M., SZÖLLÖSI, J., GOTTSCHALK, S., VEREB, G. & SZÖÖR, Á. 2021. Cytolytic Activity of CAR T Cells and Maintenance of Their CD4+ Subset Is Critical for Optimal Antitumor Activity in Preclinical Solid Tumor Models. *Cancers (Basel)*, 13.
- CURIEL, T. J., COUKOS, G., ZOU, L., ALVAREZ, X., CHENG, P., MOTTRAM, P., EVDEMON-HOGAN, M., CONEJO-GARCIA, J. R., ZHANG, L., BUROW, M., ZHU, Y., WEI, S., KRYCZEK, I., DANIEL, B., GORDON, A., MYERS, L., LACKNER, A., DISIS, M. L., KNUTSON, K. L., CHEN, L. & ZOU, W. 2004. Specific recruitment of regulatory T cells in ovarian carcinoma fosters immune privilege and predicts reduced survival. *Nat Med*, 10, 942-9.

- DAI, Q., HAN, P., QI, X., LI, F., LI, M., FAN, L., ZHANG, H., ZHANG, X. & YANG, X. 2020. 4-1BB Signaling Boosts the Anti-Tumor Activity of CD28-Incorporated 2(nd) Generation Chimeric Antigen Receptor-Modified T Cells. *Front Immunol*, 11, 539654.
- DAS, R. K., O'CONNOR, R. S., GRUPP, S. A. & BARRETT, D. M. 2020. Lingering effects of chemotherapy on mature T cells impair proliferation. *Blood Adv*, 4, 4653-4664.
- DE KONING, P. J., TESSELAAR, K., BOVENSCHEN, N., COLAK, S., QUADIR, R., VOLMAN, T. J. & KUMMER, J. A. 2010. The cytotoxic protease granzyme M is expressed by lymphocytes of both the innate and adaptive immune system. *Mol Immunol*, 47, 903-11.
- DEAS, E., WOOD, N. W. & PLUN-FAVREAU, H. 2011. Mitophagy and Parkinson's disease: the PINK1-parkin link. *Biochim Biophys Acta*, 1813, 623-33.
- DELPOUX, A., MARCEL, N., HESS MICHELINI, R., KATAYAMA, C. D., ALLISON, K. A., GLASS, C. K., QUIÑONES-PARRA, S. M., MURRE, C., LOH, L., KEDZIERSKA, K., LAPPAS, M., HEDRICK, S. M. & DOEDENS, A. L. 2021. FOXO1 constrains activation and regulates senescence in CD8 T cells. *Cell Reports*, 34, 108674.
- DENG, Q., HAN, G., PUEBLA-OSORIO, N., MA, M. C. J., STRATI, P., CHASEN, B., DAI, E., DANG, M., JAIN, N., YANG, H., WANG, Y., ZHANG, S., WANG, R., CHEN, R., SHOWELL, J., GHOSH, S., PATCHVA, S., ZHANG, Q., SUN, R., HAGEMEISTER, F., FAYAD, L., SAMANIEGO, F., LEE, H. C., NASTOUPIL, L. J., FOWLER, N., ERIC DAVIS, R., WESTIN, J., NEELAPU, S. S., WANG, L. & GREEN, M. R. 2020. Characteristics of anti-CD19 CAR T cell infusion products associated with efficacy and toxicity in patients with large B cell lymphomas. *Nature Medicine*, 26, 1878-1887.
- DENK, D., PETROCELLI, V., CONCHE, C., DRACHSLER, M., ZIEGLER, P. K., BRAUN, A., KRESS, A., NICOLAS, A. M., MOHS, K., BECKER, C., NEURATH, M. F., FARIN, H. F., BUCHHOLZ, C. J., ANDREUX, P. A., RINSCH, C. & GRETEN, F. R. 2022. Expansion of T memory stem cells with superior anti-tumor immunity by Urolithin A-induced mitophagy. *Immunity*, 55, 2059-2073.e8.
- DHATCHINAMOORTHY, K., COLBERT, J. D. & ROCK, K. L. 2021. Cancer Immune Evasion Through Loss of MHC Class I Antigen Presentation. *Front Immunol*, 12, 636568.
- DHILLON, S. 2014. Trastuzumab emtansine: a review of its use in patients with HER2-positive advanced breast cancer previously treated with trastuzumab-based therapy. *Drugs*, 74, 675-86.
- DORANTES-ACOSTA, E. & PELAYO, R. 2012. Lineage switching in acute leukemias: a consequence of stem cell plasticity? *Bone Marrow Res*, 2012, 406796.

- DUNN, G. P., OLD, L. J. & SCHREIBER, R. D. 2004. The Immunobiology of Cancer Immunosurveillance and Immunoediting. *Immunity*, 21, 137-148.
- EYQUEM, J., MANSILLA-SOTO, J., GIAVRIDIS, T., VAN DER STEGEN, S. J., HAMIEH, M., CUNANAN, K. M., ODAK, A., GONEN, M. & SADELAIN, M. 2017. Targeting a CAR to the TRAC locus with CRISPR/Cas9 enhances tumour rejection. *Nature*, 543, 113-117.
- FISHMAN, M. A. & PERELSON, A. S. 1994. Th1/Th2 Cross Regulation. *Journal of Theoretical Biology*, 170, 25-56.
- FRAIETTA, J. A., LACEY, S. F., ORLANDO, E. J., PRUTEANU-MALINICI, I., GOHIL, M., LUNDH, S., BOESTEANU, A. C., WANG, Y., O'CONNOR, R. S., HWANG, W. T., PEQUIGNOT, E., AMBROSE, D. E., ZHANG, C., WILCOX, N., BEDOYA, F., DORFMEIER, C., CHEN, F., TIAN, L., PARAKANDI, H., GUPTA, M., YOUNG, R. M., JOHNSON, F. B., KULIKOVSKAYA, I., LIU, L., XU, J., KASSIM, S. H., DAVIS, M. M., LEVINE, B. L., FREY, N. V., SIEGEL, D. L., HUANG, A. C., WHERRY, E. J., BITTER, H., BROGDON, J. L., PORTER, D. L., JUNE, C. H. & MELENHORST, J. J. 2018. Determinants of response and resistance to CD19 chimeric antigen receptor (CAR) T cell therapy of chronic lymphocytic leukemia. *Nat Med*, 24, 563-571.
- FRAUWIRTH, K. A., RILEY, J. L., HARRIS, M. H., PARRY, R. V., RATHMELL, J. C., PLAS, D. R., ELSTROM, R. L., JUNE, C. H. & THOMPSON, C. B. 2002. The CD28 signaling pathway regulates glucose metabolism. *Immunity*, 16, 769-77.
- FREY, N. V., SHAW, P. A., HEXNER, E. O., PEQUIGNOT, E., GILL, S., LUGER, S. M., MANGAN, J. K., LOREN, A. W., PERL, A. E., MAUDE, S. L., GRUPP, S. A., SHAH, N. N., GILMORE, J., LACEY, S. F., MELENHORST, J. J., LEVINE, B. L., JUNE, C. H. & PORTER, D. L. 2020. Optimizing Chimeric Antigen Receptor T-Cell Therapy for Adults With Acute Lymphoblastic Leukemia. *J Clin Oncol*, 38, 415-422.
- FRIGAULT, M. J., LEE, J., BASIL, M. C., CARPENITO, C., MOTOHASHI, S., SCHOLLER, J., KAWALEKAR, O. U., GUEDAN, S., MCGETTIGAN, S. E., POSEY, A. D., JR., ANG, S., COOPER, L. J., PLATT, J. M., JOHNSON, F. B., PAULO, C. M., ZHAO, Y., KALOS, M., MILONE, M. C. & JUNE, C. H. 2015. Identification of chimeric antigen receptors that mediate constitutive or inducible proliferation of T cells. *Cancer Immunol Res*, 3, 356-67.
- FRY, T., STETLER-STEVENSON, M, SHAH, N, YUAN, C, YATES, B, DELBROOK, C, ZHANG, L, LEE, D, STRONCEK, D. AND MACKALL, C 2015. Clinical Activity and Persistence of Anti-CD22 Chimeric Antigen Receptor in Children and Young Adults with Relapsed/Refractory Acute Lymphoblastic Leukemia (ALL). *Blood*, 126, 1324.
- FUNK, C. R., WANG, S., CHEN, K. Z., WALLER, A., SHARMA, A., EDGAR, C. L., GUPTA, V. A., CHANDRAKASAN, S., ZOINE, J. T., FEDANOV, A.,

- RAIKAR, S. S., KOFF, J. L., FLOWERS, C. R., COMA, S., PACHTER, J. A., RAVINDRANATHAN, S., SPENCER, H. T., SHANMUGAM, M. & WALLER, E. K. 2022. PI3Kdelta/gamma inhibition promotes human CART cell epigenetic and metabolic reprogramming to enhance antitumor cytotoxicity. *Blood*, 139, 523-537.
- GALON, J., COSTES, A., SANCHEZ-CABO, F., KIRILOVSKY, A., MLECNIK, B., LAGORCE-PAGÈS, C., TOSOLINI, M., CAMUS, M., BERGER, A., WIND, P., ZINZINDOHOUE, F., BRUNEVAL, P., CUGNENC, P. H., TRAJANOSKI, Z., FRIDMAN, W. H. & PAGÈS, F. 2006. Type, density, and location of immune cells within human colorectal tumors predict clinical outcome. *Science*, 313, 1960-4.
- GARDNER, R., WU, D., CHERIAN, S., FANG, M., HANAFI, L. A., FINNEY, O., SMITHERS, H., JENSEN, M. C., RIDDELL, S. R., MALONEY, D. G. & TURTLE, C. J. 2016. Acquisition of a CD19-negative myeloid phenotype allows immune escape of MLL-rearranged B-ALL from CD19 CAR-T-cell therapy. *Blood*, 127, 2406-10.
- GARDNER, R. A., FINNEY, O., ANNESLEY, C., BRAKKE, H., SUMMERS, C., LEGER, K., BLEAKLEY, M., BROWN, C., MGE BROFF, S., KELLY-SPRATT, K. S., HOGLUND, V., LINDGREN, C., ORON, A. P., LI, D., RIDDELL, S. R., PARK, J. R. & JENSEN, M. C. 2017. Intent-to-treat leukemia remission by CD19 CAR T cells of defined formulation and dose in children and young adults. *Blood*, 129, 3322-3331.
- GARRIDO, F., RUIZ-CABELLO, F., CABRERA, T., PÉREZ-VILLAR, J. J., LÓPEZ-BOTET, M., DUGGAN-KEEN, M. & STERN, P. L. 1997. Implications for immunosurveillance of altered HLA class I phenotypes in human tumours. *Immunol Today*, 18, 89-95.
- GATTINONI, L., KLEBANOFF, C. A., PALMER, D. C., WRZESINSKI, C., KERSTANN, K., YU, Z., FINKELSTEIN, S. E., THEORET, M. R., ROSENBERG, S. A. & RESTIFO, N. P. 2005. Acquisition of full effector function in vitro paradoxically impairs the in vivo antitumor efficacy of adoptively transferred CD8+ T cells. *J Clin Invest*, 115, 1616-26.
- GATTINONI, L., LUGLI, E., JI, Y., POS, Z., PAULOS, C. M., QUIGLEY, M. F., ALMEIDA, J. R., GOSTICK, E., YU, Z., CARPENITO, C., WANG, E., DOUEK, D. C., PRICE, D. A., JUNE, C. H., MARINCOLA, F. M., ROEDERER, M. & RESTIFO, N. P. 2011. A human memory T cell subset with stem cell-like properties. *Nat Med*, 17, 1290-7.
- GATTINONI, L., SPEISER, D. E., LICHTERFELD, M. & BONINI, C. 2017. T memory stem cells in health and disease. *Nat Med*, 23, 18-27.
- GATTINONI, L., ZHONG, X. S., PALMER, D. C., JI, Y., HINRICHS, C. S., YU, Z., WRZESINSKI, C., BONI, A., CASSARD, L., GARVIN, L. M., PAULOS, C. M.,

- MURANSKI, P. & RESTIFO, N. P. 2009. Wnt signaling arrests effector T cell differentiation and generates CD8+ memory stem cells. *Nat Med*, 15, 808-13.
- GHASSEMI, S., BEDOYA, F., NUNEZ-CRUZ, S., JUNE, C., MELENHORST, J. & MILONE, M. 2016. Shortened T cell culture with IL-7 and IL-15 provides the most potent chimeric antigen receptor (CAR)-modified T cells for adoptive immunotherapy. *The Journal of Immunology*, 196, 214.23-214.23.
- GHASSEMI, S., DURGIN, J. S., NUNEZ-CRUZ, S., PATEL, J., LEFEROVICH, J., PINZONE, M., SHEN, F., CUMMINS, K. D., PLESA, G., CANTU, V. A., REDDY, S., BUSHMAN, F. D., GILL, S. I., O'DOHERTY, U., O'CONNOR, R. S. & MILONE, M. C. 2022. Rapid manufacturing of non-activated potent CAR T cells. *Nature Biomedical Engineering*, 6, 118-128.
- GHASSEMI, S., NUNEZ-CRUZ, S., O'CONNOR, R. S., FRAIETTA, J. A., PATEL, P. R., SCHOLLER, J., BARRETT, D. M., LUNDH, S. M., DAVIS, M. M., BEDOYA, F., ZHANG, C., LEFEROVICH, J., LACEY, S. F., LEVINE, B. L., GRUPP, S. A., JUNE, C. H., MELENHORST, J. J. & MILONE, M. C. 2018. Reducing Ex Vivo Culture Improves the Antileukemic Activity of Chimeric Antigen Receptor (CAR) T Cells. *Cancer Immunol Res*, 6, 1100-1109.
- GHORASHIAN, S., KRAMER, A. M., ONUOHA, S., WRIGHT, G., BARTRAM, J., RICHARDSON, R., ALBON, S. J., CASANOVAS-COMPANY, J., CASTRO, F., POPOVA, B., VILLANUEVA, K., YEUNG, J., VETHAROY, W., GUVENEL, A., WAWRZYNIECKA, P. A., MEKKAOU, L., CHEUNG, G. W., PINNER, D., CHU, J., LUCCHINI, G., SILVA, J., CIOCARLIE, O., LAZAREVA, A., INGLOTT, S., GILMOUR, K. C., AHSAN, G., FERRARI, M., MANZOOR, S., CHAMPION, K., BROOKS, T., LOPES, A., HACKSHAW, A., FARZANEH, F., CHIESA, R., RAO, K., BONNEY, D., SAMARASINGHE, S., GOULDEN, N., VORA, A., VEYS, P., HOUGH, R., WYNN, R., PULE, M. A. & AMROLIA, P. J. 2019. Enhanced CAR T cell expansion and prolonged persistence in pediatric patients with ALL treated with a low-affinity CD19 CAR. *Nat Med*, 25, 1408-1414.
- GHORASHIAN, S., PULE, M. & AMROLIA, P. 2015. CD19 chimeric antigen receptor T cell therapy for haematological malignancies. *British Journal of Haematology*, 169.
- GLICK, D., BARTH, S. & MACLEOD, K. F. 2010. Autophagy: cellular and molecular mechanisms. *J Pathol*, 221, 3-12.
- GOLUBOVSKAYA, V. & WU, L. 2016. Different Subsets of T Cells, Memory, Effector Functions, and CAR-T Immunotherapy. *Cancers (Basel)*, 8.
- GRAEF, P., BUCHHOLZ, V. R., STEMBERGER, C., FLOSSDORF, M., HENKEL, L., SCHIEMANN, M., DREXLER, I., HOFER, T., RIDDELL, S. R. & BUSCH, D. H. 2014. Serial transfer of single-cell-derived immunocompetence reveals stemness of CD8(+) central memory T cells. *Immunity*, 41, 116-26.

- GREER, E. L. & BRUNET, A. 2005. FOXO transcription factors at the interface between longevity and tumor suppression. *Oncogene*, 24, 7410-7425.
- GRUPP SA, M. S., RIVES S, ET AL. . December 1-4. Updated analysis of the efficacy and safety of tisagenlecleucel in pediatric and young adult patients with relapsed/refractory acute lymphoblastic leukemia. . 60th American Society of Hematology Annual Meeting, December 1-4 2018 San Diego, CA.
- GUEDAN, S., CALDERON, H., POSEY, A. D., JR. & MAUS, M. V. 2019. Engineering and Design of Chimeric Antigen Receptors. *Mol Ther Methods Clin Dev*, 12, 145-156.
- GUEDAN, S., CHEN, X., MADAR, A., CARPENITO, C., MCGETTIGAN, S. E., FRIGAULT, M. J., LEE, J., POSEY, A. D., JR., SCHOLLER, J., SCHOLLER, N., BONNEAU, R. & JUNE, C. H. 2014. ICOS-based chimeric antigen receptors program bipolar TH17/TH1 cells. *Blood*, 124, 1070-80.
- GUO, B., CHEN, M., HAN, Q., HUI, F., DAI, H., ZHANG, W., ZHANG, Y., WANG, Y., ZHU, H. & HAN, W. 2016. CD138-directed adoptive immunotherapy of chimeric antigen receptor (CAR)-modified T cells for multiple myeloma. *Journal of Cellular Immunotherapy*, 2, 28-35.
- GUO, J. Y., KARSLI-UZUNBAS, G., MATHEW, R., AISNER, S. C., KAMPHORST, J. J., STROHECKER, A. M., CHEN, G., PRICE, S., LU, W., TENG, X., SNYDER, E., SANTANAM, U., DIPOLA, R. S., JACKS, T., RABINOWITZ, J. D. & WHITE, E. 2013. Autophagy suppresses progression of K-ras-induced lung tumors to oncocytomas and maintains lipid homeostasis. *Genes Dev*, 27, 1447-61.
- GUPTA, S. S., SHARP, R., HOFFEREK, C., KUAI, L., DORN, G. W., 2ND, WANG, J. & CHEN, M. 2019. NIX-Mediated Mitophagy Promotes Effector Memory Formation in Antigen-Specific CD8(+) T Cells. *Cell Rep*, 29, 1862-1877.e7.
- HAMAÏ, A., PIGNON, P., RAIMBAUD, I., DUPERRIER-AMOURIAUX, K., SENELLART, H., HIRET, S., DOUILLARD, J.-Y., BENNOUNA, J., AYYOUB, M. & VALMORI, D. 2012. Human TH17 Immune Cells Specific for the Tumor Antigen MAGE-A3 Convert to IFN- γ -Secreting Cells as They Differentiate into Effector T Cells In Vivo. *Cancer Research*, 72, 1059-1063.
- HAN, J. M., PATTERSON, S. J. & LEVINGS, M. K. 2012. The Role of the PI3K Signaling Pathway in CD4(+) T Cell Differentiation and Function. *Front Immunol*, 3, 245.
- HANAHAHAN, D. & WEINBERG, R. A. 2011. Hallmarks of cancer: the next generation. *Cell*, 144, 646-74.
- HAXHINASTO, S., MATHIS, D. & BENOIST, C. 2008. The AKT-mTOR axis regulates de novo differentiation of CD4+Foxp3+ cells. *J Exp Med*, 205, 565-74.

- HAY, K. A. & TURTLE, C. J. 2017. Chimeric Antigen Receptor (CAR) T Cells: Lessons Learned from Targeting of CD19 in B-Cell Malignancies. *Drugs*, 77, 237-245.
- HCP.NOVARTIS.COM. 2019. *KYMRIAH® (TISAGENLEUCCEL)* [Online]. Available: <https://www.hcp.novartis.com/products/kymriah/acute-lymphoblastic-leukemia-children/> [Accessed 2020].
- HE, J., HU, Y., HU, M. & LI, B. 2015. Development of PD-1/PD-L1 Pathway in Tumor Immune Microenvironment and Treatment for Non-Small Cell Lung Cancer. *Scientific Reports*, 5, 13110.
- HERS, I., VINCENT, E. E. & TAVARE, J. M. 2011. Akt signalling in health and disease. *Cell Signal*, 23, 1515-27.
- HINRICHS, C. S., BORMAN, Z. A., GATTINONI, L., YU, Z., BURNS, W. R., HUANG, J., KLEBANOFF, C. A., JOHNSON, L. A., KERKAR, S. P., YANG, S., MURANSKI, P., PALMER, D. C., SCOTT, C. D., MORGAN, R. A., ROBBINS, P. F., ROSENBERG, S. A. & RESTIFO, N. P. 2011. Human effector CD8+ T cells derived from naive rather than memory subsets possess superior traits for adoptive immunotherapy. *Blood*, 117, 808-14.
- HUCKS, G. & RHEINGOLD, S. R. 2019. The journey to CAR T cell therapy: the pediatric and young adult experience with relapsed or refractory B-ALL. *Blood Cancer J*, 9, 10.
- IQBAL, N. & IQBAL, N. 2014. Imatinib: a breakthrough of targeted therapy in cancer. *Chemother Res Pract*, 2014, 357027.
- JANG, I. K., LEE, Z. H., KIM, Y. J., KIM, S. H. & KWON, B. S. 1998. Human 4-1BB (CD137) signals are mediated by TRAF2 and activate nuclear factor-kappa B. *Biochem Biophys Res Commun*, 242, 613-20.
- JUNE, C. H. & SADELAIN, M. 2018. Chimeric Antigen Receptor Therapy. *N Engl J Med*, 379, 64-73.
- KALOS, M., LEVINE, B. L., PORTER, D. L., KATZ, S., GRUPP, S. A., BAGG, A. & JUNE, C. H. 2011. T cells with chimeric antigen receptors have potent antitumor effects and can establish memory in patients with advanced leukemia. *Sci Transl Med*, 3, 95ra73.
- KANEKO, S., MASTAGLIO, S., BONDANZA, A., PONZONI, M., SANVITO, F., ALDRIGHETTI, L., RADRIZZANI, M., LA SETA-CATAMANCIO, S., PROVASI, E., MONDINO, A., NAGASAWA, T., FLEISCHHAUER, K., RUSSO, V., TRAVERSARI, C., CICERI, F., BORDIGNON, C. & BONINI, C. 2009. IL-7 and IL-15 allow the generation of suicide gene-modified alloreactive self-renewing central memory human T lymphocytes. *Blood*, 113, 1006-15.
- KARA, E. E., COMERFORD, I., FENIX, K. A., BASTOW, C. R., GREGOR, C. E., MCKENZIE, D. R. & MCCOLL, S. R. 2014. Tailored Immune Responses: Novel

- Effector Helper T Cell Subsets in Protective Immunity. *PLOS Pathogens*, 10, e1003905.
- KAWAI, O., ISHII, G., KUBOTA, K., MURATA, Y., NAITO, Y., MIZUNO, T., AOKAGE, K., SAJO, N., NISHIWAKI, Y., GEMMA, A., KUDOH, S. & OCHIAI, A. 2008. Predominant infiltration of macrophages and CD8(+) T Cells in cancer nests is a significant predictor of survival in stage IV nonsmall cell lung cancer. *Cancer*, 113, 1387-95.
- KAWALEKAR, O. U., O'CONNOR, R. S., FRAIETTA, J. A., GUO, L., MCGETTIGAN, S. E., POSEY, A. D., JR., PATEL, P. R., GUEDAN, S., SCHOLLER, J., KEITH, B., SNYDER, N. W., BLAIR, I. A., MILONE, M. C. & JUNE, C. H. 2016. Distinct Signaling of Coreceptors Regulates Specific Metabolism Pathways and Impacts Memory Development in CAR T Cells. *Immunity*, 44, 380-90.
- KERDILES, Y. M., BEISNER, D. R., TINOCO, R., DEJEAN, A. S., CASTRILLON, D. H., DEPINHO, R. A. & HEDRICK, S. M. 2009. Foxo1 links homing and survival of naive T cells by regulating L-selectin, CCR7 and interleukin 7 receptor. *Nat Immunol*, 10, 176-84.
- KERSHAW, M. H., WANG, G., WESTWOOD, J. A., PACHYNSKI, R. K., TIFFANY, H. L., MARINCOLA, F. M., WANG, E., YOUNG, H. A., MURPHY, P. M. & HWU, P. 2002. Redirecting migration of T cells to chemokine secreted from tumors by genetic modification with CXCR2. *Hum Gene Ther*, 13, 1971-80.
- KIM, E. H., SULLIVAN, J. A., PLISCH, E. H., TEJERA, M. M., JATZEK, A., CHOI, K. Y. & SURESH, M. 2012. Signal integration by Akt regulates CD8 T cell effector and memory differentiation. *J Immunol*, 188, 4305-14.
- KIM, E. H. & SURESH, M. 2013. Role of PI3K/Akt signaling in memory CD8 T cell differentiation. *Front Immunol*, 4, 20.
- KIM, S. K. & CHO, S. W. 2022. The Evasion Mechanisms of Cancer Immunity and Drug Intervention in the Tumor Microenvironment. *Frontiers in Pharmacology*, 13.
- KISHTON, R. J., SUKUMAR, M. & RESTIFO, N. P. 2017. Metabolic Regulation of T Cell Longevity and Function in Tumor Immunotherapy. *Cell Metab*, 26, 94-109.
- KLEBANOFF, C. A., CROMPTON, J. G., LEONARDI, A. J., YAMAMOTO, T. N., CHANDRAN, S. S., EIL, R. L., SUKUMAR, M., VODNALA, S. K., HU, J., JI, Y., CLEVER, D., BLACK, M. A., GURUSAMY, D., KRUHLAK, M. J., JIN, P., STRONCEK, D. F., GATTINONI, L., FELDMAN, S. A. & RESTIFO, N. P. 2017. Inhibition of AKT signaling uncouples T cell differentiation from expansion for receptor-engineered adoptive immunotherapy. *JCI insight*, 2, e95103.
- KLEBANOFF, C. A., GATTINONI, L. & RESTIFO, N. P. 2012. Sorting through subsets: which T-cell populations mediate highly effective adoptive immunotherapy? *J Immunother*, 35, 651-60.

- KLOSS, C. C., LEE, J., ZHANG, A., CHEN, F., MELENHORST, J. J., LACEY, S. F., MAUS, M. V., FRAIETTA, J. A., ZHAO, Y. & JUNE, C. H. 2018. Dominant-Negative TGF-beta Receptor Enhances PSMA-Targeted Human CAR T Cell Proliferation And Augments Prostate Cancer Eradication. *Mol Ther*, 26, 1855-1866.
- KOCHENDERFER, J. N., DUDLEY, M. E., KASSIM, S. H., SOMERVILLE, R. P., CARPENTER, R. O., STETLER-STEVENSON, M., YANG, J. C., PHAN, G. Q., HUGHES, M. S., SHERRY, R. M., RAFFELD, M., FELDMAN, S., LU, L., LI, Y. F., NGO, L. T., GOY, A., FELDMAN, T., SPANER, D. E., WANG, M. L., CHEN, C. C., KRANICK, S. M., NATH, A., NATHAN, D. A., MORTON, K. E., TOOMEY, M. A. & ROSENBERG, S. A. 2015. Chemotherapy-refractory diffuse large B-cell lymphoma and indolent B-cell malignancies can be effectively treated with autologous T cells expressing an anti-CD19 chimeric antigen receptor. *J Clin Oncol*, 33, 540-9.
- KOOSHKAKI, O., DERAKHSHANI, A., HOSSEINKHANI, N., TORABI, M., SAFAEI, S., BRUNETTI, O., RACANELLI, V., SILVESTRIS, N. & BARADARAN, B. 2020. Combination of Ipilimumab and Nivolumab in Cancers: From Clinical Practice to Ongoing Clinical Trials. *Int J Mol Sci*, 21.
- KORN, T. & HILTENSPERGER, M. 2021. Role of IL-6 in the commitment of T cell subsets. *Cytokine*, 146, 155654.
- KOTANI, K., OGAWA, W., HINO, Y., KITAMURA, T., UENO, H., SANO, W., SUTHERLAND, C., GRANNER, D. K. & KASUGA, M. 1999. Dominant negative forms of Akt (protein kinase B) and atypical protein kinase C lambda do not prevent insulin inhibition of phosphoenolpyruvate carboxykinase gene transcription. *J Biol Chem*, 274, 21305-12.
- KRENCIUTE, G., PRINZING, B. L., YI, Z., WU, M. F., LIU, H., DOTTI, G., BALLYASNIKOVA, I. V. & GOTTSCHALK, S. 2017. Transgenic Expression of IL15 Improves Antiglioma Activity of IL13Ralpha2-CAR T Cells but Results in Antigen Loss Variants. *Cancer Immunol Res*, 5, 571-581.
- KUEBERUWA, G., KALAITSIDOU, M., CHEADLE, E., HAWKINS, R. E. & GILHAM, D. E. 2018a. CD19 CAR T Cells Expressing IL-12 Eradicate Lymphoma in Fully Lymphoreplete Mice through Induction of Host Immunity. *Mol Ther Oncolytics*, 8, 41-51.
- KUEBERUWA, G., ZHENG, W., KALAITSIDOU, M., GILHAM, D. E. & HAWKINS, R. E. 2018b. A Syngeneic Mouse B-Cell Lymphoma Model for Pre-Clinical Evaluation of CD19 CAR T Cells. *J Vis Exp*.
- LANGRISH, C. L., CHEN, Y., BLUMENSCHNIG, W. M., MATTSON, J., BASHAM, B., SEDGWICK, J. D., MCCLANAHAN, T., KASTELEIN, R. A. & CUA, D. J. 2005. IL-23 drives a pathogenic T cell population that induces autoimmune inflammation. *The Journal of experimental medicine*, 201, 233-240.

- LEE, D. W., KOCHENDERFER, J. N., STETLER-STEVENSON, M., CUI, Y. K., DELBROOK, C., FELDMAN, S. A., FRY, T. J., ORENTAS, R., SABATINO, M., SHAH, N. N., STEINBERG, S. M., STRONCEK, D., TSCHERNIA, N., YUAN, C., ZHANG, H., ZHANG, L., ROSENBERG, S. A., WAYNE, A. S. & MACKALL, C. L. 2015. T cells expressing CD19 chimeric antigen receptors for acute lymphoblastic leukaemia in children and young adults: a phase 1 dose-escalation trial. *The Lancet*, 385, 517-528.
- LEE, H. W., NAM, K. O., PARK, S. J. & KWON, B. S. 2003. 4-1BB enhances CD8+ T cell expansion by regulating cell cycle progression through changes in expression of cyclins D and E and cyclin-dependent kinase inhibitor p27kip1. *Eur J Immunol*, 33, 2133-41.
- LEIGHL, N. B., KARASEVA, N., NAKAGAWA, K., CHO, B. C., GRAY, J. E., HOVEY, T., WALDING, A., RYDÉN, A. & NOVELLO, S. 2020. Patient-reported outcomes from FLAURA: Osimertinib versus erlotinib or gefitinib in patients with EGFR-mutated advanced non-small-cell lung cancer. *Eur J Cancer*, 125, 49-57.
- LEMAL, R. & TOURNILHAC, O. 2019. State-of-the-art for CAR T-cell therapy for chronic lymphocytic leukemia in 2019. *J Immunother Cancer*, 7, 202.
- LEV BAR-OR, R. 2000. Feedback mechanisms between T helper cells and macrophages in the determination of the immune response. *Mathematical Biosciences*, 163, 35-58.
- LIN, H., CHENG, J., MU, W., ZHOU, J. & ZHU, L. 2021. Advances in Universal CAR-T Cell Therapy. *Frontiers in Immunology*, 12.
- LINDSLEY, C. W., ZHAO, Z., LEISTER, W. H., ROBINSON, R. G., BARNETT, S. F., DEFEO-JONES, D., JONES, R. E., HARTMAN, G. D., HUFF, J. R., HUBER, H. E. & DUGGAN, M. E. 2005. Allosteric Akt (PKB) inhibitors: discovery and SAR of isozyme selective inhibitors. *Bioorganic & Medicinal Chemistry Letters*, 15, 761-764.
- LIPPITZ, B. E. 2013. Cytokine patterns in patients with cancer: a systematic review. *Lancet Oncol*, 14, e218-28.
- LIU, D. & UZONNA, J. E. 2010. The p110 delta isoform of phosphatidylinositol 3-kinase controls the quality of secondary anti-Leishmania immunity by regulating expansion and effector function of memory T cell subsets. *J Immunol*, 184, 3098-105.
- LOCKE, F. L., GHOBADI, A., JACOBSON, C. A., MIKLOS, D. B., LEKAKIS, L. J., OLUWOLE, O. O., LIN, Y., BRAUNSCHWEIG, I., HILL, B. T., TIMMERMAN, J. M., DEOL, A., REAGAN, P. M., STIFF, P., FLINN, I. W., FAROOQ, U., GOY, A., MCSWEENEY, P. A., MUNOZ, J., SIDDIQI, T., CHAVEZ, J. C., HERRERA, A. F., BARTLETT, N. L., WIEZOREK, J. S., NAVALE, L., XUE, A., JIANG, Y., BOT, A., ROSSI, J. M., KIM, J. J., GO, W.

- Y. & NEELAPU, S. S. 2019. Long-term safety and activity of axicabtagene ciloleucel in refractory large B-cell lymphoma (ZUMA-1): a single-arm, multicentre, phase 1-2 trial. *Lancet Oncol*, 20, 31-42.
- LU, H., WANG, H., YAN, L., SHAO, H., ZHANG, W., SHEN, H., BO, H., TAO, C., XIA, S. & WU, F. 2020. Overexpression of early T cell differentiation-specific transcription factors transforms the terminally differentiated effector T cells into less differentiated state. *Cell Immunol*, 353, 104118.
- LU, T. L., PUGACH, O., SOMERVILLE, R., ROSENBERG, S. A., KOCHENDERFER, J. N., BETTER, M. & FELDMAN, S. A. 2016. A Rapid Cell Expansion Process for Production of Engineered Autologous CAR-T Cell Therapies. *Hum Gene Ther Methods*, 27, 209-218.
- MA, S., LI, X., WANG, X., CHENG, L., LI, Z., ZHANG, C., YE, Z. & QIAN, Q. 2019. Current Progress in CAR-T Cell Therapy for Solid Tumors. *Int J Biol Sci*, 15, 2548-2560.
- MACINTYRE, A. N., FINLAY, D., PRESTON, G., SINCLAIR, L. V., WAUGH, C. M., TAMAS, P., FEIJOO, C., OKKENHAUG, K. & CANTRELL, D. A. 2011. Protein kinase B controls transcriptional programs that direct cytotoxic T cell fate but is dispensable for T cell metabolism. *Immunity*, 34, 224-36.
- MAHMOUD, S. M., PAISH, E. C., POWE, D. G., MACMILLAN, R. D., GRAINGE, M. J., LEE, A. H., ELLIS, I. O. & GREEN, A. R. 2011. Tumor-infiltrating CD8+ lymphocytes predict clinical outcome in breast cancer. *J Clin Oncol*, 29, 1949-55.
- MAHNKE, Y. D., BRODIE, T. M., SALLUSTO, F., ROEDERER, M. & LUGLI, E. 2013. The who's who of T-cell differentiation: human memory T-cell subsets. *Eur J Immunol*, 43, 2797-809.
- MANURI, P. V., WILSON, M. H., MAITI, S. N., MI, T., SINGH, H., OLIVARES, S., DAWSON, M. J., HULS, H., LEE, D. A., RAO, P. H., KAMINSKI, J. M., NAKAZAWA, Y., GOTTSCHALK, S., KEBRIAIEI, P., SHPALL, E. J., CHAMPLIN, R. E. & COOPER, L. J. 2010. piggyBac transposon/transposase system to generate CD19-specific T cells for the treatment of B-lineage malignancies. *Hum Gene Ther*, 21, 427-37.
- MARKLEY, J. C. & SADELAIN, M. 2010. IL-7 and IL-21 are superior to IL-2 and IL-15 in promoting human T cell-mediated rejection of systemic lymphoma in immunodeficient mice. *Blood*, 115, 3508-19.
- MARTIN-OROZCO, N., MURANSKI, P., CHUNG, Y., YANG, X. O., YAMAZAKI, T., LU, S., HWU, P., RESTIFO, N. P., OVERWIJK, W. W. & DONG, C. 2009. T helper 17 cells promote cytotoxic T cell activation in tumor immunity. *Immunity*, 31, 787-798.
- MAUDE, S., BARRETT, D., RHEINGOLD, S., APLENC, R., TEACHEY, D., CALLAHAN, C., BANIEWICZ, D., WHITE, C., TALEKAR, M., SHAW, P,

- BROGDON, J, YOUNG, R, SCHOLLER, J, MARCUCCI, K, LEVINE, B, FREY, N, PORTER, D, LACEY, S, MELENHORST, J, JUNE, C. AND GRUPP, S 2016. Efficacy of Humanized CD19-Targeted Chimeric Antigen Receptor (CAR)-Modified T Cells in Children and Young Adults with Relapsed/Refractory Acute Lymphoblastic Leukemia. *Blood*, 128, 217.
- MAUDE, S. L., FREY, N., SHAW, P. A., APLENC, R., BARRETT, D. M., BUNIN, N. J., CHEW, A., GONZALEZ, V. E., ZHENG, Z., LACEY, S. F., MAHNKE, Y. D., MELENHORST, J. J., RHEINGOLD, S. R., SHEN, A., TEACHEY, D. T., LEVINE, B. L., JUNE, C. H., PORTER, D. L. & GRUPP, S. A. 2014. Chimeric antigen receptor T cells for sustained remissions in leukemia. *N Engl J Med*, 371, 1507-17.
- MAUDE, S. L., LAETSCH, T. W., BUECHNER, J., RIVES, S., BOYER, M., BITTENCOURT, H., BADER, P., VERNERIS, M. R., STEFANSKI, H. E., MYERS, G. D., QAYED, M., DE MOERLOOSE, B., HIRAMATSU, H., SCHLIS, K., DAVIS, K. L., MARTIN, P. L., NEMECEK, E. R., YANIK, G. A., PETERS, C., BARUCHEL, A., BOISSEL, N., MECHINAUD, F., BALDUZZI, A., KRUEGER, J., JUNE, C. H., LEVINE, B. L., WOOD, P., TARAN, T., LEUNG, M., MUELLER, K. T., ZHANG, Y., SEN, K., LEBWOHL, D., PULSIPHER, M. A. & GRUPP, S. A. 2018. Tisagenlecleucel in Children and Young Adults with B-Cell Lymphoblastic Leukemia. *N Engl J Med*, 378, 439-448.
- MAUS, M. V., HAAS, A. R., BEATTY, G. L., ALBELDA, S. M., LEVINE, B. L., LIU, X., ZHAO, Y., KALOS, M. & JUNE, C. H. 2013. T cells expressing chimeric antigen receptors can cause anaphylaxis in humans. *Cancer Immunol Res*, 1, 26-31.
- MAXIMIANO, S., MAGALHÃES, P., GUERREIRO, M. P. & MORGADO, M. 2016. Trastuzumab in the Treatment of Breast Cancer. *BioDrugs*, 30, 75-86.
- MEJSTRIKOVA, E., HRUSAK, O., BOROWITZ, M. J., WHITLOCK, J. A., BRETHON, B., TRIPPETT, T. M., ZUGMAIER, G., GORE, L., VON STACKELBERG, A. & LOCATELLI, F. 2017. CD19-negative relapse of pediatric B-cell precursor acute lymphoblastic leukemia following blinatumomab treatment. *Blood Cancer J*, 7, 659.
- MELENHORST, J. J., CHEN, G. M., WANG, M., PORTER, D. L., CHEN, C., COLLINS, M. A., GAO, P., BANDYOPADHYAY, S., SUN, H., ZHAO, Z., LUNDH, S., PRUTEANU-MALINICI, I., NOBLES, C. L., MAJI, S., FREY, N. V., GILL, S. I., TIAN, L., KULIKOVSKAYA, I., GUPTA, M., AMBROSE, D. E., DAVIS, M. M., FRAIETTA, J. A., BROGDON, J. L., YOUNG, R. M., CHEW, A., LEVINE, B. L., SIEGEL, D. L., ALANIO, C., WHERRY, E. J., BUSHMAN, F. D., LACEY, S. F., TAN, K. & JUNE, C. H. 2022. Decade-long leukaemia remissions with persistence of CD4+ CAR T cells. *Nature*, 602, 503-509.
- MILONE, M. C., FISH, J. D., CARPENITO, C., CARROLL, R. G., BINDER, G. K., TEACHEY, D., SAMANTA, M., LAKHAL, M., GLOSS, B., DANET-

- DESNOYERS, G., CAMPANA, D., RILEY, J. L., GRUPP, S. A. & JUNE, C. H. 2009. Chimeric receptors containing CD137 signal transduction domains mediate enhanced survival of T cells and increased antileukemic efficacy in vivo. *Mol Ther*, 17, 1453-64.
- MILONE, M. C. & O'DOHERTY, U. 2018. Clinical use of lentiviral vectors. *Leukemia*, 32, 1529-1541.
- MOCK, U., NICKOLAY, L., PHILIP, B., CHEUNG, G. W., ZHAN, H., JOHNSTON, I. C. D., KAISER, A. D., PEGGS, K., PULE, M., THRASHER, A. J. & QASIM, W. 2016. Automated manufacturing of chimeric antigen receptor T cells for adoptive immunotherapy using CliniMACS prodigy. *Cytotherapy*, 18, 1002-1011.
- MOUSSET, C. M., HOBBO, W., DE LIGT, A., BAARDMAN, S., SCHAAP, N. P. M., JANSEN, J. H., VAN DER WAART, A. B. & DOLSTRA, H. 2020. Cell composition and expansion strategy can reduce the beneficial effect of AKT-inhibition on functionality of CD8(+) T cells. *Cancer Immunol Immunother*, 69, 2259-2273.
- MOUSSET, C. M., HOBBO, W., JI, Y., FREDRIX, H., DE GIORGI, V., ALLISON, R. D., KESTER, M. G. D., FALKENBURG, J. H. F., SCHAAP, N. P. M., JANSEN, J. H., GATTINONI, L., DOLSTRA, H. & VAN DER WAART, A. B. 2018. Ex vivo AKT-inhibition facilitates generation of polyfunctional stem cell memory-like CD8(+) T cells for adoptive immunotherapy. *Oncoimmunology*, 7, e1488565.
- MURANSKI, P., BONI, A., ANTONY, P. A., CASSARD, L., IRVINE, K. R., KAISER, A., PAULOS, C. M., PALMER, D. C., TOULOUKIAN, C. E. & PTAK, K. 2008. Tumor-specific Th17-polarized cells eradicate large established melanoma. *Blood, The Journal of the American Society of Hematology*, 112, 362-373.
- MURANSKI, P., BORMAN, ZACHARY A., KERKAR, SID P., KLEBANOFF, CHRISTOPHER A., JI, Y., SANCHEZ-PEREZ, L., SUKUMAR, M., REGER, ROBERT N., YU, Z., KERN, STEVEN J., ROYCHOUDHURI, R., FERREYRA, GABRIELA A., SHEN, W., DURUM, SCOTT K., FEIGENBAUM, L., PALMER, DOUGLAS C., ANTONY, PAUL A., CHAN, C.-C., LAURENCE, A., DANNER, ROBERT L., GATTINONI, L. & RESTIFO, NICHOLAS P. 2011. Th17 Cells Are Long Lived and Retain a Stem Cell-like Molecular Signature. *Immunity*, 35, 972-985.
- MURPHY, K. & WEAVER, C. 2016. *Janeway's Immunobiology, 9th Edition*.
- MURPHY, K., WEAVER, C. & JANEWAY, C. 2017. *Janeway's immunobiology*, New York, W.W. Norton & Company.
- NAKAMURA, K., AMAKAWA, R., TAKEBAYASHI, M., SON, Y., MIYAJI, M., TAJIMA, K., NAKAI, K., ITO, T., MATSUMOTO, N., ZEN, K., KISHIMOTO, Y. & FUKUHARA, S. 2005. IL-4-producing CD8+ T cells may be an immunological hallmark of chronic GVHD. *Bone Marrow Transplantation*, 36, 639-647.

- NAPPO, G., HANDLE, F., SANTER, F. R., MCNEILL, R. V., SEED, R. I., COLLINS, A. T., MORRONE, G., CULIG, Z., MAITLAND, N. J. & ERB, H. H. H. 2017. The immunosuppressive cytokine interleukin-4 increases the clonogenic potential of prostate stem-like cells by activation of STAT6 signalling. *Oncogenesis*, 6, e342-e342.
- NEELAPU, S., LOCKE, F., BARTLETT, N., LEKAKIS, L., MIKLOS, D., JACOBSEN, E., BRAUNSCHWEIG, I., OLUWOLE, O., SIDDIQI, T., LIN, Y., TIMMERMAN, J., REAGAN, P., BOT, A., ROSSI, J., NAVALE, L., JIANG, Y., AYCOCK, J., ELIAS, M., WIEZOREK, J. AND GO, W 2018. Axicabtagene Ciloleucel (axi-cel; KTE-C19) in Patients with Refractory Aggressive Non-Hodgkin Lymphoma (NHL): Long-Term Follow-up of the Pivotal Zuma-1 Trial. *Biology of Blood and Marrow Transplantation*, 24, S74-S75.
- NEELAPU, S. S., LOCKE, F. L., BARTLETT, N. L., LEKAKIS, L. J., MIKLOS, D. B., JACOBSON, C. A., BRAUNSCHWEIG, I., OLUWOLE, O. O., SIDDIQI, T., LIN, Y., TIMMERMAN, J. M., STIFF, P. J., FRIEDBERG, J. W., FLINN, I. W., GOY, A., HILL, B. T., SMITH, M. R., DEOL, A., FAROOQ, U., MCSWEENEY, P., MUNOZ, J., AVIVI, I., CASTRO, J. E., WESTIN, J. R., CHAVEZ, J. C., GHOBADI, A., KOMANDURI, K. V., LEVY, R., JACOBSEN, E. D., WITZIG, T. E., REAGAN, P., BOT, A., ROSSI, J., NAVALE, L., JIANG, Y., AYCOCK, J., ELIAS, M., CHANG, D., WIEZOREK, J. & GO, W. Y. 2017. Axicabtagene Ciloleucel CAR T-Cell Therapy in Refractory Large B-Cell Lymphoma. *N Engl J Med*, 377, 2531-2544.
- NIAN, Z., ZHENG, X., DOU, Y., DU, X., ZHOU, L., FU, B., SUN, R., TIAN, Z. & WEI, H. 2021. Rapamycin Pretreatment Rescues the Bone Marrow AML Cell Elimination Capacity of CAR-T Cells. *Clin Cancer Res*, 27, 6026-6038.
- NISHIMURA, T., IWAKABE, K., SEKIMOTO, M., OHMI, Y., YAHATA, T., NAKUI, M., SATO, T., HABU, S., TASHIRO, H. & SATO, M. 1999. Distinct role of antigen-specific T helper type 1 (Th1) and Th2 cells in tumor eradication in vivo. *The Journal of experimental medicine*, 190, 617-628.
- NISHIMURA, T., NAKUI, M., SATO, M., IWAKABE, K., KITAMURA, H., SEKIMOTO, M., OHTA, A., KODA, T. & NISHIMURA, S. 2000. The critical role of Th1-dominant immunity in tumor immunology. *Cancer Chemother Pharmacol*, 46 Suppl, S52-61.
- NOVARTIS. *Novartis Press Release: Novartis announces T-Charge™, next-generation CAR-T platform with first-in-human data at ASH 2021* [Online]. Available: <https://www.novartis.com/news/media-releases/novartis-announces-t-charge-tem-next-generation-car-t-platform-first-human-data-ash-2021> [Accessed Dec 2022].
- NUMASAKI, M., WATANABE, M., SUZUKI, T., TAKAHASHI, H., NAKAMURA, A., MCALLISTER, F., HISHINUMA, T., GOTO, J., LOTZE, M. T. & KOLLS, J. K. 2005. IL-17 enhances the net angiogenic activity and in vivo growth of human non-small cell lung cancer in SCID mice through promoting CXCR-2-dependent angiogenesis. *The Journal of Immunology*, 175, 6177-6189.

- O'SULLIVAN, D., VAN DER WINDT, G. J., HUANG, S. C., CURTIS, J. D., CHANG, C. H., BUCK, M. D., QIU, J., SMITH, A. M., LAM, W. Y., DIPLATO, L. M., HSU, F. F., BIRNBAUM, M. J., PEARCE, E. J. & PEARCE, E. L. 2014. Memory CD8(+) T cells use cell-intrinsic lipolysis to support the metabolic programming necessary for development. *Immunity*, 41, 75-88.
- OCHI, A., NGUYEN, A. H., BEDROSIAN, A. S., MUSHLIN, H. M., ZARBAKHS, S., BARILLA, R., ZAMBIRINIS, C. P., FALLON, N. C., REHMAN, A., PYLAYEVA-GUPTA, Y., BADAR, S., HAJDU, C. H., FREY, A. B., BARSAGI, D. & MILLER, G. 2012. MyD88 inhibition amplifies dendritic cell capacity to promote pancreatic carcinogenesis via Th2 cells. *Journal of Experimental Medicine*, 209, 1671-1687.
- OESTE, C. L., SECO, E., PATTON, W. F., BOYA, P. & PÉREZ-SALA, D. 2013. Interactions between autophagic and endo-lysosomal markers in endothelial cells. *Histochemistry and Cell Biology*, 139, 659-670.
- OKKENHAUG, K., BILANCIO, A., FARJOT, G., PRIDDLE, H., SANCHO, S., PESKETT, E., PEARCE, W., MEEK, S. E., SALPEKAR, A., WATERFIELD, M. D., SMITH, A. J. & VANHAESEBROECK, B. 2002. Impaired B and T cell antigen receptor signaling in p110delta PI 3-kinase mutant mice. *Science*, 297, 1031-4.
- PATTON, D. T., GARDEN, O. A., PEARCE, W. P., CLOUGH, L. E., MONK, C. R., LEUNG, E., ROWAN, W. C., SANCHO, S., WALKER, L. S., VANHAESEBROECK, B. & OKKENHAUG, K. 2006. Cutting edge: the phosphoinositide 3-kinase p110 delta is critical for the function of CD4+CD25+Foxp3+ regulatory T cells. *J Immunol*, 177, 6598-602.
- PEARCE, E. L., WALSH, M. C., CEJAS, P. J., HARMS, G. M., SHEN, H., WANG, L. S., JONES, R. G. & CHOI, Y. 2009. Enhancing CD8 T-cell memory by modulating fatty acid metabolism. *Nature*, 460, 103-7.
- PETERSEN, C. T., HASSAN, M., MORRIS, A. B., JEFFERY, J., LEE, K., JAGIRDAR, N., STATON, A. D., RAIKAR, S. S., SPENCER, H. T., SULCHEK, T., FLOWERS, C. R. & WALLER, E. K. 2018. Improving T-cell expansion and function for adoptive T-cell therapy using ex vivo treatment with PI3Kdelta inhibitors and VIP antagonists. *Blood Adv*, 2, 210-223.
- PHILIP, B., KOKALAKI, E., MEKKAOU, L., THOMAS, S., STRAATHOF, K., FLUTTER, B., MARIN, V., MARAFIOTI, T., CHAKRAVERTY, R., LINCH, D., QUEZADA, S. A., PEGGS, K. S. & PULE, M. 2014. A highly compact epitope-based marker/suicide gene for easier and safer T-cell therapy. *Blood*, 124, 1277-87.
- QASIM, W. 2019. Allogeneic CAR T cell therapies for leukemia. *Am J Hematol*, 94, S50-S54.

- RAJAT K. DAS, J. S., DAVID M. BARRETT. T cell dysfunction in pediatric cancer patients at diagnosis and after chemotherapy can limit chimeric antigen receptor potential. Proceedings of the American Association for Cancer Research Annual Meeting (AACR), 2018 14-18; Chicago, IL. Philadelphia (PA). *Cancer Res* 2018;78(13 Suppl):Abstract no 1631.
- RAJE, N. S., SHAH, N., JAGANNATH, S., KAUFMAN, J. L., SIEGEL, D. S., MUNSHI, N. C., ROSENBLATT, J., LIN, Y., JAKUBOWIAK, A., TIMM, A., YERI, A., MARTIN, N., CAMPBELL, T. B., FINNEY, O., TRUPPEL-HARTMANN, A., PETROCCA, F., BERDEJA, J. G. & ALSINA, M. 2021. Updated Clinical and Correlative Results from the Phase I CRB-402 Study of the BCMA-Targeted CAR T Cell Therapy bb21217 in Patients with Relapsed and Refractory Multiple Myeloma. *Blood*, 138, 548-548.
- RAMOS, C. A., ROUCE, R., ROBERTSON, C. S., REYNA, A., NARALA, N., VYAS, G., MEHTA, B., ZHANG, H., DAKHOVA, O., CARRUM, G., KAMBLE, R. T., GEE, A. P., MEI, Z., WU, M. F., LIU, H., GRILLEY, B., ROONEY, C. M., HESLOP, H. E., BRENNER, M. K., SAVOLDO, B. & DOTTI, G. 2018. In Vivo Fate and Activity of Second- versus Third-Generation CD19-Specific CAR-T Cells in B Cell Non-Hodgkin's Lymphomas. *Mol Ther*, 26, 2727-2737.
- RAWAL, S., PARK, H. J., CHU, F., ZHANG, M., NATTAMAI, D., KANNAN, S. C., SHARMA, R., DELGADO, D. A., CHOU, T., DAVIS, R. E. & NEELAPU, S. S. 2011. Role of IL-4 in Inducing Immunosuppressive Tumor Microenvironment in Follicular Lymphoma. *Blood*, 118, 771-771.
- RICHES, J. C., DAVIES, J. K., MCCLANAHAN, F., FATAH, R., IQBAL, S., AGRAWAL, S., RAMSAY, A. G. & GRIBBEN, J. G. 2013. T cells from CLL patients exhibit features of T-cell exhaustion but retain capacity for cytokine production. *Blood*, 121, 1612-21.
- RODDIE, C., DIAS, J., O'REILLY, M. A., ABBASIAN, M., CADINANOS-GARAI, A., VISPUTE, K., BOSSHARD-CARTER, L., MITSIKAKOU, M., MEHRA, V., RODDY, H., HARTLEY, J. A., SPANSWICK, V., LOWE, H., POPOVA, B., CLIFTON-HADLEY, L., WHEELER, G., OLEJNIK, J., BLOOR, A., IRVINE, D., WOOD, L., MARZOLINI, M. A. V., DOMNING, S., FARZANEH, F., LOWDELL, M. W., LINCH, D. C., PULE, M. A. & PEGGS, K. S. 2021. Durable Responses and Low Toxicity After Fast Off-Rate CD19 Chimeric Antigen Receptor-T Therapy in Adults With Relapsed or Refractory B-Cell Acute Lymphoblastic Leukemia. *J Clin Oncol*, 39, 3352-3363.
- RODDIE, C., O'REILLY, M., DIAS ALVES PINTO, J., VISPUTE, K. & LOWDELL, M. 2019. Manufacturing chimeric antigen receptor T cells: issues and challenges. *Cytotherapy*, 21, 327-340.
- ROSENBERG, S. A., YANNELLI, J. R., YANG, J. C., TOPALIAN, S. L., SCHWARTZENTRUBER, D. J., WEBER, J. S., PARKINSON, D. R., SEIPP, C. A., EINHORN, J. H. & WHITE, D. E. 1994. Treatment of patients with metastatic

- melanoma with autologous tumor-infiltrating lymphocytes and interleukin 2. *J Natl Cancer Inst*, 86, 1159-66.
- ROSENTHAL, J., NAQVI, A. S., LUO, M., WERTHEIM, G., PAESSLER, M., THOMAS-TIKHONENKO, A., RHEINGOLD, S. R. & PILLAI, V. 2018. Heterogeneity of surface CD19 and CD22 expression in B lymphoblastic leukemia. *Am J Hematol*, 93, E352-E355.
- RUELLA, M. & MAUS, M. V. 2016. Catch me if you can: Leukemia Escape after CD19-Directed T Cell Immunotherapies. *Comput Struct Biotechnol J*, 14, 357-362.
- RUPP, L. J., SCHUMANN, K., ROYBAL, K. T., GATE, R. E., YE, C. J., LIM, W. A. & MARSON, A. 2017. CRISPR/Cas9-mediated PD-1 disruption enhances anti-tumor efficacy of human chimeric antigen receptor T cells. *Sci Rep*, 7, 737.
- SABATINO, M., CHOI, K., CHIRUVOLU, V. & BETTER, M. 2016. Production of Anti-CD19 CAR T Cells for ZUMA-3 and -4: Phase 1/2 Multicenter Studies Evaluating KTE-C19 in Patients With Relapsed/Refractory B-Precursor Acute Lymphoblastic Leukemia (R/R ALL). *Blood*, 128, 1227.
- SADELAIN, M., RIVIERE, I. & RIDDELL, S. 2017. Therapeutic T cell engineering. *Nature*, 545, 423-431.
- SAIBIL, S. D., ST PAUL, M., LAISTER, R. C., GARCIA-BATRES, C. R., ISRANI-WINGER, K., ELFORD, A. R., GRIMSHAW, N., ROBERT-TISSOT, C., ROY, D. G., JONES, R. G., NGUYEN, L. T. & OHASHI, P. S. 2019. Activation of Peroxisome Proliferator-Activated Receptors alpha and delta Synergizes with Inflammatory Signals to Enhance Adoptive Cell Therapy. *Cancer Res*, 79, 445-451.
- SALLUSTO, F., LENIG, D., FORSTER, R., LIPP, M. & LANZAVECCHIA, A. 1999. Two subsets of memory T lymphocytes with distinct homing potentials and effector functions. *Nature*, 401, 708-12.
- SALTER, A. I., IVEY, R. G., KENNEDY, J. J., VOILLET, V., RAJAN, A., ALDERMAN, E. J., VOYTOVICH, U. J., LIN, C., SOMMERMEYER, D., LIU, L., WHITEAKER, J. R., GOTTARDO, R., PAULOVICH, A. G. & RIDDELL, S. R. 2018. Phosphoproteomic analysis of chimeric antigen receptor signaling reveals kinetic and quantitative differences that affect cell function. *Sci Signal*, 11.
- SANSOM, D. M. 2000. CD28, CTLA-4 and their ligands: who does what and to whom? *Immunology*, 101, 169-77.
- SCHUSTER, S. J., BISHOP, M. R., TAM, C. S., WALLER, E. K., BORCHMANN, P., MCGUIRK, J. P., JAGER, U., JAGLOWSKI, S., ANDREADIS, C., WESTIN, J. R., FLEURY, I., BACHANOVA, V., FOLEY, S. R., HO, P. J., MIELKE, S., MAGENAU, J. M., HOLTE, H., PANTANO, S., PACAUD, L. B., AWASTHI, R., CHU, J., ANAK, O., SALLES, G., MAZIARZ, R. T. & INVESTIGATORS,

- J. 2019. Tisagenlecleucel in Adult Relapsed or Refractory Diffuse Large B-Cell Lymphoma. *N Engl J Med*, 380, 45-56.
- SCHUSTER, S. J., SVOBODA, J., CHONG, E. A., NASTA, S. D., MATO, A. R., ANAK, O., BROGDON, J. L., PRUTEANU-MALINICI, I., BHOJ, V., LANDSBURG, D., WASIK, M., LEVINE, B. L., LACEY, S. F., MELENHORST, J. J., PORTER, D. L. & JUNE, C. H. 2017. Chimeric Antigen Receptor T Cells in Refractory B-Cell Lymphomas. *N Engl J Med*, 377, 2545-2554.
- SHAH, B. D., GHOBADI, A., OLUWOLE, O. O., LOGAN, A. C., BOISSEL, N., CASSADAY, R. D., LEGUAY, T., BISHOP, M. R., TOPP, M. S., TZACHANIS, D., O'DWYER, K. M., ARELLANO, M. L., LIN, Y., BAER, M. R., SCHILLER, G. J., PARK, J. H., SUBKLEWE, M., ABEDI, M., MINNEMA, M. C., WIERDA, W. G., DEANGELO, D. J., STIFF, P., JEYAKUMAR, D., FENG, C., DONG, J., SHEN, T., MILLETTI, F., ROSSI, J. M., VEZAN, R., MASOULEH, B. K. & HOUOT, R. 2021. KTE-X19 for relapsed or refractory adult B-cell acute lymphoblastic leukaemia: phase 2 results of the single-arm, open-label, multicentre ZUMA-3 study. *Lancet*, 398, 491-502.
- SHAH, N. N. & FRY, T. J. 2019. Mechanisms of resistance to CAR T cell therapy. *Nat Rev Clin Oncol*, 16, 372-385.
- SHANKARAN, V., IKEDA, H., BRUCE, A. T., WHITE, J. M., SWANSON, P. E., OLD, L. J. & SCHREIBER, R. D. 2001. IFN γ and lymphocytes prevent primary tumour development and shape tumour immunogenicity. *Nature*, 410, 1107-1111.
- SI, S. & TEACHEY, D. T. 2020. Spotlight on Tocilizumab in the Treatment of CAR-T-Cell-Induced Cytokine Release Syndrome: Clinical Evidence to Date. *Ther Clin Risk Manag*, 16, 705-714.
- SIESS, K. M. & LEONARD, T. A. 2019. Lipid-dependent Akt-ivity: where, when, and how. *Biochem Soc Trans*, 47, 897-908.
- SINGH, H., FIGLIOLA, M. J., DAWSON, M. J., OLIVARES, S., ZHANG, L., YANG, G., MAITI, S., MANURI, P., SENYUKOV, V., JENA, B., KEBRIAEI, P., CHAMPLIN, R. E., HULS, H. & COOPER, L. J. 2013. Manufacture of clinical-grade CD19-specific T cells stably expressing chimeric antigen receptor using Sleeping Beauty system and artificial antigen presenting cells. *PLoS One*, 8, e64138.
- SINGH, N., PERAZZELLI, J., GRUPP, S. A. & BARRETT, D. M. 2016. Early memory phenotypes drive T cell proliferation in patients with pediatric malignancies. *Sci Transl Med*, 8, 320ra3.
- SINGH, R., KAUSHIK, S., WANG, Y., XIANG, Y., NOVAK, I., KOMATSU, M., TANAKA, K., CUERVO, A. M. & CZAJA, M. J. 2009. Autophagy regulates lipid metabolism. *Nature*, 458, 1131-5.

- SINGH, V. & AGREWALA, J. N. 2006. Regulatory role of pro-Th1 and pro-Th2 cytokines in modulating the activity of Th1 and Th2 cells when B cell and macrophages are used as antigen presenting cells. *BMC Immunology*, 7, 17.
- SMOLE, A., BENTON, A., POUSSIN, M. A., EIVA, M. A., MEZZANOTTE, C., CAMISA, B., GRECO, B., SHARMA, P., MINUTOLO, N. G., GRAY, F., BEAR, A. S., BAROJA, M. L., CUMMINS, C., XU, C., SANVITO, F., GOLDGEWICHT, A. L., BLANCHARD, T., RODRIGUEZ-GARCIA, A., KLICHINSKY, M., BONINI, C., JUNE, C. H., POSEY, A. D., LINETTE, G. P., CARRENO, B. M., CASUCCI, M. & POWELL, D. J. 2022. Expression of inducible factors reprograms CAR-T cells for enhanced function and safety. *Cancer Cell*, 40, 1470-1487.e7.
- SMYTH, M. J., CROWE, N. Y. & GODFREY, D. I. 2001. NK cells and NKT cells collaborate in host protection from methylcholanthrene-induced fibrosarcoma. *International Immunology*, 13, 459-463.
- SOMMERMEYER, D., HUDECEK, M., KOSASIH, P. L., GOGISHVILI, T., MALONEY, D. G., TURTLE, C. J. & RIDDELL, S. R. 2016. Chimeric antigen receptor-modified T cells derived from defined CD8+ and CD4+ subsets confer superior antitumor reactivity in vivo. *Leukemia*, 30, 492-500.
- SOTILLO, E., BARRETT, D. M., BLACK, K. L., BAGASHEV, A., OLDRIDGE, D., WU, G., SUSSMAN, R., LANAUZE, C., RUELLA, M., GAZZARA, M. R., MARTINEZ, N. M., HARRINGTON, C. T., CHUNG, E. Y., PERAZZELLI, J., HOFMANN, T. J., MAUDE, S. L., RAMAN, P., BARRERA, A., GILL, S., LACEY, S. F., MELENHORST, J. J., ALLMAN, D., JACOBY, E., FRY, T., MACKALL, C., BARASH, Y., LYNCH, K. W., MARIS, J. M., GRUPP, S. A. & THOMAS-TIKHONENKO, A. 2015. Convergence of Acquired Mutations and Alternative Splicing of CD19 Enables Resistance to CART-19 Immunotherapy. *Cancer Discov*, 5, 1282-95.
- SPRANGER, S., SPAAPEN, R. M., ZHA, Y., WILLIAMS, J., MENG, Y., HA, T. T. & GAJEWSKI, T. F. 2013. Up-regulation of PD-L1, IDO, and T(regs) in the melanoma tumor microenvironment is driven by CD8(+) T cells. *Sci Transl Med*, 5, 200ra116.
- STENSTRÖM, J., HEDENFALK, I. & HAGERLING, C. 2021. Regulatory T lymphocyte infiltration in metastatic breast cancer—an independent prognostic factor that changes with tumor progression. *Breast Cancer Research*, 23, 27.
- STOCK, S., ÜBELHART, R., SCHUBERT, M. L., FAN, F., HE, B., HOFFMANN, J. M., WANG, L., WANG, S., GONG, W., NEUBER, B., HÜCKELHOVEN-KRAUSS, A., GERN, U., CHRIST, C., HEXEL, M., SCHMITT, A., SCHMIDT, P., KRAUSS, J., JÄGER, D., MÜLLER-TIDOW, C., DREGER, P., SCHMITT, M. & SELLNER, L. 2019. Idelalisib for optimized CD19-specific chimeric antigen receptor T cells in chronic lymphocytic leukemia patients. *Int J Cancer*, 145, 1312-1324.

- STOLL, V., CALLEJA, V., VASSAUX, G., DOWNWARD, J. & LEMOINE, N. R. 2005. Dominant negative inhibitors of signalling through the phosphoinositol 3-kinase pathway for gene therapy of pancreatic cancer. *Gut*, 54, 109-16.
- STRONCEK, D. F., REN, J., LEE, D. W., TRAN, M., FRODIGH, S. E., SABATINO, M., KHUU, H., MERCHANT, M. S. & MACKALL, C. L. 2016. Myeloid cells in peripheral blood mononuclear cell concentrates inhibit the expansion of chimeric antigen receptor T cells. *Cytotherapy*, 18, 893-901.
- SUAREZ, E. R., CHANG DE, K., SUN, J., SUI, J., FREEMAN, G. J., SIGNORETTI, S., ZHU, Q. & MARASCO, W. A. 2016. Chimeric antigen receptor T cells secreting anti-PD-L1 antibodies more effectively regress renal cell carcinoma in a humanized mouse model. *Oncotarget*, 7, 34341-55.
- SUKUMAR, M., LIU, J., MEHTA, G. U., PATEL, S. J., ROYCHOUDHURI, R., CROMPTON, J. G., KLEBANOFF, C. A., JI, Y., LI, P., YU, Z., WHITEHILL, G. D., CLEVER, D., EIL, R. L., PALMER, D. C., MITRA, S., RAO, M., KEYVANFAR, K., SCHRUMP, D. S., WANG, E., MARINCOLA, F. M., GATTINONI, L., LEONARD, W. J., MURANSKI, P., FINKEL, T. & RESTIFO, N. P. 2016. Mitochondrial Membrane Potential Identifies Cells with Enhanced Stemness for Cellular Therapy. *Cell Metab*, 23, 63-76.
- SWADLING, L., PALLETT, L. J., DINIZ, M. O., BAKER, J. M., AMIN, O. E., STEGMANN, K. A., BURTON, A. R., SCHMIDT, N. M., JEFFERY-SMITH, A., ZAKERI, N., SUVEIZDYTE, K., FROGHI, F., FUSAI, G., ROSENBERG, W. M., DAVIDSON, B. R., SCHURICH, A., SIMON, A. K. & MAINI, M. K. 2020. Human Liver Memory CD8(+) T Cells Use Autophagy for Tissue Residence. *Cell Rep*, 30, 687-698.e6.
- TAKATA, H. & TAKIGUCHI, M. 2006. Three memory subsets of human CD8+ T cells differently expressing three cytolytic effector molecules. *J Immunol*, 177, 4330-40.
- TATSUMI, T., KIERSTEAD, L. S., RANIERI, E., GESUALDO, L., SCHENA, F. P., FINKE, J. H., BUKOWSKI, R. M., MUELLER-BERGHAUS, J., KIRKWOOD, J. M., KWOK, W. W. & STORKUS, W. J. 2002. Disease-associated Bias in T Helper Type 1 (Th1)/Th2 CD4+ T Cell Responses Against MAGE-6 in HLA-DRB1*0401+ Patients With Renal Cell Carcinoma or Melanoma. *Journal of Experimental Medicine*, 196, 619-628.
- TECARTUS®. 2022. ("TECARTUS® (Brexucabtagene Autoleucl)") [Online]. Available: <https://www.tecartushcp.com/car-t-cell-therapy/acute-lymphoblastic-leukemia/response>. [Accessed 2022].
- TEPPER, R. I., COFFMAN, R. L. & LEDER, P. 1992. An Eosinophil-Dependent Mechanism for the Antitumor Effect of Interleukin-4. *Science*, 257, 548-551.

- TOGASHI, Y., SHITARA, K. & NISHIKAWA, H. 2019. Regulatory T cells in cancer immunosuppression — implications for anticancer therapy. *Nature Reviews Clinical Oncology*, 16, 356-371.
- TU, W. & RAO, S. 2016. Mechanisms Underlying T Cell Immunosenescence: Aging and Cytomegalovirus Infection. *Front Microbiol*, 7, 2111.
- TUMAINI, B., LEE, D. W., LIN, T., CASTIELLO, L., STRONCEK, D. F., MACKALL, C., WAYNE, A. & SABATINO, M. 2013. Simplified process for the production of anti-CD19-CAR-engineered T cells. *Cytotherapy*, 15, 1406-15.
- TURTLE, C. J., HANAFI, L. A., BERGER, C., GOOLEY, T. A., CHERIAN, S., HUDECEK, M., SOMMERMEYER, D., MELVILLE, K., PENDER, B., BUDIARTO, T. M., ROBINSON, E., STEEVENS, N. N., CHANEY, C., SOMA, L., CHEN, X., YEUNG, C., WOOD, B., LI, D., CAO, J., HEIMFELD, S., JENSEN, M. C., RIDDELL, S. R. & MALONEY, D. G. 2016. CD19 CAR-T cells of defined CD4+:CD8+ composition in adult B cell ALL patients. *J Clin Invest*, 126, 2123-38.
- URAK, R., WALTER, M., LIM, L., WONG, C. W., BUDDE, L. E., THOMAS, S., FORMAN, S. J. & WANG, X. 2017. Ex vivo Akt inhibition promotes the generation of potent CD19CAR T cells for adoptive immunotherapy. *J Immunother Cancer*, 5, 26.
- VAN DER STEGEN, S. J., HAMIEH, M. & SADELAIN, M. 2015. The pharmacology of second-generation chimeric antigen receptors. *Nat Rev Drug Discov*, 14, 499-509.
- VAN DER WAART, A. B., VAN DE WEEM, N. M., MAAS, F., KRAMER, C. S., KESTER, M. G., FALKENBURG, J. H., SCHAAP, N., JANSEN, J. H., VAN DER VOORT, R., GATTINONI, L., HOBBO, W. & DOLSTRA, H. 2014. Inhibition of Akt signaling promotes the generation of superior tumor-reactive T cells for adoptive immunotherapy. *Blood*, 124, 3490-500.
- VAN DER WINDT, G. J., EVERTS, B., CHANG, C. H., CURTIS, J. D., FREITAS, T. C., AMIEL, E., PEARCE, E. J. & PEARCE, E. L. 2012. Mitochondrial respiratory capacity is a critical regulator of CD8+ T cell memory development. *Immunity*, 36, 68-78.
- VANHAESEBROECK, B., STEPHENS, L. & HAWKINS, P. 2012. PI3K signalling: the path to discovery and understanding. *Nature Reviews Molecular Cell Biology*, 13, 195-203.
- VANNINI, N., GIROTRA, M., NAVEIRAS, O., NIKITIN, G., CAMPOS, V., GIGER, S., ROCH, A., AUWERX, J. & LUTOLF, M. P. 2016. Specification of haematopoietic stem cell fate via modulation of mitochondrial activity. *Nature Communications*, 7.

- VARET, H., BRILLET-GUÉGUEN, L., COPPÉE, J.-Y. & DILLIES, M.-A. 2016. SARTools: A DESeq2- and EdgeR-Based R Pipeline for Comprehensive Differential Analysis of RNA-Seq Data. *PLoS one*, 11, e0157022-e0157022.
- VINAY, D. S., RYAN, E. P., PAWELEC, G., TALIB, W. H., STAGG, J., ELKORD, E., LICHTOR, T., DECKER, W. K., WHELAN, R. L., KUMARA, H. M. C. S., SIGNORI, E., HONOKI, K., GEORGAKILAS, A. G., AMIN, A., HELFERICH, W. G., BOOSANI, C. S., GUHA, G., CIRIOLO, M. R., CHEN, S., MOHAMMED, S. I., AZMI, A. S., KEITH, W. N., BILSLAND, A., BHAKTA, D., HALICKA, D., FUJII, H., AQUILANO, K., ASHRAF, S. S., NOWSHEEN, S., YANG, X., CHOI, B. K. & KWON, B. S. 2015. Immune evasion in cancer: Mechanistic basis and therapeutic strategies. *Seminars in Cancer Biology*, 35, S185-S198.
- VORMITTAG, P., GUNN, R., GHORASHIAN, S. & VERAITCH, F. S. 2018. A guide to manufacturing CAR T cell therapies. *Curr Opin Biotechnol*, 53, 164-181.
- WANG, D., AGUILAR, B., STARR, R., ALIZADEH, D., BRITO, A., SARKISSIAN, A., OSTBERG, J. R., FORMAN, S. J. & BROWN, C. E. 2018. Glioblastoma-targeted CD4+ CAR T cells mediate superior antitumor activity. *JCI Insight*, 3.
- WANG, R., DILLON, C. P., SHI, L. Z., MILASTA, S., CARTER, R., FINKELSTEIN, D., MCCORMICK, L. L., FITZGERALD, P., CHI, H., MUNGER, J. & GREEN, D. R. 2011. The transcription factor Myc controls metabolic reprogramming upon T lymphocyte activation. *Immunity*, 35, 871-82.
- WANG, X., POPPLEWELL, L. L., WAGNER, J. R., NARANJO, A., BLANCHARD, M. S., MOTT, M. R., NORRIS, A. P., WONG, C. W., URAK, R. Z., CHANG, W. C., KHALED, S. K., SIDDIQI, T., BUDDE, L. E., XU, J., CHANG, B., GIDWANEY, N., THOMAS, S. H., COOPER, L. J., RIDDELL, S. R., BROWN, C. E., JENSEN, M. C. & FORMAN, S. J. 2016. Phase 1 studies of central memory-derived CD19 CAR T-cell therapy following autologous HSCT in patients with B-cell NHL. *Blood*, 127, 2980-90.
- WEBER, E. W., PARKER, K. R., SOTILLO, E., LYNN, R. C., ANBUNATHAN, H., LATTIN, J., GOOD, Z., BELK, J. A., DANIEL, B., KLYSZ, D., MALIPATLOLLA, M., XU, P., BASHTI, M., HEITZENEDER, S., LABANIEH, L., VANDRIS, P., MAJZNER, R. G., QI, Y., SANDOR, K., CHEN, L. C., PRABHU, S., GENTLES, A. J., WANDLESS, T. J., SATPATHY, A. T., CHANG, H. Y. & MACKALL, C. L. 2021. Transient rest restores functionality in exhausted CAR-T cells through epigenetic remodeling. *Science*, 372.
- WEIDEN, P. L., FLOURNOY, N., THOMAS, E. D., PRENTICE, R., FEFER, A., BUCKNER, C. D. & STORB, R. 1979. Antileukemic effect of graft-versus-host disease in human recipients of allogeneic-marrow grafts. *N Engl J Med*, 300, 1068-73.
- WEINER, G. J. 2010. Rituximab: mechanism of action. *Semin Hematol*, 47, 115-23.

- WIEMAN, H. L., WOFFORD, J. A. & RATHMELL, J. C. 2007. Cytokine stimulation promotes glucose uptake via phosphatidylinositol-3 kinase/Akt regulation of Glut1 activity and trafficking. *Mol Biol Cell*, 18, 1437-46.
- WIKENHEISER, D. J. & STUMHOFER, J. S. 2016. ICOS Co-Stimulation: Friend or Foe? *Frontiers in Immunology*, 7.
- WILDE, S., SOMMERMEYER, D., LEISEGANG, M., FRANKENBERGER, B., MOSETTER, B., UCKERT, W. & SCHENDEL, D. J. 2012. Human Antitumor CD8⁺ T Cells Producing Th1 Polycytokines Show Superior Antigen Sensitivity and Tumor Recognition. *The Journal of Immunology*, 189, 598.
- WILSON, E. H., ZAPH, C., MOHRS, M., WELCHER, A., SIU, J., ARTIS, D. & HUNTER, C. A. 2006. B7RP-1-ICOS Interactions Are Required for Optimal Infection-Induced Expansion of CD4 Th1 and Th2 Responses. *The Journal of Immunology*, 177, 2365.
- XIA, A. L., WANG, X. C., LU, Y. J., LU, X. J. & SUN, B. 2017. Chimeric-antigen receptor T (CAR-T) cell therapy for solid tumors: challenges and opportunities. *Oncotarget*, 8, 90521-90531.
- XU, W. & LARBI, A. 2017. Markers of T Cell Senescence in Humans. *Int J Mol Sci*, 18.
- XU, X., ARAKI, K., LI, S., HAN, J. H., YE, L., TAN, W. G., KONIECZNY, B. T., BRUINSMA, M. W., MARTINEZ, J., PEARCE, E. L., GREEN, D. R., JONES, D. P., VIRGIN, H. W. & AHMED, R. 2014a. Autophagy is essential for effector CD8(+) T cell survival and memory formation. *Nat Immunol*, 15, 1152-61.
- XU, X., SUN, Q., LIANG, X., CHEN, Z., ZHANG, X., ZHOU, X., LI, M., TU, H., LIU, Y., TU, S. & LI, Y. 2019. Mechanisms of Relapse After CD19 CAR T-Cell Therapy for Acute Lymphoblastic Leukemia and Its Prevention and Treatment Strategies. *Front Immunol*, 10, 2664.
- XU, Y., ZHANG, M., RAMOS, C. A., DURETT, A., LIU, E., DAKHOVA, O., LIU, H., CREIGHTON, C. J., GEE, A. P., HESLOP, H. E., ROONEY, C. M., SAVOLDO, B. & DOTTI, G. 2014b. Closely related T-memory stem cells correlate with in vivo expansion of CAR.CD19-T cells and are preserved by IL-7 and IL-15. *Blood*, 123, 3750-9.
- YANG, J., HE, J., ZHANG, X., LI, J., WANG, Z., ZHANG, Y., QIU, L., WU, Q., SUN, Z., YE, X., YIN, W., CAO, W., SHEN, L., SERSCH, M. & LU, P. 2022. Next-day manufacture of a novel anti-CD19 CAR-T therapy for B-cell acute lymphoblastic leukemia: first-in-human clinical study. *Blood Cancer J*, 12, 104.
- YAO, C., LOU, G., SUN, H.-W., ZHU, Z., SUN, Y., CHEN, Z., CHAUSS, D., MOSEMAN, E. A., CHENG, J., D'ANTONIO, M. A., SHI, W., SHI, J., KOMETANI, K., KUROSAKI, T., WHERRY, E. J., AFZALI, B., GATTINONI, L., ZHU, Y., MCGAVERN, D. B., O'SHEA, J. J., SCHWARTZBERG, P. L. &

- WU, T. 2021. Author Correction: BACH2 enforces the transcriptional and epigenetic programs of stem-like CD8+ T cells. *Nature Immunology*, 22, 530-530.
- YATES, B., SHALABI, H., SALEM, D., DELBROOK, C., YUAN, C., STETLER-STEVENSON, M., FRY, T. AND SHAH, N 2018. Sequential CD22 Targeting Impacts CD22 CAR-T Cell Response. *Blood*, 132, 282.
- YESCARTA.COM 2019. FIRST CAR T THERAPY FOR NON-HODGKIN LYMPHOMA | YESCARTA® (AXICABTAGENE CILOLEUCEL).
- ZHANG, H., PASSANG, T., RAVINDRANATHAN, S., BOMMIREDDY, R., JAJJA, M. R., YANG, L., SELVARAJ, P., PAULOS, C. M. & WALLER, E. K. 2023. The magic of small-molecule drugs during ex vivo expansion in adoptive cell therapy. *Front Immunol*, 14, 1154566.
- ZHANG, M., JIN, X., SUN, R., XIONG, X., WANG, J., XIE, D. & ZHAO, M. 2021. Optimization of metabolism to improve efficacy during CAR-T cell manufacturing. *Journal of Translational Medicine*, 19, 499.
- ZHANG, Q., DING, J., SUN, S., LIU, H., LU, M., WEI, X., GAO, X., ZHANG, X., FU, Q. & ZHENG, J. 2019. Akt inhibition at the initial stage of CAR-T preparation enhances the CAR-positive expression rate, memory phenotype and in vivo efficacy. *Am J Cancer Res*, 9, 2379-2396.
- ZHAO, Z., CONDOMINES, M., VAN DER STEGEN, S. J. C., PERNA, F., KLOSS, C. C., GUNSET, G., PLOTKIN, J. & SADELAIN, M. 2015. Structural Design of Engineered Costimulation Determines Tumor Rejection Kinetics and Persistence of CAR T Cells. *Cancer Cell*, 28, 415-428.
- ZHAO, Z., LEISTER, W. H., ROBINSON, R. G., BARNETT, S. F., DEFEO-JONES, D., JONES, R. E., HARTMAN, G. D., HUFF, J. R., HUBER, H. E., DUGGAN, M. E. & LINDSLEY, C. W. 2005. Discovery of 2,3,5-trisubstituted pyridine derivatives as potent Akt1 and Akt2 dual inhibitors. *Bioorganic & Medicinal Chemistry Letters*, 15, 905-909.
- ZHENG, W., O'HEAR, C. E., ALLI, R., BASHAM, J. H., ABDELSAMED, H. A., PALMER, L. E., JONES, L. L., YOUNGBLOOD, B. & GEIGER, T. L. 2018. PI3K orchestration of the in vivo persistence of chimeric antigen receptor-modified T cells. *Leukemia*, 32, 1157-1167.
- ZHONG, X. S., MATSUSHITA, M., PLOTKIN, J., RIVIERE, I. & SADELAIN, M. 2010. Chimeric antigen receptors combining 4-1BB and CD28 signaling domains augment PI3kinase/AKT/Bcl-XL activation and CD8+ T cell-mediated tumor eradication. *Mol Ther*, 18, 413-20.
- ZOGHBI, A., ZUR STADT, U., WINKLER, B., MULLER, I. & ESCHERICH, G. 2017. Lineage switch under blinatumomab treatment of relapsed common acute lymphoblastic leukemia without MLL rearrangement. *Pediatr Blood Cancer*, 64.